INFLUENCE OF DIETARY CARBOHYDRATE PROFILE ON RUMEN HEALTH OF DAIRY COWS AND IDENTIFICATION OF MILK PROTEIN BIOMARKERS AS INDICATORS OF CARBOHYDRATE-INDUCED RUMINAL SHIFTS.

A Dissertation Presented

by

Bharath Kumar Mulakala

to

The Faculty of the Graduate College

of

The University of Vermont

In Partial Fulfillment of the Requirements
for the Degree of Doctor of Philosophy
Specializing in Animal Biosciences

May, 2023

Defense Date: February 28th, 2023
Dissertation Examination Committee:

Sabrina L. Greenwood, Ph.D., Advisor
Julie Dragon, Ph.D., Chairperson
Stephanie McKay, Ph.D.
John Barlow, Ph.D.
Cynthia J. Forehand, Ph.D., Dean of the Graduate College

ABSTRACT

Dietary fiber and starch content influence rumen function and ultimately impact cow health and productivity. However, little information is available assessing the influence of dietary carbohydrate profiles on rumen microbial metabolic activity and the rumen epithelial transcriptome. Further, biomarkers indicative of rumen function and health are scarce but could be useful in optimizing nutritional efficiency. The first objective was to characterize the rumen meta-proteome in cows fed different dietary contents of physically effective undegradable neutral detergent fiber (peuNDF240) and rumen fermentable starch (RFS). Eight cannulated Holstein cows were assigned to the study as part of a 4 x 4 Latin square design with a 2 x 2 factorial treatment arrangement, including four 28-d periods. Cows received one of four dietary treatments (dry matter basis); 1) low peuNDF240, low RFS, 2) high peuNDF240, low RFS, 3) low peuNDF240, high RFS, and 4) high peuNDF240, high RFS. The microbial protein fraction was isolated from rumen fluid samples collected from each cow on d 27 and 28 in each period and analyzed using LC-MS/MS techniques. The product ion spectra obtained from the samples were searched against 71 curated microbe-specific databases. Out of 46 proteins that were affected by treatments, 28 proteins across 13 microbial species were influenced due to RFS content in the diet, indicating RFS content of the diet has a greater influence on rumen microbial protein abundances.

To evaluate the use of milk proteins as indicators of changes in rumen microbial activity resulting from dietary carbohydrates, rumen fluid and milk samples were collected from the cows that received either the high peuNDF240, low RFS, or low peuNDF240, high RFS diet on the last two days in each period. Isolated proteins within each rumen fluid or milk sample were isobarically labeled and analyzed by LC-MS/MS. These results indicated that milk lipoprotein lipase (LPL) concentration may be a feasible milk biomarker indicative of an altered rumen environment.

The last objective was to examine the impact of the intra-ruminal dosage of propionate on the rumen epithelial transcriptome profile. Four ruminally-cannulated Holstein lactating were included in 2 × 2 crossover design and received an intra-ruminal dosage of either Na propionate or NaCl at 1 % and 0.6 % of dry matter intake, respectively. Rumen fluid, milk, and blood samples were collected from each cow on d 5, 6, and 7. Rumen epithelial biopsies were collected on d 7 from each cow in each period. Propionate treatment resulted in 331 differentially expressed genes in cow rumen epithelium. The results indicate that propionate dosage altered the expression of rumen epithelial genes involved in protein metabolism, cell growth and division events, lipid transport and metabolism, immune function, and transport activity, indicating major biological processes response triggered in response to an altered rumen environment.

Cumulatively, the results of this research indicate that dietary carbohydrate profile impacts rumen microbial protein abundances. In addition, diet-induced ruminal changes altered the rumen epithelial transcriptome and milk protein profile. The results of this research highlighted the use of milk proteins as a biomarker for altered rumen environment, particularly milk LPL concentration as an indicator for diet-induced ruminal changes.

CITATIONS

Material from this dissertation has been published in the following form:

Mulakala, B.K., Smith. K., Snider, M., Ayers, A., Honan, M., and Greenwood, S.L.. (2021). Impact of dietary carbohydrate profile on the dairy cow rumen meta-proteome. Journal of Dairy Science. Abstract.

Mulakala, B.K., Smith. K., Snider, M., Ayers, A., Honan, M., and Greenwood, S.L.. (2022). Influence of dietary carbohydrate profile on the dairy cow rumen meta-proteome. Journal of Dairy Science, 105, 8485-8496.

Mulakala, B.K., Smith. K., Snider, M., Ayers, A., Honan, M., and Greenwood, S.L.. (2022). Rumen Microbial Meta-Proteome and Milk Whey Proteome in Holstein Cows fed with High Starch and low Fiber Diet. Journal of Animal Science. Abstract.

Mulakala, B.K., Smith. K., Snider, M., Ayers, A., Honan, M., and Greenwood, S.L.. (2022). Use of milk proteins as biomarkers of changes in the rumen metaproteome of Holstein cows fed low fiber, high starch diets. Journal of Dairy Science. Under Revision.

AND

Material from this dissertation has been published in the following form:

Mulakala, B.K., Bhattarai, S., McKay, S., and Greenwood, S.L.. (2023). Influence of intraruminal dosage of propionate on rumen epithelial transcriptome, blood metabolites, insulin and acute phase proteins in Holstein cows. International Plant and Animal Genome Conference/PAG 30. 13-18 January 2023, San Diego, USA. Abstract.

DEDICATION PAGE

I dedicate this dissertation to God, my father and mother, and my wife, Dr. Nikitha Modupalli.

ACKNOWLEDGMENTS

I have been fortunate to receive guidance, instruction, assistance, and support from many people at different stages of my Ph.D.

Firstly, I would like to thank my advisor, Dr. Sabrina Greenwood, for her never-ending support, guidance, encouragement, invaluable advice, and immeasurable expertise, without which I would not have been in this place. I extend my sincere thankfulness for her kindest words and encouragement whenever needed.

I would like to thank Dr. Stephanie McKay, a member of my advisory committee, for allowing me to use McKay's lab Vermont Advanced Computing Core (VACC) space for analyzing transcriptomic data. Also, I would like to thank her for guiding me during the data analysis. I would like to thank Dr. John Barlow, a member of my advisory committee, for his encouragement and support. Further, I would like to thank my committee chair, Dr. Julie Dragon, for supporting the transcriptomic analysis. Overall, I would like to thank my committee members for their valuable insights and research support and for creating a great work environment filled with motivation and encouragement.

I extend my thankfulness to The United States Department of Agriculture-HATCH program for providing funding for this research study.

I would like to thank the Vermont Biomedical Research Network Proteomics Facility at the University of Vermont, specifically Dr. Ying Wai Lam, for the LC-MS/MS operation. A special thanks to my UVM friends and colleagues, Miriam Snider, Ashley Driemel, Suraj Bhattarai, Ashma Chakrawarti, Wil Sims, Gift Omoruyi, and Greenwood lab undergraduates. Thanks to the staff of the Paul R. Miller Research Complex (The

University of Vermont, Burlington, VT, USA) and William H. Miner Agriculture Research Institute (Chazy, NY) for their assistance with this research project. Further, I would like to thank Mallory Honan and Katie Smith for their assistance during the sample collection.

I would like to express my extreme gratitude towards my parents Shri. M. Nagahushanam and Smt. M. Ramadevi, my brother M. Santhosh Kumar, and my friend Dr. Subash Chander. I would like to thank my wife, Dr. Nikitha Modupalli, for her support, patience, and help.

TABLE OF CONTENTS

LIST OF TABLES

LIST OF FIGURES

LIST OF ABBREVIATIONS

A	Acetate
AA	Amino acids
ACH	Acetonitrile
APP	Acute phase protein
AREG	Amphiregulin
AST	Aminotransferase
B	Butyrate
BLAST	Basic local alignment search tool
Ca	Calcium
CH4	Methane
CLA	Conjugated linoleic acid
CO2	Carbon dioxide
CP	Crude protein
CU	Cellulose
d	Day
DAVID	Database for Annotation, Visualization and Integrated Discovery
DEGs	Differentially expressed genes
DGAT2L6	Diacylglycerol O-acyltransferase 2 like 6
DIM	Days in milk
DM	Dry matter
DMI	Dry matter intake
DMSO	Dimethyl sulfoxide
DTT	Dithiothreitol
DX	Dextrins
E	Ethanol
ELISA	Enzyme-linked immunosorbent assay
F	Formate
FA	Formic acid
Fe	Iron
GDH	Glutamate dehydrogenase
GL	Glycerol
GO	Gene ontology
h	Hour
H2	Hydrogen
HBEGF	Heparin binding EGF like growth factor
HC	Hemicellulose
High peuNDF240	High physically effective undigested NDF after 240-h of in vitro fermentation
HKDC1	Hexokinase domain containing 1
HNHS	High peundf240, high RFS
HNLS	High peundf240, low RFS

Hp	Haptoglobin
HRFS	High rumen fermentable starch
IACUC	Institutional Animal Care and Use Committee
ITIH4	Inter-α-trypsin inhibitor heavy chain 4
KIT	KIT proto-oncogene, receptor tyrosine kinase
L	Lactate
LAL	Lysosomal acid lipase
LBP	Lipopolysaccharide-binding protein
LC-MS/MS	Liquid chromatography-tandem mass spectrometry
LDLS	Low peundf240, low RFS
LNHS	Low peundf240, high RFS
Low peuNDF240	Low physically effective undigested NDF after 240-h of in vitro
LPL	Lipoprotein lipase
LPS	Lipopolysaccharide
LRFS	Low rumen fermentable starch
MAPK	Mitogen-activated protein kinase
McrI	Methyl-coenzyme M reductase
MKK5	Mitogen-activated protein kinase 5
MLYCD	Malonyl-CoA decarboxylase
mRNA	Messenger ribonucleic acid
MTOC	Microtubule organization center
MUN	Milk urea nitrogen
NDF	Neutral detergent fiber
NEFA	Non-esterified fatty acid
OA	Organic acids
P	Propionate
PAQR3	Progestin and adipoq receptor family member 3
PC	Pectin
pef	Physical effectiveness factor
peNDF	Physically effective NDF
PEPCK	Phosphoenolpyruvate carboxykinase
peuNDF240	Physically effective undf240
PFOR	Pyruvate: ferredoxin (flavodoxin) oxidoreductase
PGK	Phosphoglycerate kinase
PIK3CB	Phosphatidylinositol-4,5-bisphosphate 3-kinase catalytic subunit beta
PPDK	Pyruvate phosphate dikinase
PPP2CB	Protein phosphatase 2 catalytic subunit beta
PSPN	Persephin
RFS	Rumen fermentable starch
S	Succinate
SAA	Serum amyloid A
SARA	Subacute ruminal acidosis
SDH	Succinate dehydrogenase
SLC	Solute carriers

SPTAN1	Spectrin alpha, non-erythrocytic 1
ST	Starch
SU	Sugars
TEAB	Triethylammonium bicarbonate
TK	Transketolase
TMR	Total mixed ration
TMT	Tandem mass tag
TPI	Triosephosphate isomerase
UC	Universal control
uNDF240	The NDF fraction undigested after a 240-h in vitro fermentation
VFAs	Volatile fatty acids
XY	Xylans
Zn	Zinc

CHAPTER 1: LITERATURE REVIEW

1.1 Introduction

According to the United Nations (2017), the global human population is expected to reach over 9 billion by 2050. Consequently, global meat and milk consumption are predicted to be higher than 73% and 58% of consumption recorded in 2011, respectively (FAO, 2011). As land constraints will limit a linear increase in livestock numbers (Huws et al., 2018), efforts must be directed towards increased animal production efficiency to meet this increasing demand for ruminant products. To address this need for higher production efficiency, strategies such as operational and breeding management, host genetics, structure and composition of feed, and precise feeding are areas of intense research focus (Terry et al., 2020; Bach, 2014).

The rumen presents unique challenges for the precision feeding of ruminant livestock. Not only are there more than 100 billion microorganisms per teaspoon present in the contents of the rumen that impact feed utilization and rumen function (McCann et al., 2014; Weimer, 2015), but the rumen epithelium itself also affects net feed conversion efficiency. This is because the rumen epithelium is the physical barrier and also dictates the absorptive capacity of volatile fatty acids (**VFAs**) and several other compounds (Galfi et al., 1991). For decades, the research has focused on studying rumen microbial communities and their complex relationship with the ruminant host. As new technology has become available (meta-genomics, meta-transcriptomics, meta-proteomics and metabolomics), the methodology and tools to study the rumen microbial communities shifted from isolating and studying single stains independently in the laboratory to

simultaneously characterizing the entire rumen microbiome and their metabolic activity. Over the past decade, the adoption of these technologies was rapid and applied in most ruminant production systems to understand the rumen microbiome composition and how it influences the health and production of the animal. The results of these studies showed that diet has a major influence on the rumen microbiome composition and its activities. However, more efforts are needed to incorporate information on the impact of diet on the rumen microbial metabolic activity through omics approaches. Further, efforts have also been directed towards the characterization of functional adjustments of rumen epithelium at the molecular level in response to the altered rumen environment since ruminal epithelium undergoes adaptation in response to diet to maintain the normal function of the rumen.

Using these techniques to screen ruminal samples for rumen health biomarkers is an exciting application. They provide snapshots of an animal's metabolic status and can support rapid evaluation of rumen health in response to diet, environment, disease, or other influences. Given the currently limited catalog for reliable bioindicators of rumen health at this stage, more research is needed to explore markers, particularly non-invasive markers, to indicate ruminal function. Identifying non-invasive biomarkers for rumen health will aid in precision feeding and managing digestive functionality and efficiency. This chapter aims to summarize the previous literature on the impact of dietary carbohydrate profile on rumen health, thus helping identify the research gaps that can help better understand the impact of diet on rumen functions. Further, it discusses the potential non-invasive indicators for rumen health and performance.

1.2 Rumen Microbiome Composition

In early studies, researchers identified more than 200 species of bacteria and 100 species of protozoa and fungi inhabiting the rumen using culture-based techniques (Orpin and Joblin, 1997; White et al., 1999). The drawback of culture-based studies is that most rumen microbial species are not culturable, and the methodology is time-consuming. The development of molecular biology techniques, including restriction fragment length polymorphism, denaturing gradient gel electrophoresis, and curation of ribosomal RNA clone libraries, allowed researchers to characterize uncultivable microorganisms in various ecosystems (Whitford et al., 1998). However, these molecular techniques are inadequate if the goal is to characterize the entire diversity of complex rumen microbial communities. The application of omics techniques (such as meta-genomics, meta-transcriptomics, and meta-proteomics) is an appropriate and meaningful approach to studying the entire rumen microbiome. These techniques are not without limitations, such as inconsistencies in methodology (Clooney et al., 2016), sequencing equipment differences (D'Amore et al., 2016), unavailability of standard bioinformatic pipelines (Pollock et al., 2018), variations in databases (Soergel et al., 2012; Schloss et al., 2016) and limited sequencing facilities (Kim and Yu, 2014), causing variation across meta-omics studies that limit inter-study comparisons (Gruninger et al., 2019). However, combined with other methodologies, these techniques offer an exciting opportunity to expand our understanding of complex biological systems drastically.

While the use of omics in rumen-focused research is still in its infancy, and the lack of microbial reference databases limit is a challenge, the application of omics approaches

has already yielded valuable data elucidating the rumen microbiota (Yáñez-Ruiz et al., 2010; Morgavi et al., 2015; Wallace et al., 2015; Weimer, 2015; Huws et al., 2016); in fact, studies using next-generation sequencing techniques have estimated that rumen microbiota may contain up to 7,000 bacterial species (McSweeney and Mackie, 2012*)*. Most omic-inclusive rumen microbiome studies have been restricted to meta-genomics approaches, particularly amplicon-based, such as sequencing regions of 16S ribosomal ribonucleic acid (rRNA). The 16S rRNA gene comprises highly conserved regions interspersed with hypervariable regions (Skillman et al., 2006; Case et al., 2007; Wu et al., 2012). This makes the 16S rRNA gene suitable for characterizing phylogenetic relationships (Case et al., 2007; Rajendhran and Gunasekaran, 2011). Using a meta-genomic approach, Wu et al. (2012) described a core rumen microbiome comprised of eight phyla: *Bacteroidetes, Firmicutes, Proteobacteria, Spirochaetes, Fibrobacteres*, *Verrucomicrobia, Synergistete*s, and *Actinobacteria*. Jami and Mizrahi (2012) identified 32 genera in the ruminal contents of dairy cows, with *Prevotella* accounting for up to 72% of the bacterial population. Further, these authors reported that hundreds of species-level operational taxonomic units identified in the study belong to *Prevotella.* These observations supported the earlier hypothesis outlined by Stevenson et al. (2007), proposing the dominance of the *Prevotella* genera in the cattle rumen. In 2015, rumen microbiome profiling using a meta-genomic approach was performed [Rumen Global Census (http://www.rmgnetwork. org/global-rumen-census.html); Henderson et al., 2015]. In this project, the rumen microbiome composition was studied in 742 samples from 32 species or sub-species of ruminants in 35 countries. It concluded that a common core of bacteria and archaea dominated nearly all samples; the most abundant genera within the rumen were *Prevotella* (*Bacteroidetes*),

Butyrivibrio (*Firmicutes*), *Ruminococcus* (*Firmicutes*), and the unclassified *Lachnospiraceae, Ruminococcaceae, Bacteroidales,* and *Clostridiales*. A recent meta-omics approach confirmed these earlier findings and reported that *Prevotella* predominated the planktonic core community. Further, they reported that the share of *Prevotella* in various rumen metabolic pathways was high, such as in carbohydrate (~63%), small molecule (~50%), organic acid (~53%) metabolic pathways, oxidation-reduction processes (~44%), and generation of precursor metabolites (~42%). These researchers concluded that the *Prevotella* genera perform most of the metabolic work in the rumen fluid (Wirth et al., 2018). These previous studies demonstrate the importance of the *Prevotella* genera for ruminant nutrition and performance and guide further research to explore and characterize the functional capabilities of the *Prevotella* genera.

1.3 Impact of Dietary Carbohydrate Profile on the Rumen Microbiome

The structure and chemical composition of feedstuffs, particularly the carbohydrate profile, are primary determinants of the colonization profile of rumen microbes (Huws et al., 2014; Liu et al., 2016). Since the dietary neutral detergent fiber (**NDF**) and starch profiles and their ratio are key aspects of the ruminant diet, rumen microbiome responses revolve around the dietary concentration of NDF and starch. The relative concentration of NDF and starch in the diet influences the diversity and abundance of microbes in the rumen (Tajima et al., 2001; Krause et al., 2003; Sun et al., 2010; Sadet-Bourgeteau et al., 2010; Chen et al., 2011). Previously, repeated culture studies have validated that the predominant cellulolytic bacteria were *Fibrobacter succinogenes*, *Ruminococcus flavefaciens* and *Ruminococcus albus* (Hungate, 1966; Flint and Bayer, 2008), whereas predominant

amylolytic bacteria include *Butyrivibrio, Eubacterium, Lactobacillus, Prevotella, Ruminobacter, Selenomonas* and *Streptococcus* (Stewart et al., 1997; Tajima et al., 2000; Table 1.1). Since the advent of omics technology, using meta-genomic and meta-transcriptomic approaches, several studies have investigated dietary carbohydrate profile-induced shifts in microbial community composition of the rumen in different contexts (Petri et al., 2013; Thoetkiattikul et al., 2013; Lengowski et al., 2016). For example, transitioning from a high NDF diet to a high starch diet increased the abundance of *Bacteroidetes* while decreasing *Firmicutes* and *Proteobacteria* abundance (Petri et al., 2013). In another study, increasing the inclusion of concentrate (from 0% to 25%) in the diet increased the abundance of amylolytic bacteria such as *Ruminobacter* sp. and *Succinivibrio* sp. (Kittelmann et al., 2015). The Global Rumen Census project also reported that the abundance of *Prevotella ruminicola, P. brevis, P. bryantii* , and *P. albensis* was elevated in response to feeding of high-concentrate diets, and *Fibrobacter* abundance was elevated in samples from forage-fed ruminants (Henderson et al., 2015). Recent meta-transcriptomic analysis revealed that a high starch diet increased the expression of oxidative stress response genes and outer membrane proteins among rumen epithelial bacteria (Anderson and Schmitz-Esser, 2022). Another meta-transcriptomic analysis reported that rumen bacterial genes mapped to carbohydrate, amino acid, energy, vitamin, and co-factor metabolism pathways and bacterial biofilm formation pathways were enriched in samples from high starch-fed Holstein steers (Ogunade et al., 2019). Shotgun meta-genomics and meta-transcriptomics enhanced our knowledge of the diet's impact on rumen microbial communities and their functions. However, the above studies do not reflect specific microbial activity because gene expression does not

necessarily mean the gene is translated to protein. In contrast to meta-genomics and meta-transcriptomics, meta-proteomics measures the expressed proteins. Therefore, meta-proteomic studies provide additional insight into rumen microbial activities. Limited studies have been published using meta-proteomics to study the rumen microbiome. The first published rumen meta-proteomic study was in sheep (Toyoda et., 2009). Authors identified cellulose-binding proteins of *Fibrobacter succinogenes* and *Piromyces equi* using ID-PAGE coupled to MS/MS. In 2017, Deusch et al. (2017) were able to identify over 8000 bacterial and 350 archaeal proteins [proteins identified in 27 samples (samples are from three different diets; corn silage, grass silage, or grass hay)] in the ruminal contents of Jersey cows using ID-PAGE preceding MS/MS. Further, these authors reported that the *Prevotellaceae* proteins were abundant regardless of dietary treatments, and the proteins were linked to acetate and propionate pathways. In the same year, Snelling and Wallace (2017) identified protozoal structural proteins, prokaryotic central metabolic enzymes, and archaeal methanogenesis proteins using a 2D-PAGE separator followed by MS/MS. The method recently published by Honan and Greenwood (2020) increased the breadth of protein identification in rumen meta-proteome by excluding gels in the scientific protocol. Therefore, rumen meta-proteomic studies provide information beyond microbial diversity and aid in identifying the impact of diet on active microbial functions and metabolic pathway transformations. This information will aid in further optimization of rumen function and developing nutrition strategies to improve rumen nutrition use efficiency.

1.4 Impact of Diet on the Rumen Environment

Lactating dairy cows are often fed diets with higher starch contents to meet the demands for metabolizable energy that support milk production. The increased energy supply is necessary to support modern production levels. Feeding a high-starch diet results in increased rumen VFA concentrations, lower pH, and altered microbial composition (Hernández et al., 2014; Humer et al., 2018). For example, a decrease in ruminal pH due to high starch diets decreases cellulolytic species (*F. succinogenes*, *R. albus*, and *R. flavefaciens*) and increases lactic acid-producing (*Olsenella*) and utilizing species (*Megasphaera elsdenii*; Kim et al., 2018). This altered rumen environment results in the release of lipopolysaccharide (**LPS**) and other microbially-associated molecular patterns in the ruminal fluid (Ametaj et al., 2010; Garcia et al., 2017). For example, the free ruminal LPS concentration in non-lactating Jersey cows increased 10-fold when their diet was switched from hay to concentrate-inclusive (118 to 148 EU/mL vs. 1,600 EU/mL; Andersen et al., 1994). These changes can potentially damage the rumen epithelial barrier resulting in the translocation of pro-inflammatory signals, such as LPS, from the rumen into the blood circulation (Aschenbach et al., 2011). Translocation of LPS can lead to several other negative consequences. Translocation of LPS into the portal blood triggers systemic inflammation (Dong et al., 2011), consequently elevating the serum concentration of acute phase proteins, particularly serum amyloid A and haptoglobin (Gozho et al., 2005; Khafipour et al., 2009). Further, it impacts milk composition because, in response to systemic inflammation, the mammary gland redirects available nutrients toward synthesizing immune molecules from synthesizing milk components (Dong et al., 2011). Ma et al. (2022) reported this reprioritization in response to diet, whereby authors observed

that feeding a high-concentrate diet to dairy cows increased the blood LPS concentration within the milk vein, consequently increasing the abundance of pro-inflammatory cytokines (IL-6 and IL-1α), immune-associated factors (lingual antimicrobial peptide and tracheal antimicrobial peptide) in the mammary gland. However, the extent of damage to the ruminal epithelium due to an altered rumen environment determines whether negative consequences of rumen environment changes remain contained within the rumen or are transferred into circulation and interfere with the health and productivity of the animal (Klevenhusen et al., 2013; Liu et., 2013).

1.5 Rumen Epithelium

The rumen epithelium plays a central role in dictating the net efficiency of feed conversion, as primary functions of the ruminal epithelium include nutrient absorption and metabolism, ion transport, and physical protection (Galfi et al., 1991; Baldwin and Connor, 2017). The histological structures of the rumen epithelium support these important functions. The epithelium is a stratified squamous comprising four strata, including the stratum corneum, granulosum, stratum spinosum, and stratum basale (Graham et al., 2005; Figure 1.1). The lumen-facing side of the epithelium, the stratum corneum, is in direct contact with the ruminal lumen and is comprised of flat, cornified keratinocytes providing physical protection against tissue damage. The stratum granulosum, located below the stratum corneum, is tightly connected via tight cell junctions. The two main proteins of tight cell junctions are claudin-1 and zonula occluden-1 (Figure 1.1; Graham et al., 2005). These proteins function together to form a protective barrier that limits the translocation of large molecules such as pathogens (Klevenhusen et al., 2013) and LPS (Emmanuel et al.,

2007) across the ruminal epithelium. The stratum spinosum cells are tightly interconnected by filaments providing strength to the epithelium (Dobson et al., 1956), and the gap junctions between cells are involved in cell signaling and cell-to-cell movement of small molecules such as sugars, lactate, and butyrate (Graham and Simmons, 2005). Furthermore, stratum spinosum also contains tight-cell junction proteins claudin-1 and zonula occluden-1, but at a lower concentration than the stratum granulosum (Graham and Simmons, 2005). The final layer, the stratum basale, is tightly attached to a basal membrane, anchoring the epithelium to the central supporting core of connective tissue, and it contains larger nuclei and abundant mitochondria, indicating a high metabolic activity (Graham and Simmons, 2005; Steele et al., 2011). This membrane is mitotically active and responsible for continuous cell renewal.

The stratified squamous epithelium of the rumen epithelia acts as a selectively permeable membrane between the lumen of the rumen and arterial circulation. Despite the multiple cell cellular layers, the epithelium appears to function as a single functional entity. The cells are intimately connected through cell-to-cell gap junctions (Graham and Simmons, 2005), allowing small molecules and ions to pass from cell to cell without crossing the cell membrane repeatedly. Such molecules include such as VFAs (Aschenbach et al., 2009). Approximately 50 to 85% of the total VFA produced in the reticulo-rumen is absorbed across the rumen epithelium (Bergman, 1990; Kristensen et al., 1998). Ruminal VFA absorption occurs via passive diffusion and protein-mediated transport through bicarbonate-dependent and - independent mechanisms (Penner, 2014). After VFA uptake by the epithelium, the VFAs are metabolized within the epithelium for epithelial energy use. However, the proportion of VFA metabolization within the epithelium is not

equivalent among acetic, propionic, and butyric acids. It has been estimated that 30% of the absorbed acetic acid, 50 % of the absorbed propionic, and 90% of the absorbed butyric acid are metabolized within the ruminal epithelium (Bergman, 1990). Metabolites of these reactions, such as lactate and β-hydroxybutyric acid in the epithelium, are transported into the blood and subsequently metabolized by the liver or peripheral tissues for maintenance, growth, lactation, or lipogenesis (Bergman, 1990).

Under normal conditions, the ruminal epithelium can maintain its selective permeability. However, previous studies have shown that dietary changes challenge the integrity of the epithelium, as diet influences ruminal VFA concentrations, and pH subsequently impacts the VFA absorption rate (Aschenbach et al., 2011). For example, when transitioning from a high-forage diet (100% chopped hay) to a high-grain diet (65% grain), ruminal tissue exhibited weak tight junctions between granulosum cells in cows (Steele et al., 2011). Similarly, in goats with the same forage:concentrate ratio, the rumen tissue showed eroded tight junction proteins and the loss of stratum granulosum cell layers (Liu et al., 2013). Further, they reported that the mRNA expression of tight junction proteins claudin-4, occluden, and zonula occluden-1 was downregulated due to the high-grain diet (Liu et al., 2013). However, rumen epithelium adapts to a diet-induced altered rumen environment to account for the elevated VFA production to achieve rumen homeostasis.

One of the ruminal epithelium responses to a diet-induced altered rumen environment is surface area proliferation or degeneration (Dirksen et al., 1985; Mentschel et al., 2001). For example, Mentschel et al. (2001) reported that calves fed with increasing

amounts of propionic acid from 53 g to 390 g or butyric acid from 54 g to 326 g increased the papillae length from 1mm in controls to 2.2 mm (propionic acid) and 4 mm (butyric acid). In addition to morphological adaptation, ruminal epithelium undergoes metabolic adaptation in response to a diet-induced rumen environment. For example, net Na+ transport across the ruminal epithelium of sheep increased following the dietary transition from a 100% hay diet to a 50:50 forage:concentrate inclusion diet within 1 week (Etschmann et al., 2009). Similarly, Na+ /K+ ATPase activity was increased in sheep rumen epithelium when sheep changed from a 75:25 to a 25:75 forage:concentrate ratio (Baldwin and McLeod, 2000). Further, studies have shown that rumen epithelium undergoes adaptation at the molecular level in response to the diet-induced altered rumen environment. For example, Gholizadeh et al. (2020) reported that genes involved in filament organization, positive regulation of epithelial regulation, and immune response were differentially expressed in high grain-fed steers rumen epithelium. Baldwin et al. (2018) studied the influence of intra-ruminal butyrate infusion on epithelial transcriptomics in dry dairy cows. The authors observed the temporal effects of butyrate infusion on the epithelial transcriptome. In the early stage of intra-ruminal infusion of butyrate (on d 1 and d 3), genes related to the mitotic cell cycle process, cell cycle process, and regulation of cell cycle were influenced. On the last day (d 7) of infusion, genes related to translation, peptide biosynthetic process, peptide metabolic process, and cellular amide metabolic process were influenced. Further, these authors suggested that rumen epithelial transcriptomics changes are dynamic, strengthening the importance of studying rumen epithelial transcriptomics to increase rumen nutrition use efficiency.

As we know, a greater proportion of highly fermentable carbohydrates in ruminant diets results in a greater proportion of propionate production within the rumen. Propionate is a three-carbon VFA converted from pyruvate through the succinate or acrylate pathway (Russell, 2002). Once propionate is produced in the rumen, it is absorbed by the rumen epithelium, enters the portal vein, and is transported to the liver. In the liver, propionate is converted to glucose via gluconeogenesis. Although propionate holds a prominent position in providing energy to ruminant metabolism, the hypophagic effects of propionate have been documented in ruminants. For example, intra-ruminal propionate infusion altered feeding behaviors and decreased the energy intake of lactating dairy cows (Oba and Allen, 2003). Similarly, meal size was decreased compared with acetate with propionate infusion at spontaneous meals (Choi and Allen, 1999). In another study, intra-ruminal propionate infusion decreased serum non-esterified fatty acid concentration in steers (Oh et al., 2015). Recently, Zhan et al. (2020) reported propionate infusion upregulated the genes involved in the gluconeogenic pathway in bovine intestinal epithelial cells. Based on the above studies, it is fair to assume that propionate interacts with the genomic activities of rumen epithelium. Therefore, understanding the impact of propionate on the regulation of epithelial transcriptome is a critical component of research targeting improved rumen nutrition utilization and function.

1.6 Biomarkers Indicative of Rumen Health and Performance

The altered rumen environment alters the cow's metabolic status, commonly reflected by alterations in body fluids such as rumen fluid, blood, urine, saliva, and milk (Overton et al., 2017). For example, Nasrollahi et al. (2019) reported that aminotransferase

(**AST**) activity in the blood was high in dairy cows fed a high-concentrate diet and suggested AST activity can be used as an indicator of diet-induced altered rumen environment. Analysis of key factors in blood circulation has been a standard method for diagnosing metabolic diseases (Oetzel, 2004). However, blood collection can be time-consuming, alters the blood parameters because of animal restraining for blood collection (loose housing system), and is sometimes viewed as an animal welfare issue by the public (Fønss and Munksgaard, 2008; Solano et al., 2004). Further, most blood parameters vary diurnally, which results in a need for multiple blood collections to garner accurate metabolic assessment. For example, Hussein et al. (2020) reported that serum metabolite concentrations, such as glucose, β-hydroxybutyric acid, and urea, were influenced by the time of sampling within the day. Identifying biomarkers obtained through non-invasive sampling that are less impacted by diurnal variability or that can be easily collected for composite assessment are needed as an alternative to blood for determining the cow's metabolic and health status. Milk, as a fluid already being collected daily (often multiple times per day) from lactating cows in dairy systems, is an ideal biofluid to evaluate milk components as biomarkers of altered cow metabolic status.

1.6.1 Milk Yield and Components

While dietary starch has not consistently impacted milk yield (Stone, 1999; Gozho et al., 2007; Li et al., 2012; Danscher et al., 2015), individual milk constituents may be feasible milk biomarkers indicative of shifts in the rumen environment. Numerous studies have shown that a high starch diet can negatively impact the milk fat content (Nocek, 1997; Kleen et al., 2003; Li et al., 2012). For instance, Steele et al. (2016) reported that a high

starch diet increased the concentration of odd-chain fatty acid (including 11:0 and 13:0), cis-9, cis-12 18:2; trans-9, cis-11 conjugated linoleic acid (CLA; trans-10, cis-12 CLA; and 20:4n-6 and decreased the concentration of branched-chain fatty acid (including 14:0 iso, 15:0 iso, 15:0 anteiso, 16:0 iso, and 17:0 iso), 18:0, trans-11 18:1, cis-9, trans-11 CLA, 18:3 n-3, 20:0, cis-11 20:1, 20:4 n-3,22:0 and 24:0. In the study by Danscher et al. (2015), milk fat content was decreased (4.14% vs. 5.08%) from cows fed a high starch diet compared with cows fed a conventional TMR diet (31.8 vs. 19.6 % starch as % of DM). Similarly, Bipin et al. (2016) and Malekkhahi et al. (2016) reported reduced milk fat content due to high starch diets. Previously, Vlaeminck et al. (2006) reported feeding high starch diets reduced iso C14:0, iso C15:0 and iso C16:0 in dairy cow milk fat. Similar results were observed by Nielsen et al. (2004) when the diet was shifted from grass silage to maize silage. Woolpert et al. (2017) suggested using the bulk tank's de novo fatty acid concentration as an indicator of ruminal function on commercial Holsteins dairy farms. Loor et al. (2005) described that low rumen pH due to a high starch diet increases the biohydrogenation of C18:2n-6 to trans-10, cis-12 C18:2, which decreases the expression of genes related to milk fat content and synthesis results in milk fat depression. In support of the previous statement, infusion of CLA in dairy cows decreased the milk fat content by 51%, and authors reported the effects were most pronounced through a reduction in de novo fatty acid synthesis (Chourinard et al., 1999). However, the use of fatty acids as direct indicators of rumen health is challenging, as several factors, such as lactation state, feeding frequency, stocking density, breed, dietary ether extract content, and physical characteristics of the diet, affect the fat percentage of milk (Woolpert et al., 2016; Enemark et al., 2002; Grummer, 1991). Some studies failed to demonstrate a decrease in milk fat

content due to a high starch diet (Lean et al., 2000; Gozho et al., 2007; Gao and Oba, 2015). Plaizier et al. (2008) proposed that the differences between studies might be a repercussion of the low ruminal pH duration due to a high starch diet, with short bouts unlikely to influence milk fat content.

Other well-known milk biomarkers used as indicators of animal nutrient utilization are milk urea nitrogen (**MUN**) and lactose. Inefficient utilization of dietary nitrogen by the rumen microbes, for example resulting from a disproportion of rumen degradable: rumen undegradable protein in the diet, or a malalignment of protein and energy availability in the rumen, results in an elevated blood ammonia concentration. Elevated circulating ammonia is also reflected in a higher excretion of MUN. Previously, Stefanska et al. (2020) and Kleen et al. (2013) reported that the MUN concentration produced by dairy cows was increased in response to feeding high starch diets. Barbara et al. (2020) described that a low fermentation rate due to low pH results in a decrease in the amount of energy available for microbial protein synthesis and, at the same time increase in proteolytic bacteria in the rumen; these events increase the ammonia in the blood. However, Gao and Oba (2014, 2015) reported that dairy cows' MUN values decreased with a high starch diet. The differences in the studies need further clarification. In addition, various factors can impact the MUN concentration, such as extensive protein consumption and the degradation level of crude protein in the rumen (Aguilar et al., 2012). Therefore, further studies are needed to evaluate the use of MUN as a rumen health indicator and highlight the potential limitations of using this milk biomarker as a diagnostic tool. Plaizier et al. (2008), Guo et al. (2013), and Zhao et al. (2016) reported the concentration of lactose was increased in response to feeding dairy cows a high starch diet. However, Morar et al. (2022) recently

reported that feeding a high-starch diet did not affect dairy cow milk lactose concentration. Li et al. (2012) explained that milk lactose content increases as the starch concentrate increases in the diet because of an increased supply of propionate for gluconeogenesis and consequently milk lactose synthesis. Perhaps these discrepancies in milk lactose can be explained from the perspective of altered behavior, as previously, Nasrollahi et al. (2017) and Coon et al. (2019) reported that the risk of developing SARA can affect the sorting behavior in dairy cows, ultimately affecting the composition of feed consumed (fine particles vs. long particles) by animals. Cumulatively, the difference in the milk lactose concentration between studies may be, at least in part, because of differences in the sorting behavior between the studies.

Another milk fraction potentially rich in biomarker candidates is the protein fraction. Bovine milk contains 2.3–4.4% (w/w) of proteins. The primary group of milk proteins is casein, an acid-precipitated protein that constitutes 80% (76–86%) of bovine milk proteins with a molecular weight of ~28-30 kDa. Whey proteins comprise the non-casein protein fraction in milk (~20% of bovine milk protein). The major whey proteins are β-lactoglobulin, α-lactalbumin, bovine serum albumin, and immunoglobulins (Madureira et al., 2007). However, whey also contains thousands of low-abundance proteins, including lactoferrin, lactoperoxidase, and lysozyme (Smolenski et al., 2007; Steijns and Van Hooijdonk, 2000), as well as acute phase proteins (Eckersall et al., 2006). Tacoma et al. (2016) identified over 900 low-abundant whey proteins in bovine milk using an LC/MS technique. Studies have shown that low-abundant whey proteins include several ontological groups, including antioxidant activity, immuno-stimulating functions, and anti-inflammatory proteins (Madureira et al., 2007; Wada and Lönnerdal, 2014). Recently,

Morar et al. (2022) reported that feeding high-starch diets negatively impacted bovine milk protein content. Similarly, Colman et al. (2013), Xu et al. (2016), and Li et al. (2017) have also reported that the milk protein content was lower in milk from cows fed a high starch diet. In contrast, Khafipour et al. (2009) and Gozho et al. (2012) reported an increase in milk protein content with a high starch diet in dairy cows. However, recent studies suggested that the long-term feeding of a high starch diet to dairy cows and goats is associated with a decrease in the milk protein content (Dong et al., 2013; Chang et al., 2018). Puppel et al. (2021) recently reported that milk whey protein (β-lactoglobulin) concentration was altered due to ketosis and suggested whey proteins could be used as biomarkers for diagnosing metabolic diseases. With the help of mass spectrometry, hundreds of unique proteins have been identified in different fractions of bovine milk (Hettinga et al., 2011; Nissen et al., 2013). This makes the proteomics approach a potential tool for identifying novel biomarkers (Boehmer et al., 2010). Using the proteomics approach, van Altena et al. (2016) identified 13 significant proteins expressed differentially in dairy cow milk between the low disease resistance vs. high disease resistance dairy cows. Further, the authors confirmed the proteomics results by validation with enzyme-linked immunosorbent assays. In another study, using a proteomic approach, Abdelmegid et al. (2017) identified four candidate biomarkers (cathelicidin-4, haptoglobin, cathepsin B, and lactotransferrin) in the milk for the diagnosis of cow mastitis. Further, Delosière et al. (2019) created an atlas of 4654 unique proteins using the cow milk proteins reported in 20 recent proteomics studies. Using the atlas, authors proposed 7 proteins as biomarkers of negative energy balance in dairy cows, including phosphoenolpyruvate carboxylase, acetoacetyl-CoA thiolase, mitochondrial isovaleryl-CoA dehydrogenase,

succinate dehydrogenase flavoprotein subunit, and the leucine-rich repeat-containing protein 59. These limited studies evaluating milk proteins as indicators of animal metabolic status highlight the potential of this approach for more specific and linear causal relationship identification between rumen health and milk proteins. Therefore, evaluating milk whey proteome for representative biomarkers of an altered rumen environment could be ideal.

1.7 Conclusion

Previous studies have reported the potential impacts of dietary carbohydrate profiles on the rumen microbiome profile and rumen epithelial adaptations. However, characterization of rumen microbial metabolic activity in response to dietary carbohydrate profile and rumen epithelial functional adjustment at the molecular level in response to altered rumen environment will lead to complementary meaningful information on the impact of diet on rumen health. This information will aid in further developing precision feeding strategies that maximize rumen nutrition utilization efficiency. Impaired rumen function due to diet, particularly during periods of high-starch feeding, alters the metabolic status of the cow, consequently influencing various fractions of milk. The milk proteome is reactive to metabolic changes and could be an ideal source of biomarkers indicative of animal and rumen performance in response to diet. Identifying reliable non-invasive biomarkers for rumen health will increase the precision of feeding and managing digestive disorders.

1.8 Hypothesis and Objectives

It was hypothesized that varying dietary fiber and starch concentrations would impact the abundance of proteins involved in energetics and protein synthesis-associated pathways in rumen microbes. Further, a diet high in starch and low in fiber was hypothesized to impact the milk proteome, and milk proteins could be used as indicators of changes in rumen microbial activity resulting from diets. It was hypothesized that the genes related to biological processes will be regulated as a part of rumen epithelium adaptive responses to the altered rumen environment due to propionate, which is a consequence of high-starch feeding. The objectives of the study were;

1) Characterize the rumen meta-proteome in response to different concentrations of NDF and starch in the diet.
2) Examine the impact of a high starch and low fiber diet on the milk protein profile and evaluate milk proteins as indicators of an altered rumen environment.
3) Examine the influence of diet-induced altered rumen environment on rumen epithelial transcriptome profile.

Figure 1.1. (A) picture of rumen papillae biopsies collected from the rumen wall of the ventral sac in one of our animal trials (Photograph courtesy Dr. Sabrina Greenwood; The University of Vermont) (B) depiction of rumen papillae stratification of epithelium.

A

B

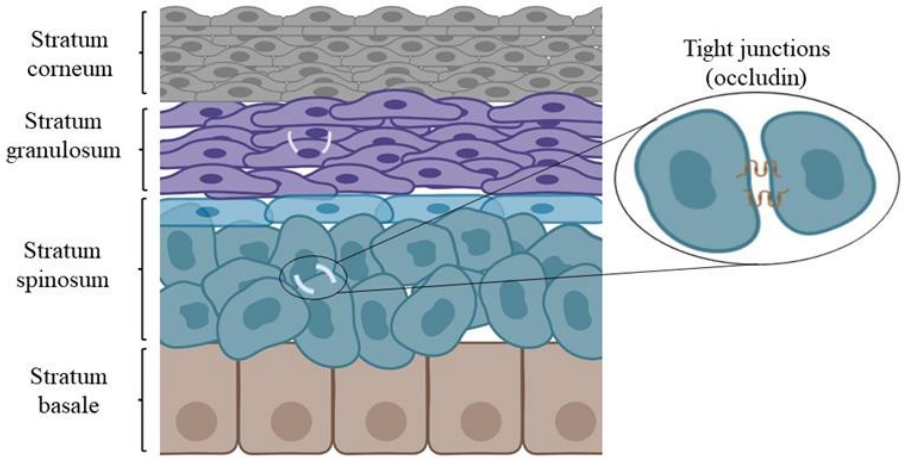

Table 1.1. The characteristics of predominant cultured ruminal microbiota adapted from Russell and Rychlik (2001).

Species	Substrate	Fermentation Products
Anaerovibrio lipolytica	GL, SU	A, S, P
Butyrivibrio fibrisolvens	ST, CU, HC, PC, SU	B, F, A, H_2
Eubacterium ruminantium	HC, DX, SU	A, F, B, L
Fibrobacter succinogenes	CU	S, F,A
Lachnospira multiparus	PC, SU	L, A, F, H_2
Megasphaera elsdenii	L, SU	P, A, B, H_2
Methanobrevibacter ruminantium	H_2, CO_2, F	CH_4
Prevotella albensis	ST, PC, XY, SU	S, A, F, P
Prevotella brevis	ST, PC, XY, SU AA	S, A, F, P
Prevotella bryantii	ST, PC, XY, SU	S, A, F, P
Prevotella ruminocola	ST, PC, XY, SU	S, A, F, P
Ruminobacter amylophilus	ST	S, F, A, E
Ruminococcus albus	CU, HC	A, F, E, H_2
Ruminococcus flavefaciens	CU, HC	S, F, A, H_2
Selenomonas ruminantium	ST, DX, SU, L, S	L, A, P, B, F, H_2
Streptococcus bovis	ST, SU	L, A, F, E
Succinomonas amylolytica	ST	S, A, P
Succinovibrio dextrinosolvens	PC, DX, SU	S, A, F, L
Wolinella succinogenes	OA, H_2, F	S

Abbreviations; CU, cellulose; HC, hemicellulose; DX, dextrins; SU, sugars; ST, starch; PC, pectin; XY, xylans; L, lactate; S, succinate; GL, glycerol, AA, amino acids; OA, organic acids; H_2, hydrogen; F, formate; CO_2, carbon dioxide; A, acetate; E, ethanol; B, butyrate; L, lactate; P, propionate; CH_4, methane.

1.9 References

Abdelmegid, S., J. Murugaiyan, M. Abo-Ismail, J. L. Caswell, D. Kelton, and G. M. Kirby. 2017. Identification of host defense-related proteins using label-free quantitative proteomic analysis of milk whey from cows with *Staphylococcus aureus* subclinical mastitis. Int. J. Mol. Sci. 19:78. https://doi.org/10.3390/ijms19010078

Abou-Ward, G. A. 2008. Effect of pre-weaning diet on lamb's rumen development. American-Eurasian Journal of Agricultural and Environmental Science. 3:561–567.

Aguilar, M., M. D. Hanigan, H. A. Tucker, B. L. Jones, S. K. Garbade, M. L. McGilliard, C. C. Stallings, K. F. Knowlton, and R. E. James. 2012. Cow and herd variation in milk urea nitrogen concentrations in lactating dairy cattle. J. Dairy Sci. 95:7261–7268. https://doi.org/10.3168/jds.2012-5582

Aschenbach, J. R., G. B. Penner, F. Stumpff, and G. Gäbel. 2011. Ruminant nutrition symposium: Role of fermentation acid absorption in the regulation of ruminal pH. J. Anim. Sci. 89:1092–1107.

van Altena, S. E. C., B. de Klerk, K. A. Hettinga, R. J. J. van Neerven, S. Boeren, H. F. J. Savelkoul, and E. J. Tijhaar. 2016. A proteomics-based identification of putative biomarkers for disease in bovine milk. Vet. Immunol. Immunopathol. 174:11–18. https://doi.org/10.1016/j.vetimm.2016.04.005

Ametaj, B. N., Q. Zebeli, F. Saleem, N. Psychogios, M. J. Lewis, S.M. Dunn, J. Xia, and D. S. Wishart. 2010. Metabolomics reveals unhealthy alterations in rumen metabolism with increased proportion of cereal grain in the diet of dairy cows. Metabolomics. 6:583–594. https://doi.org/10.1007/s11306-010-0227-6

Andersen, P. H., B. Bergelin, and K. A. Christensen. 1994. Effect of feeding regimen on concentration of free endotoxin in ruminal fluid of cattle. J. Anim. Sci. 72:487–491. https://doi.org/10.2527/1994.722487x

Andersen, T. O., B. J. Kunath, L. H. Hagen, M. O. Arntzen, and P. B. Pope. 2021. Rumen metaproteomics: Closer to linking rumen microbial function to animal productivity traits. Methods. 186:42–51. https://doi.org/10.1016/j.ymeth.2020.07.011

Anderson, C. J., and S. Schmitz-Esser. 2022. Differential Gene Expression of the Bovine Rumen Epithelial Microbiota During a Sub-acute Ruminal Acidosis (SARA) Challenge. J. Anim. Sci. Oxford Univ Press Inc Journals Dept, 2001 Evans Rd, Cary, NC 27513 USA.

Annison, E. F., and W. L. Bryden. 1998. Perspectives on ruminant nutrition and metabolism I. Metabolism in the rumen. Nutr. Res. Rev. 11:173–198. https://doi.org/10.1079/NRR19980014

Aschenbach, J. R., S. Bilk, G. Tadesse, F. Stumpff, and G. Gäbel. 2009. Bicarbonate-dependent and bicarbonate-independent mechanisms contribute to nondiffusive uptake of acetate in the ruminal epithelium of sheep. Am. J. Physiol. Gastrointest. 296:G1098–G1107. https://doi.org/10.1152/ajpgi.90442.2008

Aschenbach, J. R., G. B. Penner, F. Stumpff, and G. Gäbel. 2011. Ruminant nutrition symposium: Role of fermentation acid absorption in the regulation of ruminal pH. J. Anim. Sci. 89:1092–1107. https://doi.org/10.2527/jas.2010-3301

Bach, A. 2014. Precision feeding to increase efficiency for milk production. Adv. Dairy Technol. 26:177–189.

Baldwin, R. L., and E. E. Connor. 2017. Rumen function and development. Vet. Clin. N. Am. - Food Anim. Pract. 33:427–439.

Baldwin, R. L., R. W. Li, Y. Jia, and C. J. Li. 2018. Transcriptomic impacts of rumen epithelium induced by butyrate infusion in dairy cattle in dry period. Gene Regul. Syst. Bio. 12. https://doi.org/10.1177/1177625018774798

Baldwin, R. L., W. Li, C. Li, E. E. Connor, and R. W. Li. 2012. The bacterial community composition of the bovine rumen detected using pyrosequencing of 16S rRNA genes. Metagenomics. b1-11. https://doi.org/10.4303/mg/235571

Baldwin, R. L. T., and K. R. McLeod. 2000. Effects of diet forage: concentrate ratio and metabolizable energy intake on isolated rumen epithelial cell metabolism in vitro. J. Anim. Sci. 78:771–783. https://doi.org/10.2527/2000.783771x

Bauman, D. E., and J. M. Griinari. 2003. Nutritional regulation of milk fat synthesis. Annu. Rev. Nutr. 23:203–227. https://doi.org/10.1146/annurev.nutr.23.011702.073408

Bednar, G. E., A. R. Patil, S. M. Murray, C. M. Grieshop, N. R. Merchen, and G. C. Fahey Jr. 2001. Starch and fiber fractions in selected food and feed ingredients affect their small intestinal digestibility and fermentability and their large bowel fermentability in vitro in a canine mode. J. Nutr. 131:276–286. https://doi.org/10.1093/jn/131.2.276

Beliveau, R. M., and J. J. McKinnon. 2008. Effect of graded levels of wheat-based dried distillers' grains with solubles on performance and carcass characteristics of feedlot steers. Can. J. Anim. Sci. 88:677–684. https://doi.org/10.4141/CJAS08045

Bergman, E. N. 1990. Energy contributions of volatile fatty acids from the gastrointestinal tract in various species. Physiol. Rev. 70:567–590.

Bipin, K. C., P. T. Ramesh, and S. Yathiraj. 2016. Impact of subacute ruminal acidosis (SARA) on milk yield and milk fat content in crossbred dairy cows. Paripex-Indian J. Res. 5:290–292.

Boehmer, J. L., J. A. DeGrasse, M. A. McFarland, E. A. Tall, K. J. Shefcheck, J. L. Ward, and D. D. Bannerman. 2010. The proteomic advantage: label-free quantification of proteins expressed in bovine milk during experimentally induced coliform mastitis. Vet Immunol Immunopathol. 138:252–266. https://doi.org/10.1016/j.vetimm.2010.10.004

Brandao, V. L. N., and A. P. Faciola. 2019. Unveiling the relationships between diet composition and fermentation parameters response in dual-flow continuous culture system: a meta-analytical approach. Transl. Anim. Sci. 3:1064–1075. https://doi.org/10.1093/tas/txz019

Brulc, J. M., D. A. Antonopoulos, M. E. Berg Miller, M. K. Wilson, A. C. Yannarell, E. A. Dinsdale, R. E. Edwards, E. D. Frank, J. B. Emerson, and P. Wacklin. 2009. Gene-centric metagenomics of the fiber-adherent bovine rumen microbiome reveals forage specific glycoside hydrolases. Proc. Natl. Acad. Sci. 106:1948–1953. https://doi.org/10.1073/pnas.0806191105

Case, R. J., Y. Boucher, I. Dahllöf, C. Holmström, W. F. Doolittle, and S. Kjelleberg. 2007. Use of 16S rRNA and rpoB genes as molecular markers for microbial ecology studies. Appl. Environ. Microbiol. 73:278–288. https://doi.org/10.1128/AEM.01177-06

Chang, G., L. Wang, N. Ma, W. Zhang, H. Zhang, H. Dai, and X. 2018. Histamine activates inflammatory response and depresses casein synthesis in mammary gland of dairy cows during SARA. BMC Vet. Res. 14:168.

Chen, Y., G. B. Penner, M. Li, M. Oba, and L. L. Guan. 2011. Changes in Bacterial Diversity Associated with Epithelial Tissue in the Beef Cow Rumen during the Transition to a High-Grain Diet. Appl. Environ. Microbiol. 77:5770–5781. https://doi.org/10.1128/AEM.00375-11

Chenost, M. 1966. Fibrousness of forages: its determination and its relation to feeding value. Fibrousness of forages: Its determination and its relation to feeding value.

Choi, B. R., and M. S. Allen. 1999. Intake regulation by volatile fatty acids and physical fill. S. Afr. J. Anim. Sci. 29:40–41.

Chouinard, P. Y., L. Corneau, D. M. Barbano, L. E. Metzger, and D. E. Bauman. 1999. Conjugated linoleic acids alter milk fatty acid composition and inhibit milk fat secretion in dairy cows. J. Nutr. 129:1579–1584. https://doi.org/10.1093/jn/129.8.1579

Church, D. C. 1993. The Ruminant Animal: Digestive Physiology and Nutrition. Waveland press.

Clooney, A. G., F. Fouhy, R. D. Sleator, A. O'Driscoll, C. Stanton, P. D. Cotter, and M. J. Claesson. 2016. Comparing apples and oranges?: Next generation sequencing and its impact on microbiome analysis. PLoS One. 11:e0148028. https://doi.org/10.1371/journal.pone.0148028

Colman, E., W. B. Fokkink, M. Craninx, J. R. Newbold, B. de Baets, and V. Fievez. 2010. Effect of induction of subacute ruminal acidosis on milk fat profile and rumen parameters. J. Dairy Sci. 93:4759–4773. https://doi.org/10.3168/jds.2010-3158

Comtet-Marre, S., N. Parisot, P. Lepercq, F. Chaucheyras-Durand, P. Mosoni, E. Peyretaillade, A. R. Bayat, K. J. Shingfield, P. Peyret, and E. Forano. 2017. Metatranscriptomics reveals the active bacterial and eukaryotic fibrolytic communities in the rumen of dairy cow fed a mixed diet. Front. Microbiol. 8:67. https://doi.org/10.3389/fmicb.2017.00067

Coomey, J. H., R. Sibout, and S. P. Hazen. 2020. Grass secondary cell walls, Brachypodium distachyon as a model for discovery. New Phytol. 227:1649–1667. https://doi.org/10.1111/nph.16603

D'Amore, R., U. Z. Ijaz, M. Schirmer, J. G. Kenny, R. Gregory, A. C. Darby, M. Shakya, M. Podar, C. Quince, and N. Hall. 2016. A comprehensive benchmarking study of protocols and sequencing platforms for 16S rRNA community profiling. BMC Genomics. 17:1–20. https://doi.org/10.1186/s12864-015-2194-9

Danscher, A. M., S. Li, P. H. Andersen, E. Khafipour, N. B. Kristensen, and J. C. Plaizier. 2015. Indicators of induced subacute ruminal acidosis (SARA) in Danish Holstein cows. Acta Vet. Scand. 57:1–14. https://doi.org/10.1186/s13028-015-0128-9

Delosière, M., J. Pires, L. Bernard, I. Cassar-Malek, and M. Bonnet. 2019. Milk proteome from in silico data aggregation allows the identification of putative biomarkers of negative energy balance in dairy cows. Sci. Rep. 9:1–11.

Deusch, S., A. Camarinha-Silva, J. Conrad, U. Beifuss, M. Rodehutscord, and J. Seifert. 2017. A structural and functional elucidation of the rumen microbiome influenced by various diets and microenvironments. Front. Microbiol. 8:1605. https://doi.org/10.3389/fmicb.2017.01605

Dirksen, G. U., H. G. Liebich, and E. Mayer. 1985. Adaptive changes of the ruminal mucosa and their functional and clinical significance. Bov. Pract. (Stillwater). 116–120.

Dobson, M. J., W. C. B. Brown, A. Dobson, and A. T. Phillipson. 1956. A histological study of the organization of the rumen epithelium of sheep. Q. J. Exp. Physiol. 41:247–253. https://doi.org/10.1113/expphysiol.1956.sp001186

Dong, G., S. Liu, Y. Wu, C. Lei, J. Zhou, and S. Zhang. 2011. Diet-induced bacterial immunogens in the gastrointestinal tract of dairy cows: impacts on immunity and metabolism. Acta Vet. Scand. 53:1–7. https://doi.org/10.1186/1751-0147-53-48

Dong, H., S. Wang, Y. Jia, Y. Ni, Y. Zhang, S. Zhuang, X. Shen, and R. Zhao. 2013. Long-term effects of subacute ruminal acidosis (SARA) on milk quality and hepatic gene expression in lactating goats fed a high-concentrate diet. PLoS One. 8:850.

Eckersall, P. D., F. J. Young, A. M. Nolan, C. H. Knight, C. McComb, M. M. Waterston, C. J. Hogarth, E. M. Scott, and J. L. Fitzpatrick. 2006. Acute phase proteins in bovine milk in an experimental model of Staphylococcus aureus subclinical mastitis. J. Dairy Sci. 89:1488–1501. https://doi.org/10.3168/jds.S0022-0302(06)72216-0

Enemark, J. M. D., R. J. Jorgensen, and P. S. Enemark. 2002. Rumen acidosis with special emphasis on diagnostic aspects of subclinical rumen acidosis: a review. Vet. ir Zootech. 20:16–29.

Etschmann, B., A. Suplie, and H. Martens. 2009. Change of ruminal sodium transport in sheep during dietary adaptation. Arch. Anim. Nutr. 63:26–38. https://doi.org/10.1080/17450390802506885

Ferraretto, L. F., P. M. Crump, and R. D. Shaver. 2013. Effect of cereal grain type and corn grain harvesting and processing methods on intake, digestion, and milk production by dairy cows through a meta-analysis. J. Dairy Sci. 96:533–550. https://doi.org/10.3168/jds.2012-5932

Flint, H. J., and E. A. Bayer. 2008. Plant cell wall breakdown by anaerobic microorganisms from the mammalian digestive tract. Ann. N. Y. Acad. Sci. 1125:280–288. https://doi.org/10.1196/annals.1419.022

Fox, P. F., and A. Brodkorb. 2008. The casein micelle: Historical aspects, current concepts and significance. Int. Dairy J. 18:677–684. https://doi.org/10.1016/j.idairyj.2008.03.002

Galfi, P., S. Neogrady, and T. Sakata. 1991. Effects of volatile fatty acids on the epithelial cell proliferation of the digestive tract and its hormonal mediation. Elsevier. https://doi.org/10.1016/B978-0-12-702290-1.50010-2

Gao, X., and M. Oba. 2015. Non-invasive indicators to identify lactating dairy cows with a greater risk of subacute rumen acidosis. J. Dairy Sci. 98:5735–5739. https://doi.org/10.3168/jds.2015-9456

Gao, X., and M. Oba. 2016. Effect of increasing dietary nonfiber carbohydrate with starch, sucrose, or lactose on rumen fermentation and productivity of lactating dairy cows. J. Dairy Sci. 99:291–300. https://doi.org/10.3168/jds.2015-9871

Garcia, M., B. J. Bradford, and T. G. Nagaraja. 2017. Invited review: ruminal microbes, microbial products, and systemic inflammation. Prof. Anim. Sci. 33:635–650. https://doi.org/10.15232/pas.2017-01663

Gholizadeh, M., J. Fayazi, H. Zali, and Y. Asgari. 2020. Transcriptomic changes in the rumen epithelium of cattle after the induction of acidosis. Arch. Razi Inst. 75:109.

Giuberti, G., A. Gallo, F. Masoero, L. F. Ferraretto, P. C. Hoffman, and R. D. Shaver. 2014. Factors affecting starch utilization in large animal food production system: A review. Starch-Stärke. 66:72–90. https://doi.org/10.1002/star.201300177

Goering, H. K. 1970. Forage Fiber Analyses (Apparatus, Reagents, Procedures, and Some Applications). US Agricultural Research Service.

Gozho, G. N., D. O. Krause, and J. C. Plaizier. 2007. Ruminal lipopolysaccharide concentration and inflammatory response during grain-induced subacute ruminal acidosis in dairy cows. J. Dairy Sci. 90:856–866. https://doi.org/10.3168/jds.S0022-0302(07)71569-2

Graham, C., and N. L. Simmons. 2005. Functional organization of the bovine rumen epithelium. Am. J. Physiol. Regul. 288:R173–R181. https://doi.org/10.1152/ajpregu.00425.2004

Grant, R. 2010. Forage fragility, fiber digestibility, and chewing response in dairy cattle. Pages 27–40 in Proceedings of the 19th Annual Tri-State Dairy Nutrition Conference, Grand Wayne Center, Fort Wayne, Indiana, USA, 20-21 April, 2010. Purdue University Press.

Grant, R., W. Smith, and M. Miller. 2020. Relationships between fibre digestibility and particle size for lactating dairy cows. Adv. Dairy Technol. 32:47–57.

Greco, G., F. Hagen, S. Meibner, Z. Shen, Z. Lu, S. Amasheh, and J. R. Aschenbach. 2018. Effect of individual SCFA on the epithelial barrier of sheep rumen under physiological and acidotic luminal pH conditions. J. Anim. Sci. 96:126–142. https://doi.org/10.1093/jas/skx017

Guo, Y., X. Xu, Y. Zou, Z. Yang, S. Li, and Z. Cao. 2013. Changes in feed intake, nutrient digestion, plasma metabolites, and oxidative stress parameters in dairy cows with subacute ruminal acidosis and its regulation with pelleted beet pulp. J. Anim. Sci. Biotechnol. 4:1–10. https://doi.org/10.1186/2049-1891-4-31

Hart, E. H., C. J. Creevey, T. Hitch, and A. H. Kingston-Smith. 2018. Meta-proteomics of rumen microbiota indicates niche compartmentalisation and functional dominance in a limited number of metabolic pathways between abundant bacteria. Sci. Rep. 8:1–11. https://doi.org/10.1038/s41598-018-28827-7

Henderson, G., F. Cox, S. Ganesh, A. Jonker, W. Young, and P. H. Janssen. 2015. Rumen microbial community composition varies with diet and host, but a core microbiome is found across a wide geographical range. Sci. Rep. 5:1–15. https://doi.org/10.1038/srep14567

Hernández, J., J. L. Benedito, A. Abuelo, and C. Castillo. 2014. Ruminal acidosis in feedlot: from aetiology to prevention. Sci. World J. 2014. https://doi.org/10.1155/2014/702572

Hettinga, K., H. van Valenberg, S. de Vries, S. Boeren, T. van Hooijdonk, J. van Arendonk, and J. Vervoort. 2011. The host defense proteome of human and bovine milk. PLoS One. 6:e19433. https://doi.org/10.1371/journal.pone.0019433

Hofmann, R. R. 1989. Evolutionary steps of ecophysiological adaptation and diversification of ruminants: a comparative view of their digestive system. Oecologia. 78:443–457. https://doi.org/10.1007/BF00378733

Honan, M. C., and S. L. Greenwood. 2020. Characterization of variations within the rumen metaproteome of Holstein dairy cattle relative to morning feed offering. Sci. Rep. 10:1–8. https://doi.org/10.1038/s41598-020-59974-5

Huhtanen, P., J. Nousiainen, and M. Rinne. 2006. Recent developments in forage evaluation with special reference to practical applications.

Humer, E., J. R. Aschenbach, V. Neubauer, I. Kröger, R. Khiaosa-Ard, W. Baumgartner, and Q. Zebeli. 2018. Signals for identifying cows at risk of subacute ruminal acidosis in dairy veterinary practice. J. Anim. Physiol. Anim. Nutr. (Berl). 102:380–392. https://doi.org/10.1111/jpn.12850

Huntington, G. B. 1997. Starch utilization by ruminants: from basics to the bunk. J. Anim. Sci. 75:852–867. https://doi.org/10.2527/1997.753852x

Hussein, H. A., J.-P. Thurmann, and R. Staufenbiel. 2020. 24-h variations of blood serum metabolites in high yielding dairy cows and calves. BMC Vet. Res. 16:1–11. https://doi.org/10.1186/s12917-020-02551-9

Huws, S. A., C. J. Creevey, L. B. Oyama, I. Mizrahi, S. E. Denman, M. Popova, R. Muñoz-Tamayo, E. Forano, S. M. Waters, and M. Hess. 2018. Addressing global ruminant agricultural challenges through understanding the rumen microbiome: past, present, and future. Front. Microbiol. 9:2161. https://doi.org/10.3389/fmicb.2018.02161

Huws, S. A., J. E. Edwards, C. J. Creevey, P. Rees Stevens, W. Lin, S. E. Girdwood, J. A. Pachebat, and A. H. Kingston-Smith. 2016. Temporal dynamics of the metabolically active rumen bacteria colonizing fresh perennial ryegrass. FEMS Microbiol. Ecol. 92:137. https://doi.org/10.1093/femsec/fiv137

Isaac, N. I., D. Philippe, A. Nicholas, D. Raoult, and C. Eric. 2019. Metaproteomics of the human gut microbiota: challenges and contributions to other OMICS. Clin. Mass Spectrom. 14:18–30. https://doi.org/10.1016/j.clinms.2019.06.001

Jami, E., and I. Mizrahi. 2012. Composition and similarity of bovine rumen microbiota across individual animals. PLoS One. 7:33306. https://doi.org/10.1371/journal.pone.0033306

Jing, L., L. Dewanckele, B. Vlaeminck, W. M. van Straalen, A. Koopmans, and V. Fievez. 2018. Susceptibility of dairy cows to subacute ruminal acidosis is reflected in milk fatty acid proportions, with C18: 1 trans-10 as primary and C15: 0 and C18: 1 trans-11 as secondary indicators. J. Dairy Sci. 101:9827–9840. https://doi.org/10.3168/jds.2018-14903

Josefsen, T. D., T. H. Aagnes, and S. D. Mathiesen. 1996. Influence of diet on the morphology of the ruminal papillae in reindeer calves (*Rangifer tarandus tarandus* L.). Rangifer. 16:119–128. https://doi.org/10.7557/2.16.3.1205

Kennelly, J. J., B. Robinson, and G. R. Khorasani. 1999. Influence of carbohydrate source and buffer on rumen fermentation characteristics, milk yield, and milk composition in early-lactation Holstein cows. J. Dairy Sci. 82:2486–2496. https://doi.org/10.3168/jds.S0022-0302(99)75500-1

Kern, R. J., A. K. Lindholm-Perry, H. C. Freetly, W. M. Snelling, J. W. Kern, J. W. Keele, J. R. Miles, A. P. Foote, W. T. Oliver, and L. A. Kuehn. 2016. Transcriptome differences in the rumen of beef steers with variation in feed intake and gain. Gene. 586:12–26. https://doi.org/10.1016/j.gene.2016.03.034

Khafipour, E., D. O. Krause, and J. C. Plaizier. 2009a. Alfalfa pellet-induced subacute ruminal acidosis in dairy cows increases bacterial endotoxin in the rumen without causing inflammation. J. Dairy Sci. 92:1712–1724. https://doi.org/10.3168/jds.2008-1656

Khafipour, E., S. Li, J. C. Plaizier, and D. O. Krause. 2009b. Rumen microbiome composition determined using two nutritional models of subacute ruminal acidosis. Appl. Environ. Microbiol. 75:7115–7124. https://doi.org/10.1128/AEM.00739-09

Kim, M., and Z. Yu. 2014. Variations in 16S rRNA-based microbiome profiling between pyrosequencing runs and between pyrosequencing facilities. J. Microbiol. 52:355–365. https://doi.org/10.1007/s12275-014-3443-3

Kittelmann, S., M. R. Kirk, A. Jonker, A. McCulloch, and P. H. Janssen. 2015. Buccal swabbing as a non-invasive method to determine bacterial, archaeal, and eukaryotic microbial community structures in the rumen. Appl. Environ. Microbiol. 81:7470–7483. https://doi.org/10.1128/AEM.02385-15

Kleen, J. L., G. A. Hooijer, J. Rehage, and J. Noordhuizen. 2003. Subacute ruminal acidosis (SARA): a review. J. Vet. Med. Series A. 50:406–414. https://doi.org/10.1046/j.1439-0442.2003.00569.x

Kleen, J. L., L. Upgang, and J. Rehage. 2013. Prevalence and consequences of subacute ruminal acidosis in German dairy herds. Acta Vet. Scand. 55:1–6.

Klevenhusen, F., M. Hollmann, L. Podstatzky-Lichtenstein, R. Krametter-Frötscher, J. R. Aschenbach, and Q. Zebeli. 2013. Feeding barley grain-rich diets altered electrophysiological properties and permeability of the ruminal wall in a goat model. J. Dairy Sci. 96:2293–2302. https://doi.org/10.3168/jds.2012-6187

de Koster, J., M. Salavati, C. Grelet, M. A. Crowe, E. Matthews, R. O'Flaherty, G. Opsomer, L. Foldager, and M. Hostens. 2019. Prediction of metabolic clusters in early-lactation dairy cows using models based on milk biomarkers. J. Dairy Sci. 102:2631–2644. https://doi.org/10.3168/jds.2018-15533

Krause, D. O., S. E. Denman, R. I. Mackie, M. Morrison, A. L. Rae, G. T. Attwood, and C.S. McSweeney. 2003. Opportunities to improve fiber degradation in the rumen: microbiology, ecology, and genomics. FEMS Microbiol. Rev. 27:663–693. https://doi.org/10.1016/S0168-6445(03)00072-X

Kristensen, N. B., A. Danfaer, and N. Agergaard. 1998. Absorption and metabolism of short-chain fatty acids in ruminants. Arch. Anim. Nutr. 51:165–175. https://doi.org/10.1080/17450399809381916

Lengowski, M. B., K. H. R. Zuber, M. Witzig, J. Möhring, J. Boguhn, and M. Rodehutscord. 2016. Changes in rumen microbial community composition during adaption to an in vitro system and the impact of different forages. PLoS One. 11:e0150115. https://doi.org/10.1371/journal.pone.0150115

Li, S., G. N. Gozho, N. Gakhar, E. Khafipour, D. O. Krause, and J. C. Plaizier. 2012. Evaluation of diagnostic measures for subacute ruminal acidosis in dairy cows. Can. J. Anim. Sci. 92:353–364. https://doi.org/10.4141/cjas2012-004

Lima, R. F., J. C. Resende Júnior, S. F. Costa, J. L. P. Daniel, T. S. Teófilo, and M. G. Cardoso. 2015. Morphological response of the ruminal and omasal mucosae to the variation in diet energy. Cienc. e Agrotecnologia. 39:574–582. https://doi.org/10.1590/S1413-70542015000600004

Lindmark-Månsson, H., C. Bränning, G. Alden, and M. Paulsson. 2006. Relationship between somatic cell count, individual leukocyte populations and milk components in bovine udder quarter milk. Int. Dairy J. 16:717–727. https://doi.org/10.1016/j.idairyj.2005.07.003

Liu, J., T. Xu, Y. Liu, W. Zhu, and S. Mao. 2013. A high-grain diet causes massive disruption of ruminal epithelial tight junctions in goats. Am. J. Physiol. Regul. 305:R232–R241. https://doi.org/10.1152/ajpregu.00068.2013

Liu, J., M. Zhang, R. Zhang, W. Zhu, and S. Mao. 2016. Comparative studies of the composition of bacterial microbiota associated with the ruminal content, ruminal epithelium and in the faeces of lactating dairy cows. Microb. Biotechnol. 9:257–268. https://doi.org/10.1111/1751-7915.12345

Lopes, J. C., R. D. Shaver, P. C. Hoffman, M. S. Akins, S. J. Bertics, H. Gencoglu, and J. G. Coors. 2009. Type of corn endosperm influences nutrient digestibility in lactating dairy cows. J. Dairy Sci. 92:4541–4548. https://doi.org/10.3168/jds.2009-2090

Ma, N., J. A. Abaker, G. Wei, H. Chen, X. Shen, and G. Chang. 2022. A high-concentrate diet induces an inflammatory response and oxidative stress and depresses milk fat synthesis in the mammary gland of dairy cows. J. Dairy Sci. 105:5493–5505. https://doi.org/10.3168/jds.2021-21066

Madureira, A. R., C. I. Pereira, A. M. P. Gomes, M. E. Pintado, and F. X. Malcata. 2007. Bovine whey proteins–Overview on their main biological properties. Food Res. Int. 40:1197–1211. https://doi.org/10.1016/j.foodres.2007.07.005

Malekkhahi, M., A. M. Tahmasbi, A. A. Naserian, M. Danesh-Mesgaran, J. L. Kleen, O. AlZahal, and M. H. Ghaffari. 2016. Effects of supplementation of active dried yeast and malate during sub-acute ruminal acidosis on rumen fermentation, microbial population, selected blood metabolites, and milk production in dairy cows. Anim. Feed Sci. Technol. 213:29–43. https://doi.org/10.1016/j.anifeedsci.2015.12.018

Martin, C., and A. M. Smith. 1995. Starch biosynthesis. Plant Cell. 7:971. https://doi.org/10.1105%2Ftpc.7.7.971

McCann, J. C., T. A. Wickersham, and J. J. Loor. 2014. High-throughput methods redefine the rumen microbiome and its relationship with nutrition and metabolism. Bioinform. Biol. Insights. 8:BBI-S15389. https://doi.org/10.4137/BBI.S15389

McSweeney, C., and R. Mackie. 2012. Commission on genetic resources for food and agriculture. Micro-organisms and ruminant digestion: State of knowledge, trends and future prospects. Background Study Paper (FAO). 61:1–62.

Meissner, S., F. Hagen, C. Deiner, D. Günzel, G. Greco, Z. Shen, and J. R. Aschenbach. 2017. Key role of short-chain fatty acids in epithelial barrier failure during ruminal acidosis. J. Dairy Sci. 100:6662–6675. https://doi.org/10.3168/jds.2016-12262

Mentschel, J., R. Leiser, C. Mülling, C. Pfarrer, and R. Claus. 2001. Butyric acid stimulates rumen mucosa development in the calf mainly by a reduction of apoptosis. Arch. Anim. Nutr. 55:85–102. https://doi.org/10.1080/17450390109386185

Mizrahi, I. 2013. Rumen symbioses. Springer-Verlag Berlin Heidelberg. https://doi.org/10.1007/978-3-642-30194-0_1

Morar, D., C. Văduva, A. Morar, M. Imre, C. Tulcan, and K. Imre. 2022. Paraclinical Changes Occurring in Dairy Cows with Spontaneous Subacute Ruminal Acidosis under Field Conditions. Animals. 12:2466.

Morgavi, D. P., E. Forano, C. Martin, and C. J. Newbold. 2010. Microbial ecosystem and methanogenesis in ruminants. Animals. 4:1024–1036. https://doi.org/10.1017/S1751731110000546

Morgavi, D. P., E. Rathahao-Paris, M. Popova, J. Boccard, K. F. Nielsen, and H. Boudra. 2015. Rumen microbial communities influence metabolic phenotypes in lambs. Front. Microbiol. 6:1060. https://doi.org/10.3389/fmicb.2015.01060

Nielsen, T. S., K. Sejrsen, H. R. Andersen, P. Lund, and E. M. Straarup. 2004. Effect of silage type and energy concentration on conjugated linoleic acid (CLA) in milk fat from dairy cows. J. Anim. Feed Sci. 13:697–700.

Nissen, A., E. Bendixen, K. L. Ingvartsen, and C. M. Røntved. 2013. Expanding the bovine milk proteome through extensive fractionation. J. Dairy Sci. 96:7854–7866. https://doi.org/10.3168/jds.2013-7106

Nocek, J. E. 1997. Bovine acidosis: Implications on laminitis. J. Dairy Sci. 80:1005–1028.

Nocek, J. E., and J. Russell. 1988. Protein and energy as an integrated system. Relationship of ruminal protein and carbohydrate availability to microbial synthesis and milk production. J. Dairy Sci. 71:2070–2107. https://doi.org/10.3168/jds.S0022-0302(97)76026-0

Oba, M., and M. S. Allen. 2003a. Dose-response effects of intrauminal infusion of propionate on feeding behavior of lactating cows in early or midlactation. J. Dairy Sci. 86:2922–2931. https://doi.org/10.3168/jds.S0022-0302(03)73889-2

Oba, M., and M. S. Allen. 2003b. Intraruminal infusion of propionate alters feeding behavior and decreases energy intake of lactating dairy cows. J. Nutr. 133:c–1099. https://doi.org/10.1093/jn/133.4.1094

Oetzel, G. R. 2004. Monitoring and testing dairy herds for metabolic disease. Vet. Clin. North Am. Food Anim. 20:651–674. https://doi.org/10.1016/j.cvfa.2004.06.006

Ogunade, I., A. Pech-Cervantes, and H. Schweickart. 2019. Metatranscriptomic analysis of sub-acute ruminal acidosis in beef cattle. Animals. 9:232. https://doi.org/10.3390/ani9050232

Orpin, C. G., and K. N. Joblin. 1997. The rumen anaerobic fungi. Springer.

Overton, T. R., J. A. A. McArt, and D. v Nydam. 2017. A 100-Year Review: Metabolic health indicators and management of dairy cattle. J. Dairy Sci. 100:10398–10417. https://doi.org/10.3168/jds.2017-13054

Parker, R., and S. G. Ring. 2001. Aspects of the physical chemistry of starch. J. Cereal Sci. 34:1–17. https://doi.org/10.1006/jcrs.2000.0402

Penner, G. B. 2014. Mechanisms of volatile fatty acid absorption and metabolism and maintenance of a stable rumen environment. Pages 92–104 in 25th Florida Ruminant Nutrition Symposium.

Petri, R. M., T. Schwaiger, G. B. Penner, K. A. Beauchemin, R. J. Forster, J. J. McKinnon, and T. A. McAllister. 2013. Characterization of the core rumen microbiome in cattle during transition from forage to concentrate as well as during and after an acidotic challenge. PLoS One. 8:e83424. https://doi.org/10.1371/journal.pone.0083424

Philippeau, C., J. Landry, and B. Michalet-Doreau. 2000. Influence of the protein distribution of maize endosperm on ruminal starch degradability. J. Sci. Food Agric. 80:404–408. https://doi.org/10.1002/1097-0010(200002)80:3%3C404::AID-JSFA541%3E3.0.CO;2-Z

Pilachai, R., J. T. Schonewille, C. Thamrongyoswittayakul, S. Aiumlamai, C. Wachirapakorn, H. Everts, and W.H. Hendriks. 2012. Starch source in high concentrate rations does not affect rumen pH, histamine and lipopolysaccharide concentrations in dairy cows. Livest. Sci. 150:135–142. https://doi.org/10.1016/j.livsci.2012.08.009

Plaizier, J. C., D. O. Krause, G. N. Gozho, and B. W. McBride. 2008a. Subacute ruminal acidosis in dairy cows: the physiological causes, incidence and consequences. Vet. J. 176:21–31. https://doi.org/10.1016/j.tvjl.2007.12.016

Pollock, J., L. Glendinning, T. Wisedchanwet, and M. Watson. 2018. The madness of microbiome: attempting to find consensus “best practice” for 16S microbiome studies. Appl. Environ. Microbiol. 84:e02627-17. https://doi.org/10.1128/AEM.02627-17

Poppi, D. P., R. E. Hendricksen, and D. J. Minson. 1985. The relative resistance to escape of leaf and stem particles from the rumen of cattle and sheep. J. Agric. Sci. 105:9–14. https://doi.org/10.1017/S0021859600055623

Puppel, K., M. Gołębiewski, J. Slósarz, G. Grodkowski, P. Solarczyk, P. Kostusiak, K. Grodkowska, M. Balcerak, and T. Sakowski. 2021. Interaction between the level of immunoglobulins and number of somatic cells as a factor shaping the immunomodulating properties of colostrum. Sci. Rep. 11:1–9. https://doi.org/10.1038/s41598-021-95283-1

Rajendhran, J., and P. Gunasekaran. 2011. Microbial phylogeny and diversity: small subunit ribosomal RNA sequence analysis and beyond. Microbiol. Res. 166:99–110. https://doi.org/10.1016/j.micres.2010.02.003

Reinhardt, T. A., and J. D. Lippolis. 2006. Bovine milk fat globule membrane proteome. J. Dairy Res. 73:406–416. https://doi.org/10.1017/S0022029906001889

Sadet-Bourgeteau, S., C. Martin, and D. P. Morgavi. 2010. Bacterial diversity dynamics in rumen epithelium of wethers fed forage and mixed concentrate forage diets. Vet. Microbiol. 146:98–104. https://doi.org/10.1016/j.vetmic.2010.04.029

Santana, Á. L., and M. A. A. Meireles. 2014. New starches are the trend for industry applications: a review. Food Public Health. 4:229–241.

Schiebenhoefer, H., T. van den Bossche, S. Fuchs, B. Y. Renard, T. Muth, and L. Martens. 2019. Challenges and promise at the interface of metaproteomics and genomics: an overview of recent progress in metaproteogenomic data analysis. Expert Rev. Proteomics. 16:375–390. https://doi.org/10.1080/14789450.2019.1609944

Schloss, P. D., M. L. Jenior, C. C. Koumpouras, S. L. Westcott, and S. K. Highlander. 2016. Sequencing 16S rRNA gene fragments using the PacBio SMRT DNA sequencing system. Peer J. 4:e1869. https://doi.org/10.7717/peerj.1869

Schwartzkopf-Genswein, K. S., K. A. Beauchemin, D. J. Gibb, D. H. Crews Jr, D. D. Hickman, M. Streeter, and T.A. McAllister. 2003. Effect of bunk management on feeding behavior, ruminal acidosis and performance of feedlot cattle: A review. J. Anim. Sci. 81:E149–E158. https://doi.org/10.2527/2003.8114_suppl_2E149x

Skillman, L. C., P. N. Evans, C. Strömpl, and K. N. Joblin. 2006. 16S rDNA directed PCR primers and detection of methanogens in the bovine rumen. Lett. Appl. Microbiol. 42:222–228. https://doi.org/10.1111/j.1472-765X.2005.01833.x

Smith, W. A. 2019. Relationships between Undigested and Physically Effective Fiber in Lactating Dairy Cow Diets. The University of Vermont and State Agricultural College.

Smolenski, G., S. Haines, F. Y.-S. Kwan, J. Bond, V. Farr, S. R. Davis, K. Stelwagen, and T. T. Wheeler. 2007. Characterisation of host defence proteins in milk using a proteomic approach. J. Proteome Res. 6:207–215. https://doi.org/10.1021/pr0603405

Snelling, T. J., and R. J. Wallace. 2017. The rumen microbial metaproteome as revealed by SDS-PAGE. BMC Microbiol. 17:1–10. https://doi.org/10.1186/s12866-016-0917-y

Sniffen, C. J., J. D. O'connor, P. J. van Soest, D. G. Fox, and J. B. Russell. 1992. A net carbohydrate and protein system for evaluating cattle diets: II. Carbohydrate and protein availability. J. Anim. Sci. 70:3562–3577. https://doi.org/10.2527/1992.70113578x

Soergel, D. A. W., N. Dey, R. Knight, and S. E. Brenner. 2012. Selection of primers for optimal taxonomic classification of environmental 16S rRNA gene sequences. ISME J. 6:1440–1444. https://doi.org/10.1038/ismej.2011.208

van Soest, P. J. 1994. Nutritional Ecology of the Ruminant. Cornell university press.

Solano, J., F. Galindo, A. Orihuela, and C. S. Galina. 2004. The effect of social rank on the physiological response during repeated stressful handling in Zebu cattle (*Bos indicus*). Physiol. Behav. 82:679–683. https://doi.org/10.1016/j.physbeh.2004.06.005

Steele, M. A., J. Croom, M. Kahler, O. AlZahal, S. E. Hook, K. Plaizier, and B. W. McBride. 2011. Bovine rumen epithelium undergoes rapid structural adaptations during grain-induced subacute ruminal acidosis. Am. J. Physiol. Regul. 300:R1515–R1523. https://doi.org/10.1152/ajpregu.00120.2010

Stefańska, B., J. Komisarek, and W. Nowak. 2020. Noninvasive indicators associated with subacute ruminal acidosis in dairy cows. Ann. Anim. Sci. 20:1325–1338.

Steijns, J. M., and A. C. M. van Hooijdonk. 2000. Occurrence, structure, biochemical properties and technological characteristics of lactoferrin. Br. J. Nutr. 84:11–17. https://doi.org/10.1017/S0007114500002191

Sterk, A., B. E. O. Johansson, H. Z. H. Taweel, M. Murphy, A. M. van Vuuren, W. H. Hendriks, and J. Dijkstra. 2011. Effects of forage type, forage to concentrate ratio, and crushed linseed supplementation on milk fatty acid profile in lactating dairy cows. J. Dairy Sci. 94:6078–6091. https://doi.org/10.3168/jds.2011-4617

Stevenson, D. M., and P. J. Weimer. 2007. Dominance of Prevotella and low abundance of classical ruminal bacterial species in the bovine rumen revealed by relative quantification real-time PCR. Appl. Microbiol. Biotechnol. 75:165–174. https://doi.org/10.1007/s00253-006-0802-y

Stevnebø, A., S. Sahlström, and B. Svihus. 2006. Starch structure and degree of starch hydrolysis of small and large starch granules from barley varieties with varying amylose content. Anim. Feed Sci. Technol. 130:23–38. https://doi.org/10.1016/j.anifeedsci.2006.01.015

Stone, W. C. 1999. The effect of subclinical rumen acidosis on milk components. Page. Proceedings Cornell Nutrition Conference For Feed Manufacturers.

Sun, Y. Z., S. Y. Mao, and W. Y. Zhu. 2010. Rumen chemical and bacterial changes during stepwise adaptation to a high-concentrate diet in goats. Animals. 4:210–217. https://doi.org/10.1017/S175173110999111X

Tacoma, R., J. Fields, D. B. Ebenstein, Y. W. Lam, and S. L. Greenwood. 2016. Characterization of the bovine milk proteome in early-lactation Holstein and Jersey breeds of dairy cows. J. Proteomics. 130:200–210. https://doi.org/10.1016/j.jprot.2015.09.024

Tajima, K., R. I. Aminov, T. Nagamine, H. Matsui, M. Nakamura, and Y. Benno. 2001. Diet-dependent shifts in the bacterial population of the rumen revealed with real-time PCR. Appl. Environ. Microbiol. 67:2766–2774. https://doi.org/10.1128/AEM.67.6.2766-2774.2001

Tajima, K., S. Arai, K. Ogata, T. Nagamine, H. Matsui, M. Nakamura, R. I. Aminov, and Y. Benno. 2000. Rumen bacterial community transition during adaptation to high-grain diet. Anaerobe. 6:273–284. https://doi.org/10.1006/anae.2000.0353

Thoetkiattikul, H., W. Mhuantong, T. Laothanachareon, S. Tangphatsornruang, V. Pattarajinda, L. Eurwilaichitr, and V. Champreda. 2013. Comparative analysis of microbial profiles in cow rumen fed with different dietary fiber by tagged 16S rRNA gene pyrosequencing. Curr. Microbiol. 67:130–137. https://doi.org/10.1007/s00284-013-0336-3

Toyoda, A., W. Iio, M. Mitsumori, and H. Minato. 2009. Isolation and identification of cellulose-binding proteins from sheep rumen contents. Appl. Environ. Microbiol. 75:1667–1673. https://doi.org/10.1128/AEM.01838-08

Woolpert, M. E., H.M. Dann, K. W. Cotanch, C. Melilli, L. E. Chase, R. J. Grant, and D. M. Barbano. 2016. Management, nutrition, and lactation performance are related to bulk tank milk de novo fatty acid concentration on northeastern US dairy farms. J. Dairy Sci. 99:8486–8497.

Woolpert, M. E., H. M. Dann, K. W. Cotanch, C. Melilli, L. E. Chase, R. J. Grant, and D. M. Barbano. 2017. Management practices, physically effective fiber, and ether extract are related to bulk tank milk de novo fatty acid concentration on Holstein dairy farms. J. Dairy Sci. 100:5097–5106.

Vlaeminck, B., V. Fievez, D. Demeyer, and R. J. Dewhurst. 2006. Effect of forage: concentrate ratio on fatty acid composition of rumen bacteria isolated from ruminal and duodenal digesta. J. Dairy Sci. 89:2668–2678. https://doi.org/10.3168/jds.S0022-0302(06)72343-8

Wada, Y., and B. Lönnerdal. 2014. Bioactive peptides derived from human milk proteins—mechanisms of action. J. Nutr. Biochem. 25:503–514. https://doi.org/10.1016/j.jnutbio.2013.10.012

Wallace, R. J., J. A. Rooke, N. McKain, C. A. Duthie, J. J. Hyslop, D. W. Ross, A. Waterhouse, M. Watson, and R. Roehe. 2015. The rumen microbial metagenome associated with high methane production in cattle. BMC Genomics. 16:1–14. https://doi.org/10.1186/s12864-015-2032-0

Weimer, P. J. 2015. Redundancy, resilience, and host specificity of the ruminal microbiota: implications for engineering improved ruminal fermentations. Front. Microbiol. 6:296. https://doi.org/10.3389/fmicb.2015.00296

White, B. A., I. K. O. Cann, S. A. Kocherginskaya, R. I. Aminov, L. A. Thill, R. I. Mackie, and R. Onodera. 1999. Molecular analysis of Archaea, Bacteria and Eucarya communities in the rumen-review. Asian-Australas J. Anim. Sci. 12:129–138. https://doi.org/10.5713/ajas.1999.129

Whitford, M. F., R. J. Forster, C. E. Beard, J. Gong, and R. M. Teather. 1998. Phylogenetic analysis of rumen bacteria by comparative sequence analysis of cloned 16S rRNA genesß. Anaerobe 4:153–163. https://doi.org/10.1006/anae.1998.0155

Williams, A. G., and G. S. Coleman. 1997. The rumen protozoa. Springer. https://doi.org/10.1007/978-94-009-1453-7_3

Winter, K. A., and D. P. Collins. 1987. Fibrosity index as an estimate of forage digestibility. Can. J. Plant Sci. 67:445–449. https://doi.org/10.4141/cjps87-063

Wirth, R., G. Kádár, B. Kakuk, G. Maróti, Z. Bagi, Á. Szilágyi, G. Rákhely, J. Horváth, and K. L. Kovács. 2018. The planktonic core microbiome and core functions in the cattle rumen by next generation sequencing. Front. Microbiol. 9:2285. https://doi.org/10.3389/fmicb.2018.02285

Xu, C., T. Shen, W. Yang, H. Yu, S. Gao, and B. Huang. 2016. The effect of subacute ruminal acidosis of dairy cows on productivity, digestibility and greenhouse gas emission. J. Agric. Sci. 8:92. http://dx.doi.org/10.5539/jas.v8n4p9

Yáñez-Ruiz, D. R., B. Macías, E. Pinloche, and C. J. Newbold. 2010. The persistence of bacterial and methanogenic archaeal communities residing in the rumen of young lambs. FEMS Microbiol. Ecol. 72:272–278. https://doi.org/10.1111/j.1574-6941.2010.00852.x

Yang, W. Z., K. A. Beauchemin, and L. M. Rode. 2000. Effects of barley grain processing on extent of digestion and milk production of lactating cows. J. Dairy Sci. 83:554–568. https://doi.org/10.3168/jds.S0022-0302(00)74915-0

Zebeli, Q., J. Dijkstra, M. Tafaj, H. Steingass, B. N. Ametaj, and W. Drochner. 2008. Modeling the adequacy of dietary fiber in dairy cows based on the responses of ruminal pH and milk fat production to composition of the diet. J. Dairy Sci. 91:2046–2066. https://doi.org/10.3168/jds.2007-0572

Zebeli, Q., M. Tafaj, H. Steingass, B. Metzler, and W. Drochner. 2006. Effects of physically effective fiber on digestive processes and milk fat content in early lactating dairy cows fed total mixed rations. J. Dairy Sci. 89:651–668. https://doi.org/10.3168/jds.S0022-0302(06)72129-4

Zhan, K., T. Y. Yang, Y. Chen, M. C. Jiang, and G. Q. Zhao. 2020. Propionate enhances the expression of key genes involved in the gluconeogenic pathway in bovine intestinal epithelial cells. J. Dairy Sci. 103:5514–5524. https://doi.org/10.3168/jds.2019-17309

Zhao, M., D. Bu, J. Wang, X. Zhou, D. Zhu, T. Zhang, J. Niu, and L. Ma. 2016. Milk production and composition responds to dietary neutral detergent fiber and starch ratio in dairy cows. Anim. Sci. J. 87:756–766. https://doi.org/10.1111/asj.12482

CHAPTER 2: IMPACT OF DIETARY CARBOHYDRATE PROFILE ON THE DAIRY COW RUMEN META-PROTEOME

2.1 Abstract

Diet starch and fiber content influence the rumen microbial profile and its fermentation products, yet there is no information about the impact of these dietary carbohydrate fractions on the metabolic activity of these microbes. The objective of this experiment was to evaluate the effects of dietary carbohydrate profile changes on the rumen meta-proteome profile. Eight cannulated Holstein cows were assigned to the study as part of a 4 x 4 Latin square design with a 2 x 2 factorial treatment arrangement including four 28-d periods. Cows received one of four dietary treatments on a dry matter (DM) basis. Diets included different concentrations of rumen fermentable starch (RFS) and physically effective undigested NDF (peuNDF240) content in the diet: 1) low peuNDF240, low RFS (LNLS), 2) high peuNDF240, low RFS (HNLS), 3) low peuNDF240, high RFS (LNHS), and 4) high peuNDF240, high RFS (HNHS). Rumen fluid samples were collected from each cow on the last two days of each period at three-time points (0600, 1000, and 1400 h). The microbial protein fraction was isolated, isobarically labeled and analyzed using liquid chromatography combined with tandem mass spectrometry techniques. Product ion spectra were searched using the SEQUEST search on Proteome Discoverer 2.4 against 71 curated microbe-specific databases. Data were analyzed using PROC MIXED procedure in SAS 9.4. A total of 138 proteins were characterized across 26 of the searched microbial species. In total, 46 proteins were affected by treatments across 17 of the searched microbial species. Of these 46 proteins, 28 were affected by RFS content across 13

microbial species, with 20 proteins having higher abundance with higher dietary RFS and 8 proteins having higher abundance with lower dietary RFS. The majority of these proteins have roles in energetics, carbon metabolism, and protein synthesis. Examples include pyruvate, phosphate dikinase (*Ruminococcus albus* SY3), 30S ribosomal protein S11 (*Clostridium aminophilum*), and methyl-coenzyme M reductase subunit alpha (*Methanobrevibacter ruminantium* strain 35063), which had higher abundances with higher dietary RFS. Conversely, glutamate dehydrogenase (*Butyrivibrio fibrisolvens*) and 50S ribosomal protein L5 (*Pseudobutyrivibrio ruminis*) and L15 (*Ruminococcus bromii*) had lower abundances with higher dietary RFS content. Among the remaining 18 proteins unaffected by RFS content alone, five proteins were impacted by peuNDF240 content, and 13 were affected by peuNDF240 × RFS interactions. Our results suggest that the RFS content of the diet may have a greater influence on rumen microbial protein abundances than dietary peuNDF240 content or peuNDF240 × RFS interactions. This research highlights that dietary carbohydrate profile changes can impact rumen microbial protein abundances. Further research is needed to fully characterize the impact of diet on the rumen meta-proteome and manipulate the various roles of rumen microbes. This will aid in designing strategies to maximize nutrient use efficiency in the rumen.

2.2 Introduction

Carbohydrates form the basis of a ruminant's diet and are necessary for synthesizing body tissues and animal products (McDonald, 2002). As carbohydrates are the primary nutrient in ruminant diets, they directly impact rumen microbial populations. In vitro and in vivo studies support the suggestion that the availability of carbohydrates in the rumen is

the critical factor controlling the energy availability for rumen microbes (Koenig et al., 2003; Zhang et al., 2015). Availability directly depends on the type of carbohydrate fraction and structure present, which, in turn, influences ruminal fermentation kinetics and dynamics (Villalba et al., 2006). While starch is a readily fermentable source of energy for rumen microbes and is a crucial component to support the energetic demands of high-yielding dairy cows, the dietary NDF and its physical characteristics, such as particle size and digestibility, are the main factors responsible for ruminal health and DMI regulation (Conrad et al., 1964). Physically effective NDF (**peNDF**) and the NDF fraction undigested after a 240-h in vitro fermentation (**uNDF240**) are essential indicators of rumen function and health. Smith (2019) proposed a method to combine fiber's physical and chemical nature into a single measurement, termed physically effective uNDF240 (**peuNDF240**). Further, the author reported that the inclusion of peuNDF240 within ration characterization further identifies pertinent fiber fractions and their impact on rumen function. Formulating rations with an optimal balance between NDF fractions and rumen fermentable starch (**RFS**) is critical to optimize digestion, nutrient utilization, and productivity.

Previous studies have investigated the effect of the dietary content of fiber and starch on the rumen microbial profile and activity via meta-genomic and meta-transcriptomic approaches (Thoetkiattikul et al., 2013; Ogunade et al., 2019). The results of these studies reported that feeding a high fiber diet increased the abundance of *Firmicutes* while feeding a high starch diet resulted in an increased abundance of *Bacteroidetes* and enriched the genes related to carbohydrate, amino acid, energy, vitamin, and cofactor metabolism pathways. While these results identify potential impacts of dietary carbohydrates on the rumen microbial profiles, they do not identify the specific fiber or

starch fractions being modified. Additionally, many rumen microbes have multiple functions and niches; the results of the above studies do not reflect specific microbial activity, as transcript abundance does not necessarily correlate to protein expression.

Identifying and quantifying proteins from rumen microbial communities will lead to meaningful complementary information characterizing the metabolic activity of rumen microbes in response to different diets. This information is critical for further optimization of rumen function and improvement of nutrient use efficiency. This could be achieved using meta-proteomics, an analytical approach that supports the characterization of the entire protein complement within the microbial environment (Hart et al., 2018) and provides a snapshot of microbial activity at a given point in time. Although proteomics technologies are not without limitations, the use of this omics approach can expand characterization and biological understanding. Limitations of the meta-proteomics approach include: 1) limited available databases for protein identification, 2) high false discovery rate from the use of large databases, and 3) search engine sensitivity (Andersen et al., 2001; Isaac et al., 2019). However, with advanced sensitivity and accuracy in mass spectrometry analysis and the development of proteomics software platforms, the meta-proteomics approach is a useful tool to develop a deeper insight into the functional and taxonomic interplay of proteins in complex microbial communities and its implication on animal health and the environment (Schiebenhoefer et al., 2019). Previous research by Snelling and Wallace (2017) and Hart et al. (2018) provided the first glimpses of microbe-specific proteins in the rumen using gel-based proteomic techniques. Recent modifications by Honan and Greenwood (2020) eliminated the use of gels to expand the breadth of proteins identified in the rumen meta-proteome. This modified approach was applied in

this study as a tool to characterize shifts in the meta-proteome in response to the dietary carbohydrate profile changes. We hypothesized that dietary carbohydrate profile changes would impact the abundance of proteins associated with energetics and protein synthesis-associated pathways in cellulolytic and amylolytic microbes because of changes in the availability of primary substrates for their growth and production. As there was little published information exploring the impact of dietary carbohydrate profile changes on the rumen microbial meta-proteome profile, this study aims to evaluate the effects of varying concentrations of dietary RFS and peuNDF240 content on the rumen microbial protein abundances in Holstein dairy cows using non-gel-based proteomic techniques.

2.3 Materials and Methods

2.3.1 Animals and Experimental Design

Samples analyzed in this experiment were collected from a larger study conducted at the William H. Miner Agricultural Research Institute (Chazy, NY) from July 2019 to September 2019. Experimental procedures were conducted as per protocol approved by the William H. Miner Agricultural Research Institute Animal Care and Use Committee. Eight ruminally-cannulated lactating Holstein cows (85 + 15 DIM) were included in a 4×4 Latin square experiment with a 2 x 2 factorial treatment design consisting of four 28-d periods. Cows were paired randomly at the beginning of each period and assigned randomly to one of four dietary treatments (DM basis) of different concentrations of RFS and peuNDF240 content in the diet. Each cow was exposed to each dietary treatment once. Blinding was not used. Dietary treatments were as follows: 1) low peuNDF240, low RFS (6.35 % of DM,16.7 % of DM; **LNLS**), 2) high peuNDF240, low RFS (8.60 % of DM,16.7 % of

DM; **HNLS**), 3) low peuNDF240, high RFS (6.7 % of DM,19.2 % of DM; **LNHS**), and 4) (8.00 % of DM,19.2 % of DM; **HNHS**). Dietary crude protein (**CP**; as % of DM) of the LNLS, HNLS, LNHS and HNHS diets were 16.1 %, 16.0 %, 15.3 % and 15.2 %, respectively. The complete list of diet ingredients, chemical composition, and particle size distribution, as outlined by Smith (2021), can be found in the supplementary file (Supplementary Tables S1 and S2; https://data.mendeley.com/datasets/bv3y4ffnc6/1). Briefly, different concentrations of peuNDF240 were achieved through inclusion of either brown midrib-3 or conventional corn silages, and the different concentrations of RFS were achieved with different inclusion amounts of corn meal. Diet peuNDF240 was calculated by multiplying the physically effective factor by the uNDF240 organic matter (uNDF240om) content of the diet that was retained on the ≥1.18 mm sieve. The RFS of the diet was calculated by multiplying the starch digestibility measured at 7-h by the starch content of the diet. Smith (2021) reported that total tract digestibility of NDF was higher with the low peuNDF240 diets compared with feeding a high peuNDF240 diet. Smith (2021) also observed that there was no effect of dietary treatments of peuNDF240 or RFS, or their interaction, on DMI, rumen fermentation profiles, or rumen pH.

2.3.2 Rumen Fluid Sampling

Rumen fluid samples for this experiment were collected from each cow on d 27 (1400 h) and d 28 (0600 h and 1000 h) of each period. Two samples from one cow during the second period (0600 h and 1000 h) and eight samples from period four (1000 h) were not available for analysis. At each of the three sampling time points, rumen fluid samples were collected from three locations in the mid-ventral ruminal sac of each cow and

composited within the time point within the cow as previously described (Steele et al., 2012). Samples (n=1 sample/cow/time point) were flash-frozen immediately after each collection using a dry-ice ethanol bath, transported on dry ice to the laboratory and stored at -80 °C until processing.

2.3.3 Protein Extraction from Rumen Fluid

Frozen rumen fluid samples (n = 96) were thawed overnight at 4 °C. Once thawed, samples were strained through four layers of cheesecloth (Lion Services Inc., Charlotte, NC) to separate coarse fibers. Samples were then pooled within the cow within the period across the three points, creating one composite sample per cow per period (n=32 samples). A universal control (**UC**) was generated by pooling equal volumes of rumen fluid from each cow from each time point across the four periods. The samples and UC were then centrifuged at 16,000 x g for 20 min at 4 °C to collect the pellet.

The collected pellets were processed as Honan and Greenwood (2020) described. Briefly, RIPA lysis buffer containing protease inhibitor (Pierce Protease Inhibitor Mini Tablets, Thermo Scientific, Rockford, IL) and a 5 mm stainless steel bead (Qiagen, Hilden, Germany) were added to collected pellets. Samples were homogenized (TissueLyser II, Qiagen) at 30 Hz for 30 sec followed by a 3 min incubation on ice, and this homogenization/incubation process was repeated for a total of six repetitions. The resulting homogenate samples were then precipitated by adding a 6 M trichloroacetic acid/80 mM dithiothreitol (**DTT**) solution at a 1:3 protein extract ratio. The samples were then vortexed and incubated overnight at 4°C. Following the overnight incubation, samples were vortexed and centrifuged at 16,000 x g for 20 min at 4°C. Pellets were washed twice with

ice-cold 20 % dimethyl sulfoxide in acetone and twice with were homogenized (TissueLyser II, Qiagen) at 30 Hz for 30 sec followed by a 3 min incubation on ice, and this homogenization/incubation process Following the overnight incubation, samples were vortexed and centrifuged at 16,000 x *g* for 20 min at 4°C. Pellets were washed twice with ice-cold 20 % dimethyl sulfoxide in acetone and twice with 100 % ice-cold acetone. Precipitated pellets were air-dried and resuspended in phosphate-buffered saline. The total protein extract concentrations were quantified using a bicinchoninic acid assay kit (Pierce, Rockford, IL).

2.3.4 Tandem Mass Tag (TMT) Peptide Labeling

Tandem mass tag peptide labeling (an isobaric label) was performed as per manufacturer instructions (Thermo Scientific). Briefly, 72 μg of protein from each sample was aliquoted, and the volume of each sample was normalized to 100 μL with 100 mM triethylammonium bicarbonate (**TEAB**). Samples were then reduced with 0.5 mM of DTT for 60 min at 37 °C followed by iodoacetamide alkylation in the dark for 30 min. Trypsin was then added at a 1:50 (w/w) ratio and the samples were digested overnight at 37°C. Dissolved TMT reagents were added to the digested samples and incubated for 1 hr, subsequently quenched with 8 μL of 5% hydroxylamine. Multiplexes were created by combining equal volumes (100 μL) of a random subset of individual TMT-labeled samples (a maximum of 9 experimental samples per multiplex) + 1 aliquot of UC per plex. A 100 μL aliquot from each plex (total 5 plexes) was dried to remove TEAB. Peptides were then fractionated using a high pH reversed-phase peptide fractionation kit (Thermo Scientific) as per kit instructions resulting in eight fractions for each plex. Fractionated plex samples

were submitted to The Vermont Biomedical Research Network Proteomics Facility (The University of Vermont, Burlington, VT) for liquid chromatography-tandem mass spectrometry **(LC-MS/MS**).

2.3.5 LC-MS/MS Analysis

Protein identification and quantification were performed on a Q-Exactive Plus MS coupled to an EASY-nLC 1200 (Thermo Scientific), similar to the workflow described by Honan and Greenwood (2020). Briefly, the fractionated peptide samples were dissolved in 10 µL of 2.5% formic acid (**FA**) and 2.5% acetonitrile (**ACH**) in water and then loaded onto a 100 µm x 500 mm capillary column packed with Halo C18 (2.7 µm particle size, 90 nm pore size, Michrom Bioresources, CA, USA) at a flow rate of 300 nL/min. The column end was laser pulled to a ~3 µm orifice and packed with a minimal amount of 5µm MAGIC C18AQ before packing with the 3-µm particle size chromatographic materials. Solvent gradient conditions were as follows: 2.5 to 35% of ACH/0.1% FA for 60 min and increase from 35 to 100% ACH /0.1% FA in 1 min and then 100% ACH /0.1% FA for 4 min, an immediate return to 2.5% ACH /0.1% FA, and a final hold at 2.5% ACH/0.1% FA. Peptides were introduced into the MS via a nanospray ionization source with a spray voltage of 2.0 kV. Full MS scans were acquired in a data-dependent "Top 10" acquisition mode with lock mass function activated (m/z 371.1012). The scans were acquired in the mass range of 300-1,600 m/z with a mass resolution of 70,000, and the AGC target value was set at $1e^6$. The top ten intense peaks in MS were fragmented with higher-energy collisional dissociation of 10. The LC-MS/MS spectra were obtained at a 35,000 resolution, with an AGC target

of $1e^5$ and a maximum injection time of 100 ms. Dynamic exclusion was enabled (peptide match: preferred; exclude isotopes: on; underfill ratio: 1%).

2.3.6 Data Analysis

Product ion spectra were searched using the SEQUEST search engine with percolator node (false discovery rate to less than 1%) on Proteome Discoverer 2.4 (Thermo Scientific) against 71 composite databases downloaded on September 12, 2020, from UniProt. Methionine oxidation (+15.995 Da) and TMT10plex modification on N-termini and lysine (+229.163 Da) were chosen as variable modifications, and cysteine alkylation by iodoacetamide was selected as a fixed modification. Precursor mass ion tolerance was defined at + 10 ppm and fragment mass ion tolerance at + 0.02 Da. The protease was specified as trypsin with two maximum missing cleavages. The TMT labeled peptides were quantified with the Reporter Ions Quantifier node in the consensus workflow, and parameters were specified as follows: unique, and razor peptides were used for quantification; Reject Quan results with missing channels and apply Quan value corrections were set as false; Co-Isolation Threshold value was set as 50; Average Reporter S/N Threshold was 10; "Total Peptide Amount" was used for normalization and Scaling Mode was set "on Control Averages," so that the peptide abundances in the UC labels were set as 100 and the abundances in other channels were scaled accordingly. The scaled abundance values of the samples were used for further statistical analyses. For protein identification, 71 microbial composite proteome databases were manually selected for peptide comparison searches in SEQUEST. Microbes to be included in this analysis were selected because of their known prevalence in the rumen, and their involvement in rumen

microbial carbohydrate metabolism. The SEQUEST engine then comparatively searched protein/peptide masses detected in the sample against the selected 71 composite proteome databases by statistical matching to identify proteins, their microorganism and strain source. For any proteins identified as uncharacterized, the FASTA sequence was retrieved from UniProt (http://www.uniprot.org/) and searched through the Basic Local Alignment Search Tool (BLAST; http://blast.ncbi.nlm.nih.gov/Blast.cgi). The top hit protein was selected as an identified protein if the hit was 100% matched with the searched query. A mixed procedure model of SAS 9.4 (SAS Institute, Cary, NC) was performed, including peuNDF240, RFS, peuNDF240 × RFS interactions, replicate and cow(replicate) as the fixed effects and cow as the random effect. The impact of diet on protein abundance was considered significant if $P < 0.05$.

2.4 Results

In this study, the meta-proteomic analysis identified 138 proteins labeled in all samples across 26 of the searched microbial species (Supplementary Table S3; https://data.mendeley.com/datasets/bv3y4ffnc6/1). The following microbes and their strains were identified: *Prevotella ruminicola*, *Prevotella ruminicola* strain *ATCC 19189*, *Prevotella bryantii*, *Ruminococcus albus 8*, *Ruminococcus albus* strain *27210*, *Ruminococcus albus* strain *SY3*, *Ruminococcus bromii*, *Butyrivibrio hungatei*, *Prevotella aff. Ruminicola Tc2-24*, *Methanobrevibacter ruminantium* strain *35063*, *Eubacterium cellulosolvens* 6, *Ruminococcus flavefaciens*, *Pseudobutyrivibrio ruminis*, *Selenomonas ruminantium*, *Eubacterium ruminantium*, *Fibrobacter succinogenes* strain *ATCC 19169*, *Treponema bryantii*, *Pseudobacteroides cellulosolvens ATCC 35603*, *Clostridium*

aminophilum, *Oxalobacter formigenes HOxBLS*, *Megasphaera elsdenii DSM 20460*, *Treponema saccharophilum*, *Butyrivibrio fibrisolvens*, *Butyrivibrio proteoclasticus* strain *ATCC 51982*, *Selenomonas ruminantium subsp lacilytica* strain *NBRC 103574*, and *Methanosarcina barkeri*. The diet treatments affected 46 proteins across 17 of the searched microbial species. Of these 46 proteins, 28 proteins were impacted by RFS content, 5 were affected by peuNDF240 content, and 13 were affected by peuNDF240 × RFS interactions.

2.4.1 Microbial Protein Profile Affected by RFS Content in the Diet

Dietary RFS content affected 28 microbial proteins (63% of affected proteins; Table 2.1), with 20 proteins having higher abundance with higher dietary RFS and 8 proteins having higher abundance with lower dietary RFS. These proteins were associated with 13 searched microbial species; *P. ruminicola*, *P. ruminicola* strain *ATCC 19189*, *P. aff. Ruminicola Tc2-24*, *R. albus SY3*, *M. ruminantium* strain 35063, *B. fibrisolvens*, *B. hungatei*, *R. albus 8*, *C. aminophilum*, *P. cellulosolvens ATCC 35603*, *P. ruminis*, *E. cellulosolvens 6*, and *R. bromii*.

2.4.2 Microbial Protein Profile Affected by peuNDF240 Content in the Diet

Of the 138 proteins identified in this experiment, only 5 microbial proteins were affected by peuNDF240 content (Table 2.2), with 4 proteins having higher abundance with higher dietary peuNDF240 and 1 protein having higher abundance with lower dietary peuNDF240. These proteins originated from 3 microbial species: Pyruvate, phosphate dikinase, and sn-glycerol-3-phosphate ABC transporter ATP-binding protein UgpC from *R. bromii*, 30s ribosomal protein S5 from *Ruminococcus sp*., and acyl-CoA dehydrogenase from *E. cellulosolvens* 6 had higher abundances with higher dietary peuNDF240 content.

Conversely, 30s ribosomal protein S16 from *P. ruminicola* had a lower abundance with higher dietary peuNDF240 content.

2.4.3 Microbial Protein Profile Affected by peuNDF240 × RFS Interactions in the Diet

Thirteen microbial proteins were affected by the peuNDF240 × RFS interactions (Table 2.3). These proteins were associated with 10 searched microbial species; *C. aminophilum, R. bromii, P. ruminicola, T. bryantii, P. bryantii, P. ruminis, S. ruminantium, B. fibrisolvens, Prevotella sp.,* and *P. ruminicola strain ATCC 19189*.

2.5 Discussion

In the present study, not surprisingly, higher numbers of proteins were identified from microbial genera that are more completely cataloged in the available databases. Additionally, many proteins were identified across multiple species, likely resulting from conserved sequences or similar functional roles. The five proteins most highly identified across microbial species were elongation factor Tu, 30S and 50S ribosomal proteins, GAPDH and glutamate dehydrogenase (**GDH**). These results were not surprising given that elongation factor Tu accounts for 5 to 10% of total cell protein (Weijland et al., 1992), and ribosomal proteins account for 20% of bacterial dry weight (Russell, 2002). In line with these observations, Hart et al. (2018) reported elongation factor Tu, GAPDH, and GDH as all being in the top 25 most abundant proteins found within the bovine rumen. Similarly, Honan and Greenwood (2020) reported that elongation Tu and ribosomal proteins were widely represented proteins across the microbial species characterized in their study. Given the importance of GAPDH in glycolysis and GDH's essential role in

enabling ammonia assimilation within the rumen and microbial protein synthesis (Wallace et al., 1997), the high prevalence of these proteins is also not surprising.

2.5.1 Impact of Diet on the Rumen Meta-proteome

The altered dietary carbohydrate profile affected the abundance of 46 microbial proteins in the present study, representing 33% of identified proteins. Not surprisingly, most of these proteins were functionally associated with energetics (Figure 2.1), protein biosynthesis, and carbon metabolism pathways, but interestingly, many of these proteins were primarily associated with *Prevotella*. At the ingredient level, a previous rumen meta-proteomic study reported that the abundances of proteins assigned to the *Prevotellaceae* family were not affected by the provision of different feedstuffs, including comparisons of corn silage vs. grass silage vs. grass hay fed to Jersey cows (Deusch et al., 2017). However, studies have reported a shift in the abundance of *Prevotella* in response to diet nutrient profiles. For example, Zhang et al. (2014) reported that primary dietary forage sources affected the abundance the *Prevotella*. In their study, intake of an alfalfa diet increased the proportion of the *Prevotella* genera compared with the proportion observed in cows fed a corn-stalk diet. Additionally, Thoetkiattikul et al. (2013) and Zeng et al. (2019) reported an increased abundance of *Prevotella* in cows fed a high starch diet. These differences might be due to changes in nutrient profile, as *Prevotella* can utilize a range of carbohydrates, from simple mono- or oligo- saccharides to complex plant polysaccharides such as pectins, mannans, starch, and hemicelluloses (Matsui et al., 2000; Miyazaki et al., 1997).

2.5.2 Influence of RFS Content on Rumen Meta-proteome

Rumen fermentable starch content had a much greater impact on the characterized rumen meta-proteome compared with peuNDF240. In the current study, 28 proteins, representing 63% of affected proteins, were affected due to RFS content. Many of these proteins were associated with 1) energetics, 2) carbon metabolism, and 3) protein biosynthesis pathways.

Glyceraldehyde-3-phosphate dehydrogenase is involved in oxidative phosphorylation of D-glyceraldehyde-3-phosphate to 1,3-bisphosphate-D-glycerate (Ferri et al., 1978), a central step in glycolysis. *B. hungatei* GAPDH abundance was higher with lower dietary RFS content, which is not unexpected, given that *B. hungatei* is a secondary degrader species that utilizes fiber degradation as substrates for their growth (Kopečný et al., 2003). *P. ruminicola* GAPDH abundance was higher with lower dietary RFS content. In contrast, *P. ruminicola* pyruvate: ferredoxin (flavodoxin) oxidoreductase (**PFOR**) was higher with higher dietary RFS content. Oxidative decarboxylation of pyruvate to form acetyl-coenzyme A is catalyzed by PFOR, a crucial step in many metabolic pathways. The shift in the abundance of *P. ruminicola*'s GAPDH and PFOR may be part of *P. ruminicola*'s versatile behavior in response to different dietary substrates available in the rumen. As *Prevotella* constitutes one of the most predominant genera in the rumen, with major roles in carbohydrate metabolism, further research is needed to explore the regulation of carbohydrate metabolism associated protein in *Prevotella* in response to different dietary substrate availability and their concentrations.

The abundances of phosphoglycerate kinase (**PGK**), pyruvate phosphate dikinase (**PPDK**), and (**TPI**) from *R. albus* were higher in response to higher dietary RFS content.

Phosphoglycerate kinase and anaerobic PPDK are involved in glycolysis and gluconeogenesis pathways. Phosphoglycerate kinase catalyzes the reversible interconversion of 1,3-bisphosphoglycerate and 3-bisphosphoglycerate. Anaerobic PPDK catalyzes the reversible reactions from phosphoenolpyruvate to pyruvate (Chastain et al., 2011). The increase in abundance of these proteins from *R. albus* with high dietary RFS content may indicate an increase in the rate of gluconeogenesis as *R. albus* utilizes cellulose as their primary substrate for growth in the rumen, though this was not validated in the current trial. To support this suggestion, we observed the abundance of TPI, a gluconeogenic protein responsible for catalyzing the interconversion of dihydroxyacetone phosphate to D-glyceraldehyde- 3-phosphate, was higher with higher dietary RFS. Transketolase (**TK**), an enzyme involved in the pentose phosphate pathway of carbohydrate metabolism, is an alternative branch of glycolysis used to produce the sugars that form DNA and RNA (Appel and Parrot, 1970). An increase in the abundance of TK with higher dietary RFS may indicate that *P.aff. ruminicola* utilizes starch as the primary substrate for their growth. The higher abundance of PGK from *P.aff. ruminicola* with higher dietary RFS content further supports the species growth with high RFS content. However, these postulated impacts of RFS on *P.aff. ruminicola* require further investigation for validation.

We also observed a higher abundance of *P. ruminicola* succinate dehydrogenase (**SDH**) with higher RFS content. Succinate dehydrogenase catalyzes the synthesis of fumarate from succinate, which is required for both aerobic and anaerobic growth. The higher abundance of this protein from *P. ruminicola* with a higher RFS fraction in the diet is in agreement with the previous observation that *Bacteroides* use the succinate pathway

for growth (Macy and Probst, 1979). Glutamate dehydrogenase from *B. fibrisolvens* was lower with higher dietary RFS content, whereas GDH from *P.aff. ruminicola* was lower with lower dietary RFS content. Given that GDH is thought to be a major ammonia assimilatory enzyme in the rumen, our results agree with the premise that GDH activity is repressed when rumen bacteria are grown under the glucose limiting condition (Pengpeng and Tan, 2013). *B. fibrisolvens* utilize fiber as their primary substrate for growth, whereas *P.aff. ruminicola* uses starch as their primary substrate for growth.

In this study, the higher abundance of 30s ribosomal proteins S1, S5, S3, and 50s ribosomal protein L22 from *P. ruminicola* in response to higher dietary RFS suggests increased *P. ruminicola* protein synthesis. An increase in the abundance of 50S ribosomal protein L1 from *R. bromii* with lower dietary RFS content may indicate an increase in microbial biomass with a lower fraction RFS diet, though shifts in biomass were not measured in our current study. It may be because of increased NDF digestibility due to low RFS content in the diet, as *R. bromii* relies on dietary NDF as a substrate to support their growth. To support the possible explanation of increased NDF digestibility due to low RFS content in the diet, Smith (2021) reported that higher RFS diets had to tendency to result in lower NDF digestibility. Further, Ferraretto et al. (2013) observed a decrease in rumen NDF degradability with an increase in dietary starch content. *P. ruminis* is a fibrolytic bacterium, and Asma et al. (2013) reported a decrease in the abundance of *P. ruminis* with high starch diets. An increase in the abundance of 50s ribosomal protein L5 from *P. ruminis* with lower RFS was not unexpected, but an increase in the abundance of glycine-tRNA ligase with higher RFS content was not expected. The glycine-tRNA ligase catalyzes an amino acid's attachment to its cognate tRNA molecules and is consequently vital for

consequent protein biosynthesis (Kaiser et al., 2020). Previously, Huws et al. (2020) reported that *Pseudobutyrivibrio* species contain an abundance of carbohydrate-active enzyme isoforms that facilitate metabolic plasticity and resilience under dietary perturbations. Thus, the observed increase of glycine-tRNA ligase abundance with higher dietary RFS content may result from their metabolic plasticity and resilience characteristics under dietary perturbations.

An increase in the abundance of 30s ribosomal protein S11 from *C. aminophilum* with higher dietary RFS content was observed. Because *C. aminophilum* is an obligatory amino acid fermenting bacterium in the rumen, this could indicate that protein synthesis is increasing with high RFS fraction diets. While increased abundance could be due to increased concentration of microbial metabolites in the rumen environment, particularly amino acids, and peptides, because of high starch digestibility, this causal relationship is speculative and requires validation. The enzyme D-3-phosphoglycerate dehydrogenase catalyzes the first step in the L-serine biosynthetic pathway by converting D-3-phosphoglycerate, an intermediate metabolite in glycolysis, to phosphohydroxypyruvate (Grant, 2018). A higher D-3-phosphoglycerate dehydrogenase protein abundance from *P.aff. ruminicola* in response to higher dietary RFS content may indicate protein synthesis is likely increasing with a high diet RFS inclusion. An increased abundance of *P.aff. ruminicola* DNA-directed RNA polymerase subunit alpha with higher dietary RFS content further supports our suggestion that total protein synthesis by *P.aff. ruminicola* may be increasing in response to a higher dietary RFS content. A higher abundance of *E. cellulosolvens* 6 polyribonucleotide nucleotidyl transferase with higher dietary RFS content may indicate that protein synthesis is likely decreasing as polyribonucleotide

nucleotidyl transferase is involved in mRNA degradation. This was not surprising as *E. cellulosolvens* 6 is a fibrolytic bacterium. An increased abundance of polyribonucleotide nucleotidyl transferase may have occurred because *E. cellulosolvens* 6 prioritized their functions to low energy requiring pathways rather than replication due to limited substrate availability with a higher dietary RFS content diet. Also supportive of the suggestion of shifts in protein synthesis was our observation of a higher abundance of *P. cellulosolvens ATCC 35603* heat shock chaperone protein DnaK with lower dietary RFS content, as molecular chaperones exist inside cells as families of diverse molecular mass proteins (e.g., 90, 70, 60, and 30 kDa) that involve folding and refolding proteins to prevent denaturation.

In the present study, higher abundances of methanogenesis-associated proteins (5,10-methylenetetrahydromethanopterin reductase and Methyl-coenzyme M reductase subunit alpha -component of methyl-coenzyme M reductase (**McrI**)) from *M. ruminantium* were observed with higher dietary RFS content. While methane measurements were not collected in the current trial, known relationships could provide some insight into this observation. Specifically, the abundance of *M. ruminantium* is typically related to low methane production (Danielsson et al., 2017; Danielsson et al., 2012). Methyl-CoM reductase exists in two isomeric forms, McrI and McrII, with McrI expressed at low hydrogen concentrations and McrII being expressed at high hydrogen concentrations (Reeve et al., 1997). With past research identifying that *M. ruminantium* M1 does not code for McrII (Leahy et al., 2010), Danielsson et al. (2017) speculated that *M. ruminantium* might be unable to scavenge hydrogen for methanogenesis in an environment with higher hydrogen concentrations, which may also be the explanation for our finding.

The increased abundance of McrI and 5,10-methylenetetrahydromethanopterin reductase from *M. ruminantium* likely occurred because increased starch content favors propionate production, thus reducing hydrogen production and methanogenic substrate availability (Hassanat et al., 2013; Pirondini et al., 2015; Rooke et al., 2014). This study further supports the suggestion that the activity of *M. ruminantium* is associated with low methane production.

2.5.3 Influence of peuNDF240 on the Rumen Meta-proteome

In the present study, we observed a shift in the abundance of PPDK from *R. bromii* in response to peuNDF240 content in the diet, indicating a relationship between *R. bromii* and dietary fiber shifts. In line with our observation, *R. bromii* has historically been considered fibrolytic in its activity (Deng et al., 2007). An increased abundance of 30s ribosomal protein S16 from *Ruminococcus sps.* in cows fed higher dietary peuNDF240 content suggests that protein synthesis could be increasing; however, this was not directly measured or validated in the current study. This may indicate that *Ruminococcus sps*., growth is likely increasing with the higher dietary peuNDF240 content due to an increase in the availability of NDF for fermentation, likely resulting from an increased rumen NDF retention rate.

A higher abundance of acyl-CoA dehydrogenase from *E. ruminantium* was also observed with higher dietary peuNDF240 content. This enzyme catalyzes the first step of fatty acids β-oxidation, and the rate of fatty acid oxidation is high during fasting but low in the fed animal (Schulz, 2013). *E. ruminantium* is a primary cellulolytic bacterium; therefore, an increase in abundance of acyl-CoA dehydrogenase from *E. ruminantium* with

higher dietary peuNDF240 content may be a result of shifting NDF degradability, as high uNDF240 diets have less NDF degradability, which may have ultimately limited the substrate availability for *E. ruminantium* fermentation. As only five proteins were affected by peuNDF240, it appears that 1) the peuNDF240 contents were too similar across diets in the current study to create a microbial activity response, 2) the response variables other than protein abundance, for example, enzymatic rate, may be the more appropriate variables to assess when studying the impact of uNDF240 on microbial metabolism, or 3) other microbes not included in this characterization may need to be considered in future studies.

2.5.4 Influence of peuNDF240 × RFS Interactions on Rumen Meta-proteome

Thirteen microbial proteins were affected by the interaction of peuNDF240 × RFS and are associated with carbohydrate metabolism and protein biosynthesis pathways. Some interactive effects are not unexpected, as studies have shown that peNDF interacts with the starch degradation kinetics, modifying the response of ruminal fermentation and performance in dairy cows. For example, Zebeli et al. (2008) reported that the passage rate of rumen degradable starch was accelerated from the reticulorumen when the peNDF content of the diet was increased. Additionally, Yang & Beauchemin (2006) have shown that feeding longer size fiber particles shifted the starch digestion from the rumen into the intestine, lowering the development of acidosis.

The function of phosphoenolpyruvate carboxykinase (**PEPCK**) is to catalyze oxaloacetate conversion to phosphoenolpyruvate as part of the gluconeogenesis pathway. A higher abundance of PEPCK from *S. ruminantium* in cows fed with the LNLS diet than those fed

the HNHS diet was observed. It may be because of a decreased substrate availability, and ultimately energy availability, associated with the LNLS diet, as *S. ruminantium* is an amylolytic bacteria. Supporting this observation, Asanuma and Hino et al. (2001) reported that the mRNA expression of PEPCK was inversely related to the sufficiency of energy in *S. ruminantium*, suggesting that PEPCK synthesis is regulated at the transcriptional level when energy supply was altered. A higher abundance of *P. bryantii* PFOR with HNHS and LNLS compared with the HNLS diet may indicate the species' growth with HNHS and LNLS diets. A higher abundance of acyl-CoA dehydrogenase from *B. fibrisolvens* in response to the HNHS diet compared with the HNLS and LNLS diet may be due to decreased primary substrate availability for energy production by *B. fibrisolvens*, as this is primarily a cellulolytic bacterium. Further research is required to confirm this postulated relationship.

The abundance of 30s ribosomal protein S3 from *R. bromii* was higher in response to the HNLS diet compared with the LNLS or HNHS diets. Additionally, the abundance of elongation factor from *R. bromii* was higher with HNLS compared with the LNLS diet. These observations may indicate that protein synthesis in *R. bromii* is increasing with the HNLS diet. While any shift in protein synthesis requires further validation, in support of this suggestion, we also observed an increased abundance of 50s ribosomal proteins L1 from *R. bromii* with the HNLS diet. The abundance of proteins related to protein biosynthesis, such as pseudouridine synthetase, 60 kDa chaperonin, and 30S ribosomal protein S12 from *P. ruminicola* was affected by peuNDF240 x RFS. However, the abundances were varied with no clear trend across treatments. This is somewhat expected, as *Prevotella* has a remarkable degree of genetic diversity (Purushe et al., 2010), therefore

can occupy various ecological niches within the rumen (Jami and Mizrahi, 2012). These observations also further support *P. ruminicola*'s metabolic versatility characteristic, enabling them to adapt to different dietary changes in the rumen.

2.6 Conclusion

In this experiment, we identified 138 rumen microbial proteins and the shifts in their abundance relative to peuNDF240 and the RFS content of the diet. Alteration of dietary carbohydrate profiles affected 46 proteins across 17 of the searched microbial species, mainly due to RFS content. Many of the proteins affected by diet have known functions related to energetics, protein biosynthesis, and carbon metabolism. This research demonstrates the breadth and specificity of shifts in the protein-mediated microbial activity in the rumen with altered carbohydrate substrate availability. Additionally, our results highlight the need to further examine and characterize the rumen meta-proteome in relation to the diet to improve our understanding of rumen microbial responsiveness. Furthermore, this is some of the first research that contributes to the identification of diet-directed mechanisms that impact the core microbial metabolic pathways and ruminant productivity using proteomic approaches.

Table 2.1. The rumen microbial protein abundances of Holstein dairy cows affected by high and low dietary concentrations of RFS.

Accession no.	Proteins	Species	HRFS[1]	LRFS[2]	*P* value
A0A1I6IX72	30s ribosomal protein S11	*[Clostridium] aminophilum*	139	107	0.001
I5AW29	Polyribonucleotide nucleotidyltransferase	*[Eubacterium] cellulosolvens*	102	90	0.024
A0A317G314	Glutamate dehydrogenase	*Butyrivibrio fibrisolvens*	93	103	0.016
A0A1G5DIH3	Glyceraldehyde-3-phosphate dehydrogenase	*Butyrivibrio hungatei*	77	95	0.001
D3E050	Methyl-coenzyme M reductase subunit alpha	*Methanobrevibacter ruminantium*	106	85	0.001
D3E1K9	5,10-methylenetetrahydromethanopterin reductase	*Methanobrevibacter ruminantium*	102	85	0.001
A0A1I0LYZ3	Transketolase	*Prevotella aff. ruminicola*	147	96	0.005
A0A1I0P5C6	Glutamate dehydrogenase	*Prevotella aff. ruminicola*	103	95	0.024
A0A1I0M5Y7	D-3-phosphoglycerate dehydrogenase	*Prevotella aff. ruminicola Tc2-24*	102	94	0.023
A0A1I0MM67	Phosphoglycerate kinase	*Prevotella aff. ruminicola Tc2-24*	86	65	0.032
A0A1I0P5I5	DNA-directed RNA polymerase subunit alpha	*Prevotella aff. ruminicola Tc2-24*	96	75	0.037
A0A1H5ULG9	Glyceraldehyde-3-phosphate dehydrogenase	*Prevotella ruminicola*	113	127	0.043
A0A1H5VSL2	Pyruvate-ferredoxin/flavodoxin oxidoreductase	*Prevotella ruminicola*	96	76	0.020
A0A1H5WM35	Elongation factor G	*Prevotella ruminicola*	108	122	0.011
A0A1H5WWH7	30s ribosomal protein S3	*Prevotella ruminicola*	98	81	0.025
A0A1M6U8F7	50s ribosomal protein L22	*Prevotella ruminicola*	93	84	0.014
A0A1M6U920	30s ribosomal protein S5	*Prevotella ruminicola*	110	99	0.024
UPI0008EEAC0D	30S ribosomal protein S1	*Prevotella ruminicola*	106	93	0.015
D5EX27	L-arabinose isomerase	*Prevotella ruminicola (strain ATCC 19189)*	114	87	0.002
D5EUX2	50s ribosomal protein L11	*Prevotella ruminicola (strain ATCC 19189)*	122	131	0.045

D5EWF4	Succinate dehydrogenase/fumarate reductase, flavoprotein subunit	*Prevotella ruminicola strain ATCC 19189*	117	94	0.007
A0A0L6JLZ7	Chaperone protein DnaK	*Pseudobacteroides cellulosolvens ATCC 35603*	63	97	0.001
A0A1H7FGA7	Glycine--tRNA ligase	*Pseudobutyrivibrio ruminis*	110	93	0.006
A0A2G3E9W1	50S ribosomal protein L5	*Pseudobutyrivibrio ruminis*	41	110	0.007
E9SA28	Triosephosphate isomerase	*Ruminococcus albus 8*	116	88	0.034
E9SBQ5	Phosphoglycerate kinase	*Ruminococcus albus 8*	122	86	0.006
A0A011V1T4	Pyruvate, phosphate dikinase	*Ruminococcus albus SY3*	98	86	0.018
A0A1G5IE59	50S ribosomal protein L15	*Ruminococcus bromii*	74	99	<0.001

[1]HRFS = High rumen fermentable starch
[2]LRFS = Low rumen fermentable starch

Table 2.2. The rumen microbial protein abundances of Holstein dairy cows affected by low and high dietary concentration of peuNDF240.

Accession no.	Proteins	Species	High peuNDF240[1]	Low peuNDF240[2]	*P* value
A0A1H5UBN2	30s ribosomal protein S16	*Prevotella ruminicola*	94	105.4	0.036
A0A1T4JZ88	Acyl-CoA dehydrogenase	*Eubacterium ruminantium*	135	108.0	0.013
A0A412UNB6	Pyruvate, phosphate dikinase	*Ruminococcus bromii*	102	91.3	0.005
A0A414DYV0	sn-glycerol-3-phosphate ABC transporter ATP-binding protein UgpC	*Ruminococcus bromii*	94	74.3	0.019
UPI00031FF12C	30s ribosomal protein S5	*Ruminococcus*	119	79.7	0.014

[1]High peuNDF240 = High physically effective undigested NDF after 240-h of in vitro fermentation
[2]Low peuNDF240 = Low physically effective undigested NDF after 240-h of in vitro fermentation

Table 2.3. The rumen microbial protein profile of Holstein dairy cows affected by different dietary concentration levels of peuNDF240 and RFS.

Accession no.	Proteins	Species	High peuNDF240[1]		Low peuNDF240[2]		*P* value
			HRFS[3]	LRFS[4]	HRFS[3]	LRFS[4]	
A0A1G5IDN6	30s ribosomal protein S3	*Ruminococcus bromii*	71^{b}	107^{a}	92^{ab}	79^{b}	<0.05
A0A1H5RLC4	Pseudouridine synthase	*Prevotella ruminicola*	85^{b}	104^{ab}	100^{b}	123^{a}	<0.05
A0A1H6GDE8	Phosphoenolpyruvate carboxykinase	*Selenomonas ruminantium*	74^{b}	81^{b}	80^{b}	104^{a}	<0.05
A0A1H9IAR9	Flagellin	*Treponema bryantii*	117^{a}	85^{b}	90^{ab}	87^{b}	<0.05
A0A1I0C755	ABC transporter substrate-binding protein	*[Clostridium]aminophilum*	101^{a}	91^{ab}	82^{b}	101^{a}	<0.05
A0A1M7JI43	30S ribosomal protein S12	*Ruminococcus flavefaciens*	70^{b}	104^{ab}	122^{a}	80 ^{ab}	<0.05
A0A2G3EDW8	GGGtGRT protein	*Pseudobutyrivibrio ruminis*	114^{ab}	124^{a}	99^{b}	113^{ab}	<0.05
A0A2N0UM52	50s ribosomal protein L1	*Ruminococcus bromii*	115^{b}	173^{a}	95^{b}	109^{b}	<0.05
A0A317G571	Acyl-CoA dehydrogenase	*Butyrivibrio fibrisolvens*	188^{a}	144^{b}	158 ^{ab}	117^{c}	<0.05
A0A412LBR6	Elongation factor	*Ruminococcus bromii*	124^{ab}	137^{a}	129^{ab}	109^{b}	<0.05
D5EWS5	60 kDa chaperonin	*Prevotella ruminicola (strain ATCC 19189)*	84^{b}	80^{b}	110^{a}	83^{b}	<0.05
UPI0001D0765C	30s ribosomal protein S12	*Prevotella*	73^{b}	95^{ab}	87^{b}	101^{a}	<0.05
UPI0001DB225B	ferredoxin oxidoreductase	*Prevotella bryantii*	106^{b}	80^{b}	101^{ab}	110^{a}	<0.05

$^{a–c}$Mean values in the same row with different superscripts differ ($P < 0.05$)
[1]High peuNDF240 = High physically effective undigested NDF after 240-h of in vitro fermentation
[2]Low peuNDF240 = Low physically effective undigested NDF after 240-h of in vitro fermentation
[3]HRFS = High rumen fermentable starch
[4]LRFS = Low rumen fermentable starch

Figure 2.1. Metabolic pathways involved in the degradation of carbohydrates in the rumen (adapted from Wirth et al., 2018, Russell, 2002). The proteins identified in this study are identified by a ■ Unidirectional arrows indicate that the protein catalyzes a reaction in one direction, while bidirectional arrows indicate that the protein can catalyze forward and reverse reactions. Abbreviations: TPI, triosephosphate isomerase; GAPDH, glyceraldehyde 3-phosphate dehydrogenase; TK, transketolase; PGK, phosphoglycerate kinase; PFOR, pyruvate ferredoxin oxidoreductase; PPDK, pyruvate phosphate dikinase; PEPCK, phosphenol pyruvate carboxy kinase; SDH, succinate dehydrogenase.

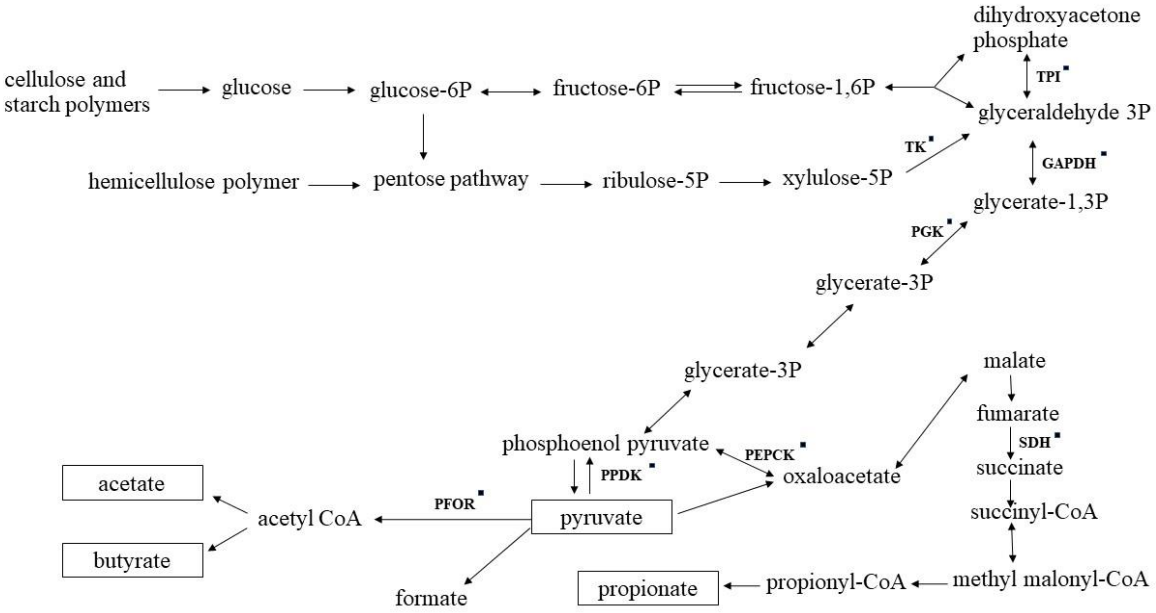

2.7 References

Andersen, T. O., B. J. Kunath, L. H. Hagen, M. O. Arntzen, and P. B. J. M. Pope. 2021. Rumen Metaproteomics: Closer to linking rumen microbial function to animal productivity traits. Methods. 186:42-51. https://doi.org/10.1016/j.clinms.2019.06.001.

Appel, S. H. and B. L. Parrot. 1970. Hexose monophosphate pathway in synapses. J. Neurochem. 17:1619-1626. https://doi.org/10.1111/j.1471-4159.1970.tb11386.x.

Asanuma, N. and T. Hino. 2001. Molecular characterization, enzyme properties and transcriptional regulation of phosphoenolpyruvate carboxykinase and pyruvate kinase in a ruminal bacterium, Selenomonas ruminantium. Microbiology. 147:681-690. https://doi.org/10.1099/00221287-147-3-681.

Asma, Z., C. Sylvie, C. Laurent, M. Jérôme, K. Christophe, B. Olivier, T. M. Annabelle, and E. Francis. 2013. Microbial ecology of the rumen evaluated by 454 GS FLX pyrosequencing is affected by starch and oil supplementation of diets. FEMS Microbiol. Ecol. 83:504-514. https://doi.org/10.1111/1574-6941.12011.

Chastain, C. J., C. J. Failing, L. Manandhar, M. A. Zimmerman, M. M. Lakner, and T. H. Nguyen. 2011. Functional evolution of C4 pyruvate, orthophosphate dikinase. J. Exp. Bot. 62:3083-3091. https://doi.org/10.1093/jxb/err058.

Conrad, H., A. D. Pratt, and J. W. Hibbs. 1964. Regulation of feed intake in dairy cows. I. Change in importance of physical and physiological factors with increasing digestibility. J. Dairy Sci. 47:54-62. https://doi.org/10.3168/jds.S0022-0302(64)88581-7.

Danielsson, R., J. Dicksved, L. Sun, H. Gonda, B. Müller, A. Schnürer, and J. Bertilsson. 2017. Methane production in dairy cows correlates with rumen methanogenic and bacterial community structure. Front. Microbiol. 8:226. https://doi.org/10.3389/fmicb.2017.00226.

Danielsson, R., A. Schnürer, V. Arthurson, and J. Bertilsson. 2012. Methanogenic population and CH4 production in Swedish dairy cows fed different levels of forage. Appl. Environ. Microbiol. 78:6172-6179. https://doi.org/10.1128/AEM.00675-12.

Deng, W., M. Wanapat, S. Ma, J. Chen, D. Xi, T. He, Z. Yang, and H. Mao. 2007. Phylogenetic analysis of 16S rDNA sequences manifest rumen bacterial diversity in gayals (Bos frontalis) fed fresh bamboo leaves and twigs (Sinarumdinaria). Asian-Australas. J. Anim. Sci. 20:1057-1066. https://doi.org/10.5713/ajas.2007.1057.

Deusch, S., A. Camarinha-Silva, J. Conrad, U. Beifuss, M. Rodehutscord, and J. Seifert. 2017. A structural and functional elucidation of the rumen microbiome influenced by various diets and microenvironments. Front. Microbiol. 8:1605. https://doi.org/10.3389/fmicb.2017.01605.

Ferraretto, L., P. Crump, and R. J. Shaver. 2013. Effect of cereal grain type and corn grain harvesting and processing methods on intake, digestion, and milk production by dairy cows through a meta-analysis. J. Dairy Sci. 96:533-550. https://doi.org/10.3168/jds.2012-5932.

Ferri, G., G. Comerio, P. Ladarola, M. Zapponi, and M. Speranza. 1978. Subunit structure and activity of glyceraldehyde-3-phosphate dehydrogenase from spinach chloroplasts. Biochim Biophys Acta- Enzymology. 522: 19-31. https://doi.org/10.1016/0005-2744(78)90318-2.

Grant, G. A. 2018. d-3-phosphoglycerate dehydrogenase. Front Mol Biosci. 5:110. https://doi.org/10.3389/fmolb.2018.00110.

Hart, E., C. Creevey, T. Hitch, and A. H. Kingston-Smith. 2018. Meta-proteomics of rumen microbiota indicates niche compartmentalisation and functional dominance in a limited number of metabolic pathways between abundant bacteria. Sci. Rep. 8:1-11. https://doi.org/10.1038/s41598-018-28827-7.

Hassanat, F., R. Gervais, C. Julien, D. Massé, A. Lettat, P. Y. Chouinard, H. V. Petit, and C. Benchaar. 2013. Replacing alfalfa silage with corn silage in dairy cow diets: Effects on enteric methane production, ruminal fermentation, digestion, N balance, and milk production. J. Dairy Sci. 96:4553-4567. https://doi.org/10.3168/jds.2012-6480.

Honan, M. C. and S. L. Greenwood. 2020. Characterization of variations within the rumen metaproteome of Holstein dairy cattle relative to morning feed offering. Sci. Rep. 10:1-8. https://doi.org/10.1038/s41598-020-59974-5.

Isaac, N. I., D. Philippe, A. Nicholas, D. Raoult, and C. J. C. M. S. Eric. 2019. Metaproteomics of the human gut microbiota: challenges and contributions to other OMICS. Clin. Mass Spectrom. 14:18-30. https://doi.org/10.1016/j.clinms.2019.06.001.

Jami, E. and I. Mizrahi. 2012. Composition and similarity of bovine rumen microbiota across individual animals. PloS One. 7:e33306. https://doi.org/10.1371/journal.pone.0033306.

Kaiser, F., S. Krautwurst, S. Salentin, V. J. Haupt, C. Leberecht, S. Bittrich, D. Labudde, and M. Schroeder. 2020. The structural basis of the genetic code: amino acid recognition by aminoacyl-tRNA synthetases. Sci. Rep. 10:1-17. https://doi.org/10.1038/s41598-020-69100-0.

Kim, J. N., C. Méndez–García, R. R. Geier, M. Iakiviak, J. Chang, I. Cann, and R. I. Mackie. 2017. Metabolic networks for nitrogen utilization in Prevotella ruminicola 23. Sci. Rep. 7:1-11. https://doi.org/10.1038/s41598-017-08463-3.

Koenig, K. M, K. A. Beauchemin, and L. M. Rode. 2003. Effect of grain processing and silage on microbial protein synthesis and nutrient digestibility in beef cattle fed barley-based diets. J. Anim. Sci. 81:1057-1067. https://doi.org/10.2527/2003.8141057x.

Kopečný, J., M. Zorec, J. Mrazek, Y. Kobayashi, and R. Marinšek-Logar. 2003. Butyrivibrio hungatei sp. nov. and Pseudobutyrivibrio xylanivorans sp. nov., butyrate-producing bacteria from the rumen. Int. J. Syst. Evol. 53:201-209. https://doi.org/10.1099/ijs.0.02345-0.

Leahy, S. C., W. J. Kelly, E. Altermann, R. S. Ronimus, C. J. Yeoman, D. M. Pacheco, and G. T. Attwood. 2010. The genome sequence of the rumen methanogen Methanobrevibacter

ruminantium reveals new possibilities for controlling ruminant methane emissions. PloS one. 5:e8926. https://doi.org/10.1371/journal.pone.0008926.

Schiebenhoefer, H., T. Van Den Bossche, S. Fuchs, B. Y. Renard, T. Muth, and L. J. Martens. 2019. Challenges and promise at the interface of metaproteomics and genomics: an overview of recent progress in metaproteogenomic data analysis. Expert Rev Proteomics**.** 16:375-390. https://doi.org/10.1080/14789450.2019.1609944.

Schulz, H. 2013. Fatty acid oxidation. Pages 281-284 in Encyclopedia of biological chemistry (second edition). W. J. Lennarz, and M. D. Lane. Academic Press, Waltham. https://doi.org/10.1016/B978-0-12-378630-2.00071-2.

Macy, J. M. and I. Probst. 1979. The biology of gastrointestinal bacteroides. Annu. Rev. Microbiol. 33:561-594. https://doi.org/10.1146/annurev.mi.33.100179.003021.

Matsui, H., K. Ogata, K. Tajima, M. Nakamura, T. Nagamine, R. I. Aminov, and Y. Benno. 2000. Phenotypic characterization of polysaccharidases produced by four Prevotella type strains. Curr. Microbiol. 41:45-49. https://doi.org/10.1007/s002840010089.

McDonald, P. 2002. Animal nutrition. Pearson Education Publisher, Harlow, UK.

Miyazaki, K., J. C. Martin, R. Marinsek-Logar, and H. J. Flint. 1997. Degradation and utilization of xylans by the rumen anaerobe Prevotella bryantii (formerly P. ruminicola subsp. brevis) $B_1$4. Anaerobe. 3:373-381. https://doi.org/10.1006/anae.1997.0125.

Mulakala, B. K. 2022. Impact of dietary carbohydrate profile on the dairy cow rumen meta-proteome. Mendeley Data, V1. https://data.mendeley.com/datasets/bv3y4ffnc6/1.

Ogunade, I., A. Pech-Cervantes, and H. Schweickart. 2019. Metatranscriptomic analysis of sub-acute ruminal acidosis in beef cattle. Animals. 9:232. https://doi.org/10.3390/ani9050232.

Pengpeng, W. and Z. Tan. 2013. Ammonia assimilation in rumen bacteria: a review. Anim. Biotechnol. 24:107-128. https://doi.org/10.1080/10495398.2012.756402.

Pirondini, M., S. Colombini, M. Mele, L. Malagutti, L. Rapetti, G. Galassi, and G. M. Crovetto. 2015. Effect of dietary starch concentration and fish oil supplementation on milk yield and composition, diet digestibility, and methane emissions in lactating dairy cows. J. Dairy Sci. 98:357-372. https://doi.org/10.3168/jds.2014-8092.

Purushe, J., D. E. Fouts, M. Morrison, B. A. White, R. I. Mackie, P. M. Coutinho, B. Henrissat, and K. E. Nelson. 2010. Comparative genome analysis of Prevotella ruminicola and Prevotella bryantii: insights into their environmental niche. Microb. Ecol. 60:721-729. https://doi.org/10.1007/s00248-010-9692-8.

Reeve, J. N., J. Nölling, R. M. Morgan, and D. R. Smith. 1997. Methanogenesis: genes, genomes, and who's on first?. J. Bacteriol. 179:5975-5986. https://doi.org/10.1128/jb.179.19.5975-5986.1997.

Rooke, J. A., R. J. Wallace, C. A. Duthie, N. McKain, S. M. de Souza, J. J. Hyslop, D. W. Ross, T. Waterhouse, and R. Roehe. 2014. Hydrogen and methane emissions from beef

cattle and their rumen microbial community vary with diet, time after feeding and genotype. Br. J. Nutr. 112:398-407. https://doi.org/10.1017/S0007114514000932.

Russell, J. B. 2002. Rumen microbiology and its role in ruminant nutrition. Department of Microbiology, Cornell University. https://www.ars.usda.gov/research/software/download/?softwareid=409 , Ithaca, NY.

Smith, W. A. 2019. Relationships between undigested and physically effective fiber in lactating dairy cow diets. MS Thesis. The University of Vermont, Burlington, VT.

Smith, K. M. 2021. The effect of physically effective undegradable neutral detergent fiber and rumen fermentable starch on lactating Holstein cows. MS Thesis. The University of Vermont, Burlington, VT.

Snelling, T. J. and R. J. Wallace. 2017. The rumen microbial metaproteome as revealed by SDS-PAGE. J. Dairy Sci. 95:318-327. https://doi.org/10.1186/s12866-016-0917-y.

Sniffen, C. J., J. D. O'connor, P. J. Van Soest, D. G. Fox, and J. B. Russell. 1992. A net carbohydrate and protein system for evaluating cattle diets: II. Carbohydrate and protein availability. J. Anim. Sci. 70:3562-3577. https://doi.org/10.2527/1992.70113562x.

Steele, M., L. Dionissopoulos, O. AlZahal, J. Doelman, and B. W. McBride. 2012. Rumen epithelial adaptation to ruminal acidosis in lactating cattle involves the coordinated expression of insulin-like growth factor-binding proteins and a cholesterolgenic enzyme. J. Dairy Sci. 95:318-327. https://doi.org/10.3168/jds.2011-4465.

Thoetkiattikul, H., W. Mhuantong, T. Laothanachareon, S. Tangphatsornruang, V. Pattarajinda, L. Eurwilaichitr, and V. Champreda. 2013. Comparative analysis of microbial profiles in cow rumen fed with different dietary fiber by tagged 16S rRNA gene pyrosequencing. Curr. Microbiol. 67:130-137. https://doi.org/10.1007/s00284-013-0336-3.

Villalba, J. J., F. D. Provenza, and K. C. Olson. 2006. Terpenes and carbohydrate source influence rumen fermentation, digestibility, intake, and preference in sheep. J. Anim. Sci. 84:2463-2473. https://doi.org/10.2527/jas.2005-716.

Wallace, R., R. Onodera, and M. A. Cotta. 1997. Metabolism of nitrogen-containing compounds. Pages 283-328 in The rumen microbial ecosystem. Springer, Dordrecht. https://doi.org/10.1007/978-94-009-1453-7_7.

Weijland, A., K. Harmark, R. H. Cool, P. H. Anborgh, and A. Parmeggiani. 1992. Elongation factor Tu: a molecular switch in protein biosynthesis. Mol. Microbiol. 6:683-688. https://doi.org/10.1111/j.1365-2958.1992.tb01516.x.

Wirth, R., G. Kádár, B. Kakuk, G. Maróti, Z. Bagi, Á. Szilágyi, G. Rákhely, J. Horváth, and K. L. Kovács. 2018. The planktonic core microbiome and core functions in the cattle rumen by next generation sequencing. Front. Microbiol. 9:2285. https://doi.org/10.3389/fmicb.2018.02285.

Yang, W. and K. A. Beauchemin. 2006. Increasing the physically effective fiber content of dairy cow diets may lower efficiency of feed use. 89:2694-2704. https://doi.org/10.3168/jds.2008-1379.

Zebeli, Q., J. Dijkstra, M. Tafaj, H. Steingass, B. N. Ametaj, and W. J. Drochner. 2008. Modeling the adequacy of dietary fiber in dairy cows based on the responses of ruminal pH and milk fat production to composition of the diet. J. Dairy Sci. 91:2046-2066. https://doi.org/10.3168/jds.2007-0572.

Zeng, H., C. Guo, D. Sun, H. E. Seddik, and S. Mao. 2019. The ruminal microbiome and metabolome alterations associated with diet-induced milk fat depression in dairy cows. Metabolites. 9:154. https://doi.org/10.3390/metabo9070154.

Zhang, R., W. Zhu, W. Zhu, J. Liu, S. Mao. 2014. Effect of dietary forage sources on rumen microbiota, rumen fermentation and biogenic amines in dairy cows. J. Sci. Food Agric. 94:1886-1895. https://doi.org/10.1002/jsfa.6508.

Zhang, X., H. Zhang, Z. Wang, X. Zhang, H. Zou, C. Tan, and Q. Peng. 2015. Effects of dietary carbohydrate composition on rumen fermentation characteristics and microbial population in vitro. Ital. J. Anim. Sci. 14:3366. https://doi.org/10.4081/ijas.2015.3366

CHAPTER 3: USE OF MILK PROTEINS AS BIOMARKERS OF CHANGES IN THE RUMEN METAPROTEOME OF HOLSTEIN COWS FED LOW FIBER, HIGH STARCH DIETS

3.1 Abstract

Dietary levels of undegraded neutral detergent fiber (uNDF240) and rumen fermentable starch (RFS) can impact the rumen microbiome and milk composition. The objective of the study is to investigate the use of milk proteins as biomarkers of rumen microbial activity through a comparative evaluation of the rumen microbial and milk protein profiles produced by Holstein cows fed diets with varying contents of physically effective uNDF240 (peuNDF240) and RFS. Eight ruminally cannulated lactating Holstein cows were included in a larger study as part of a 4 x 4 Latin square design with four 28-d periods to assess 4 diets varying in peuNDF240 and RFS content. For this experiment, cows received one of two dietary treatments: 1) low peuNDF240, high RFS (LNHS) diet, or 2) high peuNDF240, low RFS (HNLS) diet. Within each period, rumen fluid samples were collected from each cow on d 26 (1400 h) and d 27 (0600 h and 1000 h), and milk samples were collected from each cow on d 25 (2030 h), d 26 (0430 h, 1230 h, and 2030 h), and d 27 (0430 h and 1230 h). Microbial proteins were isolated from each rumen fluid sample. For milk samples, milk proteins were fractionated, and the whey fraction was subsequently isolated. Isolated proteins within each rumen fluid or milk sample were isobarically labeled and analyzed by LC-MS/MS. Product ion spectra acquired from rumen fluid samples were searched using SEQUEST against 71 composite databases. In contrast, product ion spectra acquired from milk samples were searched against the *Bos taurus*

database. Data were analyzed using the PROC MIXED procedure in SAS 9.4 to assess the impact of diet and time of sampling. A total of 129 rumen microbial proteins were quantified across 24 searched microbial species. Of these, the abundance of 14 proteins across 9 microbial species was impacted due to diet and diet × time interaction, including 7 proteins associated with energetics pathways. Among the 159 quantified milk proteins, the abundance of 21 proteins was impacted due to the diet and diet × time interaction. The abundance of 19 of these milk proteins was impacted due to diet × time interactions. Of these, 16 proteins had the disparity across diets at the 0430 h sampling time, including proteins involved in host defense, nutrient synthesis, and transportation, suggesting that biological shifts resulting from diet-induced rumen changes are not diurnally uniform across milkings. The concentration of lipoprotein lipase (LPL) was higher in the milk from the cows fed with the LNHS diet, which was numerically confirmed with an ELISA. Further, as determined by ELISA, the LPL concentration was significantly higher in the milk from the cows fed with the LNHS diet at 0430 h sampling point, suggesting that LPL concentration may indicate dietary carbohydrate-induced ruminal changes. The results of this study suggest that diet-induced rumen changes can be reflected in milk in a diurnal pattern, further highlighting the need to consider sampling time points for using milk proteins as a representative biomarker of rumen microbial activity.

3.2 Introduction

Diets formulated for high-producing dairy cows typically include a high proportion of rapidly fermentable carbohydrates to meet the cow's energy demands. However, feeding dairy cows rich in rapidly fermentable carbohydrates and low in fiber can impact their

DMI, performance, and milk quality (Grant, 1997; Zebeli et al., 2008; Fustini et al., 2017). For example, Akhlaghi et al. (2022) reported that cows fed a high starch, low fiber diet (29.2% of DM, 32.9 % DM) produced, on average, 1.2 kg/d more milk and consumed an additional 0.04 kg DM/d, compared with cows fed a low starch, high fiber diet (22.3% of DM, 29.2% of DM). To maintain healthy ruminal function, the NASEM (2021) recommends a minimum of 25 to 33% fiber (on a dry matter (DM) basis) for lactating cows, measured as NDF content. In addition to the fiber content of the diet, its physical characteristics such as particle size, digestibility, impact ruminal fill, and daily DMI (Conrad et al., 1964). To better characterize the fibrous content of the diet, Mertens (1997) proposed the concept of physically effective NDF (**peNDF**), which is calculated by multiplying the NDF content by its physical effectiveness factor (**pef**). The estimation of pef equates to the proportion of particles retained on the ≥ 4 mm sieve of the Penn State Particle Separator (Heinrichs and Kononoff, 2013). A common method for measuring the digestibility of fiber is the determination of undegraded NDF at 240 h (**uNDF240**). The uNDF240 is the percentage of NDF that is not degraded after 240 h of incubation with mixed ruminal microbes (Allen and Mertens, 1988, Raffrenato et al., 2018). Recently, Grant et al. (2020) proposed the concept of physically effective undegraded NDF at 240 h (**peuNDF240**), which summarizes the chemical and physical properties of fiber; it is calculated by multiplying the uNDF240 by the pef. Previously, Smith (2021) reported that diets containing lower peuNDF240 (~6% of DM) and higher rumen fermentable starch (**RFS**; 19% of DM) induced negative associative effects on milk fat %, total tract digestibility of NDF, and acetate: propionate ratio in dairy cows. Therefore, an optimal

balance between peuNDF240 fractions and RFS is important to optimizing nutrient utilization and productivity.

The impact of dietary carbohydrate profile on animal productivity is mainly the result of a modified ruminal microbial environment, and several studies have reported a shifting rumen microbiota during feeding of diets containing a high proportion of rapidly fermentable carbohydrates with inadequate fiber content (Hook et al., 2011; Ogunade et al., 2019; Ramos et al., 2021). Methodologically, these studies investigated rumen microbial changes at the DNA (meta-genomics) and RNA (meta-transcriptomics) levels; however, these studies did not assess the actual metabolic response of the microbial population at the protein level. Previously, Hart et al. (2018) reported the mismatch between the cows' rumen microbial transcriptomic and translated data. More recently, Mulakala et al. (2022) characterized the rumen meta-proteome impacted by varying levels of peuNDF240 and RFS content in the diet fed to lactating dairy cows.

The impact of diet-induced modifications to the rumen microbial environment alters the cow's metabolic status, which is commonly reflected by alterations in body fluids such as blood, urine, saliva, and milk (Overton et al., 2017). The standard method used for diagnosing metabolic diseases is the analysis of key factors in blood circulation (Oetzel, 2004). However, obtaining blood via venous puncture can be considered an animal welfare issue in public perception (Solano et al., 2004). Further, blood collection at multiple time points may be required for metabolic assessment, highlighted by Hussein et al. (2020), who recently reported diurnal variations in serum metabolites concentrations, such as glucose, β-hydroxybutyric acid, and urea from dairy cows. Therefore, diagnostic capacity using

non-invasively obtained biological fluid such as milk could prove to be a useful alternative to blood in determining cow metabolic and health status. Previously, Zhao et al. (2016) reported that different levels of dietary NDF and starch altered milk fat, protein, and lactose content and production. In another study, milk protein content increased when cows were fed diets rich in starch, partly due to an increase in rumen's available energy (Cantalapiedra-Hijar et al., 2014). Puppel et al. (2021) recently reported that the concentrations of selected milk whey proteins were altered due to ketosis and suggested whey proteins could be used as biomarkers for diagnosing biological dysfunction and metabolic diseases. Evaluating potential non-invasive biomarkers for diagnosing diet-induced rumen dysfunction may be used to diagnose metabolic shifts resulting from high RFS and low NDF diets. We hypothesized that the milk proteome would change in response to a low peuNDF240, high RFS diet. More specifically, we hypothesized that the abundance of immune-associated proteins in milk would change due to a high RFS diet. This study aims to characterize the milk proteome in response to feeding cows a low peuNDF240, high RFS diet and relate this milk proteome to the characterized rumen metaproteome.

3.3 Materials and Methods

3.3.1 Animals and Experimental Design

The experimental protocol for this study was approved by the William H. Miner Agricultural Research Institute Animal Care and Use Committee (IACUC# 2017AUR02). Samples analyzed in this experiment were collected from a larger study conducted at the William H. Miner Agricultural Research Institute (Chazy, NY) from July 2019 to September 2019. The experimental design of the larger study utilized eight lactating

cannulated Holstein cows (85 ± 15 DIM) included in a 4 × 4 Latin square experiment with a 2 x 2 factorial treatment design consisting of four 28-d periods as described by Smith (2021). The 8 cows used in this study were cannulated at the beginning of their previous dry (non-lactating) period, and these cannulas were cleaned regularly throughout the dry period and lactation. The rumen cannulation was performed according to the William H. Miner Agricultural Research Institute guidelines. Briefly, the procedure was a one-step fistulation procedure whereby a circular incision was created in the left paralumbar fossa after analgesic and anesthetic administration, subsequently followed by an incision in the rumen wall. The rumen wall was sutured to the abdominal skin to form a fistula, into which a 3-inch flexible rubber cannula was placed. The surgery site was inspected until healed, and the vital signs of the cows were recorded throughout the inspection. The 3-inch cannula was replaced with a 4-inch cannula after day 14 or when well healed. In each period, cows were paired randomly and assigned to one of four dietary treatments (DM basis) of different concentrations of RFS and peuNDF240 content in the diet. Blinding was not used. For this study, samples were collected from the cows fed a diet containing low peuNDF240, high RFS (6.7 % of DM, 19.2 % of DM**; LNHS**) or high peuNDF240, low RFS (8.60 % of DM, 16.7 % of DM; **HNLS**) in each period. The complete diet ingredient and nutritional profiles can be found in the supplementary file (Supplementary Tables S1 and S2; https://data.mendeley.com/datasets/bv3y4ffnc6/1).

3.3.2 Rumen Fluid Sampling and Protein Fractionation

Rumen fluid samples were collected from each cow in each period on d 26 (1400 h) and d 27 (0600 h and 1000 h), resulting in 42 samples [2 cows per treatment per period

× 2 treatments per period × 4 periods × 3 samples per cow per period; 6 samples were not collected]. As described by Steele et al. (2012), rumen fluid samples were collected from three areas in the mid-ventral ruminal sac of each cow's rumen and pooled within the cow within the sampling point to create one composite sample/cow/time point. The samples were flash-frozen using a dry-ice ethanol bath and stored at -80 °C until further processing.

Frozen rumen fluid samples (n = 42) were thawed overnight at 4 °C and strained through four layers of cheesecloth (Lion Services Inc., Charlotte, NC) to separate coarse fibers. A universal control (**UC**) was generated by pooling equal volumes of rumen fluid from each cow at each time point across the four periods. The samples and UC were centrifuged at 16,000 x *g* for 20 min at 4 °C, and the supernatant was discarded to collect the cell pellets. The collected pellets were processed as described by Honan and Greenwood (2020). Briefly, one mini-tablet protease inhibitor (Pierce Protease Inhibitor Mini Tablets, Thermo Scientific, Rockford, IL) dissolved in RIPA lysis buffer, and a 5 mm stainless steel bead (Qiagen, Hilden, Germany) was added to tubes containing pellets. Sample pellets were homogenized (TissueLyser II, Qiagen) at 30 Hz for 30 sec, followed by a 3-min incubation on ice. Six repetitions of this homogenization and incubation process were performed. The resulting homogenate samples were precipitated by adding a 6 M trichloroacetic acid/80 mM dithiothreitol (**DTT**) solution at a 1:3 protein extract ratio, and then samples were incubated overnight at 4 °C. Following overnight incubation, samples were centrifuged at 16,000 x *g* for 20 min at 4 °C, and the supernatant was discarded. The collected pellets were washed twice with 20% dimethyl sulfoxide (**DMSO**) in acetone and twice with 100 % ice-cold acetone. The wash step protocol was as follows: 20% DMSO in acetone was added to cell pellets, incubated for 1 hour at -20 ℃, and then centrifuged at

10,000 x g for 5 minutes at 4 ℃ to collect the cell pellet. The collected pellet was washed twice with 100% ice-cold acetone instead of 20% DMSO in acetone by following the wash step protocol described above. The collected pellets were air-dried and resuspended in phosphate-buffered saline and total protein extract concentrations were quantified using a bicinchoninic acid assay kit (Pierce, Rockford, IL).

3.3.3 Milk Sample Collection and Milk Protein Isolation

Cows were milked thrice daily at 0430, 1230, and 2030 h throughout the study. Milk samples were collected from each cow on d 25 (2030 h), d 26 (0430 h, 1230 h, and 2030 h), and d 27 (0430 h and 1230 h) of each period. Milk samples were collected using the commercially available in-line sampling unit attached to each cow's milk line. At each milk sampling time point, a BouMatic (Madison, WI, USA) in-line sampling unit was attached to an individual milk meter. A subsample of the milk was automatically pumped into the sampling unit throughout the milking time for each cow, which provided a representative composite sample within cow within milking. The samples were thoroughly mixed in the sampling unit and then transferred into collection tubes. The collection tubes were flash-frozen using a dry-ice ethanol bath and stored at -80 °C until further processing.

After thawing milk samples (n = 94, including 6 milk samples per cow per period × 2 cows per treatment per period × 2 treatments per period × 4 periods; 2 samples were not collected) overnight at 4 ℃, the samples were composited within a period within cow within time point across the day, creating 47 samples that include 3 samples (one 0430 h sample, one 1230 h sample, and one 2030 h sample) per cow (n=4) per period (n=4). A UC was generated by pooling equal milk volumes from each cow at each time point across the

four periods. A mammalian protease inhibitor cocktail (0.24 mL/g milk protein; Protease Inhibitor Cocktail**,** Sigma, Milwaukee, WI, USA) was added to each composite milk sample and the UC. Samples were then centrifuged at 4,000 × *g* for 15 min at 4 °C. The cream layer was then removed, and the depletion of casein from skimmed samples was performed as described by Tacoma et al. (2016). Briefly, $CaCl_2$ (60 mM) was added to the skimmed sample, and the pH was adjusted to 4.3 using 30% acetic acid (Fisher Scientific, Fair Lawn, NJ, USA). Samples were then ultra-centrifuged at 189,000 × *g* at 4 °C for 70 min, and the supernatant was collected and stored at -80 °C until processing. The samples were analyzed using the bicinchoninic acid assay kit (Pierce, Rockford, IL, USA) for protein quantification.

3.3.4 Tandem Mass Tag (TMT) Peptide Labeling

Tandem mass tag peptide labeling was performed using 10 plex TMT reagents kits (Thermo Scientific) per the manufacturer's instructions. Briefly, 72 µg of protein from each rumen fluid and milk sample was aliquoted, and the volume was adjusted to 100 µL with 100 mM triethylammonium bicarbonate (**TEAB**). Samples were incubated with 0.5 mM of DTT for 60 min at 37 °C and then with iodoacetamide for 30 min in the dark. After incubation, trypsin was added, and samples were digested overnight at 37 °C. The TMT reagents (0.8 mg dissolved in 41 µL of acetonitrile) were added to the digested samples and incubated for 1 h at room temperature. After incubation, 8 µL of 5% hydroxylamine was added to quench the reaction. Each multiplex was created by pooling an equal volume (25 µL) from each subset of individual TMT-labeled samples (9 experimental samples + 1 aliquot of UC per 10 plex TMT reagents kit). Rumen fluid (n=42) and milk samples (n=47) were processed separately. A 100 µL aliquot from each multiplex was dried to remove

TEAB and then fractionated using a high pH reversed-phase peptide fractionation kit (Thermo Scientific) as per kit instructions resulting in 8 fractions for each multiplex. The fractionated samples were submitted to The Vermont Biomedical Research Network Proteomics Facility (The University of Vermont, Burlington, VT) for liquid chromatography-tandem mass spectrometry **(LC-MS/MS**).

3.3.5 LC-MS/MS Analysis

The fractionated peptide samples were dissolved in 10 µL of 2.5% formic acid (**FA**), and 2.5% acetonitrile (**ACH**) in water for subsequent LC-MS/MS peptide identification and quantification. The LC-MS/MS analysis was performed on a Q-Exactive Plus MS coupled to an EASY-nLC 1200 (Thermo Scientific), similar to the methods described by Honan and Greenwood (2020). Briefly, samples were loaded onto a 100 µm x 500 mm capillary column packed with Halo C18 (2.7 µm particle size, 90 nm pore size, Michrom Bioresources, CA, USA) at a flow rate of 300 nL/min. Following solvent gradient conditions were used to separate peptides; 2.5 to 35% of ACH/0.1% FA for 60 min and increase from 35 to 100% ACH /0.1% FA in 1 min and then 100% ACH /0.1% FA for 4 min, an immediate return to 2.5% ACH /0.1% FA, and a final hold at 2.5% ACH/0.1% FA. Peptides were introduced into the MS via a nanospray ionization source, and laser pulled ~3 µm orifice with a spray voltage of 2.0 kV. Full MS scans were acquired in a data-dependent "Top 10" acquisition mode with lock mass function activated (*m/z* 371.1012). The scans were acquired in the mass range of 350-1,600 m/z with a mass resolution of 70,000, and the AGC target value was set at $1e^6$. The top ten intense peaks in MS were fragmented with higher-energy collisional dissociation of 10. MS/MS spectra were

obtained at a 35,000 resolution, with an AGC target of $1e^5$ and a maximum injection time of 100 ms. Dynamic exclusion was enabled (peptide match: preferred; exclude isotopes: on; underfill ratio: 1%).

3.3.6 Data Analysis

Product ion spectra acquired from rumen fluid samples were searched using the SEQUEST search engine with percolator node (false discovery rate to less than 1%) on Proteome Discoverer 2.4 (Thermo Scientific) against 71 rumen-relevant composite databases downloaded on September 12, 2020. In contrast, product ion spectra acquired from milk samples were searched against the *Bos taurus* database downloaded from UniProt on October 28, 2021. Product ion spectra acquired from rumen fluid (n=1) and milk samples (n=3) from a cow with a high milk somatic cell count were excluded from the product ion spectra search and all further data analysis. Search Parameters were as follows: (1) full trypsin enzymatic activity; (2) maximum missed cleavages = 2; (3) minimum peptide length = 6, (4) mass tolerance at 10 ppm for precursor ions and 0.02 Da for fragment ions; (5) dynamic modifications on methionines (+15.9949 Da: oxidation), Dynamic TMT6plex modification (The TMT6plex and TMT10plex have the same isobaric mass) on N-termini and lysines (229.163 Da); (6) static carbamidomethylation modification on cysteines (+57.021 Da). As Reporter Ions Quantifier node in the consensus workflow, the TMT labeled peptides were quantified, and parameters were specified as follows: unique and razor peptides were used for quantification; Reject Quan results with missing channels and apply Quan value corrections were set as false; Co-Isolation Threshold value was set as 75; Average Reporter S/N Threshold was 10; "Total Peptide

Amount" was used for normalization and Scaling Mode was set "on Control Averages," so that the peptide abundances in the UC labels were set as 100 and the abundances in other channels were scaled accordingly. All the protein identification and quantification information (<1% FP; with protein grouping enabled) was exported from the MSF result files to excel spreadsheets. The scaled abundance values of the samples were used for further statistical analysis. For any proteins identified as uncharacterized, the FASTA sequence was retrieved from UniProt (http://www.uniprot.org/) and searched through the Basic Local Alignment Search Tool (BLAST; http://blast.ncbi.nlm.nih.gov/Blast.cgi). The top hit protein was selected as an identified protein if the hit was 100% matched with the searched query. A mixed procedure model of SAS 9.4 (SAS Institute, Cary, NC) was performed, including diet, period, time, diet × time interaction as the fixed effects and cow, cow × diet × time as random effects. The diet and diet × time interaction effect on protein abundance was considered significant if $P < 0.05$.

3.3.7 ELISA

An ELISA was used to validate the concentration of lipoprotein lipase (**LPL**) in milk samples. While it must be noted that the commercially available ELISA used in this study has not been extensively validated and has some limitations in terms of the linear range of detection, this assay is commercially available, allowing for repeatability and LPL detection within bovine milk. The LPL protein was selected for validation for two reasons 1) it is the protein that had the highest statistically significant difference due to the LNHS diet in this study, and further, its abundance was also affected by a diet × time interaction, 2) LPL protein quantification with techniques such as ELISA using commercially available

products is possible, whereas protein quantification assays or antibodies are not currently available for all differentially affected proteins. The concentration of LPL in the milk serum was measured in triplicate using a commercially available ELISA kit (Bovine Lipoprotein Lipase, MBS005972; My BioSource, Inc., San Diego, CA). The ELISA, including standard curve creation, was performed according to the manufacturer's instructions. The kit's sensitivity was 5 ng/mL and the detection range of the kit was 25 – 800 ng/mL. Minimum acceptable r^2 of the standard curve was 0.99. Both intra-assay CV (%) and inter-assay CV (%) of the kit were less than 15% [CV (%) = SD/mean ×100]. The data was analyzed using the same statistical model used to analyze the LC-MS/MS data as described above. The diet and diet × time interaction effect on protein abundance was considered significant if $P < 0.05$.

3.4 Results

3.4.1 Rumen Metaproteome

The rumen meta-proteomic analysis in this study identified 129 proteins labeled in all samples across 24 searched microbes (Supplementary Table S4; http://dx.doi.org/10.17632/78v4rvnrwx.1). Identified microbes and their strains were as follows; *Prevotella ruminicola, Prevotella ruminicola strain ATCC 19189, Ruminococcus albus 8, Ruminococcus albus strain 27210, Ruminococcus albus strain SY3, Ruminococcus bromii, Butyrivibrio hungatei, Prevotella aff. ruminicola Tc2-24, Methanobrevibacter ruminantium strain 35063, Eubacterium cellulosolvens 6, Ruminococcus flavefaciens, Ruminococcus flavefaciens 007c, Pseudobutyrivibrio ruminis, Selenomonas ruminantium, Eubacterium ruminantium, Pseudobacteroides cellulosolvens ATCC 35603, Clostridium*

aminophilum, Oxalobacter formigenes HOxBLS, Treponema saccharophilum DSM 2985, Butyrivibrio fibrisolvens, Butyrivibrio proteoclasticus strain ATCC 51982, Methanosarcina barkeri 3, Prevotella bryantii B14 and *Peptostreptococcus anaerobius CAG:621*. In the present study, 14 proteins across 9 microbial species were impacted due to diet and diet × time interaction (Table 3.1). Of these 14 proteins, the abundance of 12 proteins across 8 microbial species was impacted due to diet × time interaction, and only 2 proteins across 2 microbial species were impacted due to diet. Among the 12 proteins affected by diet × time interactions, 6 proteins were impacted due to diet at the 1400 h sampling point.

The abundances of pyruvate, phosphate dikinase (*P. ruminis*, *R. flavefaciens*) and NADH dehydrogenase (*R. albus SY3*) were higher in cows fed the HNLS diet compared with the cows fed the LNHS diet at 0600h sampling point. At the same time point, the abundances of glutamate dehydrogenase (*P. ruminicola*), fructose-bisphosphate aldolase (*P. ruminicola*), and 60 kDa chaperonin (*P. ruminicola strain ATCC 19189*) were higher in cows fed the LNHS diet compared with cows fed the HNLS diet. At the 1000 h sampling point, the abundances of glutamate dehydrogenase (*B. hungatei*), TonB-linked outer membrane protein, SusC/RagA family (*P. ruminicola*), and pyruvate-ferredoxin/flavodoxin oxidoreductase (*P. bryantii B14*) were higher in cows fed the LNHS diet, whereas the abundance of NifU homolog involved in Fe-S cluster formation (*P. ruminis*) was higher in cows fed the HNLS diet. The abundance of NifU_N domain-containing protein (*P. cellulosolvens ATCC 35603*) and Glyceraldehyde-3-phosphate dehydrogenase (*P. bryantii B14*) was higher in the cows fed the HNLS diet compared with the cows fed with the LNHS diet at 1400 h sampling point.

The abundance of pyruvate, phosphate dikinase (*R. albus SY3*), and BMC domain-containing protein (*C. aminophilum*) were impacted due to diet, and their abundance was higher in the cows fed the HNLS diet compared with those fed the LNHS diet.

3.4.2 Milk Proteome Profile

Proteomic analysis identified 159 milk proteins labeled in all samples (Supplementary Table S5; http://dx.doi.org/10.17632/78v4rvnrwx.1). Of these 159 identified proteins, the abundances of 21 proteins were affected due to diet and the diet × time interaction (Table 3.2), including 19 proteins affected by the diet × time interaction and 2 proteins affected by diet. Among 19 proteins affected by the diet × time interaction, 16 were impacted by the diet at the 0430 h sampling point, with 6 proteins having a higher abundance in milk collected from cows fed the LNHS diet compared with samples from those fed the HNLS diet.

The abundance of immunoglobulin M heavy chain secretory form, kininogen-1, inter-alpha-trypsin inhibitor heavy chain H4, complement factor H, monocyte differentiation antigen CD14, complement factor I isoform X1, ribonuclease 4, inter-alpha-trypsin inhibitor heavy chain H2 were lower in milk from LNHS-fed cows at 0430 h collection time point compared with samples from the HNLS-fed cows, whereas, the abundance of alpha-S1-casein, kappa-casein, and secretoglobin family 1D member were higher in milk samples from LNHS-fed cows at the same collection time point. The abundances of mitogen-activated protein kinase 5, complement component C9 and vitamin D-binding protein were higher in milk from cows fed the HNLS diet at 1230 h collection time point compared with milk samples from those fed the LNHS diet.

The abundance of CTSL1 and lipoprotein lipase (LPL) were impacted due to diet. The abundance of the CST1 protein was higher in cows fed the HNLS diet (112 vs. 90; $P = 0.03$), whereas the abundance of LPL was higher in cows fed the LNHS diet (1210 vs. 604; $P < 0.01$).

3.4.3 Lipoprotein Lipase ELISA Validation

The concentration of LPL, as determined by ELISA, was higher in milk samples from cows fed the LNHS diet compared with milk samples from cows fed the HNLS diet at the 0430 h sampling point ($P = 0.01$; Figure 3.1B). This treatment difference was not observed for the other milk sampling times ($P = 0.42$ and 0.77 for sampling at 1230 and 2030 h, respectively: Figure 3.1B). The concentration of LPL was not significantly affected by diet ($P = 0.12$; Figure 3.1A) when the time was not considered.

3.5 Discussion

Previous research clearly demonstrates that the diet's concentration and profile of fiber and starch can influence milk composition and component profiles produced by dairy cows. For example, Zhao et al. (2016) reported a linear decrease in milk protein content and production, lactose content, and production as the diet's NDF: starch ratio increased. Alzahal et al. (2009) observed that cows fed a lower fiber diet (32.7% of DM) produced lower levels of polyunsaturated fatty acids in milk compared with cows fed with a higher fiber diet (40% of DM). In the current trial, the LNHS diet impacted the abundance of 21 milk proteins isolated from the skimmed milk fraction. Most of the milk proteins affected by the LNHS diet in this study were immune-related, suggesting systemic inflammation. As cows were cannulated at the beginning of their dry period, and the study was not started

until 80 d DIM, it indicates that systemic inflammation was probably not due to rumen cannulation during the study. Previous studies evaluating the impact of subacute ruminal acidosis (**SARA**), typically resulting from highly fermentable and low fiber diets, may provide insight into this observed protein response. In the larger study associated with this trial, Smith (2021) reported that cows fed the LNHS diet had a rumen pH < 5.8 for approximately 5.8 h/d. According to Zebeli et al. (2008), cows with a rumen pH lower than 5.8 for more than 5 to 6 h/d are at a high risk of developing SARA. Therefore, cows fed the LNHS diet in this study could be assumed to be at risk. Previous studies have reported that rumen pH depression increased free ruminal concentrations of lipopolysaccharides (**LPS**; Gozho et al., 2007; Emmanuel et al., 2008), and this increased the translocation of LPS from the gut into the blood circulation and activation of an inflammatory response (Khafipour et al., 2009b). In response to diet-induced systemic inflammation, the mammary gland shifts its priorities from synthesizing milk components to repartitioning more nutrients toward synthesizing immune molecules (Dong et al., 2011). This homeorhetic reprioritization in response to diet was recently highlighted in the research of Ma et al. (2022), who reported that feeding a high concentrate diet to dairy cows increased the blood LPS concentration within the milk vein, increasing the abundance of proinflammatory cytokines (IL-6 and IL-1α), immune-associated factors (lingual antimicrobial peptide and tracheal antimicrobial peptide) in the mammary gland. While we did not measure blood or free ruminal LPS concentrations in the current trial, this previously characterized relationship could provide insight into our observations.

To confirm the dietary induction of altered rumen microbial function in the current study, we did observe shifts in the abundance of microbial proteins due to a diet × time

interaction. In this current trial, the abundance of 12 proteins across 8 microbial species was impacted due to the diet × time interaction, highlighting the relevance to diurnal variation in rumen meta-proteome characterization studies. This aligns with our previous research, where we investigated the impact of not only LNHS and HNLS diets on the rumen meta-proteome but also the impact of diets high in peuNDF240 and RFS and low in peuNDF240 and RFS (Mulakala et al., 2022). In agreement with our previous observations, many of the affected proteins were associated with energetic pathways in terms of functionality. For example, the abundance of pyruvate phosphate dikinase from *P. ruminis* and *R. flavefaciens*, which is involved in glycolysis and gluconeogenesis pathways, was higher in the cows fed the HNLS diet at the 1400 h sampling point in the current study. At the same time, the abundance of fructose-bisphosphate aldolase from *P. ruminicola*, which is also involved in the glycolysis and gluconeogenesis pathways, was higher in the cows fed with the LNHS diet.

The results of the rumen meta-proteome in this study indicate an alteration of microbial metabolic activity due to the LNHS diet, which can subsequently alter the fermentation type and ultimately impact the composition of bodily fluids such as milk. For example, studies have shown that; milk fat was decreased because of the changes in the concentration of volatile fatty acids and the alteration of microbiota in the rumen due to the high starch diet in dairy cows (Pitta et al., 2018; Zeng et al., 2019). Therefore, in this current experiment, we sought to identify milk proteins that could be potential biomarkers of a diet-induced altered ruminal environment. Identifying potential biomarkers of diet-induced altered ruminal environment can be rapid, pertinent decision tools as they provide snapshots of cow metabolic status and help evaluate the impact of diet on rumen health.

Herein we successfully identified 21 milk proteins affected by the peuNDF240 and RFS content of the diet, including several milk protein candidates that may be appropriate biomarkers indicative of an altered rumen environment. The diet impacted the abundance of 16 milk proteins, with the 0430 h sampling point specifically being distinctive. In addition, most of the proteins affected by diet were immune-related. These findings cumulatively suggest that biological shifts resulting from diet-induced rumen changes can be reflected in milk but that these changes are not diurnally uniform across milking times. To identify the most representative biomarker with a feasible prospect of industry application, both aspects require consideration.

In terms of biological assessment, we observed a lower abundance of RNase4 in milk from cows fed the LNHS diet. Several proteins within the ribonuclease (**RNase**) family are present in cow milk and have previously been reported to have host defense-associated activities. For example, RNase family proteins, such as eosinophil cationic protein and eosinophil-derived neurotoxin, have been reported to have antibacterial and antiviral properties, respectively (Lehrer et al., 1989; Rosenberg and Domachowske, 2001). Previously, RNase4 in bovine milk has been reported to have antimicrobial activity against *Candida albicans* (Harris et al., 2010). Further, Murata et al. (2013) reported that the antimicrobial activity of lactoferrin and lactofericin was enhanced in the presence of RNase4, suggesting that lactoferrin, lactofericin and RNase4 may be concomitantly active antimicrobial agents in milk. The lower measured abundance of milk RNase4 in the current study may suggest immune suppression in the LNHS-fed cows. To support this possible explanation, we also observed a decreased abundance of immunoglobulin M heavy chain secretory form, and immunoglobulin-like protein in milk from cows fed the LNHS diet.

This supports further investigation of these proteins as biomarkers of immune function but would not likely serve as specific biomarkers indicative of shifts in rumen function resulting from dietary carbohydrate profiles.

The CD14 protein is a glycosylphosphatidylinositol-anchored protein expressed on the membrane of monocytes/macrophages and neutrophils (Haziot et al., 1988; Wright et al., 1991), It also serves as an immune cellular receptor for interactions with LPS. In this study, we observed lower abundance of CD14 in milk samples from LNHS-fed cows compared with samples from those fed the HNLS diet. The primary source of soluble CD14 (**sCD4**) in body fluids is from shedding of membrane-bound CD14 from monocytes and neutrophils (Bazil and Strominger, 1991; Haziot et al., 1993). Studies have shown that sCD14 modulates immune responses by interacting with B and T lymphocytes (Arias et al., 2000; Filipp et al., 2001) and plays a measurable role in supporting host defense in response to LPS challenges. For example, recombinant bovine sCD14 decreased the mortality of mice during an intraperitoneal LPS challenge (Lee et al., 2003b). In another study, the administration of recombinant sCD14 prevented LPS-induced TNF-α production in whole human blood (Haziot et al., 1994). Previously, it has been reported that SARA stimulated the expression of genes associated with the functions of LPS receptors, such as CD14 in white blood cells (Stefanska et al., 2018). While sCD14 has been primarily studied in blood, identifying this protein in milk is not new. Lee et al. (2003a) reported that milk sCD14 abundances were increased with intramammary LPS challenge in cows and speculated that possible sources of sCD14 in milk could result from serum leakage or cells in the mammary gland. However, Lee et al. (2003a) also observed that milk collected from the mastitis-infected quarters had lower sCD14 than uninfected quarters of the same cow;

the possible explanation outlined by Lee et al. (2003a) was that increased sCD14 resulted in an increase in binding to the bacteria that could not be detected in the whey samples due to their removal by centrifugation. Previously, the direct binding of sCD14 to gram-negative bacteria has been reported (Jack et al., 1995). Ultimately, it could be postulated that the decrease in the abundance of milk sCD14 protein in samples from cows fed the LNHS diet in the current trial may be because either (1) it is less detected due to increased sCD14 association with LPS and their removal by centrifugation, or (2) decrease in shedding of sCD14 by neutrophils and macrophages into the milk. While this protein warrants further exploration, it is not likely the optimal biomarker for targeted identification of dietary carbohydrate-induced shifts.

The acute-phase immunological response elevates acute-phase proteins (**APP**) in animal circulation and tissues because of infection, inflammation, or trauma. Acute-phase proteins, such as serum amyloid A, and haptoglobin, have been studied in cattle, particularly as potential biomarkers of mastitis in milk (Grönlund et al., 2003; Miglio et al., 2013). Recently, studies have focused on identifying new APP inter-α-trypsin inhibitor heavy chain 4 (**ITIH4**) in the milk and whey of cow milk during mastitis (Huang et al., 2014; Soler et al., 2019). Boehmer (2011) suggested ITIH4 and kininogen can be potential candidates for inflammatory biomarkers in bovine milk. Previously, studies have shown the increase of ITIH4 in different inflammatory processes (Piñeiro et al., 1999; Jostins et al., 2012). However, an essential indicator of the disease process may also be a decrease in ITIH4 level. For example, Kashyap et al. (2009) reported that ITIH4 protein was completely absent in patients with acute ischemic stroke compared with the control group, and serum levels returned to normal as acute ischemic stroke patients recovered. Similarly,

the lower abundance of ITIH4 in milk from cows fed the LNHS diet may indicate a diet-induced inflammatory response. Further decreases in the abundance of ITIH4 suggest immune suppression in cows fed the LNHS diet, as the role of the acute phase response is to restore a healthy physiological function (Kushner, 1982). Additionally, kininogens are precursor proteins for kinins and are known to play key roles in complement activation (Discipio, 1982). Like ITIH4, the abundance of kininogen-1 was lower in milk from cows fed the LNHS diet, indicating immune suppression. To support these suggestions, we observed a decrease in the abundance of complement factor I isoform X1, complement factor I isoform X1, and Inter-alpha-trypsin inhibitor heavy chain H2 in milk from cows fed the LNHS diet. While each of these proteins may be potentially valid biomarkers, not all of these proteins can currently be analyzed via commercially available kits, reducing the rapidity of application.

Mitogen-activated protein kinase (**MAPK**) acts as an integration point for multiple biochemical signals and is involved in various cellular processes, including cell proliferation and differentiation, transcriptional regulation, and development. Mitogen-activated protein kinase kinase (**MKK5**) is involved in the innate immune MAPK signaling cascade. Moyes et al. (2010) reported that MAPK9 is implicated as part of cows' immune response to intramammary challenges and negative energy balance. Memon et al. (2019) recently reported that feeding a high concentrate diet to lactating dairy cows alters the udder activity by triggering the MAPK-Nrf2 signaling pathway. In this current trial, we did not measure the LPS concentration, which may have explained our observation of an increase in the abundance of MKK5 in milk from LNHS-fed cows. However, an increase in the abundance of MKK5 may suggest MAPK signaling pathway was triggered in the cows fed

with the LNHS diet. Therefore, further exploration of the impact of diet on the MAPK signaling pathway proteins in the mammary gland could support further characterization and identification of potentially valid biomarkers.

Lipoprotein lipase was a protein of focus herein, as the abundance of LPL in milk was affected by diet in this current study. Lipoprotein lipase is an enzyme associated with triacylglycerol hydrolysis in chylomicrons and very-low-density lipoproteins, converting each triacylglycerol into glycerol and non-esterified fatty acids for tissue utilization (Stins et al., 1992; Bernard et al., 2008). The mammary gland takes up long-chain fatty acids through the action of LPL. The transcript abundance and activity of LPL markedly increase at the onset of lactation to augment the availability of fatty acids to the mammary tissue (Shirley et al., 1973). Alternatively, the transcription of LPL in the mammary gland is decreased by feeding a high concentrate diet in dairy, goats, and cows (Zhao et al., 2014; Ma et al., 2022). Surprisingly, the abundance of LPL was higher in milk from cows fed the LNHS diet in the current trial. We performed an ELISA on the same samples to validate the higher LPL identified by LC-MS/MS. Though a lower magnitude of change, we similarly measured higher concentrations of LPL in milk from cows fed the LNHS diet. As measured through the ELISA validation, the concentration of LPL was significantly higher in the milk from cows fed the LNHS diet at the 0430 h sampling point, supporting our suggestion that biological shifts reflected in the milk due to diet-induced rumen changes are not diurnally uniform across milkings. Studies have reported that LPL is primarily regulated at transcription and post-transcription levels (Doolittle et al., 1990; Muhammad et al., 1998; Hughes et al., 2002). Therefore, LPL mRNA expression is not always accompanied by corresponding increases in LPL synthesis. For example, when rat

adipocytes were treated with epinephrine, there was a decrease in LPL synthesis with no corresponding change in LPL mRNA level (Ong et al., 1992). Jensen et al. (1994) reported that LPL is also regulated at transcription and post-transcriptional levels in the mammary gland of the mouse. Increased abundance of LPL in milk from cows fed the LNHS diet may result from differentially regulating LPL at transcription and post-transcriptional levels. The results of this study indicate that LPL can be a potential biomarker candidate for diet-induced rumen microbial changes and should be further investigated.

3.6 Conclusion

In the present study, 14 rumen microbial proteins across 9 microbial species were impacted due to different diet combinations of peuNDF240 and RFS, with the abundances of 12 microbial proteins across 8 microbial species being impacted due to the diet × time interaction; some of these affected proteins were associated with the energetics pathway. While the functionality of these proteins was predominantly energetics-related and is in line with previous research, the current trial demonstrates the importance of sampling time. Concurrently, 21 milk proteins were affected by dietary treatment, with the abundance of 19 milk proteins being impacted due to the diet × time interaction. Most of these proteins were related to host defense, nutrient synthesis, and transportation. While many of these affected milk proteins warrant further investigation, the impact of diet on milk LPL protein abundance was the focus of our subsequent validation. The higher concentration of LPL with the LNHS diet, confirmed with LC-MS/MS analysis and ELISA, may be a feasible milk biomarker indicative of an altered rumen environment resulting from an altered dietary carbohydrate profile. The results of this study suggest that biological shifts resulting

from diet-induced changes to the rumen microbial environment can be reflected in milk, and milk proteins may be feasible biomarkers for such changes with careful consideration for function and diurnal variability.

Figure 3.1. (A) The average lipoprotein lipase concentration in the milk from cows fed with the low peuNDF240 and high rumen fermentable starch content diet (LNHS) or high peuNDF240 and low rumen fermentable starch content diet (HNLS) determined by ELISA (B) The average lipoprotein lipase concentration in the milk from cows fed with the LNHS or HNLS diet at different sampling time points determined by ELISA. n = 8 cows per treatment (LNHS or HNLS) per time point.

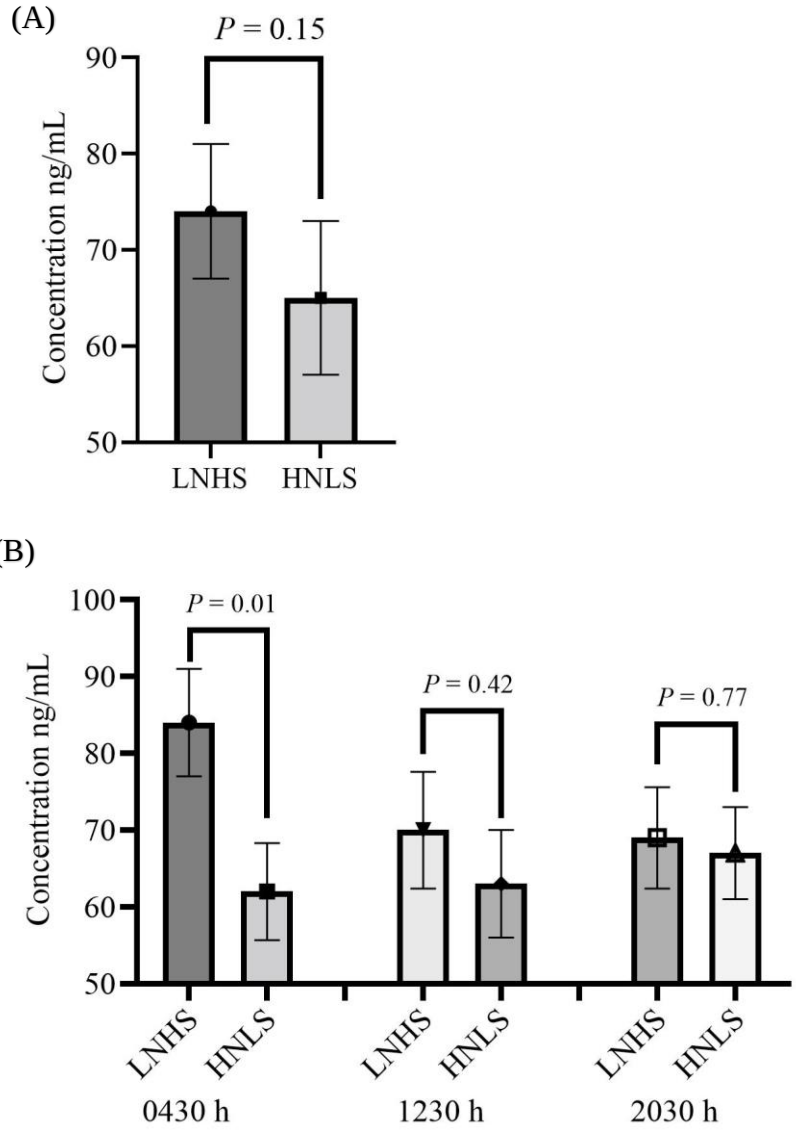

Table 3.1. Impact of a low peuNDF240, high RFS diet fed to lactating Holstein dairy cows on rumen microbial protein abundances at different sampling time points. n = 8 cows per treatment (LNHS or HNLS) per time point.

Accession no.	Proteins	Species	0600 h		1000 h		1400 h		*P*
			HNLS	LNHS	HNLS	LNHS	HNLS	LNHS	value
A0A1H7FBX7	Pyruvate, phosphate dikinase	*Pseudobutyrivibrio ruminis*	84[a]	88[a]	91[a]	85[a]	98[a]	82[b]	<0.05
A0A1M6YX51	Glutamate dehydrogenase	*Prevotella ruminicola*	101[a]	111[a]	102[a]	104[a]	93[a]	124[b]	<0.05
A0A1M7L8N4	Pyruvate, phosphate dikinase	*Ruminococcus flavefaciens*	91[a]	92[a]	105[a]	106[a]	112[a]	95[b]	<0.05
D5EWS5	60 kDa chaperonin	*Prevotella ruminicola (strain ATCC 19189)*	125[a]	129[a]	112[a]	94[a]	89[a]	123[b]	<0.05
A0A1M6VCT7	Fructose-bisphosphate aldolase	*Prevotella ruminicola*	136[a]	124[a]	117[a]	109[a]	101[a]	146[b]	<0.05
A0A011VU56	NADH dehydrogenase	*Ruminococcus albus*	98[a]	107[a]	125[a]	114[a]	116[a]	84[b]	<0.05
A0A1D9P306	Glutamate dehydrogenase	*Butyrivibrio hungatei*	93[a]	98[a]	91[a]	106[b]	92[a]	99[a]	<0.05
A0A1H7G5V3	NifU homolog involved in Fe-S cluster formation	*Pseudobutyrivibrio ruminis*	105[a]	83[a]	124[a]	80[b]	90[a]	84[a]	<0.05
D8DWJ0	Pyruvate-ferredoxin/flavodoxin oxidoreductase	*Prevotella bryantii B14*	107[a]	109[a]	105[a]	126[b]	98[a]	99[a]	<0.05
A0A1H6LFS4	TonB-linked outer membrane protein, SusC/RagA family	*Prevotella ruminicola*	97[a]	96[a]	91[a]	116[b]	111[a]	112[a]	<0.05
A0A0L6JXI6	NifU_N domain-containing protein	*Pseudobacteroides cellulosolvens ATCC*	69[a]	55[b]	76[a]	68[a]	78[a]	73[a]	<0.05
D8DZJ1	Glyceraldehyde-3-phosphate dehydrogenase	*Prevotella bryantii B14*	131[a]	108[b]	126[a]	122[a]	113[a]	123[a]	<0.05

[a-b]Mean values in the sampling point with different superscripts differ ($P < 0.05$)

[1]HNLS = high peuNDF240 and low rumen fermentable starch content diet

[2]LNHS = low peuNDF240 and high rumen fermentable starch content diet

Table 3.2. Impact of feeding a low peuNDF240, high RFS diet to lactating Holstein cows on milk protein abundances at different milking times. n = 8 cows per treatment (LNHS or HNLS) per time point.

Accession no.	Proteins	0430 h		1230 h		2030 h		*P* value
		HNLS	LNHS	HNLS	LNHS	HNLS	LNHS	
A0A140T8A9	Kappa-casein	260[a]	479[b]	303[a]	276[a]	479[a]	410[a]	<0.05
A0JNP2	Secretoglobin family 1D member	144[a]	357[b]	229[a]	256[a]	357[a]	304[a]	<0.05
E1BI01	Mitogen-activated protein kinase 5	64[a]	66[a]	53[a]	118[b]	66[a]	92[a]	<0.05
F1MMD7	Inter-alpha-trypsin inhibitor heavy chain H4	104[a]	70[b]	89[a]	85[a]	70[a]	88[a]	<0.05
F1MNT4	Laminin subunit beta 1	90[a]	56[b]	72[a]	66[a]	56[a]	73[a]	<0.05
F1MNV5	Kininogen-1	98[a]	71[b]	84[a]	90[a]	71[a]	90[a]	<0.05
F1MNW4	Inter-alpha-trypsin inhibitor heavy chain H2	105[a]	77[b]	97[a]	104[a]	77[a]	92[a]	<0.05
F1N4M7	Complement factor I isoform X1	87[a]	63[b]	74[a]	85[a]	63[a]	77[a]	<0.05
F1N5M2	Vitamin D-binding protein	80[a]	64[a]	68[a]	86[b]	64[a]	75[a]	<0.05
G5E5T5	Immunogloin M heavy chain secretory form	81[a]	62[b]	81[a]	75[a]	62[a]	68[a]	<0.05
P02662	Alpha-S1-casein	256[a]	562[b]	430[a]	405[a]	562[a]	462[a]	<0.05
P11151	Lipoprotein lipase	428[a]	1331[b]	720[a]	1042[a]	666[a]	1256[b]	<0.05
P17690	Beta-2-glycoprotein	89[a]	56[b]	82[a]	92[a]	56[a]	91[a]	<0.05
P79345	Epididymal secretory protein E1	111[a]	73[b]	83[a]	95[a]	73[a]	97[a]	<0.05
Q0IIH5	Nucleobindin 2	86[a]	64[b]	77[a]	87[a]	64[a]	86[a]	<0.05
Q28085	Complement factor H	173[a]	134[b]	177[a]	138[a]	134[a]	162[a]	<0.05
Q3MHN2	Complement component C9	70 [a]	69[a]	62[a]	86[b]	69[a]	90[a]	<0.05
Q3T000	Synaptobrevin homolog YKT6	100[a]	77[b]	95[a]	89[a]	77[a]	103[a]	<0.05
Q58DP6	Ribonuclease 4	98[a]	67[b]	80[a]	93[a]	67[a]	94[a]	<0.05
Q95122	Monocyte differentiation antigen CD14	106[a]	76[b]	92[a]	85[a]	76[a]	92[a]	<0.05

[a-b]Mean values in the sampling point with different superscripts differ ($P < 0.05$)

[1]HNLS = high peuNDF240 and low rumen fermentable starch content diet

[2]LNHS = low peuNDF240 and high rumen fermentable starch content diet

3.7 References

Akhlaghi, B., E. Ghasemi, M. Alikhani, A. Ghaedi, S. Nasrollahi, and M. H. Ghaffari. 2022. Influence of reducing starch in the diets with similar protein and energy contents on lactation performance, ruminal fermentation, digestibility, behaviour and blood metabolites in primiparous and multiparous dairy cows. Vet. Med. Sci. 8:808-821. https://doi.org/10.1002/vms3.722

Allen, M. and D. J. Mertens 1988. Evaluating constraints on fiber digestion by rumen microbes. J. Nutr. 118:261-270. https://doi.org/10.1093/jn/118.2.261

Alzahal, O., M. Or-Rashid, S. L. Greenwood, M. Douglas, and B. J. McBride. 2009. The effect of dietary fiber level on milk fat concentration and fatty acid profile of cows fed diets containing low levels of polyunsaturated fatty acids. J. Dairy Sci. 92:1108-1116. https://doi.org/10.3168/jds.2008-1472

Aoki, T. and S. Narumiya. 2012. Prostaglandins and chronic inflammation. Trends Pharmacol. Sci. 33:304-311. https://doi.org/10.1016/j.tips.2012.02.004

Arias, M. A., J. Nores, N. Vita, F. Stelter, L. K. Borysiewicz, P. Ferrara, and M. Labéta. 2000. Cutting edge: human B cell function is regulated by interaction with soluble CD14: opposite effects on IgG1 and IgE production. J. Immunol. 164:3480-3486. https://doi.org/10.4049/jimmunol.164.7.3480

Bazil, V. and J. Strominger. 1991. Shedding as a mechanism of down-modulation of CD14 on stimulated human monocytes. J. Immunol. 147:1567-1574.

Beauchemin, K., W. Yang, and L. Rode. 2003. Effects of particle size of alfalfa-based dairy cow diets on chewing activity, ruminal fermentation, and milk production. J. Dairy Sci. 86:630-643. https://doi.org/10.3168/jds.S0022-0302(03)73641-8

Bernard, L., C. Leroux, and Y. Chilliard. 2008. Expression and nutritional regulation of lipogenic genes in the ruminant lactating mammary gland. Pages 67-108 in Bioactive Components of Milk. Z. Bösze, ed. Springer, New York, NY. https://doi.org/10.1017/S1751731110000510

Boehmer, J., D. Bannerman, K. Shefcheck, and J. Ward. 2008. Proteomic analysis of differentially expressed proteins in bovine milk during experimentally induced Escherichia coli mastitis. J. Dairy Sci. 91:4206-4218. https://doi.org/10.3168/jds.2008-1297

Boehmer, J. L. 2011. Proteomic analyses of host and pathogen responses during bovine mastitis. Mammary Gland Biol Neoplasia. 16:323-338. https://doi.org/10.1007/s10911-011-9229-x

Cantalapiedra-Hijar, G., J. L. Peyraud, S. Lemosquet, E. Molina-Alcaide, H. Boudra, P. Noziere, and I. Ortigues-Marty. 2014. Dietary carbohydrate composition modifies the milk N efficiency in late lactation cows fed low crude protein diets. Animals. 8:275-285. https://doi.org/10.1017/S1751731113002012

Conrad, H., A. Pratt, and J. W. Hibbs. 1964. Regulation of feed intake in dairy cows. I. Change in importance of physical and physiological factors with increasing digestibility. J. Dairy Sci. 47:54-62. https://doi.org/10.3168/jds.S0022-0302(64)88581-7

Cook, N. B., K. V. Nordlund, and G. Oetzel. 2004. Environmental influences on claw horn lesions associated with laminitis and subacute ruminal acidosis in dairy cows. J. Dairy Sci. 87:E36-E46. https://doi.org/10.3168/jds.S0022-0302(04)70059-4

Danscher, A. M., S. Li, P. H. Andersen, E. Khafipour, N. B. Kristensen, and J. C. Plaizier. 2015a. Indicators of induced subacute ruminal acidosis (SARA) in Danish Holstein cows. Acta Vet. Scand. 57:1-14. https://doi.org/10.1186/s13028-015-0128-9

Dirksen, G., H. Liebich, and E. Mayer. 1985. Adaptive changes of the ruminal mucosa and their functional and clinical significance. AABP. 116-120. https://doi.org/10.21423/bovine-vol1985no20p116-120

Discipio, R. J. 1982. The activation of the alternative pathway C3 convertase by human plasma kallikrein. BSI. 45:587.

Dong, G., S. Liu, Y. Wu, C. Lei, J. Zhou, and S. Zhang. 2011. Diet-induced bacterial immunogens in the gastrointestinal tract of dairy cows: impacts on immunity and metabolism. Acta Vet. Scand. 53:1-7. https://doi.org/10.1186/1751-0147-53-48

Doolittle, M. H., O. Ben-Zeev, J. Elovson, D. Martin, and T. Kirchgessner. 1990. The response of lipoprotein lipase to feeding and fasting. Evidence for posttranslational regulation. J. Biol. Chem. 265:4570-4577.

Emmanuel, D., S. Dunn, and B. Ametaj. 2008. Feeding high proportions of barley grain stimulates an inflammatory response in dairy cows. J. Dairy Sci. 91:606-614. https://doi.org/10.3168/jds.2007-0256

Filipp, D., K. Alizadeh-Khiavi, C. Richardson, A. Palma, N. Paredes, O. Takeuchi, S. Akira, and M. Julius. 2001. Soluble CD14 enriched in colostrum and milk induces B cell growth and differentiation. PNAS. 98:603-608. https://doi.org/10.1073/pnas.98.2.603

Fustini, M., A. Palmonari, G. Canestrari, E. Bonfante, L. Mammi, M. Pacchioli, G. Sniffen, R. Grant, K. Cotanch, and A. Formigoni. 2017. Effect of undigested neutral detergent fiber content of alfalfa hay on lactating dairy cows: Feeding behavior, fiber digestibility, and lactation performance. J. Dairy Sci. 100:4475-4483. https://doi.org/10.3168/jds.2016-12266

Garrett, E., M. Pereira, K. Nordlund, L. Armentano, W. Goodger, and G. Oetzel. 1999. Diagnostic methods for the detection of subacute ruminal acidosis in dairy cows. J. Dairy Sci. 82:1170-1178. https://doi.org/10.3168/jds.S0022-0302(99)75340-3

Gozho, G., D. Krause, and J. C. Plaizier. 2007. Ruminal lipopolysaccharide concentration and inflammatory response during grain-induced subacute ruminal acidosis in dairy cows. J. Dairy Sci. 90:856-866. https://doi.org/10.3168/jds.S0022-0302(07)71569-2

Grant, R. J. 1997. Interactions among forages and nonforage fiber sources. J. Dairy Sci. 80:1438-1446. https://doi.org/10.3168/jds.S0022-0302(97)76073-9

Grant, R., W. Smith, and M. J. Miller. 2020. Relationships between fibre digestibility and particle size for lactating dairy cows. Adv. Dairy Technol. 32:47-57.

Grönlund, U., C. Hultén, P. D. Eckersall, C. Hogarth, and K. Waller. 2003. Haptoglobin and serum amyloid A in milk and serum during acute and chronic experimentally induced Staphylococcus aureus mastitis. J. Dairy Res. 70:379-386. https://doi.org/10.1017/S0022029903006484

Harris, P., K. M. Johannessen, G. Smolenski, M. Callaghan, M. K. Broadhurst, K. Kim, and T. Wheeler. 2010. Characterisation of the antimicrobial activity of bovine milk ribonuclease4 and ribonuclease5 (angiogenin). Int. Dairy J. 20:400-407. https://doi.org/10.1016/j.idairyj.2009.12.018

Hart, E., C. Creevey, T. Hitch, and A. Kingston-Smith. 2018. Meta-proteomics of rumen microbiota indicates niche compartmentalisation and functional dominance in a limited number of metabolic pathways between abundant bacteria. Sci. Rep. 8:1-11. https://doi.org/10.1038/s41598-018-28827-7

Haziot, A., S. Chen, E. Ferrero, M. Low, R. Silber, and S. Goyert. 1988. The monocyte differentiation antigen, CD14, is anchored to the cell membrane by a phosphatidylinositol linkage. J. Immunol. Res. 141:547-552.

Haziot, A., G. W. Rong, V. Bazil, J. Silver, and S. Goyert. 1994. Recombinant soluble CD14 inhibits LPS-induced tumor necrosis factor-alpha production by cells in whole blood. J. Immunol. Res. 152:5868-5876.

Haziot, A., B.-Z. Tsuberi, and S. Goyert. 1993. Neutrophil CD14: biochemical properties and role in the secretion of tumor necrosis factor-alpha in response to lipopolysaccharide. J. Immunol. Res. 150:5556-5565.

Heinrichs, J. and P. Kononoff, University Park, PA. DSE. 2013. The Penn state particle separator. 186:1-8.

Honan, M. C. and S. L. Greenwood. 2020. Characterization of variations within the rumen metaproteome of Holstein dairy cattle relative to morning feed offering. Sci. Rep. 10:1-8. https://doi.org/10.1038/s41598-020-59974-5

Hook, S. E., M. A. Steele, K. S. Northwood, J. Dijkstra, J. France, A.-D. G. Wright, and B. W. McBride. 2011. Impact of subacute ruminal acidosis (SARA) adaptation and recovery on the density and diversity of bacteria in the rumen of dairy cows. FEMS Microbiol. Ecol. 78:275-284. https://doi.org/10.1111/j.1574-6941.2011.01154.x

Hughes, T. R., T. S. Tengku-Muhammad, S. A. Irvine, and D. P. Ramji. 2002. A novel role of Sp1 and Sp3 in the interferon-γ-mediated suppression of macrophage lipoprotein lipase gene transcription. J. Biol. Chem. 277:11097-11106. https://doi.org/10.1074/jbc.M106774200

Hussein, H. A., J.-P. Thurmann, and R. J. B. Staufenbiel. 2020. 24-h variations of blood serum metabolites in high yielding dairy cows and calves. BMC Vet. Res. 16:1-11. https://doi.org/10.1186/s12917-020-02551-9

Jack, R. S., U. Grunwald, F. Stelter, G. Workalemahu, and C. J. Schütt. 1995. Both membrane-bound and soluble forms of CD14 bind to Gram-negative bacteria. Eur. J. Immunol. 25:1436-1441. https://doi.org/10.1002/eji.1830250545

Jensen, D. R., S. Gavigan, V. Sawicki, D. L. Witsell, R. H. Eckel, and M. C. Neville. 1994. Regulation of lipoprotein lipase activity and mRNA in the mammary gland of the lactating mouse. Biochem. 298:321-327. https://doi.org/10.1042/bj2980321

Jostins, L., S. Ripke, R. K. Weersma, R. H. Duerr, D. P. McGovern, K. Y. Hui, J. C. Lee, L. Philip Schumm, Y. Sharma, and C. A. Anderson. 2012. Host–microbe interactions have shaped the genetic architecture of inflammatory bowel disease. Nature. 491:119-124. https://doi.org/10.1038/nature11582

Kashyap, R. S., A. R. Nayak, P. S. Deshpande, D. Kabra, H. J. Purohit, G. M. Taori, and H. F. Daginawala. 2009. Inter-α-trypsin inhibitor heavy chain 4 is a novel marker of acute ischemic stroke. Clin. Chim. Acta. 402:160-163. https://doi.org/10.1016/j.cca.2009.01.009

Khafipour, E., D. Krause, and J. Plaizier. 2009a. Alfalfa pellet-induced subacute ruminal acidosis in dairy cows increases bacterial endotoxin in the rumen without causing inflammation. J. Dairy Sci. 921712-1724. https://doi.org/10.3168/jds.2008-1656

Kushner, I. J. 1982. The phenomenon of the acute phase response. Ann. N. Y. Acad. Sci. 389:39-48. https://doi.org/10.1111/j.1749-6632.1982.tb22124.x

Lee, J.-W., M. Paape, T. Elsasser, and X. J. Zhao. 2003a. Elevated milk soluble CD14 in bovine mammary glands challenged with Escherichia coli lipopolysaccharide. J. Dairy Sci. 86:2382-2389. https://doi.org/10.3168/jds.S0022-0302(03)73832-6

Lee, J. W., M. J. Paape, and X. J. Zhao. 2003b. Recombinant bovine soluble CD14 reduces severity of experimental Escherichia coli mastitis in mice. Vet. Res**.** 34:307-316. https://doi.org/10.1051/vetres:2003006

Lehrer, R. I., D. Szklarek, A. Barton, T. Ganz, K. Hamann, and G. J. Gleich. 1989. Antibacterial properties of eosinophil major basic protein and eosinophil cationic protein. J. Immunol. Res. 142:4428-4434.

Ma, N., J. Abaker, G. Wei, H. Chen, X. Shen, and G. J. Chang. 2022. A high-concentrate diet induces an inflammatory response and oxidative stress and depresses milk fat synthesis in the mammary gland of dairy cows. J. Dairy Sci. 105: 5493-5505. https://doi.org/10.3168/jds.2021-21066

Maes, P., D. Damart, C. Rommens, J. Montreuil, G. Spik, and A. J. Tartar. 1988. The complete amino acid sequence of bovine milk angiogenin. FEBS Lett. 241:41-45. https://doi.org/10.1016/0014-5793(88)81027-5

Mertens, D. J. 1997. Creating a system for meeting the fiber requirements of dairy cows. J. Dairy Sci. 80:1463-1481. https://doi.org/10.3168/jds.S0022-0302(97)76075-2

Memon, M. A., Y. Wang, T. Xu, N. Ma, H. Zhang, A.-C. Roy, Z. ul Aabdin, and X. Shen. 2019. Lipopolysaccharide induces oxidative stress by triggering MAPK and Nrf2 signalling pathways in mammary glands of dairy cows fed a high-concentrate diet. Microb. Pathog. 128:268-275. https://doi.org/10.1002/vms3.615

Miglio, A., L. Moscati, G. Fruganti, M. Pela, E. Scoccia, A. Valiani, and C. J. Maresca. 2013. Use of milk amyloid A in the diagnosis of subclinical mastitis in dairy ewes. J. Dairy Res. 80:496-502. https://doi.org/10.1017/S0022029913000484

Moyes, K. M., J. K. Drackley, D. E. Morin, S. L. Rodriguez-Zas, R. E. Everts, H. A. Lewin, and J. J. Loor. 2010. Mammary gene expression profiles during an intramammary challenge reveal potential mechanisms linking negative energy balance with impaired immune response. Physiol. Genomics. 41:161-170. https://doi.org/10.1152/physiolgenomics.00197.2009

Mulakala, B., K. Smith, M. Snider, A. Ayers, M. Honan, and S. Greenwood. 2022. Influence of dietary carbohydrate profile on the dairy cow rumen meta-proteome. J. Dairy Sci. 105:8485-8496. https://doi.org/10.3168/jds.2022-21812

Mulakala, Bharath kumar (2022), "Mulakala et al. 2022. JDS, Supplementary Tables", Mendeley Data, v1.

Murata, M., H. Wakabayashi, K. Yamauchi, and F. J. Abe. 2013. Identification of milk proteins enhancing the antimicrobial activity of lactoferrin and lactoferricin. J. Dairy Sci. 96:4891-4898. https://doi.org/10.3168/jds.2013-6612

National Academies of Sciences, Enginnering, and Medicine. 2021. Nutrient Requirements of Dairy Cattle. 8th rev. ed. Natl. Acad. Sci., Washington, DC. https://doi.org/10.17226/25806

Ogunade, I., A. Pech-Cervantes, and H. J. Schweickart. 2019. Metatranscriptomic analysis of sub-acute ruminal acidosis in beef cattle. Animals. 9:232. https://doi.org/10.3390/ani9050232

Ong, J. M., B. Saffari, R. B. Simsolo, and P. A. Kern. 1992. Epinephrine inhibits lipoprotein lipase gene expression in rat adipocytes through multiple steps in post-transcriptional processing. Mol. Endocrinol. 6:61-69. https://doi.org/10.1210/mend.6.1.1738372

Overton, T., J. McArt, and D. J. Nydam. 2017. A 100-Year Review: Metabolic health indicators and management of dairy cattle. J. Dairy Sci. 100:10398-10417. https://doi.org/10.3168/jds.2017-13054

Pitta, D. W., N. Indugu, B. Vecchiarelli, D. E. Rico, and K. J. Harvatine. 2018. Alterations in ruminal bacterial populations at induction and recovery from diet-induced milk fat

depression in dairy cows. J Dairy Sci 101:295–309. https://doi.org/10.3390/metabo9070154

Piñeiro, M., M. A. A. Alava, N. González-Ramón, J. Osada, P. Lasierra, L. Larrad, A. Piñeiro, and F. Lampreave. 1999. ITIH4 serum concentration increases during acute-phase processes in human patients and is up-regulated by interleukin-6 in hepatocarcinoma HepG2 cells. Biochem. Biophys. Res. Commun. 263:224-229. https://doi.org/10.1006/bbrc.1999.1349

Puppel, K., P. Staniszewska, M. Gołębiewski, J. Slósarz, G. Grodkowski, P. Solarczyk, M. Kunowska-Slósarz, P. Kostusiak, B. Kuczyńska, and T. J. Przysucha. 2021. Using the Relationship between Concentrations of Selected Whey Proteins and BHBA to Characterize the Metabolism of Dairy Cows in Early Lactation. Animals. 11:2298. https://doi.org/10.3390/ani11082298

Raffrenato, E., D. Ross, and M. J. Van Amburgh. 2018. Development of an in vitro method to determine rumen undigested aNDFom for use in feed evaluation. J. Dairy Sci. 101:9888-9900. https://doi.org/10.3168/jds.2018-15101

Ramos, S. C., C. D. Jeong, L. L. Mamuad, S. H. Kim, S. H. Kang, E. T. Kim, Y. I. Cho, S. S. Lee, and S. S. Lee. 2021. Diet transition from high-forage to high-concentrate alters rumen bacterial community composition, epithelial transcriptomes and ruminal fermentation parameters in dairy cows. Animals. 11:838. https://doi.org/10.3390/ani11030838

Rosenberg, H. F. and J. B. Domachowske. 2001. Eosinophils, eosinophil ribonucleases, and their role in host defense against respiratory virus pathogens. J. Leukoc. Biol. 70:691-698.

Shirley, J., R. Emery, E. Convey, and W. J. Oxender. 1973. Enzymic changes in bovine adipose and mammary tissue, serum and mammary tissue hormonal changes with initiation of lactation. J. Dairy Sci. 56:569-574.

Solano, J., F. Galindo, A. Orihuela, and C. Galina. 2004. The effect of social rank on the physiological response during repeated stressful handling in Zebu cattle (*Bos indicus*). Physiol. Behav. 82:679-683.

Soler, L., R. Dąbrowski, N. García, M. A. Alava, F. Lampreave, M. Piñeiro, W. Wawron, M. Szczubiał, and M. J. Bochniarz. 2019. Acute-phase inter-alpha-trypsin inhibitor heavy chain 4 (ITIH4) levels in serum and milk of cows with subclinical mastitis caused by *Streptococcus* species and coagulase-negative *Staphylococcus* species. J. Dairy Sci. 102:539-546. https://doi.org/10.1016/j.physbeh.2004.06.005

Smith, K. M. 2021. The effect of physically effective undegradable neutral detergent fiber and rumen fermentable starch on lactating Holstein cows. MS Thesis. Department of Animal and Veterinary Sciences, The University of Vermont, Burlington, VT. https://scholarworks.uvm.edu/graddis/1384

Steele, M., L. Dionissopoulos, O. Alzahal, J. Doelman, and B. W. McBride. 2012. Rumen epithelial adaptation to ruminal acidosis in lactating cattle involves the coordinated expression of insulin-like growth factor-binding proteins and a cholesterolgenic enzyme. J. Dairy Sci. 95:318-327. https://doi.org/10.3168/jds.2011-4465

Stefanska, B., W. Człapa, E. Pruszynska-Oszmałek, D. Szczepankiewicz, V. Fievez, J. Komisarek, K. Stajek, and W. J. Nowak. 2018. Subacute ruminal acidosis affects fermentation and endotoxin concentration in the rumen and relative expression of the CD14/TLR4/MD2 genes involved in lipopolysaccharide systemic immune response in dairy cows. J. Dairy Sci. 101:1297-1310. https://doi.org/10.3168/jds.2017-12896

Stins, M. F., F. R. Maxfield, and I. J. Goldberg. 1992. Polarized binding of lipoprotein lipase to endothelial cells. Implications for its physiological actions. Arterioscler. Thromb. Vasc. Biol.12:1437-1446.
https://doi.org/10.1161/01.ATV.12.12.1437

Tacoma, R., J. Fields, D. B. Ebenstein, Y.-W. Lam, and S. L. Greenwood. 2016. Comparative proteomics dataset of skimmed milk samples from Holstein and Jersey dairy cattle. Data Br. 6:843-846. https://doi.org/10.1016/j.dib.2016.01.038

Wright, S. D., R. A. Ramos, A. Hermanowski-Vosatka, P. Rockwell, and P. A. Detmers. 1991. Activation of the adhesive capacity of CR3 on neutrophils by endotoxin: dependence on lipopolysaccharide binding protein and CD14. J. Exp. Med. 173:1281-1286. https://doi.org/10.1084/jem.173.5.1281

Zebeli, Q., J. Dijkstra, M. Tafaj, H. Steingass, B. Ametaj, and W. J. Drochner. 2008. Modeling the adequacy of dietary fiber in dairy cows based on the responses of ruminal pH and milk fat production to composition of the diet. J. Dairy Sci. 91:2046-2066. https://doi.org/10.3168/jds.2007-0572

Zeng, H., C. Guo, D. Sun, H. Seddik, and S. Mao. 2019. The ruminal microbiome and metabolome alterations associated with diet-induced milk fat depression in dairy cows. Metabolites 9:154. https://doi.org/10.3390/metabo9070154

Zhang, L., S. Boeren, A. Van Hooijdonk, J. Vervoort, and K. J. Hettinga. 2015. A proteomic perspective on the changes in milk proteins due to high somatic cell count. J. Dairy Sci. 98:5339-5351. https://doi.org/10.3168/jds.2014-9279

Zhao, M., D. Bu, J. Wang, X. Zhou, D. Zhu, T. Zhang, J. Niu, and L. Ma. 2016. Milk production and composition responds to dietary neutral detergent fiber and starch ratio in dairy cows. Anim. Sci. J. 87:756-766. https://doi.org/10.1111/asj.12482

Zhao, W. S., S. L. Hu, K. Yu, H. Wang, W. Wang, J. Loor, and J. Luo. 2014. Lipoprotein lipase, tissue expression and effects on genes related to fatty acid synthesis in goat mammary epithelial cells. Int. J. Mol. Sci. 15:22757-22771.

CHAPTER 4: INTRA-RUMINAL PROPIONATE DOSAGE ALTERS THE RUMEN EPITHELIAL TRANSCRIPTOME PROFILE OF HOLSTEIN COWS.

4.1 Abstract

The rumen epithelium undergoes substantial functional adjustments at the molecular level in response to the altered rumen environment induced by increasing the fermentability of the diet. As the ruminal propionate concentration is positively correlated with diet fermentability, further characterization of rumen transcriptome changes in response to rumen propionate concentration supports the refinement of nutritional strategies supportive of dairy cow health and productivity. The objective of this study was to investigate the effects of intra-ruminal propionate dosing on the rumen epithelial transcriptome. Four ruminally-cannulated Holstein cows were included in a 2 × 2 crossover design with two 7-d experimental periods. In each period, cows were ruminally dosed daily with either sodium propionate [1 % of dry matter intake (DMI)] or sodium chloride (0.6% of DMI)]. On d 5, 6, and 7 of each period, rumen fluid and blood samples were collected from each cow at 1000 and 1430 h, and composite milk samples were collected from each cow during both a.m. and p.m. milkings (0430 and 1630 h, respectively). Rumen fluid was filtered through four layers of cheesecloth, and fluid was stored until analysis of rumen metabolite concentrations. Plasma was harvested from blood and stored prior to analysis. The plasma concentrations of insulin, glucose, non-esterified fatty acid (NEFA), lipopolysaccharide (LPS), haptoglobin (Hp), lipopolysaccharide-binding protein (LBP), and serum amyloid A (SAA) were determined using bovine-specific ELISA kits. Contents of milk fat, protein, other solids, Hp, LPL, LBP and SAA were also determined. Rumen epithelial biopsies

were collected on d 7 from each cow in each period and stored in a stabilization solution. Biopsy samples were submitted for commercial mRNA extraction and sequencing. The PROC MIXED procedure of SAS 9.4 was used to assess the impact of treatment and time of sampling on analyzed parameters. Using the HISAT2 alignment tool, the clean reads obtained from samples were aligned to the *Bos taurus* genome assembly ARS-UCD 1.3, while DESEQ2 was used to detect differentially expressed genes (DEGs). Functional annotation of DEGs was performed using the PANTHER classification system, and pathway enrichment analysis of DEGs was performed using g:Profiler. Milk protein content was lower due to propionate treatment. No other plasma or milk parameters were affected by treatment. Rumen metabolite concentrations did not differ across treatments. However, propionate treatment resulted in 331 DEGs, of which 146 and 185 were down- and up-regulated, respectively. The identified DEGs were involved in cell growth division events, lipid transport and metabolism, protein metabolism, transport activity, and immune function. For example, the expressions of immune-associated genes *TLR 2*, *CD46*, *CD63*, *HM13*, *CCL20*, and *IRF2BPL*, were down-regulated in response to propionate dosage. In contrast, expression of immune-associated genes *LOC101909777*, *LOC104973096*, *LOC112441460* and *IL37* were up-regulated in response to propionate dosage. The pathway enrichment analysis of identified DEGs in this study revealed that MAPK1/MAPK3 signaling pathway was significantly enriched. Further, DEGs involved in the MAPK1/MAPK3 signaling pathway were down-regulated, indicating negative regulation of cell growth in the rumen epithelium of propionate-treated cows. These results indicate that the rumen epithelial adaptation in response to propionate-induced altered rumen environment includes regulating epithelial genes involved in a diversity of

functions, including some critical to cellular and animal health. The results of this study highlight that intra-ruminal propionate dosage resulted in significant changes in transcriptome profiles of rumen epithelium.

4.2 Introduction

Lactating dairy cows are often fed a highly fermentable diet to maximize energy intake and production. Maximizing energy is important; however, feeding a highly fermentable diet also results in physiologic changes. For instance, increasing the fermentability of the dairy diet alters rumen function, leading to increased volatile fatty acid (**VFA**) production, reduced rumination and salivation, decreased rumen pH, and altered rumen microbial composition (Dias et al., 2018; Li et al., 2021). These changes impact rumen nutrients utilization efficiency and ultimately impact cow production and health.

The ruminal epithelium plays an essential role in the dairy cow's adaptation to a highly fermentable diet. In these conditions, the initial response of the rumen epithelium is to increase its surface area for VFA absorption (Goodlad and Integration, 1981; Gäbel et al., 1987) to maintain the normal function of the rumen. In addition to morphological adaptations, the rumen epithelium undergoes functional adjustments at the molecular level in response to the diet-induced altered rumen environment. For example, Gholizadeh et al. (2020) reported that feeding a high-grain diet to beef steers resulted in differential expression of rumen epithelial genes involved in filament organization, positive regulation of epithelial regulation, and immune response. In another study, the genes involved in cell signaling and morphogenesis were differentially expressed in the rumen epithelial tissue

of high starch-fed beef calves (Li et al., 2019). Further, the presence and magnitude of diet-induced rumen epithelial tissue damage determines the animal's susceptibility to post-absorptive metabolic dysfunction. For example, Liu et al. (2013) reported that the ruminal free lipopolysaccharide (**LPS**) concentration was higher in high grain-fed goats compared with hay-fed goats. Further, the authors reported an increase in the LPS concentration in the peripheral blood of high grain-fed goats while not in the hay-fed goats as a result of altered epithelial structure and mRNA expression of epithelial tight junction proteins in high grain-fed goats. Cumulatively, these earlier reports suggest that the regulation of epithelial transcriptomic changes is due to an altered rumen environment. Given the importance of nutrient uptake across the rumen epithelium for productivity and animal health, particularly for production parameters such as lactation that are intensely energy-demanding and reliant on nutritional management, further characterization of these epithelial changes in response to diet is critical.

While alteration of the base diet in experimental conditions supports this research, another method to determine causal impacts is to use intra-ruminal dosing techniques to explore more direct relationships. An example is the recent work published by Baldwin et al. (2018), who studied rumen epithelial transcriptomic changes in dairy cows in response to intra-ruminal butyrate infusion. Authors reported that rumen epithelial genes related to the mitotic cell cycle process, cell cycle process, regulation of cell cycle, translation, peptide biosynthetic process, peptide metabolic process, and cellular amide metabolic process were regulated due to intra-ruminal butyrate infusion. These findings suggest that individual VFA produced in the rumen can regulate the genomic activities of rumen

epithelium, ultimately influencing rumen nutrient utilization efficiency. Since ruminant consumption of high starch diets results in a greater proportion of propionate production within the rumen, understanding the epithelial transcriptomic changes in response to the propionate concentration in the rumen would be beneficial. Previously, intra-ruminal propionate infusion induced a hypophagic effect in lactating dairy cows (Oba and Allen, 2003), and in another study, intra-ruminal propionate infusion decreased serum non-esterified fatty acid (**NEFA**) concentration in steers (Oh et al., 2015). Recently, Zhan et al. (2020) reported propionate infusion up-regulated genes related to gluconeogenic pathways in bovine intestinal epithelial cells. However, there are limited studies on the impact of propionate on rumen epithelial transcriptome, a critical piece to devising strategies that improve rumen nutrition utilization and function in high starch feeding systems. We hypothesized that ruminal propionate regulates genes related to major biological processes in the ruminal epithelial tissue. This study aimed to characterize the rumen transcriptomic profile changes in response to propionate-induced altered rumen environment using intra-ruminal dosage as a model of increased nutritionally induced propionate concentration in the rumen.

4.3 Materials and Methods

4.3.1 Animals, Diets, and Experimental Design

The experimental protocol was reviewed and approved by the Institutional Animal Care and Use Committee of the University of Vermont (Protocol # 2021-00072), and animal procedures were done in accordance with the requirements of the Office of Laboratory Animal Welfare. Four ruminally-cannulated lactating Holstein dairy cows were

selected and blocked by days in milk (**DIM**) and parity. The cows were included in a 2 × 2 crossover design trial with two 7-d experimental periods at the Paul R. Miller Research and Educational Center (The University of Vermont, Burlington, VT, USA). All cows were fed a balanced dietary ration (Supplementary Table S6) ad libitum and offered TMR twice daily at 0630 and 1430 h. Cows within the block received either a ruminal dosage of 1) sodium propionate (propionate; Sigma-Aldrich St. Louis, MO) at a dosage of 1% of DMI or 2) sodium chloride (control; Sigma-Aldrich St. Louis, MO) at a dosage of 0.6% of DMI and received the opposite treatment in the second period. The control dose of sodium chloride was calculated to provide an equal amount of moles of sodium ions as the propionate treatment. Experimental periods were separated by a 7-d washout period during which all cows received only the balanced TMR.

4.3.2 Feed Sampling and Analyses

For 3 d prior to period 1 and during each experimental period, the weight of the TMR offered to each cow each day was recorded and refused feed per cow was removed and weighed each day before morning feeding (0630 h) to determine individual DMI. Samples of TMR and feed refusals were collected throughout each experimental period and stored at -20 °C for further analysis. Refusal samples were dried at 65 °C for 48 h to determine the DM content. The TMR samples were composited within the period (n=2; one sample from each period) and submitted for wet chemistry analysis (Dairy One, Ithaca, NY).

4.3.3 Blood and Rumen Fluid Samples Collection

Blood and rumen fluid samples were collected from each cow on the last three days of each experimental period (d 5, 6, and 7) at 1030 and 1430 h. Blood samples were taken from the tail vein and collected in dipotassium and tri potassium ethylene diamine tetra acetic acid 10-mL vacutainer tubes (Fisher Scientific). Blood samples were inverted and then placed on ice. Plasma was harvested within 1 h of blood collection by centrifuging the vacutainers at 1,900 × g for 15 min. Plasma was stored at –20 °C until analyzed. Rumen fluid was collected from four areas in the ventral rumen sac, pooled, squeezed through 4 layers of cheesecloth, flash-frozen using a dry-ice ethanol bath, and stored at -80 °C. Individual rumen fluid samples (n=48) were submitted to the William H. Miner Agricultural Research Institute (Chazy, NY) for VFA analysis.

4.3.4 Blood Samples Analysis

The plasma concentration of glucose (Glucose kit #510, Sigma Chemical Co., St. Louis, MO), insulin (Bovine Insulin ELISA Kit, Invitrogen, Carlsbad, CA), and NEFA (SFA-1 kit, ZenBio Inc, Durham, NC) were determined using commercial kits following the manufacturer's instructions. The plasma concentrations of haptoglobin (**Hp**), and serum amyloid A (**SAA**), were determined using specific enzyme-linked immunosorbent assay (**ELISA**) kits (My BioSource, Inc., San Diego, CA) according to the manufacturer's protocols. The plasma concentrations of lipopolysaccharide (**LPS**) and lipopolysaccharide

binding protein (**LBP**) were also determined using ELISA kits (AFG Bioscience LLC, Northbrook, IL) according to the manufacturer's protocols.

4.3.5 Milk Sampling and Analysis

Cows were milked twice daily at 0430 and 1630 h. Milk samples from each cow were collected during a.m. and p.m. milking on the last three days of each experimental period (d 5, 6, and 7). Milk samples were collected from individual cows using commercial inline milk samplers (DeLaval Inc., Tumba, Sweden). Collected milk was thoroughly mixed to ensure homogeneity, and samples from each cow were divided into two subsamples. The first subsample was preserved using 2-bromo-2-nitropropane-1,3-diol and submitted to Lancaster DHIA (Manheim, Philadelphia) for commercial analyses of milk parameters [fat, protein, other solids, and milk urea nitrogen (**MUN**)]. The second subsample was flash-frozen using a dry-ice ethanol bath and stored at -80 °C until further analysis. For analysis, these second subsamples were thawed at 4 °C overnight and subsequently centrifuged at 4,000 × g for 15 min at 4 °C. The fat layer was then removed using a clean spatula. This centrifugation and fat removal step was repeated. The supernatant was then collected and stored at −80 °C until analyzed for LBP, LPL, Hp, and SAA concentration, using the same ELISA kits to determine their plasma concentrations.

4.3.6 Rumen Papillae Sampling

Rumen papillae were harvested from the rumen ventral sac at 1100 h from each cow on d 7 of each experimental period. Rumen papillae were collected according to the procedure outlined by Wetzels et al. (2017). In brief, rumen digesta was partially evacuated

via the cannula (the rumen was never emptied for more than 10 min). Using aseptic scissors, approximately 150 mg of rumen papillae were harvested from the rumen wall of the ventral sac, approximately 30-40 cm below the bottom edge of the rumen cannula. Biopsies were placed into copious amounts of 1x ice-cold PBS to detach adherent feed particles. Individual papillae were then collected using forceps, transferred into a stabilization agent (RNAlater, Qiagen, Hilden, Germany), and stored at -20 °C for further processing. Total mRNA extraction and sequencing were performed commercially (Novogene Company LTD, Beijing, China).

4.3.7 RNA extraction and Sequencing

Total mRNA extraction and sequencing were performed by Novogene Co., LTD (Beijing, China). Briefly, total RNA from the samples were extracted using the TRIzol reagent (Invitrogen, Carlsbad, CA, USA) in accordance with the manufacturer's recommendations. Extracted RNA purity, integrity, and quantification were determined using an Agilent Fragment Analyzer 5400 (Agilent Technologies, Santa Clara, CA, USA). Subsequently, mRNA was isolated from the total RNA using poly-T oligo-attached magnetic beads. After fragmentation of isolated mRNA, the first strand cDNA was synthesized using random hexamer primers. Second strand cDNA was synthesized using deoxyuridine triphosphate (dUTP) instead of using deoxythymidine triphosphate (dTTP). Next, cDNAs were fragmented by sonication (Covaris, Woburn, MA, USA) and overhangs were converted into blunt ends using exonuclease and polymerase. After adenylation of the 3' ends of the cDNA fragments, the Illumina Y-adapters (Illumina TruSeq indexed forked adapters, San Diego, CA, USA) was ligated to prepare for hybridization. Using AMPure

XP beads (Beckman Coulter, Beverly, USA) cDNA fragments of 150bp in length were selected. The directional libraries were prepared by eliminating the second strand using USER Enzyme (NEB, USA) and then subjected to amplification. The library was checked with Qubit 2.0 Fluorometer (Life Technologies, CA, USA), real-time PCR for quantification, and Agilent Bioanalyzer 2100 system (Agilent Technologies, CA, USA) for size distribution detection. The library preparations were sequenced on Illumina NovaSeq 6000 (Novogene Co. Ltd., Beijing, China), and 150 bp paired-end reads were generated.

4.3.8 RNA-seq Reads Mapping and Annotation

The quality of sequencing raw reads was assessed using FastQC (v.11.5; Andrews, 2010). The data were preprocessed using the Trimmomatic software (v.0.38; Bolger et al., 2014) to filter out low-quality reads and remove adaptors. High-quality RNA-seq reads were aligned to the *Bos taurus* genome assembly ARS-UCD 1.3 (RefSeq accession GCF_002263795.2) using HISAT2 (v.2.1; Kim et al., 2015). Samtools (v.13; Li et al., 2009) was used to sort the BAM alignment files generated from HISAT2 by coordinates. Reads were counted using StringTie (Pertea et al., 2016), and expression values were normalized as reads per kilobase of transcript per million mapped reads (cut-off > 1). Differential gene expression analysis was performed using DESeq2 (Love et al., 2014). Differentially expressed genes (**DEGs**) were counted and considered significant if the Benjamini-Hochberg method adjusted *P*-value (P_{FDR}) was less than 0.05 and log2fc > 2. Software tool default parameters were used in most instances, with the following exceptions: --rna-strandness argument was specified as reverse (RF) in the HISAT2 and StringTie protocol; --mapq (mapping quality score) argument was specified as 5 in

Samtools protocol. The functional annotation tool of the PANTHER classification System (v.13.1; Mi et al., 2016) was used to inspect Gene Ontology (**GO**) terms. Pathway enrichment analysis of DEGs was performed using g:Profiler (http://biit.cs.ut.ee/gprofiler/).

4.3.9 Statistical Analysis

A mixed procedure model of SAS 9.4 (SAS Institute, Cary, NC) was performed, including treatment, treatment × time interaction as the fixed effects. Random effects included cowID and cowID × treatment. The effects of treatment and the treatment × time interaction were considered significant if $P < 0.05$.

4.4 Results

4.4.1 Dry Matter Intake and Milk Component Analysis

Dry matter intake, milk fat content, other solids, and MUN were not different between cows fed the propionate and control treatments (Table 4.1). Milk protein content was lower in the propionate treatment cows samples than in the control cows (3.3% vs. 3.4%; $P = 0.01$). Milk fat content was numerically lower in samples from cows in the propionate treatment (4.0%) compared with the control (4.0% vs. 4.3%; $P = 0.27$). However, treatment had a significant effect on fat content when the sample collection time point was considered. Milk fat content was lower in milk from cows given the propionate treatment at the p.m. collection compared with control cows (4.3% vs. 5.0%; $P = 0.03$; Supplementary Table S8). The concentration of milk acute phase proteins SAA, LPL, LBP, and Hp are presented in Table 4.1. Their concentrations did not differ across treatments.

4.4.2 Ruminal Metabolites and Blood parameters

The concentration of rumen metabolites did not differ between cows receiving the propionate and control treatments (Table 4.2). Similarly, treatment did not affect the concentration of plasma glucose, NEFA, insulin, LBP, and LPS (Table 4.3). The concentration of plasma LBP was impacted by treatment × time interaction, whereby the concentration was higher in samples from the a.m. control cows compared with a.m. samples from the propionate cows (270.7 vs. 218.8 ng/mL; P = 0.04). The plasma concentrations of acute phase proteins SAA and Hp are presented in Table 4.3. Their concentrations did not differ across treatments.

4.4.3 Rumen Epithelial Transcriptome Profile

A total of 350 million (43 $\pm$ 3.8 million per sample) high-quality 150 bp paired reads were generated from 8 ruminal papillae samples by RNA-seq. An average of 90.1% of input reads were aligned to the *Bos taurus* genome assembly ARS-UCD 1.3, of which 82.8% were mapped uniquely. A total of 331 significant DEGs were identified between the propionate and control groups, of which 186 were down-regulated and 145 were up-regulated in the propionate group compared with the control group (Supplementary Table S7; Figure 4.1). Functional analysis by PANTHER using a list of DEGs identified different molecular functions and biological process terms (Figure 4.2). For example, the biological process includes the cellular process (GO:0009987), immune system process (GO:0002376), and metabolic process (GO:0008152). Further, the expression of genes

involved in various biological processes such as protein metabolism, lipid transport and metabolism, immune process, transport activity, and cell growth and division events (Table 4.4) were affected due to propionate dosage. A total of 25 DEGs were involved in protein metabolism, of which 17 and 8 were down- and up-regulated, respectively, in the propionate group compared with the control group; 8 DEGs were involved in cell division events, of which 6 and 2 were down- and up-regulated, respectively, in the propionate group compared with the control group; 10 DEGs were involved in transport activity, of which 7 and 3 were down- and up-regulated, respectively, in the propionate group compared with the control group; 14 DEGs were involved in the immune process, of which 6 and 8 were down- and up-regulated, respectively, in the propionate group compared with the control group; 8 DEGs were involved in the lipid transport and metabolism, of which 6 and 2 were down- and up-regulated, respectively, in the propionate group compared with the control group. Pathway enrichment analysis of DEGs using g:Profiler showed that the REACTOME_pathway mitogen-activated protein kinases (**MAPK1/MAPK3**) signaling was significantly enriched (P_{FDR} = 0.04) due to treatment. A total of 8 DEGs were involved in the MAPK1/MAPK3 signaling pathway, of which were all down-regulated in the propionate group compared with the control group - [(amphiregulin (***AREG***), heparin binding EGF like growth factor (***HBEGF***), KIT proto-oncogene, receptor tyrosine kinase (***KIT***), persephin (***PSPN***), phosphatidylinositol-4,5-bisphosphate 3-kinase catalytic subunit beta (***PIK3CB***), progestin and adipoQ receptor family member 3 (***PAQR3***), protein phosphatase 2 catalytic subunit beta (***PPP2CB***), spectrin alpha, non-erythrocytic 1 (***SPTAN1***)].

4.5 Discussion

The result of this analysis showed that the propionate dosage resulted in 331 DEG, which includes genes involved in major biological processes. As a specific outcome, the MAPK1/MAPK3 signaling pathway, also known as the ERK1/ERK2 signaling pathway, was significantly enriched due to treatment. It is well documented that MAPK families are involved in various complex cellular processes such as proliferation, differentiation, development, transformation, and apoptosis. Enrichment of MAPK1/MAPK3 signaling pathway in this study may provide some insight into mechanistic adaptations of the rumen epithelium as activated MAPK1/MAPK3 has been previously demonstrated to enter the nucleus and change the gene expression of the cell to promote growth, differentiation, or mitosis (Zhang and Liu, 2002). Further, it was suggested that MAPK1/3 may involve controlling the Microtubule organization center (**MTOC**) function. The MTOC controls the organization of microtubular structures in interphase cells and the mitotic spindle of dividing cells (Zhang and Liu, 2002). In addition, the expression of genes involved in microtubule binding and formation and actin-cytoskeleton organization were downregulated due to propionate dosage. Microtubules play an important role in cell division, cell polarity, cell motility, cell signaling, and intracellular transport (Kollman et al., 2010; Conduit, 2016). Microtubules are critical cytoskeleton components that drive essential cellular functions such as cell division and migration (Logan et al., 2019). Further, DEGs such as cyclin T1 (***CCNT1***), cyclin Pas1/PHO80 domain containing 1 (***CNPPD1***), cell division cycle associated 3 (***CDCA3***) and cyclin dependent kinase 2 (***CDK2***) were down-regulated due to propionate dosage. These genes encode proteins which are involved

in cell cycle regulations. Cyclins bind and activate cyclin-dependent kinases and activation of cyclin-dependent kinases is required for the next phase of the cell cycle. For example, by phosphorylating cell division cycle-associated proteins and E2F transcriptional factors, the cyclin/cyclin-dependent kinase complex terminates the S phase and drives the cell-cycle transition to G2 (Ding et al., 2020). Down-regulation of *CCNT, CNPPD1*, *CDCA3*, *CDK2* and down-regulation of DEGs involved in the MAPK1/MAPK3 signaling pathway, microtubule binding and formation and actin-cytoskeleton organization may suggest the decreased cell growth and division function in the rumen epithelium of propionate treated cows. Recently, Baldwin et al. (2018) reported that the top enriched biological terms in the rumen epithelial transcriptome on the first day of intra-ruminal butyrate infusion in Holstein cows were mitotic cell processes, cell cycle processes, regulation of cell cycle, and microtubules-based processes. Conversely, on the third day of intra-ruminal butyrate infusion, gene ontology analysis highlighted a negative regulation of the biological process, negative regulation of the cellular process, and negative regulation of cell proliferation. While the above study was conducted using non-lactating cows, the characterization results of ruminal epithelial changes in response to diet-induced altered rumen environment could still provide insight into our observations. Therefore, the negative regulation of rumen epithelial cell growth observed in this study may be part of a dynamic adaptation by rumen epithelium in response to an altered rumen environment, whereby these epithelial cells respond to propionate dosage through an initial up-regulation of cell proliferation-related genes, followed by an adaptation period that includes down-regulation of these cell proliferation-related genes.

The primary function of the ruminal epithelium is nutrient absorption; therefore, we speculated that the expression of genes involved in transport activity might be affected due to propionate dosage. In the present study, a total of 10 DEGs were involved in the transport activity, 7 (*SLC6A6*, *SLC25A1*, *SLC39A2*, *UCP3*, *TMEM110*, *ANO6*, *WNK3*), and 3 (*SLC23A1*, *KCNS1*, *LOC112447392*) of which were down- and up-regulated, respectively, in the propionate group compared with the control group. Solute carriers (**SLC**) are inner plasma membrane transport proteins, the largest transporters that import and export most nutrients, such as sugars, amino acids, and VFAs (Aschenbach et al., 2009). Previous studies have shown that a high-grain diet enhanced rumen epithelial absorption by enhancing *SLC* gene family expression (Zhao et al., 2017). However, Ogata et al. (2020) reported that 11 out of 13 *SLC* family genes were downregulated in Japanese black bull's rumen epithelium when fed a 26:74 forage:concentrate diet, and then 12 out of 19 *SLC* family genes were up-regulated when these bulls were fed an 87:13 forage:concentrate diet. While it should be noted that Japanese black bulls have been selectively bred for higher depositions of intramuscular fat (Gotoh et al., 2018), this selective breeding could have influenced the variation of *SLC* family gene expression in the above study. In the present study, 3 out of 4 *SLC* DEGs were down-regulated by the propionate dosage. This may suggest that the differential regulation of *SLC* gene expression may be part of the rumen epithelial response to altered nutrient composition due to an altered rumen environment. Differential regulation of *SLC* genes may also suggest that the rumen epithelium transitions to altered nutrient absorptive functions. Therefore, it was not surprising to see gene expression of ion transporters was affected. Calcium (**Ca**) ion transporter *TMEM110*, zinc (**Zn**)/Iron (**Fe**) transporter *SLC39A2*, as well as chloride ion

transporter *ANO6* were down-regulated in the propionate group compared with the control group. At the same time, potassium ion transporter *KCNS1* and magnesium ion transporter *LOC112447392* were up-regulated in the propionate group compared with the control group. This suggests mineral flux perturbation in the rumen epithelium of cows that received intra-ruminal propionate dosage. To further support the suggestion, Dong et al. (2011) previously reported plasma mineral (Ca, Fe, and Zn) perturbations as the proportion of starch content in the diet increased.

Besides efficient absorption and metabolism of VFAs, the rumen epithelium has an essential role in immune and barrier functions. Previous studies have reported that the immune system is involved in rumen epithelial adaptation to a high-starch diet (Chen and Oba, 2012; Dionissopoulos et al., 2012). In this study, the expression of the *TLR2* gene was down-regulated in the rumen epithelium of propionate-treatment cows. Toll-like receptor 2, an important member of the *TLR* family, plays a vital role in pathogen recognition and mediates the secretion of chemokines to develop effective immunity. Previously, Kent-Dennis et al. (2019) reported the down-regulation of expression of *TLR*2 and *TLR*4 in the rumen epithelium of high grain-fed dairy cows. However, other studies have reported an up-regulation of *TLR* expression in the rumen epithelium of dairy cows in response to a high starch diet (Stefanska et al., 2018; Chen and Oba, 2012). Kent-Dennis et al. (2019) explained the variation of *TLR* expression among studies might be because of temporal regulation of *TLR* gene expression in response to a diet-induced altered rumen environment, which can be apparent only through repeated tissue sample collection. The idea of temporal variability of *TLR* gene expression postexposure to a diet-induced altered

rumen may not be restricted to the *TLR* gene. Zhang et al. (2016) reported that a high starch diet up-regulated the immune-related genes in the cattle rumen epithelium. In contrast, Gholizadeh et al. (2020) reported the down-regulation of immune-related genes in rumen epithelial fed on a high starch diet. In this study, we observed the expression of genes such as complement regulatory (*CD46*), surface antigen (*CD63*), histocompatibility minor 13 (*HM13*), C-C motif chemokine ligand 20 (*CCL20*), and interferon regulatory factor 2 binding protein like (*IRF2BPL*) was down-regulated in the rumen epithelium of propionate-treatment cows. At the same time, the expression of T cell receptors (*LOC10029843*, *LOC10190977*, *LOC104973096*, LOC112441460), immunoglobulin lambda-1 light chain-like (*LOC112441460*) and interleukin 37 (*IL37*) were up-regulated. This might suggest that the expression of immune related genes in the rumen epithelial may also follow the complex temporal pattern in response to the altered rumen environment. Therefore, future studies investigating the dynamic regulation of expression of immune-associated genes in response to a diet-induced altered rumen environment might be ideal. These studies may aid in understanding rumen epithelial inflammatory response to increased ruminal LPS concentration following high fermentable diets. The differential regulation of immune-related genes observed in this study could be part of the epithelial tissue's return to a homeostatic state in response to a propionate-induced altered rumen environment. While gene regulation in the rumen epithelial tissue paints a cohesive image of the likely cellular regulation occurring in the current trial, the biofluid parameters are less reflective. For example, the plasma LPS concentration in samples from cows receiving the propionate treatment was numerically higher compared with the control but not significantly different (P = 0.19). This suggests that there is more variability in the

magnitude of plasma LPS response compared with the epithelial response and may be a result of variable translocation of the LPS from the rumen into the bloodstream. Consequently, the biofluid concentrations of acute phase proteins LBP, SAA, and Hp were not different between the propionate and control treatments. Although the concentration of milk acute phase protein LBP, SAA, and Hp were not different across the treatment, the milk protein content was significantly lower due to propionate dosage. Numerous studies have previously reported a decrease in milk protein content with a high-starch diet in dairy cows (Morar et al., 2022; Colman et al., 2013; Xu et al., 2016; Li et al., 2017). Since milk protein synthesis during lactation is a complex biological process, only a little perturbation in lactation can impact the milk protein content (Guo et al., 2022).

In this study, the expression of genes involved in lipids transport and metabolism differed between propionate and control treatments. Fatty acid-binding proteins, such as *FABP4*, bind to fatty acids and lipids to transport and deliver them to different sites for utilization (Furuhashi and Hotamisligil, 2008). Malonyl-CoA decarboxylase (***MLYCD***) is involved in the fatty acid oxidation process; it converts malonyl-CoA to acetyl-CoA, which enters into the Krebs cycle to produce cellular energy. Phospholipases A2 are enzymes that hydrolyze phospholipids and release fatty acids and phospholipids in the tissues. Previous studies have shown that *PLA2G* influences lipid metabolism and mobilization by generating free fatty acids (Dennis et al., 2912). The *LRP1* gene encodes for the low-density lipoprotein receptor-related protein, which is involved in regulating the metabolism of intracellular triglycerides. Previous studies have reported that decreased expression of *LRP1* was associated with the accumulation of triglycerides in human adipocytes (Actis

Dato and Chiabrando, 2018). Diacylglycerol O-acyltransferase 2 like 6 (***DGAT2L6***) is involved in the final step of triacylglycerol triglyceride synthesis, which catalyzes the formation of the ester bond between the hydroxyl group of 1,2-diacylglycerol and a long-chain fatty acyl-CoA (Karantonis et al., 2009). Down-regulation of *FABP4*, *PLA2G*, *LRP1* and up-regulation of *DGAT2L6* in the propionate group compared with the control group may suggest an increase in the accumulation of lipids in the rumen epithelial tissue of propionate-treated cows, resulting in lower efficiency of exporting fatty acids out of rumen epithelia. To further support the suggestion of altered fatty acid synthesis in the propionate-treated cows, milk fat content was lower in p.m. collected milk from the propionate-treated cows compared with samples collected from control cows. Previous studies have shown a decrease in milk fat content from cows fed a high starch diet (Pitta et al., 2018; Zeng et al., 2019).

Sequencing results provided some insight into glucose and protein metabolism regulation as well. Similar to lipid metabolism-associated genes, the expression hexokinase domain containing 1 (***HKDC1***) was down-regulated by the propionate dosage. The hexokinase domain containing 1 involved in glucose metabolism, catalyzes the phosphorylation of glucose to produce glucose-6-phosphate, the rate-limiting step in glycolysis. Downregulation of *HKDC1* may indicate an increase in glucose synthesis in the propionate-treatment cow rumen epithelium; however, the plasma glucose concentration only partially validated this postulation as it was numerically higher (P = 0.51) in the propionate-treated cows. Similarly, the genes related to protein post-translational modification and catabolism were markedly downregulated in the propionate

group compared with the control group. Conversely, translation genes were up-regulated in the rumen epithelium tissue of propionate-treated cows. Cumulatively, these may suggest a protein synthesis perturbation in the rumen epithelium of propionate-treated cows. Overall, propionate dosage trigged genes involved in major biological processes, which may impact rumen epithelium's nutritive absorption capacity, ultimately impacting the feed conversion efficiency. Future studies are needed to examine the variation of animal feed efficiency because of rumen epithelium changes in response to diet-induced altered rumen environment. These studies may aid in designing nutritional strategies to increase animal production.

4.6 Conclusion

The results of this study provided a snapshot of the cow rumen epithelial transcriptome profile changes in response to the propionate-induced altered rumen environment. In total, 331 DEGs were identified in the cow rumen epithelium that received intra-ruminal propionate dosage, of which 146 and 185 were up-and down-regulated, respectively. The results showed a decrease in the expression of genes involved in cell growth and division events, lipid transport and metabolism, protein metabolism, and transport activity in response to the propionate dosage. Further, genes related to the immune system were differentially regulated, cumulatively suggesting that propionate's intra-ruminal dosage drastically alters the rumen epithelial transcriptome. Ultimately, the findings of this study enhanced our understanding of the adaptive responses of rumen epithelium to a diet-induced altered rumen environment. This information may aid in

developing precise nutritional management strategies that support both productivity and health, particularly in high-grain feeding management systems.

Figure 4.1. Volcano plot displaying the differentially expressed genes (DEGs) in rumen epithelium collected from cows dosed with intra-ruminal sodium propionate (propionate) or sodium chloride (control). Red and blue points are DEGs. n = 4 cows/treatment (propionate or control).

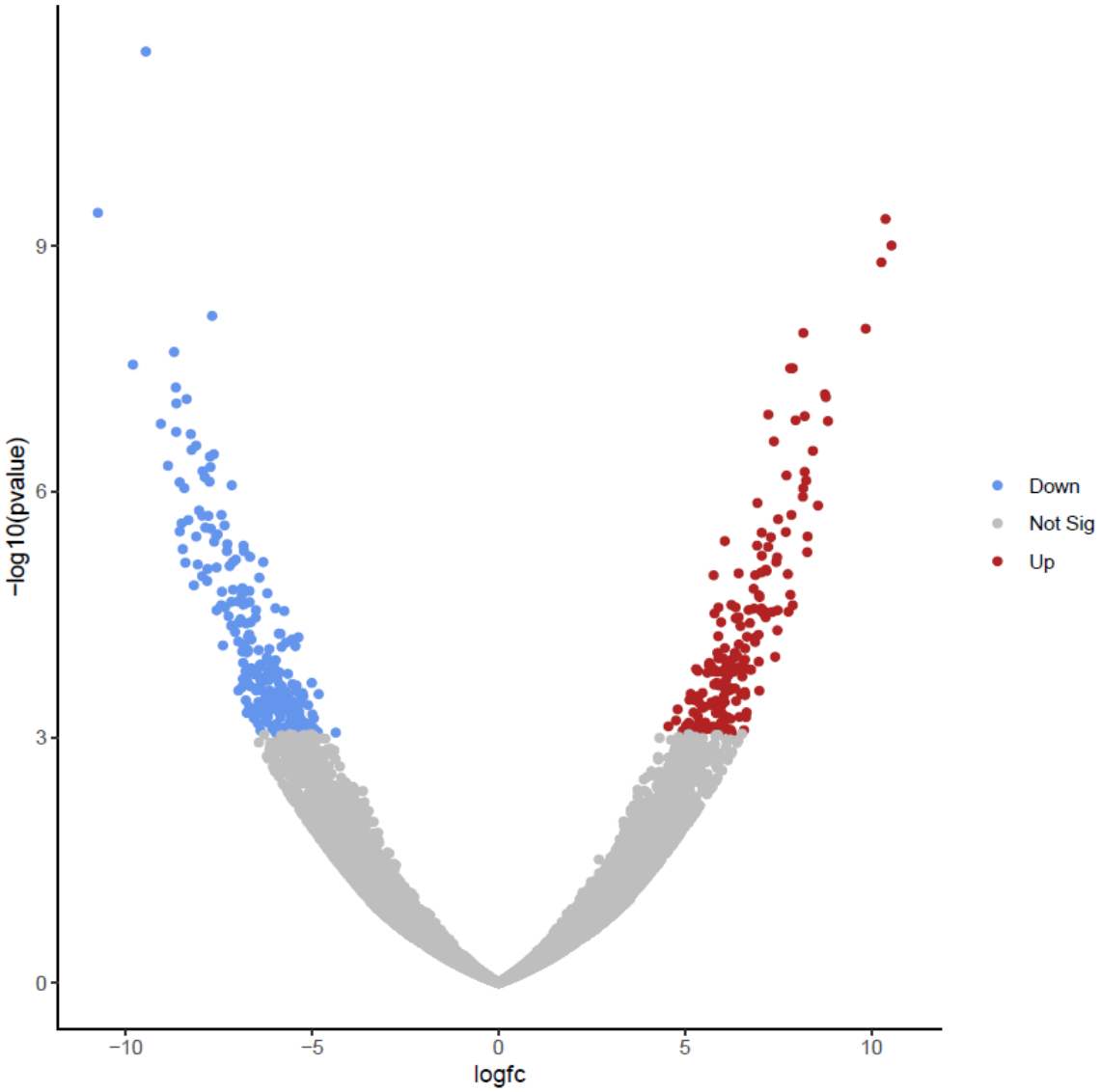

Figure 4.2. Biological process (A) and Molecular functions (B) of differentially expressed genes in ruminal epithelium between cows dosed with intra-ruminal sodium propionate (propionate) or sodium chloride (control) as identified by PANTHER. n = 4 cows/treatment (propionate or control).

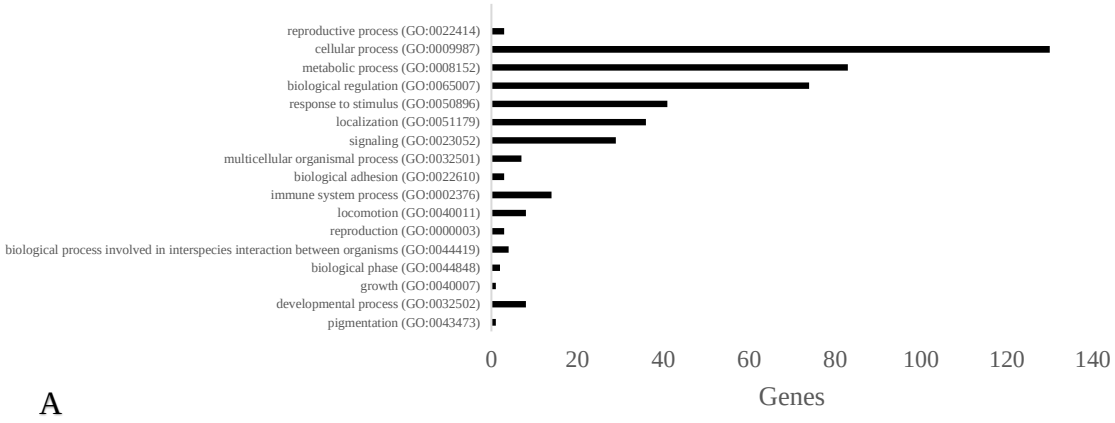

A

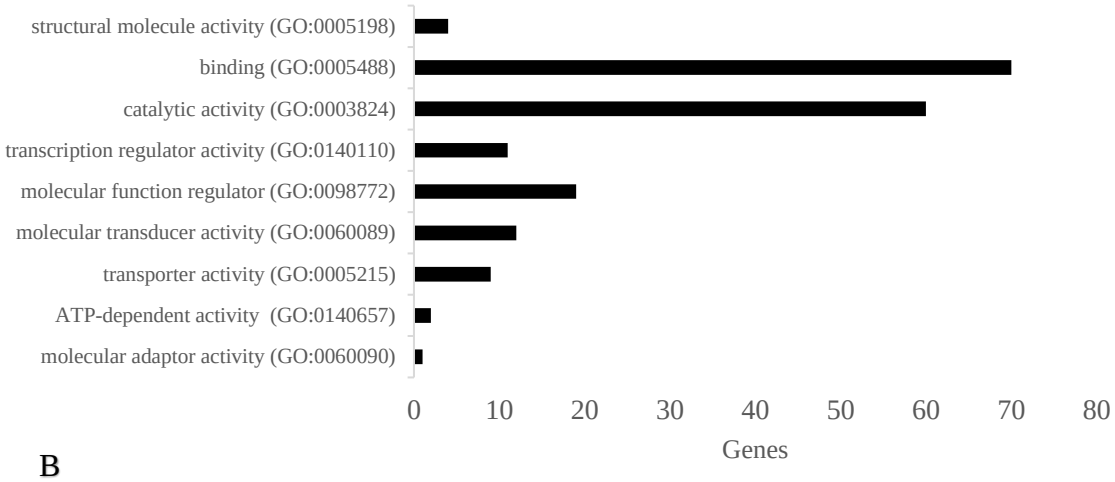

B

Table 4.1. DMI, milk fat content, milk protein content and the average concentration of other solids, MUN, SAA, Hp, and LBP in the milk samples from cows dosed with intra-ruminal sodium propionate (propionate) or sodium chloride (control). n = 4 cows/treatment (propionate or control).

	Control	**Propionate**	***P* - value**
DMI (kg/d)	20.5	21.3	0.74
Milk fat (%)	4.3	4.0	0.27
Milk protein (%)	3.4	3.3	0.01
Other solids (%)	5.7	5.6	0.17
Milk urea nitrogen (mg/dL)	11.5	11.6	0.94
Serum amyloid A (μg/mL)	20.8	21.5	0.42
Haptoglobin (ng/mL)	244.3	268.5	0.82
Lipopolysaccharide Binding Protein (ng/mL)	170.6	181.7	0.82
Lipoprotein lipase (ng/mL)	180.3	181.2	0.85

Table 4.2. The average rumen fluid metabolite concentration in the samples from cows dosed with intra-ruminal sodium propionate (propionate) or sodium chloride (control). n = 4 cows/treatment (propionate or control).

	Control	**Propionate**	***P* - value**
Total volatile fatty acid (mM)	121.1	119.3	0.82
Propionic (mM)	27.4	25.4	0.56
Acetic acid (mM)	76.6	76.1	0.81
Butyric acid (mM)	13.3	13.1	0.73
Isovaleric acid (mM)	0.9	1.2	0.13
Isobutyric acid (mM)	0.7	0.8	0.58
Valeric acid (mM)	2.0	2.6	0.75
Acetic:Propionic acid ratio	2.8	3.1	0.07

Table 4.3. The average plasma concentration of SAA, Hp, LBP, LPS, NEFA, glucose, and insulin from cows dosed with intra-ruminal sodium propionate (propionate) or sodium chloride (control). n = 4 cows/treatment (propionate or control).

	Control	**Propionate**	***P* - value**
Serum amyloid A (μg/mL)	6.6	5.7	0.39
Haptoglobin (μg/mL)	5.3	7.4	0.52
Lipopolysaccharide Binding Protein (ng/mL)	253.4	227.3	0.21
Lipopolysaccharide (ng/mL)	3.2	4.3	0.19
Non-esterified fatty acid (μM)	68.2	72.1	0.45
Glucose (mg/dL)	74.4	78.5	0.51
Insulin (μIU/mL)	101.9	115.8	0.66

Table 4.4. Rumen epithelial differential expressed genes identified between cows dosed with intra-ruminal sodium propionate (propionate) or sodium chloride (control) involved in protein metabolism, cell division, transport activity, immune process, lipid transport, and metabolism as identified by PANTHER. n = 4 cows/treatment (propionate or control).

Entrez Gene ID	Description	log2FoldChange	P_{FDR}- value	Biological process
519017	adenine phosphoribosyl transferase(*APRT*)	-7.5	<0.05	Nucleobase metabolic process
525394	ADP ribosylation factor related protein 1(*ARFRP1*)	-5.0	<0.05	Protein localization
281108	cathepsin V(*CTSV*)	6.2	<0.05	Protein catabolic process
613935	EARP complex and GARP complex interacting protein 1(*EIPR1*)	-5.6	<0.05	Protein ubiquitination
101902938	HEAT repeat containing 4(*HEATR4*)	-6.2	<0.05	Protein maturation
527520	HECT and RLD domain containing E3 ubiquitin protein ligase family member 6(*HERC6*)	-6.4	<0.05	Protein catabolic process
281831	heat shock protein family A (*Hsp70*) member 8(*HSPA8*)	-7.3	<0.05	Protein folding
107131803	serpin B3-like(*LOC107131803*)	-7.8	<0.05	Proteolysis
540984	OTU deubiquitinase, ubiquitin aldehyde binding 1(*OTUB1*)	-7.0	<0.05	Protein ubiquitination
514957	pumilio RNA binding family member 3(*PUM3*)	-6.6	<0.05	Translational elongation
510205	serpin family B member 10(*SERPINB10*)	-5.8	<0.05	Proteolysis
615950	spermine synthase(*SMS*)	-8.2	<0.05	Polyamine biosynthetic process
538785	STAM binding protein like 1(*STAMBPL1*)	-8.6	<0.05	Protein deubiquitination
280706	thyroglobulin(*TG*)	-8.0	<0.05	Amino acid metabolic process
281528	transglutaminase 2(*TGM2*)	-5.8	<0.05	Protein modification process

281225	ubiquitin conjugating enzyme E2 K(*UBE2K*)	-7.5	<0.05	Protein catabolic process
534262	ubiquitin specific peptidase 38(*USP38*)	-5.9	<0.05	Protein deubiquitination
107133112	40S ribosomal protein S26-like(*LOC107133112*)	6.4	<0.05	Translation^{U}
112442039	40S ribosomal protein S29 pseudogene(*LOC112442039*)	-6.5	<0.05	Translation^{U}
101903101	40S ribosomal protein S3a pseudogene(*LOC101903101*)	7.4	<0.05	Translation^{KO}
781565	40S ribosomal protein S6 pseudogene(*LOC781565*)	5.7	<0.05	Translation^{U}
112442704	60S ribosomal protein L10-like(*LOC112442704*)	7.6	<0.05	Translation^{U}
617130	60S ribosomal protein L12 pseudogene(*LOC617130*)	6.3	<0.05	Translation^{U}
107132302	60S ribosomal protein L23a pseudogene(*LOC107132302*)	7.2	<0.05	Translation^{U}
107132785	60S ribosomal protein L30 pseudogene(*LOC107132785*)	7.8	<0.05	Translation^{R}
540108	spectrin alpha, non-erythrocytic 1(*SPTAN1*)	-5.7	<0.05	actin cytoskeleton organization
540479	NF2, moesin-ezrin-radixin like tumor suppressor(*NF2*)	-5.6	<0.05	actin binding
511853	tubulin tyrosine ligase like 4(*TTLL4*)	6.3	<0.05	microtubule cytoskeleton organization
100295202	telomere repeat binding bouquet formation protein 1(*TERB1*)	5.5	<0.05	chromosome localization
100139988	ras homolog family member Q(*RHOQ*)	-6.3	<0.05	actin cytoskeleton organization
539332	cofilin 2(*CFL2*)	-6.4	<0.05	actin filament depolymerization

519789	dynein cytoplasmic 1 light intermediate chain 2 (*DYNC1LI2*)	-5.7	<0.05	Microtubule binding
282531	GABA type A receptor associated protein like 2 (*GABARAPL2*)	-8.1	<0.05	Microtubule binding
784525	interferon beta-2(*LOC784525*)	6.8	<0.05	Immune function
281666	C-C motif chemokine ligand 20(*CCL20*)	-5.7	<0.05	Immune function
280851	CD46 molecule(*CD46*)	-5.6	<0.05	Immune function
786493	interleukin 37(*IL37*)	6.3	<0.05	Immune function
613845	interferon regulatory factor 2 binding protein like(*IRF2BPL*)	-7.1	<0.05	Immune function
100298434	T cell receptor alpha variable 38-1-like(*LOC100298434*)	8.4	<0.05	Immune function[U]
101909777	T cell receptor alpha variable 25-like(*LOC101909777*)	6.5	<0.05	Immune function[U]
104973096	T cell receptor alpha variable 22-like(*LOC104973096*)	6.5	<0.05	Immune function[U]
112441460	immunoglobulin lambda-1 light chain-like(*LOC112441460*)	6.4	<0.05	Immune function[U]
112446441	T-cell receptor beta chain V region 3H.25-like(*LOC112446441*)	8.5	<0.05	Immune function[U]
404156	CD63 molecule(*CD63*)	-5.4	<0.05	Immune function
281534	toll like receptor 2(*TLR2*)	-6.0	<0.05	Immune function
512534	histocompatibility minor 13(*HM13*)	-7.6	<0.05	Immune function
505492	solute carrier family 23 member 1(*SLC23A1*)	6.2	<0.05	Transport activity
282476	solute carrier family 25 member 1(*SLC25A1*)	-7.2	<0.05	Transport activity
508989	solute carrier family 39 member 2(*SLC39A2*)	-5.6	<0.05	Transport activity
282366	solute carrier family 6 member 6(*SLC6A6*)	-7.0	<0.05	Transport activity
112447392	membrane magnesium transporter 1 pseudogene(*LOC112447392*)	7.0	<0.05	Transport activity

538654	transmembrane protein 110(*TMEM110*)	-7.7	<0.05	Transport activity
521338	potassium voltage-gated channel modifier subfamily S member 1(*KCNS1*)	8.9	<0.05	Transport activity
521784	anoctamin 6(*ANO6*)	-8.3	<0.05	Transport activity
100337119	WNK lysine deficient protein kinase 3(*WNK3*)	-7.9	<0.05	Transport activity
281563	uncoupling protein 3(*UCP3*)	7.8	<0.05	Transport activity
281759	fatty acid binding protein 4, adipocyte(*FABP4*)	-3.6	<0.05	Lipid transport
533894	LDL receptor related protein 1(*LRP1*)	-6.7	<0.05	Lipid metabolism
505958	diacylglycerol O-acyltransferase 2 like 6(*DGAT2L6*)	10.1	<0.05	Lipid metabolism
614911	phospholipase A2 group V(*PLA2G5*)	-6.8	<0.05	Lipid metabolism
512341	malonyl-CoA decarboxylase(*MLYCD*)	-9.6	<0.05	Lipid metabolism
523479	ATP binding cassette subfamily A member 12(*ABCA12*)	8.8	<0.05	Lipid transport
535900	Star related lipid transfer domain containing 8(*STARD8*)	-7.5	<0.05	Lipid transport
513533	phosphomevalonate kinase(*PMVK*)	-8.1	<0.05	Lipid metabolism

[U]Biological process as identified by UniProt database.

[KO]Biological process as identified by Kegg orthology database.

[R]Biological process as identified by Reactome database.

4.7 References

Actis Dato, V., and G. A. Chiabrando. 2018. The role of low-density lipoprotein receptor-related protein 1 in lipid metabolism, glucose homeostasis and inflammation. Int. J. Mol. Sci. 19:1780.

Andrews, S. 2010. FastQC: a quality control tool for high throughput sequence data.

Aschenbach, J. R., S. Bilk, G. Tadesse, F. Stumpff, and G. Gäbel. 2009. Bicarbonate-dependent and bicarbonate-independent mechanisms contribute to nondiffusive uptake of acetate in the ruminal epithelium of sheep. Am. J. Physiol. Liver Physiol. 296:G1098–G1107. https://doi.org/10.1152/ajpgi.90442.2008

Baldwin, R. L., R. W. Li, Y. Jia, and C. Li. 2018. Transcriptomic impacts of rumen epithelium induced by butyrate infusion in dairy cattle in dry period. Gene Regul. Syst. Biol. 12:11776250-18774798. https://doi.org/10.1177/1177625018774798

Bionaz, M., and J. J. Loor. 2008. ACSL1, AGPAT6, FABP3, LPIN1, and SLC27A6 are the most abundant isoforms in bovine mammary tissue and their expression is affected by stage of lactation. J. Nutr. 138:1019–1024. https://doi.org/10.1093/jn/138.6.1019

Bolger, A. M., M. Lohse, and B. Usadel. 2014. Trimmomatic: a flexible trimmer for Illumina sequence data. Bioinformatics 30:2114–2120.

Carman, G. M., and G. S. Han. 2009. Phosphatidic acid phosphatase, a key enzyme in the regulation of lipid synthesis. J. Biol. Chem. 284:2593–2597. https://doi.org/10.1074/jbc.R800059200

Chen, Y., and M. Oba. 2012. Variation of bacterial communities and expression of Toll-like receptor genes in the rumen of steers differing in susceptibility to subacute ruminal acidosis. Vet. Microbiol. 159:451–459. https://doi.org/10.1016/j.vetmic.2012.04.032

Colman, E., W. B. Fokkink, M. Craninx, J. R. Newbold, B. de Baets, and V. Fievez. 2010. Effect of induction of subacute ruminal acidosis on milk fat profile and rumen parameters. J. Dairy Sci. 93:4759–4773. https://doi.org/10.3168/jds.2010-3158

Conduit, P. T. 2016. Microtubule organization: A complex solution. J. Cell Biol. 213:609. https://doi.org/10.1083%2Fjcb.201606008

Deák, F., R. E. Anderson, J. L. Fessler, and D. M. Sherry. 2019. Novel cellular functions of very long chain-fatty acids: insight from ELOVL4 mutations. Front. Cell. Neurosci. 13:428. https://doi.org/10.3389/fncel.2019.00428

Dias, A. L. G., J. A. Freitas, B. Micai, R. A. Azevedo, L. F. Greco, and J. E. P. Santos. 2018. Effects of supplementing yeast culture to diets differing in starch content on performance and feeding behavior of dairy cows. J. Dairy Sci. 101:186–200. https://doi.org/10.3168/jds.2017-13240

Ding, L., J. Cao, W. Lin, H. Chen, X. Xiong, H. Ao, M. Yu, J. Lin, and Q. Cui. 2020. The roles of cyclin-dependent kinases in cell-cycle progression and therapeutic strategies in human breast cancer. Int. J. Mol. Sci. 21:1960. https://doi.org/10.3390/ijms21061960

Dionissopoulos, L., M. A. Steele, O. Alzahal, and B. W. McBride. 2012. Adaptation to high grain diets proceeds through minimal immune system stimulation and differences in extracellular matrix protein expression in a model of subacute ruminal acidosis in non-lactating dairy cows. Am. J. Anim. Vet. Sci. 7:84–91.

Dong, G., S. Liu, Y. Wu, C. Lei, J. Zhou, and S. Zhang. 2011. Diet-induced bacterial immunogens in the gastrointestinal tract of dairy cows: impacts on immunity and metabolism. Acta Vet. Scand. 53:1–7. https://doi.org/10.1186/1751-0147-53-48

Furuhashi, M., and G. S. Hotamisligil. 2008. Fatty acid-binding proteins: role in metabolic diseases and potential as drug targets. Nat. Rev. Drug Discov. 7:489–503.

Gäbel, G., H. Martens, M. Sündermann, and P. Galfi. 1987. The effect of diet, intraruminal pH and osmolarity on sodium, chloride and magnesium absorption from the temporarily isolated and washed reticulo-rumen of sheep. Q. J. Exp. Physiol. Transl. Integr. 72:501–511. https://doi.org/10.1113/expphysiol.1987.sp003092

Gholizadeh, M., J. Fayazi, H. Zali, and Y. Asgari. 2020. Transcriptomic changes in the rumen epithelium of cattle after the induction of acidosis. Arch. Razi Inst. 75:109. https://doi.org/10.22092%2FARI.2019.125930.1326

Goodlad, R. A. 1981. Some effects of diet on the mitotic index and the cell cycle of the ruminal epithelium of sheep. Q. J. Exp. Physiol. Transl. Integr. 66:487–499. https://doi.org/10.1113/expphysiol.1981.sp002590

Gotoh, T., T. Nishimura, K. Kuchida, and H. Mannen. 2018. The Japanese Wagyu beef industry: Current situation and future prospects—A review. Asian-Australasian J. Anim. Sci. 31:933.

Graham, C., and N. L. Simmons. 2005. Functional organization of the bovine rumen epithelium. Am. J. Physiol. Integr. Comp. Physiol. 288:R173–R181. https://doi.org/10.1152/ajpregu.00425.2004

Greenwood, S. L., and M. C. Honan. 2019. Symposium review: Characterization of the bovine milk protein profile using proteomic techniques. J. Dairy Sci. 102:2796–2806. https://doi.org/10.3168/jds.2018-15266

Guo, Z., L. Ma, and D. Bu. 2022. Omics, the New Technological Approaches to the Milk Protein Researches. Milk Protein New Res. Approaches 37.

Karantonis, H. C., T. Nomikos, and C. A. Demopoulos. 2009. Triacylglycerol metabolism. Curr. Drug Targets 10:302–319.

Kent-Dennis, C., A. Pasternak, J.C. Plaizier, and G. B. Penner. 2019. Potential for a localized immune response by the ruminal epithelium in nonpregnant heifers following a short-term subacute ruminal acidosis challenge. J. Dairy Sci. 102:7556–7569.

Khafipour, E., D. Krause, and J. Plaizier. 2009a. Alfalfa pellet-induced subacute ruminal acidosis in dairy cows increases bacterial endotoxin in the rumen without causing inflammation. J. Dairy Sci. 92:1712-1724. https://doi.org/10.3168/jds.2008-1656

Kihara, A. 2012. Very long-chain fatty acids: elongation, physiology and related disorders. J. Biochem. 152:387–395. https://doi.org/10.1093/jb/mvs105

Kim, D., B. Langmead, and S. L. Salzberg. 2015. HISAT: a fast spliced aligner with low memory requirements. Nat. Methods 12:357–360.

Kollman, J. M., J. K. Polka, A. Zelter, T. N. Davis, and D. A. Agard. 2010. Microtubule nucleating γ-TuSC assembles structures with 13-fold microtubule-like symmetry. Nature 466:879–882. https://doi.org/10.1038/nature09207

Leduc, A., S. Le Guillou, L. Bianchi, L. O. Correia, M. Gelé, J. Pires, P. Martin, C. Leroux, F. Le Provost, and M. Boutinaud. 2022. Milk proteins as a feed restriction signature indicating the metabolic adaptation of dairy cows. Sci. Rep. 12:18886. https://doi.org/10.1038/s41598-022-21804-1.

Levine, A. J. 1997. p53, the cellular gatekeeper for growth and division. Cell 88:323–331. https://doi.org/10.1016/S0092-8674(00)81871-1

Li, F., and H. Zhang. 2019. Lysosomal acid lipase in lipid metabolism and beyond. Arterioscler. Thromb. Vasc. Biol. 39:850–856.

Li, H., B. Handsaker, A. Wysoker, T. Fennell, J. Ruan, N. Homer, G. Marth, G. Abecasis, R. Durbin, and 1000 Genome Project Data Processing Subgroup. 2009. The sequence alignment/map format and SAMtools. bioinformatics 25:2078–2079.

Li, M. M., R. R. White, L. L. Guan, L. Harthan, and M. D. Hanigan. 2021. Metatranscriptomic analyses reveal ruminal pH regulates fiber degradation and fermentation by shifting the microbial community and gene expression of carbohydrate-active enzymes. Anim. microbiome 3:1–17. https://doi.org/10.1186/s42523-021-00092-6

Li, Q., R. Liang, Y. Li, Y. Gao, Q. Li, D. Sun, and J. Li. 2020. Identification of candidate genes for milk production traits by RNA sequencing on bovine liver at different lactation stages. BMC Genet. 21:1–12. https://doi.org/10.1186/s12863-020-00882-y

Li, S., G. N. Gozho, N. Gakhar, E. Khafipour, D. O. Krause, and J. C. Plaizier. 2012. Evaluation of diagnostic measures for subacute ruminal acidosis in dairy cows. Can. J. Anim. Sci. 92:353–364. https://doi.org/10.4141/cjas2012-004

Li, W., S. Gelsinger, A. Edwards, C. Riehle, and D. Koch. 2019. Transcriptome analysis of rumen epithelium and meta-transcriptome analysis of rumen epimural microbial community in young calves with feed induced acidosis. Sci. Rep. 9:1–13. https://doi.org/10.1038/s41598-019-39286-z

Liu, J., T. Xu, Y. Liu, W. Zhu, and S. Mao. 2013. A high-grain diet causes massive disruption of ruminal epithelial tight junctions in goats. Am. J. Physiol. Integr. Comp. Physiol. 305:R232–R241. https://doi.org/10.1152/ajpregu.00068.2013

Logan, C. M., and A. S. Menko. 2019. Microtubules: Evolving roles and critical cellular interactions. Exp. Biol. Med. 244:1240–1254. https://doi.org/10.1177/1535370219867296

Love, M. I., W. Huber, and S. Anders. 2014. Moderated estimation of fold change and dispersion for RNA-seq data with DESeq2. Genome Biol. 15:1–21.

Mi, H., S. Poudel, A. Muruganujan, J. T. Casagrande, and P. D. Thomas. 2016. PANTHER version 10: expanded protein families and functions, and analysis tools. Nucleic Acids Res. 44:D336–D342.

Monte, M., R. Benetti, G. Buscemi, P. Sandy, G. Del Sal, and C. Schneider. 2003. The cell cycle-regulated protein human GTSE-1 controls DNA damage-induced apoptosis by affecting p53 function. J. Biol. Chem. 278:30356–30364. https://doi.org/10.1074/jbc.M302902200

Morar, D., C. Văduva, A. Morar, M. Imre, C. Tulcan, and K. Imre. 2022. Paraclinical Changes Occurring in Dairy Cows with Spontaneous Subacute Ruminal Acidosis under Field Conditions. Animals. 12:2466.

Oba, M., and M. S. Allen. 2003. Intraruminal infusion of propionate alters feeding behavior and decreases energy intake of lactating dairy cows. J. Nutr. 133:1099. https://doi.org/10.1093/jn/133.4.1094

Ogata, T., H. Makino, N. Ishizuka, E. Iwamoto, T. Masaki, K. Kizaki, Y. H. Kim, and S. Sato. 2020. Long-term high-grain diet alters ruminal pH, fermentation, and epithelial transcriptomes, leading to restored mitochondrial oxidative phosphorylation in Japanese Black cattle. Sci. Rep. 10:1–11. https://doi.org/10.1038/s41598-020-63471-0

Pertea, M., D. Kim, G.M. Pertea, J. T. Leek, and S. L. Salzberg. 2016. Transcript-level expression analysis of RNA-seq experiments with HISAT, StringTie and Ballgown. Nat. Protoc. 11:1650–1667.

Stefanska, B., W. Człapa, E. Pruszynska-Oszmałek, D. Szczepankiewicz, V. Fievez, J. Komisarek, K. Stajek, and W. Nowak. 2018. Subacute ruminal acidosis affects fermentation and endotoxin concentration in the rumen and relative expression of the CD14/TLR4/MD2 genes involved in lipopolysaccharide systemic immune response in dairy cows. J. Dairy Sci. 101:1297–1310.

Uppal, S. K., K. Wolf, and H. Martens. (2003). The effect of short chain fatty acids on calcium flux rates across isolated rumen epithelium of hay-fed and concentrate-fed sheep. J. Anim. Physiol. Anim. Nutr. 87:12-20. https://doi.org/10.1046/j.1439-0396.2003.00401.x

Verlhac, M.-H., H. De Pennart, B. Maro, M. H. Cobb, and H. J. Clarke. 1993. MAP kinase becomes stably activated at metaphase and is associated with microtubule-organizing centers during meiotic maturation of mouse oocytes. Dev. Biol. 158:330–340.

Wang, X., H. Zhou, J. G. Hickford, S. Li, J. Wang, X. Liu, J. Hu and Y. Luo. (2020). Variation in the yak lipin-1 gene and its association with milk traits. J. Dairy Res. 87:166-169. https://doi.org/10.1017/S002202991900089X

Xu, C., T. Shen, W. Yang, H. Yu, S. Gao, and B. Huang. 2016. The effect of subacute ruminal acidosis of dairy cows on productivity, digestibility and greenhouse gas emission. J. Agric. Sci. 8:92. http://dx.doi.org/10.5539/jas.v8n4p9

Zhang, W., and H. T. Liu. 2002. MAPK signal pathways in the regulation of cell proliferation in mammalian cells. Cell Res. 12:9–1.

CHAPTER 5: GENERAL DISCUSSION AND CONCLUSIONS

5.1 General Discussion

Dietary fiber and starch content influence the rumen microbial profile and fermentation products, consequently altering the rumen environment and influencing the rumen epithelial functions. These changes impact rumen nutrient utilization efficiency and ultimately impact cow production and health through postulated mechanisms of altered rumen microbial metabolic activity and rumen epithelial integrity. Characterizing these mechanisms and identifying biomarkers reflecting a diet-induced altered rumen environment would provide much-needed support for the further development of dairy nutritional management strategies. A series of 3 objectives were developed to address these needs.

In this dissertation, Chapter 2 explores the impact of dietary carbohydrate profile changes on the rumen microbial metabolic activity. In this study (Chapter 2), the effects of varying concentrations of dietary fiber and starch content on the rumen microbial protein abundances in Holstein dairy cows were evaluated using a non-gel-based proteomic technique. The altered carbohydrate profile impacted the abundance of rumen microbial protein. Interestingly, most of the proteins were primarily associated with the *Prevotella* genera. The results of this study provided a snapshot of metabolic adjustments of *Prevotella* at the protein level with dietary carbohydrate profile changes. Interestingly, the *Prevotella* undergoes metabolic adjustments by differentially regulating the proteins involved in the same metabolic pathway. For example, GAPDH and PFOR were involved in the glycolysis pathway; *P. ruminicola* GAPDH abundance was higher with lower dietary RFS content,

whereas *P. ruminicola* PFOR was higher with higher dietary RFS content. As *Prevotella* is the predominant genera within the rumen and has a major share in various rumen metabolic pathways (Wirth et al., 2018), further research on the regulation of proteins associated with core metabolic pathways in *Prevotella* in response to different carbohydrate profiles could be ideal. In addition, most of the microbial proteins impacted by diets in this study were involved in energetics, protein biosynthesis, and carbon metabolism pathways, indicating that diet demonstrates the breadth of dietary impact on protein-mediated activity. Further characterization of shifts in the protein-mediated microbial activity in the rumen with altered carbohydrate substrate, along with correlating changes with changes in microbial outputs such as ruminal VFA profile, will aid in designing strategies to manipulate the functional roles of various microbes within the rumen.

Diet-induced altered rumen environment challenges the rumen epithelial integrity (Aschenbach et al., 2011). In this dissertation, the impact of diet-induced altered rumen environment on rumen epithelium at the molecular level was explored by intra-ruminal propionate dosing (Chapter 4). Propionate-induced down-regulation of rumen epithelial genes involved in the cell growth and division events indicates negative regulation of rumen epithelial cell growth when ruminal propionate is increased. In addition, the propionate dosage affected the expression of genes involved in transport activity, lipid transport and metabolism, protein metabolism, and immune functions. The results of this study suggest that the molecular adaptation of rumen epithelium in response to an altered rumen environment seems to be mediated through tight regulation of the expression of genes involved in various biological processes. Previous studies have identified that rumen

epithelial gene expression involved in fatty acid metabolism, ion transport, immune functions, cell growth, and transport activity are dominantly affected by the highly fermentable diet (Penner et al., 2011). This may further suggest that tight regulation of the expression of genes involved in major biological processes may be part of the coordinated response of rumen epithelium to the altered rumen environment.

Another consequence of diet-induced altered rumen microbial metabolic activity was an alteration of the metabolic status of the animal. This altered metabolic status can be reflected by alterations in body fluids such as milk (Overton et al., 2017). Therefore, we evaluated the use of milk proteins as indicators of changes in rumen microbial activity resulting from the diet-induced modifications to the rumen microbial environment (Chapter 3). In this study (Chapter 3), high starch diet impacted the abundance of milk proteins. Most of the impacted proteins were immune-related, suggesting systematic inflammation in the cows fed with a high starch diet. A higher concentration of LPL with the high starch diet, confirmed with LC-MS/MS analysis and ELISA, may indicate that LPL could be an indicator of a diet-induced altered rumen environment. However, propionate dosage (Chapter 4) did not affect the milk LPL concentration. These may suggest that using milk LPL concentration as an indicator has some limitations. I speculate that the difference in the impact of the altered rumen environment on milk LPL concentration may have to deal with the difference in the cow's lactation stage in the two trials; the cows used in Chapter 3 were at early lactation (85$\pm$15 DIM), whereas those used in Chapter 4 were at the late lactation period (240$\pm$13 DIM). Previously, Zhao et al. (2014) reported that mRNA expression of LPL in the goat mammary gland reached maximum levels within one month

at early lactation, followed by a decline in expression at late lactation and undetectable expression during the dry period. The propionate-induced altered rumen environment has shown no impact on milk LPL concentration may be because of decreased *LPL* gene expression activity during the late lactation period. These may suggest that the cow lactation stage needs to be considered for using milk LPL concentration as a representative biomarker of diet-induced ruminal shifts. The results of this study (Chapter 3) indicate that diet-induced rumen changes can be reflected in milk, suggesting milk proteins can be feasible markers for reflecting diet-induced physiological stress. Therefore, further studies investigating milk proteins as biomarkers of digestive disorders such as SARA could be beneficial.

5.2 Limitations

We utilized samples collected as part of a larger study with different objectives for objectives 1 and 2. Since NDF is the major substrate for numerous rumen microbes for fermentation, only 5 proteins were impacted by the peuNDF240 content in the study (Chapter 2), which indicates that peuNDF240 contents were perhaps too similar across diets to create a microbial activity response that was the focus of our objectives, but not the objectives of the greater study. Variation of peuNDF240 content across the diet would have resulted in variation in the study results. Other limitations include those related to rumen sampling and sample processing. Given the complexity of the rumen ecosystem, the rumen sampling method representing an accurate reflection of the original microbiome and its functional properties is essential (Kunath et al., 2019). Previous studies have shown that rumen sampling via a rumen fistula offers accuracy and allows the collection of

representative rumen fluid samples (Geishauser and Gitzel, 1996). As outlined in chapters 2 and 3, the rumen fluid was collected from three locations in the mid-ventral ruminal sac of each cow via a rumen fistula. However, the inconsistency of sampling region within the rumen across the animals in the study may not reflect the original microbiome and its functional properties because previous studies have shown that rumen microbiota composition was affected by sampling region (Henderson et al., 2013). As Andersen et al. (2021) suggested, given the complexity of rumen microbial function, the development of standardization of protocols for rumen sampling is needed for comparable results.

Humic substances in the rumen fluid samples decreases the number of microbial protein identification. Therefore, TCA was used to precipitate the humic substance in the sample. However, TCA was associated with the loss of proteins and difficulty in resolubilizing proteins in the buffer (Keiblinger et al., 2016; Terry et al., 2018). Loss of proteins impacts our understanding of rumen microbial response in response to the carbohydrate profile. Although proteomic approaches can expand our biological understanding of rumen microbes at the protein level, it has limitations. The major limitation was the limited available databases for protein identification. Because of the complex rumen microbial community, the rumen meta-proteome consists of diverse mixtures of proteins. The ideal database should include all the proteins expected to be expressed within the rumen microbiome. As outlined in Chapters 2 and 3, peptide masses detected in the rumen fluid samples were searched against the selected 71 composite proteome databases for protein identification. The selected databases included only dominant ruminal bacterial species. This results in less protein identification in the samples

and excludes the rumen microbial community's important family members, including protozoal and fungal species, in the analysis. Altogether, largely impacts our understanding of rumen microbial responses at the protein level in response to the dietary carbohydrate profile.

As outlined in Chapter 3, during the milk sample preparation for proteomic analysis, efforts were made to remove high-abundance proteins such as casein via acidification to enrich the detection of low-abundance proteins in the milk; despite the efforts, some of these proteins were still present in our results. The presence of high-abundance proteins masks the detection of low-abundance proteins. Further, removing processes of casein may alter the structure of low-abundance proteins. These factors may impact the identification of total low-abundance proteins in the samples and contribute to variation in the results. In the third study (Chapter 4), rumen papillae biopsies were taken only from one region of the rumen, which may not represent the host transcriptome. Further, the time gap between the rumen papillae biopsies collected across the animals during the trial might impact the rumen epithelial transcriptome, subsequently influencing the transcriptome results. Another limitation of the third study is related to the data analysis; there is no standard bioinformatic pipeline to analyze the rumen epithelial transcriptome data. The results can vary based on the pipeline used to analyze the transcriptome data. Further, multiple freeze-thaw cycles of blood plasma and milk samples limit ELISA's precise measurement of protein concentration in Chapter 4.

5.3 Future Studies

Given the complexity of rumen microbial communities, understanding the rumen microbial response to diet carbohydrate profile using a single omic approach leads to the development of an incomplete picture. For example, Dai et al. (2015) reported that GH5, GH9, GH45, and GH48 were the most expressed carbohydrate-active enzymes (CAZymes) in the rumen of dairy cows fed with a forage diet using a meta-transcriptomic approach. Similarly, Hess et al. (2011), using a meta-genomics approach, reported that the abundance of GH5 and GH9 CAZymes was high but not the abundance of GH45 and GH48 in the rumen of high-forage-fed dairy cows. Therefore, future studies integrating multi-omic (meta-transcriptomics, meta-proteomics, and metabolomics) approaches to study the rumen microbial responses in response to the various concentrations of peuNDF240 and RFS content will lead to developing a complete picture of rumen microbial response to diet. Integrating meta-transcriptomics, meta-proteomics, and metabolomics will provide valuable information about the 'taxon-protein-metabolite' axis. This information will be critical in developing nutrition strategies against metabolic disorders such as sub-acute ruminal acidosis. Of course, the major limitation of this approach will be the limited databases. However, more research has recently been directed toward developing rumen-specific protein databases (Hagen et al., 2021).

The rumen epithelium controls the cow's nutrient availability. During the transition period, cows must adapt to lactation-associated challenges and require significant rumen epithelial functional adjustments to provide the cow with nutrients to support the physiologic state. Therefore, characterizing the rumen epithelial tissue gene expression pattern in response to ruminal pH changes due to the gradual transition of a high

fermentable diet in dairy cows would be beneficial. This information will lead to developing nutritional strategies to support these metabolic adaptations.

As mentioned, identifying non-invasive biomarkers for rumen health and performance can be an interesting decision tool as they provide snapshots of a cow's physiological imbalance. Though the relationship between SARA and milk fat depression is controversial, studies have shown that one of the consequences of SARA in dairy cows is milk fat depression (Koch and Lascano, 2018). It is known that LPL supplies circulating lipids to the mammary gland for fatty acid synthesis, and further studies have shown that LPL was regulated at transcription and translation levels. Therefore, evaluating milk LPL protein concentration, LPL activity in milk, and mammary gland LPL gene expression in dairy cows fed with a SARA-inducing diet might be beneficial. Previously, numerous studies have evaluated various milk fractions, such as milk protein, fat, and MUN, for potential biomarkers for cow metabolic status. However, milk also contains several other signaling components, such as extracellular vesicles, particularly exosomes, which can be potential biomarkers for cow metabolic status. Exosomes are small membrane vesicles ranging from 30 to 100 nm, secreted by multiple cell types under normal and abnormal conditions (Colitti et al., 2020). Exosomes can be used as potential biomarkers for the following reasons; 1) exosomes are involved in cell-to-cell communication (Théry et al., 2002), 2) exosomes are replicative of the donor cell and are composed of mRNA, microRNA, rRNA, long noncoding RNA, tRNA, protein, and DNA, which can affect the recipient cell protein production (Yamamoto et al., 2019), and 3) exosomes can be isolated from various biological fluids, such as milk (Lässer et al., 2011). Considering the strong

relationship between early lactation and liver metabolic changes, we can assume that the liver exosome composition also changes during lactation. Recently, it has been shown that liver-specific exosomes can be isolated from human blood by targeting a liver-specific exosome surface protein (anti-asialoglycoprotein receptor) (Newman et al., 2022). Therefore, the isolation of liver-specific exosomes from lactating dairy cow's milk and the characterization of its transcriptome and proteome profile with diet modification could be beneficial. This information helps monitor changes in the liver during the lactation period and will aid in developing biomarkers for metabolic disorders. However, there are limitations to the proposed idea, namely 1) isolation of exosomes is still challenging because some components of biological fluids, such as microvesicles, lipoprotein have size overlaps with exosomes (Yakubovich et al., 2022), 2) the mRNA or protein yield from exosomes is too low to process with current technology, and 3) isolation of milk liver-specific exosomes using human liver-specific exosome antibodies is questionable. With the rapid advancement in technology, these potential additions to the field of focus may be tangible in the near future.

5.4 Conclusions

The research presented in this dissertation demonstrated that the altered carbohydrate profile impacts the rumen microbial core metabolic pathways. This research also provided a snapshot of the cow rumen epithelial transcriptome profile changes in response to the altered rumen environment. Further, this research demonstrated that the biological shifts resulting from diet-induced altered ruminal changes could be reflected in milk, and milk proteins can be used as biomarkers of diet-induced altered rumen

environment. In addition, we proposed using milk LPL concentration as an indicator of an altered rumen environment resulting from an altered dietary carbohydrate profile. The overall results of this research improved our understanding of rumen microbial responsiveness to the dietary carbohydrate profile along with the impact of diet-induced altered rumen environment on the rumen epithelial gene expression and milk protein profile. Additionally, our results highlight the need to further examine changes in the rumen microbial activity and rumen epithelial gene expression in response to alterations in dietary carbohydrate composition. This information will lead to a complete understanding of the impact of diet on rumen health. Further, combining the above information with identified biomarkers for diet-induced altered rumen environment will aid in developing precision feeding strategies that maximize rumen nutrition utilization efficiency.

CHAPTER 6: COMPREHENSIVE BIBLIOGRAPHY

Abdelmegid, S., J. Murugaiyan, M. Abo-Ismail, J. L. Caswell, D. Kelton, and G. M. Kirby. 2017. Identification of host defense-related proteins using label-free quantitative proteomic analysis of milk whey from cows with Staphylococcus aureus subclinical mastitis. Int. J. Mol. Sci. 19:78. https://doi.org/10.3390/ijms19010078

Abou-Ward, G. A. 2008. Effect of pre-weaning diet on lamb's rumen development. American-Eurasian Journal of Agricultural and Environmental Science. 3:561–567.

Actis Dato, V., and G. A. Chiabrando. 2018. The role of low-density lipoprotein receptor-related protein 1 in lipid metabolism, glucose homeostasis and inflammation. Int. J. Mol. Sci. 19:1780.

Aguilar, M., M. D. Hanigan, H. A. Tucker, B. L. Jones, S. K. Garbade, M. L. McGilliard, C. C. Stallings, K. F. Knowlton, and R. E. James. 2012. Cow and herd variation in milk urea nitrogen concentrations in lactating dairy cattle. J. Dairy Sci. 95:7261–7268. https://doi.org/10.3168/jds.2012-5582

Akhlaghi, B., E. Ghasemi, M. Alikhani, A. Ghaedi, S. Nasrollahi, and M. H. Ghaffari. 2022. Influence of reducing starch in the diets with similar protein and energy contents on lactation performance, ruminal fermentation, digestibility, behaviour and blood metabolites in primiparous and multiparous dairy cows. Vet. Med. Sci. 8:808-821. https://doi.org/10.1002/vms3.722

Allen, M. and D. J. Mertens 1988. Evaluating constraints on fiber digestion by rumen microbes. J. Nutr. 118:261-270. https://doi.org/10.1093/jn/118.2.261

Alzahal, O., M. Or-Rashid, S. L. Greenwood, M. Douglas, and B. J. McBride. 2009. The effect of dietary fiber level on milk fat concentration and fatty acid profile of cows fed diets containing low levels of polyunsaturated fatty acids. J. Dairy Sci. 92:1108-1116. https://doi.org/10.3168/jds.2008-1472

Ametaj, B. N., Q. Zebeli, F. Saleem, N. Psychogios, M. J. Lewis, S.M. Dunn, J. Xia, and D. S. Wishart. 2010. Metabolomics reveals unhealthy alterations in rumen metabolism with increased proportion of cereal grain in the diet of dairy cows. Metabolomics. 6:583–594. https://doi.org/10.1007/s11306-010-0227-6

Andersen, P. H., B. Bergelin, and K. A. Christensen. 1994. Effect of feeding regimen on concentration of free endotoxin in ruminal fluid of cattle. J. Anim. Sci. 72:487–491. https://doi.org/10.2527/1994.722487x

Andersen, T. O., B. J. Kunath, L. H. Hagen, M. O. Arntzen, and P. B. Pope. 2021. Rumen metaproteomics: Closer to linking rumen microbial function to animal productivity traits. Methods. 186:42–51. https://doi.org/10.1016/j.ymeth.2020.07.011

Anderson, C. J., and S. Schmitz-Esser. 2022. Differential Gene Expression of the Bovine Rumen Epithelial Microbiota During a Sub-acute Ruminal Acidosis (SARA) Challenge. J. Anim. Sci. Oxford Univ Press Inc Journals Dept, 2001 Evans Rd, Cary, NC 27513 USA.

Andrews, S. 2010. FastQC: a quality control tool for high throughput sequence data.

Annison, E. F., and W. L. Bryden. 1998. Perspectives on ruminant nutrition and metabolism I. Metabolism in the rumen. Nutr. Res. Rev. 11:173–198. https://doi.org/10.1079/NRR19980014

Aoki, T. and S. Narumiya. 2012. Prostaglandins and chronic inflammation. Trends Pharmacol. Sci. 33:304-311. https://doi.org/10.1016/j.tips.2012.02.004

Appel, S. H. and B. L. Parrot. 1970. Hexose monophosphate pathway in synapses. J. Neurochem. 17:1619-1626. https://doi.org/10.1111/j.1471-4159.1970.tb11386.x.

Arias, M. A., J. Nores, N. Vita, F. Stelter, L. K. Borysiewicz, P. Ferrara, and M. Labéta. 2000. Cutting edge: human B cell function is regulated by interaction with soluble CD14: opposite effects on IgG1 and IgE production. J. Immunol. 164:3480-3486. https://doi.org/10.4049/jimmunol.164.7.3480

Asanuma, N. and T. Hino. 2001. Molecular characterization, enzyme properties and transcriptional regulation of phosphoenolpyruvate carboxykinase and pyruvate kinase in a ruminal bacterium, Selenomonas ruminantium. Microbiology. 147:681-690. https://doi.org/10.1099/00221287-147-3-681.

Aschenbach, J. R., G. B. Penner, F. Stumpff, and G. Gäbel. 2011. Ruminant nutrition symposium: Role of fermentation acid absorption in the regulation of ruminal pH. J. Anim. Sci. 89:1092–1107. https://doi.org/10.2527/jas.2010-3301

Aschenbach, J. R., S. Bilk, G. Tadesse, F. Stumpff, and G. Gäbel. 2009. Bicarbonate-dependent and bicarbonate-independent mechanisms contribute to nondiffusive uptake of acetate in the ruminal epithelium of sheep. Am. J. Physiol. Liver Physiol. 296:G1098–G1107. https://doi.org/10.1152/ajpgi.90442.2008

Asma, Z., C. Sylvie, C. Laurent, M. Jérôme, K. Christophe, B. Olivier, T. M. Annabelle, and E. Francis. 2013. Microbial ecology of the rumen evaluated by 454 GS FLX pyrosequencing is affected by starch and oil supplementation of diets. FEMS Microbiol. Ecol. 83:504-514. https://doi.org/10.1111/1574-6941.12011.

Bach, A. 2014. Precision feeding to increase efficiency for milk production. Adv. Dairy Technol. 26:177–189.

Baldwin, R. L. T., and K. R. McLeod. 2000. Effects of diet forage: concentrate ratio and metabolizable energy intake on isolated rumen epithelial cell metabolism in vitro. J. Anim. Sci. 78:771–783. https://doi.org/10.2527/2000.783771x

Baldwin, R. L., and E. E. Connor. 2017. Rumen function and development. Vet. Clin. North Am. Food Anim. Pract. 33:427–439.

Baldwin, R. L., R. W. Li, Y. Jia, and C. Li. 2018. Transcriptomic impacts of rumen epithelium induced by butyrate infusion in dairy cattle in dry period. Gene Regul. Syst. Biol. 12:11776250-18774798. https://doi.org/10.1177/1177625018774798

Baldwin, R. L., W. Li, C. Li, E. E. Connor, and R. W. Li. 2012. The bacterial community composition of the bovine rumen detected using pyrosequencing of 16S rRNA genes. Metagenomics. b1-11. https://doi.org/10.4303/mg/235571

Bauman, D. E., and J. M. Griinari. 2003. Nutritional regulation of milk fat synthesis. Annu. Rev. Nutr. 23:203–227. https://doi.org/10.1146/annurev.nutr.23.011702.073408

Bazil, V. and J. Strominger. 1991. Shedding as a mechanism of down-modulation of CD14 on stimulated human monocytes. J. Immunol. 147:1567-1574.

Beauchemin, K., W. Yang, and L. Rode. 2003. Effects of particle size of alfalfa-based dairy cow diets on chewing activity, ruminal fermentation, and milk production. J. Dairy Sci. 86:630-643. https://doi.org/10.3168/jds.S0022-0302(03)73641-8

Bednar, G. E., A. R. Patil, S. M. Murray, C. M. Grieshop, N. R. Merchen, and G. C. Fahey Jr. 2001. Starch and fiber fractions in selected food and feed ingredients affect their small intestinal digestibility and fermentability and their large bowel fermentability in vitro in a canine mode. J. Nutr. 131:276–286. https://doi.org/10.1093/jn/131.2.276

Beliveau, R. M., and J. J. McKinnon. 2008. Effect of graded levels of wheat-based dried distillers' grains with solubles on performance and carcass characteristics of feedlot steers. Can. J. Anim. Sci. 88:677–684. https://doi.org/10.4141/CJAS08045

Bergman, E. N. 1990. Energy contributions of volatile fatty acids from the gastrointestinal tract in various species. Physiol. Rev. 70:567–590.

Bernard, L., C. Leroux, and Y. Chilliard. 2008. Expression and nutritional regulation of lipogenic genes in the ruminant lactating mammary gland. Pages 67-108 in Bioactive Components of Milk. Z. Bösze, ed. Springer, New York, NY. https://doi.org/10.1017/S1751731110000510

Bionaz, M., and J. J. Loor. 2008. ACSL1, AGPAT6, FABP3, LPIN1, and SLC27A6 are the most abundant isoforms in bovine mammary tissue and their expression is affected by stage of lactation. J. Nutr. 138:1019–1024. https://doi.org/10.1093/jn/138.6.1019

Bipin, K. C., P. T. Ramesh, and S. Yathiraj. 2016. Impact of subacute ruminal acidosis (SARA) on milk yield and milk fat content in crossbred dairy cows. Paripex-Indian J. Res. 5:290–292.

Boehmer, J. L. 2011. Proteomic analyses of host and pathogen responses during bovine mastitis. Mammary Gland Biol Neoplasia. 16:323-338. https://doi.org/10.1007/s10911-011-9229-x

Boehmer, J. L., J. A. DeGrasse, M. A. McFarland, E. A. Tall, K. J. Shefcheck, J. L. Ward, and D. D. Bannerman. 2010. The proteomic advantage: label-free quantification of proteins

expressed in bovine milk during experimentally induced coliform mastitis. Vet. Immunol. Immunopathol. 138:252–266. https://doi.org/10.1016/j.vetimm.2010.10.004

Boehmer, J., D. Bannerman, K. Shefcheck, and J. Ward. 2008. Proteomic analysis of differentially expressed proteins in bovine milk during experimentally induced *Escherichia coli mastitis*. J. Dairy Sci. 91:4206-4218. https://doi.org/10.3168/jds.2008-1297

Bolger, A. M., M. Lohse, and B. Usadel. 2014. Trimmomatic: a flexible trimmer for Illumina sequence data. Bioinformatics 30:2114–2120.

Brandao, V. L. N., and A. P. Faciola. 2019. Unveiling the relationships between diet composition and fermentation parameters response in dual-flow continuous culture system: a meta-analytical approach. Transl. Anim. Sci. 3:1064–1075. https://doi.org/10.1093/tas/txz019

Brulc, J. M., D. A. Antonopoulos, M. E. Berg Miller, M. K. Wilson, A. C. Yannarell, E. A. Dinsdale, R. E. Edwards, E. D. Frank, J. B. Emerson, and P. Wacklin. 2009. Gene-centric metagenomics of the fiber-adherent bovine rumen microbiome reveals forage specific glycoside hydrolases. Proc. Natl. Acad. Sci. 106:1948–1953. https://doi.org/10.1073/pnas.0806191105

Brulc, J. M., D. A. Antonopoulos, M. E. Berg Miller, M. K. Wilson, A. C. Yannarell, E. A. Dinsdale, R. E. Edwards, E. D. Frank, J. B. Emerson, and P. Wacklin. 2009. Gene-centric metagenomics of the fiber-adherent bovine rumen microbiome reveals forage specific glycoside hydrolases. Proc. Natl. Acad. Sci. 106:1948–1953. https://doi.org/10.1073/pnas.0806191105

Cantalapiedra-Hijar, G., J. L. Peyraud, S. Lemosquet, E. Molina-Alcaide, H. Boudra, P. Noziere, and I. Ortigues-Marty. 2014. Dietary carbohydrate composition modifies the milk N efficiency in late lactation cows fed low crude protein diets. Animals. 8:275-285. https://doi.org/10.1017/S1751731113002012

Carman, G. M., and G. S. Han. 2009. Phosphatidic acid phosphatase, a key enzyme in the regulation of lipid synthesis. J. Biol. Chem. 284:2593–2597. https://doi.org/10.1074/jbc.R800059200

Case, R. J., Y. Boucher, I. Dahllöf, C. Holmström, W. F. Doolittle, and S. Kjelleberg. 2007. Use of 16S rRNA and rpoB genes as molecular markers for microbial ecology studies. Appl. Environ. Microbiol. 73:278–288. https://doi.org/10.1128/AEM.01177-06

Chang, G., L. Wang, N. Ma, W. Zhang, H. Zhang, H. Dai, and X. 2018. Histamine activates inflammatory response and depresses casein synthesis in mammary gland of dairy cows during SARA. BMC Vet. Res. 14:168.

Chastain, C. J., C. J. Failing, L. Manandhar, M. A. Zimmerman, M. M. Lakner, and T. H. Nguyen. 2011. Functional evolution of C4 pyruvate, orthophosphate dikinase. J. Exp. Bot. 62:3083-3091. https://doi.org/10.1093/jxb/err058.

Chen, Y., and M. Oba. 2012. Variation of bacterial communities and expression of Toll-like receptor genes in the rumen of steers differing in susceptibility to subacute ruminal acidosis. Vet. Microbiol. 159:451–459. https://doi.org/10.1016/j.vetmic.2012.04.032

Chen, Y., G. B. Penner, M. Li, M. Oba, and L. L. Guan. 2011. Changes in Bacterial Diversity Associated with Epithelial Tissue in the Beef Cow Rumen during the Transition to a High-Grain Diet. Appl. Environ. Microbiol. 77:5770–5781. https://doi.org/10.1128/AEM.00375-11

Chenost, M. 1966. Fibrousness of forages: its determination and its relation to feeding value. Fibrousness of forages: Its determination and its relation to feeding value.

Choi, B. R., and M. S. Allen. 1999. Intake regulation by volatile fatty acids and physical fill. S. Afr. J. Anim. Sci. 29:40–41.

Chouinard, P. Y., L. Corneau, D. M. Barbano, L. E. Metzger, and D. E. Bauman. 1999. Conjugated linoleic acids alter milk fatty acid composition and inhibit milk fat secretion in dairy cows. J. Nutr. 129:1579–1584. https://doi.org/10.1093/jn/129.8.1579

Church, D. C. 1993. The Ruminant Animal: Digestive Physiology and Nutrition. Waveland press.

Clooney, A. G., F. Fouhy, R. D. Sleator, A. O'Driscoll, C. Stanton, P. D. Cotter, and M. J. Claesson. 2016. Comparing apples and oranges?: Next generation sequencing and its impact on microbiome analysis. PLoS One. 11:e0148028. https://doi.org/10.1371/journal.pone.0148028

Colitti, M., S. Sgorlon, and B. Stefanon. 2020. Exosome cargo in milk as a potential marker of cow health. J. Dairy Res. 87:79–83.

Colman, E., W. B. Fokkink, M. Craninx, J. R. Newbold, B. de Baets, and V. Fievez. 2010. Effect of induction of subacute ruminal acidosis on milk fat profile and rumen parameters. J. Dairy Sci. 93:4759–4773. https://doi.org/10.3168/jds.2010-3158

Comtet-Marre, S., N. Parisot, P. Lepercq, F. Chaucheyras-Durand, P. Mosoni, E. Peyretaillade, A. R. Bayat, K. J. Shingfield, P. Peyret, and E. Forano. 2017. Metatranscriptomics reveals the active bacterial and eukaryotic fibrolytic communities in the rumen of dairy cow fed a mixed diet. Front. Microbiol. 8:67. https://doi.org/10.3389/fmicb.2017.00067

Conduit, P. T. 2016. Microtubule organization: A complex solution. J. Cell Biol. 213:609. https://doi.org/10.1083%2Fjcb.201606008

Conrad, H., A. D. Pratt, and J. W. Hibbs. 1964. Regulation of feed intake in dairy cows. I. Change in importance of physical and physiological factors with increasing digestibility. J. Dairy Sci. 47:54-62. https://doi.org/10.3168/jds.S0022-0302(64)88581-7.

Cook, N. B., K. V. Nordlund, and G. Oetzel. 2004. Environmental influences on claw horn lesions associated with laminitis and subacute ruminal acidosis in dairy cows. J. Dairy Sci. 87:E36-E46. https://doi.org/10.3168/jds.S0022-0302(04)70059-4

Coomey, J. H., R. Sibout, and S. P. Hazen. 2020. Grass secondary cell walls, Brachypodium distachyon as a model for discovery. New Phytol. 227:1649–1667. https://doi.org/10.1111/nph.16603

D'Amore, R., U. Z. Ijaz, M. Schirmer, J. G. Kenny, R. Gregory, A. C. Darby, M. Shakya, M. Podar, C. Quince, and N. Hall. 2016. A comprehensive benchmarking study of protocols and sequencing platforms for 16S rRNA community profiling. BMC Genomics. 17:1–20. https://doi.org/10.1186/s12864-015-2194-9

Dai, X., Y. Tian, J. Li, X. Su, X. Wang, S. Zhao, L. Liu, Y. Luo, D. Liu, and H. Zheng. 2015. Metatranscriptomic analyses of plant cell wall polysaccharide degradation by microorganisms in the cow rumen. Appl. Environ. Microbiol. 81:1375–1386.

Danielsson, R., A. Schnürer, V. Arthurson, and J. Bertilsson. 2012. Methanogenic population and CH4 production in Swedish dairy cows fed different levels of forage. Appl. Environ. Microbiol. 78:6172-6179. https://doi.org/10.1128/AEM.00675-12

Danielsson, R., J. Dicksved, L. Sun, H. Gonda, B. Müller, A. Schnürer, and J. Bertilsson. 2017. Methane production in dairy cows correlates with rumen methanogenic and bacterial community structure. Front. Microbiol. 8:226. https://doi.org/10.3389/fmicb.2017.00226

Danscher, A. M., S. Li, P. H. Andersen, E. Khafipour, N. B. Kristensen, and J. C. Plaizier. 2015. Indicators of induced subacute ruminal acidosis (SARA) in Danish Holstein cows. Acta Vet. Scand. 57:1–14. https://doi.org/10.1186/s13028-015-0128-9

de Koster, J., M. Salavati, C. Grelet, M. A. Crowe, E. Matthews, R. O'Flaherty, G. Opsomer, L. Foldager, and M. Hostens. 2019. Prediction of metabolic clusters in early-lactation dairy cows using models based on milk biomarkers. J. Dairy Sci. 102:2631–2644. https://doi.org/10.3168/jds.2018-15533

Deák, F., R. E. Anderson, J. L. Fessler, and D. M. Sherry. 2019. Novel cellular functions of very long chain-fatty acids: insight from ELOVL4 mutations. Front. Cell. Neurosci. 13:428. https://doi.org/10.3389/fncel.2019.00428

Delosière, M., J. Pires, L. Bernard, I. Cassar-Malek, and M. Bonnet. 2019. Milk proteome from in silico data aggregation allows the identification of putative biomarkers of negative energy balance in dairy cows. Sci. Rep. 9:1–11.

Deng, W., M. Wanapat, S. Ma, J. Chen, D. Xi, T. He, Z. Yang, and H. Mao. 2007. Phylogenetic analysis of 16S rDNA sequences manifest rumen bacterial diversity in gayals (*Bos frontalis*) fed fresh bamboo leaves and twigs (*Sinarumdinari*a). Asian-Australas. J. Anim. Sci. 20:1057-1066. https://doi.org/10.5713/ajas.2007.1057.

Deusch, S., A. Camarinha-Silva, J. Conrad, U. Beifuss, M. Rodehutscord, and J. Seifert. 2017. A structural and functional elucidation of the rumen microbiome influenced by various diets and microenvironments. Front. Microbiol. 8:1605. https://doi.org/10.3389/fmicb.2017.01605

Dias, A. L. G., J. A. Freitas, B. Micai, R. A. Azevedo, L. F. Greco, and J. E. P. Santos. 2018. Effects of supplementing yeast culture to diets differing in starch content on performance and feeding behavior of dairy cows. J. Dairy Sci. 101:186–200. https://doi.org/10.3168/jds.2017-13240

Ding, L., J. Cao, W. Lin, H. Chen, X. Xiong, H. Ao, M. Yu, J. Lin, and Q. Cui. 2020. The roles of cyclin-dependent kinases in cell-cycle progression and therapeutic strategies in human breast cancer. Int. J. Mol. Sci. 21:1960. https://doi.org/10.3390/ijms21061960

Dionissopoulos, L., M. A. Steele, O. Alzahal, and B. W. McBride. 2012. Adaptation to high grain diets proceeds through minimal immune system stimulation and differences in extracellular matrix protein expression in a model of subacute ruminal acidosis in non-lactating dairy cows. Am. J. Anim. Vet. Sci. 7:84–91.

Dirksen, G. U., H. G. Liebich, and E. Mayer. 1985. Adaptive changes of the ruminal mucosa and their functional and clinical significance. Bov. Pract. (Stillwater). 116–120.

Discipio, R. J. 1982. The activation of the alternative pathway C3 convertase by human plasma kallikrein. BSI. 45:587.

Dobson, M. J., W. C. B. Brown, A. Dobson, and A. T. Phillipson. 1956. A histological study of the organization of the rumen epithelium of sheep. Q. J. Exp. Physiol. 41:247–253. https://doi.org/10.1113/expphysiol.1956.sp001186

Dong, G., S. Liu, Y. Wu, C. Lei, J. Zhou, and S. Zhang. 2011. Diet-induced bacterial immunogens in the gastrointestinal tract of dairy cows: impacts on immunity and metabolism. Acta Vet. Scand. 53:1–7. https://doi.org/10.1186/1751-0147-53-48

Dong, H., S. Wang, Y. Jia, Y. Ni, Y. Zhang, S. Zhuang, X. Shen, and R. Zhao. 2013. Long-term effects of subacute ruminal acidosis (SARA) on milk quality and hepatic gene expression in lactating goats fed a high-concentrate diet. PLoS One. 8:850.

Doolittle, M. H., O. Ben-Zeev, J. Elovson, D. Martin, and T. Kirchgessner. 1990. The response of lipoprotein lipase to feeding and fasting. Evidence for posttranslational regulation. J. Biol. Chem. 265:4570-4577.

Eckersall, P. D., F. J. Young, A. M. Nolan, C. H. Knight, C. McComb, M. M. Waterston, C. J. Hogarth, E. M. Scott, and J. L. Fitzpatrick. 2006. Acute phase proteins in bovine milk in an experimental model of Staphylococcus aureus subclinical mastitis. J. Dairy Sci. 89:1488–1501. https://doi.org/10.3168/jds.S0022-0302(06)72216-0

Emmanuel, D., S. Dunn, and B. Ametaj. 2008. Feeding high proportions of barley grain stimulates an inflammatory response in dairy cows. J. Dairy Sci. 91:606-614. https://doi.org/10.3168/jds.2007-0256

Enemark, J. M. D., R. J. Jorgensen, and P. S. Enemark. 2002. Rumen acidosis with special emphasis on diagnostic aspects of subclinical rumen acidosis: a review. Vet. ir Zootech. 20:16–29.

Etschmann, B., A. Suplie, and H. Martens. 2009. Change of ruminal sodium transport in sheep during dietary adaptation. Arch. Anim. Nutr. 63:26–38. https://doi.org/10.1080/17450390802506885

Ferraretto, L. F., P. M. Crump, and R. D. Shaver. 2013. Effect of cereal grain type and corn grain harvesting and processing methods on intake, digestion, and milk production by dairy cows through a meta-analysis. J. Dairy Sci. 96:533–550. https://doi.org/10.3168/jds.2012-5932

Ferri, G., G. Comerio, P. Ladarola, M. Zapponi, and M. Speranza. 1978. Subunit structure and activity of glyceraldehyde-3-phosphate dehydrogenase from spinach chloroplasts. Biochim Biophys Acta- Enzymology. 522: 19-31. https://doi.org/10.1016/0005-2744(78)90318-2

Filipp, D., K. Alizadeh-Khiavi, C. Richardson, A. Palma, N. Paredes, O. Takeuchi, S. Akira, and M. Julius. 2001. Soluble CD14 enriched in colostrum and milk induces B cell growth and differentiation. PNAS. 98:603-608. https://doi.org/10.1073/pnas.98.2.603

Flint, H. J., and E. A. Bayer. 2008. Plant cell wall breakdown by anaerobic microorganisms from the mammalian digestive tract. Ann. N. Y. Acad. Sci. 1125:280–288. https://doi.org/10.1196/annals.1419.022

Fox, P. F., and A. Brodkorb. 2008. The casein micelle: Historical aspects, current concepts and significance. Int. Dairy J. 18:677–684. https://doi.org/10.1016/j.idairyj.2008.03.002

Furuhashi, M., and G. S. Hotamisligil. 2008. Fatty acid-binding proteins: role in metabolic diseases and potential as drug targets. Nat. Rev. Drug Discov. 7:489–503.

Fustini, M., A. Palmonari, G. Canestrari, E. Bonfante, L. Mammi, M. Pacchioli, G. Sniffen, R. Grant, K. Cotanch, and A. Formigoni. 2017. Effect of undigested neutral detergent fiber content of alfalfa hay on lactating dairy cows: Feeding behavior, fiber digestibility, and lactation performance. J. Dairy Sci. 100:4475-4483. https://doi.org/10.3168/jds.2016-12266

Gäbel, G., H. Martens, M. Sündermann, and P. Galfi. 1987. The effect of diet, intraruminal pH and osmolarity on sodium, chloride and magnesium absorption from the temporarily isolated and washed reticulo-rumen of sheep. Q. J. Exp. Physiol. Transl. Integr. 72:501–511. https://doi.org/10.1113/expphysiol.1987.sp003092

Galfi, P., S. Neogrady, and T. Sakata. 1991. Effects of volatile fatty acids on the epithelial cell proliferation of the digestive tract and its hormonal mediation. Elsevier. https://doi.org/10.1016/B978-0-12-702290-1.50010-2

Gao, X., and M. Oba. 2015. Non-invasive indicators to identify lactating dairy cows with a greater risk of subacute rumen acidosis. J. Dairy Sci. 98:5735–5739. https://doi.org/10.3168/jds.2015-9456

Gao, X., and M. Oba. 2016. Effect of increasing dietary nonfiber carbohydrate with starch, sucrose, or lactose on rumen fermentation and productivity of lactating dairy cows. J. Dairy Sci. 99:291–300. https://doi.org/10.3168/jds.2015-9871

Garcia, M., B. J. Bradford, and T. G. Nagaraja. 2017. Invited review: ruminal microbes, microbial products, and systemic inflammation. Prof. Anim. Sci. 33:635–650. https://doi.org/10.15232/pas.2017-01663

Garrett, E., M. Pereira, K. Nordlund, L. Armentano, W. Goodger, and G. Oetzel. 1999. Diagnostic methods for the detection of subacute ruminal acidosis in dairy cows. J. Dairy Sci. 82:1170-1178. https://doi.org/10.3168/jds.S0022-0302(99)75340-3

Geishauser, T., and A. Gitzel. 1996. A comparison of rumen fluid sampled by oro-ruminal probe versus rumen fistula. Small Rumin. Res. 21:63–69.

Gholizadeh, M., J. Fayazi, H. Zali, and Y. Asgari. 2020. Transcriptomic changes in the rumen epithelium of cattle after the induction of acidosis. Arch. Razi Inst. 75:109. https://doi.org/10.22092%2FARI.2019.125930.1326

Giuberti, G., A. Gallo, F. Masoero, L. F. Ferraretto, P. C. Hoffman, and R. D. Shaver. 2014. Factors affecting starch utilization in large animal food production system: A review. Starch-Stärke. 66:72–90. https://doi.org/10.1002/star.201300177

Goering, H. K. 1970. Forage Fiber Analyses (Apparatus, Reagents, Procedures, and Some Applications). US Agricultural Research Service.

Goodlad, R. A. 1981. Some effects of diet on the mitotic index and the cell cycle of the ruminal epithelium of sheep. Q. J. Exp. Physiol. Transl. Integr. 66:487–499. https://doi.org/10.1113/expphysiol.1981.sp002590

Gotoh, T., T. Nishimura, K. Kuchida, and H. Mannen. 2018. The Japanese Wagyu beef industry: Current situation and future prospects—A review. Asian-Australasian J. Anim. Sci. 31:933.

Gozho, G. N., D. O. Krause, and J. C. Plaizier. 2007. Ruminal lipopolysaccharide concentration and inflammatory response during grain-induced subacute ruminal acidosis in dairy cows. J. Dairy Sci. 90:856–866. https://doi.org/10.3168/jds.S0022-0302(07)71569-2

Graham, C., and N. L. Simmons. 2005. Functional organization of the bovine rumen epithelium. Am. J. Physiol. Integr. Comp. Physiol. 288:R173–R181. https://doi.org/10.1152/ajpregu.00425.2004

Grant, G. A. 2018. d-3-phosphoglycerate dehydrogenase. Front. Mol. Biosci. 5:110. https://doi.org/10.3389/fmolb.2018.00110.

Grant, R. 2010. Forage fragility, fiber digestibility, and chewing response in dairy cattle. Pages 27–40 in Proceedings of the 19th Annual Tri-State Dairy Nutrition Conference, Grand Wayne Center, Fort Wayne, Indiana, USA, 20-21 April, 2010. Purdue University Press.

Grant, R. J. 1997. Interactions among forages and nonforage fiber sources. J. Dairy Sci. 80:1438-1446. https://doi.org/10.3168/jds.S0022-0302(97)76073-9

Grant, R., W. Smith, and M. J. Miller. 2020. Relationships between fibre digestibility and particle size for lactating dairy cows. Adv. Dairy Technol. 32:47-57.

Greco, G., F. Hagen, S. Meibner, Z. Shen, Z. Lu, S. Amasheh, and J. R. Aschenbach. 2018. Effect of individual SCFA on the epithelial barrier of sheep rumen under physiological and acidotic luminal pH conditions. J. Anim. Sci. 96:126–142. https://doi.org/10.1093/jas/skx017

Greenwood, S. L., and M. C. Honan. 2019. Symposium review: Characterization of the bovine milk protein profile using proteomic techniques. J. Dairy Sci. 102:2796–2806. https://doi.org/10.3168/jds.2018-15266

Grönlund, U., C. Hultén, P. D. Eckersall, C. Hogarth, and K. Waller. 2003. Haptoglobin and serum amyloid A in milk and serum during acute and chronic experimentally induced Staphylococcus aureus mastitis. J. Dairy Res. 70:379-386. https://doi.org/10.1017/S0022029903006484

Guo, Y., X. Xu, Y. Zou, Z. Yang, S. Li, and Z. Cao. 2013. Changes in feed intake, nutrient digestion, plasma metabolites, and oxidative stress parameters in dairy cows with subacute ruminal acidosis and its regulation with pelleted beet pulp. J. Anim. Sci. Biotechnol. 4:1–10. https://doi.org/10.1186/2049-1891-4-31

Guo, Z., L. Ma, and D. Bu. 2022. Omics, the New Technological Approaches to the Milk Protein Researches. Milk Protein New Res. Approaches 37.

Hagen, L.H., C. G. Brooke, C. A. Shaw, A. D. Norbeck, H. Piao, M.Ø. Arntzen, H.M. Olson, A. Copeland, N. Isern, and A. Shukla. 2021. Proteome specialization of anaerobic fungi during ruminal degradation of recalcitrant plant fiber. ISME J. 15:421–434.

Harris, P., K. M. Johannessen, G. Smolenski, M. Callaghan, M. K. Broadhurst, K. Kim, and T. Wheeler. 2010. Characterisation of the antimicrobial activity of bovine milk ribonuclease4 and ribonuclease5 (angiogenin). Int. Dairy J. 20:400-407. https://doi.org/10.1016/j.idairyj.2009.12.018

Hart, E. H., C. J. Creevey, T. Hitch, and A. H. Kingston-Smith. 2018. Meta-proteomics of rumen microbiota indicates niche compartmentalisation and functional dominance in a limited number of metabolic pathways between abundant bacteria. Sci. Rep. 8:1–11. https://doi.org/10.1038/s41598-018-28827-7

Hassanat, F., R. Gervais, C. Julien, D. Massé, A. Lettat, P. Y. Chouinard, H. V. Petit, and C. Benchaar. 2013. Replacing alfalfa silage with corn silage in dairy cow diets: Effects on enteric methane production, ruminal fermentation, digestion, N balance, and milk production. J. Dairy Sci. 96:4553-4567. https://doi.org/10.3168/jds.2012-6480.

Haziot, A., B.-Z. Tsuberi, and S. Goyert. 1993. Neutrophil CD14: biochemical properties and role in the secretion of tumor necrosis factor-alpha in response to lipopolysaccharide. J. Immunol. Res. 150:5556-5565.

Haziot, A., G. W. Rong, V. Bazil, J. Silver, and S. Goyert. 1994. Recombinant soluble CD14 inhibits LPS-induced tumor necrosis factor-alpha production by cells in whole blood. J. Immunol. Res. 152:5868-5876.

Haziot, A., S. Chen, E. Ferrero, M. Low, R. Silber, and S. Goyert. 1988. The monocyte differentiation antigen, CD14, is anchored to the cell membrane by a phosphatidylinositol linkage. J. Immunol. Res. 141:547-552.

Heinrichs, J. and P. Kononoff, University Park, PA. DSE. 2013. The Penn state particle separator. 186:1-8.

Henderson, G., F. Cox, S. Ganesh, A. Jonker, W. Young, and P. H. Janssen. 2015. Rumen microbial community composition varies with diet and host, but a core microbiome is found across a wide geographical range. Sci. Rep. 5:1–15. https://doi.org/10.1038/srep14567

Hernández, J., J. L. Benedito, A. Abuelo, and C. Castillo. 2014. Ruminal acidosis in feedlot: from aetiology to prevention. Sci. World J. 2014. https://doi.org/10.1155/2014/702572

Hess, M., A. Sczyrba, R. Egan, T.-W. Kim, H. Chokhawala, G. Schroth, S. Luo, D. S. Clark, F. Chen, and T. Zhang. 2011. Metagenomic discovery of biomass-degrading genes and genomes from cow rumen. Science. 331:463–467.

Hettinga, K., H. van Valenberg, S. de Vries, S. Boeren, T. van Hooijdonk, J. van Arendonk, and J. Vervoort. 2011. The host defense proteome of human and bovine milk. PLoS One. 6:e19433. https://doi.org/10.1371/journal.pone.0019433

Hofmann, R. R. 1989. Evolutionary steps of ecophysiological adaptation and diversification of ruminants: a comparative view of their digestive system. Oecologia. 78:443–457. https://doi.org/10.1007/BF00378733

Honan, M. C. and S. L. Greenwood. 2020. Characterization of variations within the rumen metaproteome of Holstein dairy cattle relative to morning feed offering. Sci. Rep. 10:1-8. https://doi.org/10.1038/s41598-020-59974-5.

Hook, S. E., M. A. Steele, K. S. Northwood, J. Dijkstra, J. France, A.-D. G. Wright, and B. W. McBride. 2011. Impact of subacute ruminal acidosis (SARA) adaptation and recovery on the density and diversity of bacteria in the rumen of dairy cows. FEMS Microbiol. Ecol. 78:275-284. https://doi.org/10.1111/j.1574-6941.2011.01154.x

Hughes, T. R., T. S. Tengku-Muhammad, S. A. Irvine, and D. P. Ramji. 2002. A novel role of Sp1 and Sp3 in the interferon-γ-mediated suppression of macrophage lipoprotein lipase gene transcription. J. Biol. Chem. 277:11097-11106. https://doi.org/10.1074/jbc.M106774200

Huhtanen, P., J. Nousiainen, and M. Rinne. 2006. Recent developments in forage evaluation with special reference to practical applications.

Humer, E., J. R. Aschenbach, V. Neubauer, I. Kröger, R. Khiaosa-Ard, W. Baumgartner, and Q. Zebeli. 2018. Signals for identifying cows at risk of subacute ruminal acidosis in dairy veterinary practice. J. Anim. Physiol. Anim. Nutr. (Berl). 102:380–392. https://doi.org/10.1111/jpn.12850

Huntington, G. B. 1997. Starch utilization by ruminants: from basics to the bunk. J. Anim. Sci. 75:852–867. https://doi.org/10.2527/1997.753852x

Hussein, H. A., J.-P. Thurmann, and R. Staufenbiel. 2020. 24-h variations of blood serum metabolites in high yielding dairy cows and calves. BMC Vet. Res. 16:1–11. https://doi.org/10.1186/s12917-020-02551-9

Huws, S. A., C. J. Creevey, L. B. Oyama, I. Mizrahi, S. E. Denman, M. Popova, R. Muñoz-Tamayo, E. Forano, S. M. Waters, and M. Hess. 2018. Addressing global ruminant agricultural challenges through understanding the rumen microbiome: past, present, and future. Front. Microbiol. 9:2161. https://doi.org/10.3389/fmicb.2018.02161

Huws, S. A., J. E. Edwards, C. J. Creevey, P. Rees Stevens, W. Lin, S. E. Girdwood, J. A. Pachebat, and A. H. Kingston-Smith. 2016. Temporal dynamics of the metabolically active rumen bacteria colonizing fresh perennial ryegrass. FEMS Microbiol. Ecol. 92:fiv137. https://doi.org/10.1093/femsec/fiv137

Isaac, N. I., D. Philippe, A. Nicholas, D. Raoult, and C. Eric. 2019. Metaproteomics of the human gut microbiota: challenges and contributions to other OMICS. Clin. Mass Spectrom. 14:18–30. https://doi.org/10.1016/j.clinms.2019.06.001

Jack, R. S., U. Grunwald, F. Stelter, G. Workalemahu, and C. J. Schütt. 1995. Both membrane-bound and soluble forms of CD14 bind to Gram-negative bacteria. Eur. J. Immunol. 25:1436-1441. https://doi.org/10.1002/eji.1830250545

Jami, E., and I. Mizrahi. 2012. Composition and similarity of bovine rumen microbiota across individual animals. PLoS One. 7:e33306. https://doi.org/10.1371/journal.pone.0033306

Jensen, D. R., S. Gavigan, V. Sawicki, D. L. Witsell, R. H. Eckel, and M. C. Neville. 1994. Regulation of lipoprotein lipase activity and mRNA in the mammary gland of the lactating mouse. Biochem. 298:321-327. https://doi.org/10.1042/bj2980321

Jing, L., L. Dewanckele, B. Vlaeminck, W. M. van Straalen, A. Koopmans, and V. Fievez. 2018. Susceptibility of dairy cows to subacute ruminal acidosis is reflected in milk fatty acid proportions, with C18: 1 trans-10 as primary and C15: 0 and C18: 1 trans-11 as secondary indicators. J. Dairy Sci. 101:9827–9840. https://doi.org/10.3168/jds.2018-14903

Josefsen, T. D., T. H. Aagnes, and S. D. Mathiesen. 1996. Influence of diet on the morphology of the ruminal papillae in reindeer calves (*Rangifer tarandus tarandus* L.). Rangifer. 16:119–128. https://doi.org/10.7557/2.16.3.1205

Jostins, L., S. Ripke, R. K. Weersma, R. H. Duerr, D. P. McGovern, K. Y. Hui, J. C. Lee, L. Philip Schumm, Y. Sharma, and C. A. Anderson. 2012. Host–microbe interactions have shaped the genetic architecture of inflammatory bowel disease. Nature. 491:119-124. https://doi.org/10.1038/nature11582

Kaiser, F., S. Krautwurst, S. Salentin, V. J. Haupt, C. Leberecht, S. Bittrich, D. Labudde, and M. Schroeder. 2020. The structural basis of the genetic code: amino acid recognition by aminoacyl-tRNA synthetases. Sci. Rep. 10:1-17. https://doi.org/10.1038/s41598-020-69100-0.

Karantonis, H. C., T. Nomikos, and C. A. Demopoulos. 2009. Triacylglycerol metabolism. Curr. Drug Targets 10:302–319.

Kashyap, R. S., A. R. Nayak, P. S. Deshpande, D. Kabra, H. J. Purohit, G. M. Taori, and H. F. Daginawala. 2009. Inter-α-trypsin inhibitor heavy chain 4 is a novel marker of acute ischemic stroke. Clin. Chim. Acta. 402:160-163. https://doi.org/10.1016/j.cca.2009.01.009

Keiblinger, K. M., S. Fuchs, S. Zechmeister-Boltenstern, and K. Riedel. 2016. Soil and leaf litter metaproteomics—a brief guideline from sampling to understanding. FEMS Microbiol. Ecol. 92.

Kennelly, J. J., B. Robinson, and G. R. Khorasani. 1999. Influence of carbohydrate source and buffer on rumen fermentation characteristics, milk yield, and milk composition in early-lactation Holstein cows. J. Dairy Sci. 82:2486–2496. https://doi.org/10.3168/jds.S0022-0302(99)75500-1

Kent-Dennis, C., A. Pasternak, J.C. Plaizier, and G. B. Penner. 2019. Potential for a localized immune response by the ruminal epithelium in nonpregnant heifers following a short-term subacute ruminal acidosis challenge. J. Dairy Sci. 102:7556–7569.

Kern, R. J., A. K. Lindholm-Perry, H. C. Freetly, W. M. Snelling, J. W. Kern, J. W. Keele, J. R. Miles, A. P. Foote, W. T. Oliver, and L. A. Kuehn. 2016. Transcriptome differences in the rumen of beef steers with variation in feed intake and gain. Gene. 586:12–26. https://doi.org/10.1016/j.gene.2016.03.034

Khafipour, E., D. O. Krause, and J. C. Plaizier. 2009a. Alfalfa pellet-induced subacute ruminal acidosis in dairy cows increases bacterial endotoxin in the rumen without causing inflammation. J. Dairy Sci. 92:1712–1724. https://doi.org/10.3168/jds.2008-1656

Khafipour, E., S. Li, J. C. Plaizier, and D. O. Krause. 2009b. Rumen microbiome composition determined using two nutritional models of subacute ruminal acidosis. Appl. Environ. Microbiol. 75:7115–7124. https://doi.org/10.1128/AEM.00739-09

Kihara, A. 2012. Very long-chain fatty acids: elongation, physiology and related disorders. J. Biochem. 152:387–395. https://doi.org/10.1093/jb/mvs105

Kim, D., B. Langmead, and S. L. Salzberg. 2015. HISAT: a fast spliced aligner with low memory requirements. Nat. Methods 12:357–360.

Kim, J. N., C. Méndez–García, R. R. Geier, M. Iakiviak, J. Chang, I. Cann, and R. I. Mackie. 2017. Metabolic networks for nitrogen utilization in Prevotella ruminicola 23. Sci. Rep. 7:1-11. https://doi.org/10.1038/s41598-017-08463-3.

Kim, M., and Z. Yu. 2014. Variations in 16S rRNA-based microbiome profiling between pyrosequencing runs and between pyrosequencing facilities. J. Microbiol. 52:355–365. https://doi.org/10.1007/s12275-014-3443-3

Kittelmann, S., M. R. Kirk, A. Jonker, A. McCulloch, and P. H. Janssen. 2015. Buccal swabbing as a non-invasive method to determine bacterial, archaeal, and eukaryotic microbial community structures in the rumen. Appl. Environ. Microbiol. 81:7470–7483. https://doi.org/10.1128/AEM.02385-15

Kleen, J. L., G. A. Hooijer, J. Rehage, and J. Noordhuizen. 2003. Subacute ruminal acidosis (SARA): a review. J. Vet. Med. Series A. 50:406–414. https://doi.org/10.1046/j.1439-0442.2003.00569.x

Kleen, J. L., L. Upgang, and J. Rehage. 2013. Prevalence and consequences of subacute ruminal acidosis in German dairy herds. Acta Vet. Scand. 55:1–6.

Klevenhusen, F., M. Hollmann, L. Podstatzky-Lichtenstein, R. Krametter-Frötscher, J. R. Aschenbach, and Q. Zebeli. 2013. Feeding barley grain-rich diets altered electrophysiological properties and permeability of the ruminal wall in a goat model. J. Dairy Sci. 96:2293–2302. https://doi.org/10.3168/jds.2012-6187

Koch, L.E., and G. J. Lascano. 2018. Milk fat depression: etiology, theories, and soluble carbohydrate interactions. J Anim Res Nutr. 3:1–21.

Koenig, K. M, K. A. Beauchemin, and L. M. Rode. 2003. Effect of grain processing and silage on microbial protein synthesis and nutrient digestibility in beef cattle fed barley-based diets. J. Anim. Sci. 81:1057-1067. https://doi.org/10.2527/2003.8141057x.

Kollman, J. M., J. K. Polka, A. Zelter, T. N. Davis, and D. A. Agard. 2010. Microtubule nucleating γ-TuSC assembles structures with 13-fold microtubule-like symmetry. Nature 466:879–882. https://doi.org/10.1038/nature09207

Kopečný, J., M. Zorec, J. Mrazek, Y. Kobayashi, and R. Marinšek-Logar. 2003. Butyrivibrio hungatei sp. nov. and Pseudobutyrivibrio xylanivorans sp. nov., butyrate-producing bacteria from the rumen. Int. J. Syst. Evol. 53:201-209. https://doi.org/10.1099/ijs.0.02345-0.

Krause, D. O., S. E. Denman, R. I. Mackie, M. Morrison, A. L. Rae, G. T. Attwood, and C.S. McSweeney. 2003. Opportunities to improve fiber degradation in the rumen: microbiology, ecology, and genomics. FEMS Microbiol. Rev. 27:663–693. https://doi.org/10.1016/S0168-6445(03)00072-X

Kristensen, N. B., A. Danfaer, and N. Agergaard. 1998. Absorption and metabolism of short-chain fatty acids in ruminants. Arch. Anim. Nutr. 51:165–175. https://doi.org/10.1080/17450399809381916

Kunath, B. J., G. Minniti, M. Skaugen, L. H. Hagen, G. Vaaje-Kolstad, V. G. H. Eijsink, P. B. Pope, and M. Ø. Arntzen. 2019. Metaproteomics: sample preparation and methodological considerations. Emerg. sample Treat. proteomics 187–215.

Kushner, I. J. 1982. The phenomenon of the acute phase response. Ann. N. Y. Acad. Sci. 389:39-48. https://doi.org/10.1111/j.1749-6632.1982.tb22124.x

Lässer, C., V. Seyed Alikhani, K. Ekström, M. Eldh, P. Torregrosa Paredes, A. Bossios, M. Sjöstrand, S. Gabrielsson, J. Lötvall, and H. Valadi. 2011. Human saliva, plasma and breast milk exosomes contain RNA: uptake by macrophages. J. Transl. Med. 9:1–8.

Leahy, S. C., W. J. Kelly, E. Altermann, R. S. Ronimus, C. J. Yeoman, D. M. Pacheco, and G. T. Attwood. 2010. The genome sequence of the rumen methanogen Methanobrevibacter ruminantium reveals new possibilities for controlling ruminant methane emissions. PloS one. 5:e8926. https://doi.org/10.1371/journal.pone.0008926.

Leduc, A., S. Le Guillou, L. Bianchi, L. O. Correia, M. Gelé, J. Pires, P. Martin, C. Leroux, F. Le Provost, and M. Boutinaud. 2022. Milk proteins as a feed restriction signature indicating the metabolic adaptation of dairy cows. Sci. Rep. 12:18886. https://doi.org/10.1038/s41598-022-21804-1.

Lee, J. W., M. J. Paape, and X. J. Zhao. 2003b. Recombinant bovine soluble CD14 reduces severity of experimental Escherichia coli mastitis in mice. Vet. Res. 34:307-316. https://doi.org/10.1051/vetres:2003006

Lehrer, R. I., D. Szklarek, A. Barton, T. Ganz, K. Hamann, and G. J. Gleich. 1989. Antibacterial properties of eosinophil major basic protein and eosinophil cationic protein. J. Immunol. Res. 142:4428-4434.

Lengowski, M. B., K. H. R. Zuber, M. Witzig, J. Möhring, J. Boguhn, and M. Rodehutscord. 2016. Changes in rumen microbial community composition during adaption to an in vitro system and the impact of different forages. PLoS One. 11:e0150115. https://doi.org/10.1371/journal.pone.0150115

Levine, A. J. 1997. p53, the cellular gatekeeper for growth and division. Cell 88:323–331. https://doi.org/10.1016/S0092-8674(00)81871-1

Li, F., and H. Zhang. 2019. Lysosomal acid lipase in lipid metabolism and beyond. Arterioscler. Thromb. Vasc. Biol. 39:850–856.

Li, H., B. Handsaker, A. Wysoker, T. Fennell, J. Ruan, N. Homer, G. Marth, G. Abecasis, R. Durbin, and 1000 Genome Project Data Processing Subgroup. 2009. The sequence alignment/map format and SAMtools. Bioinformatics 25:2078–2079.

Li, M. M., R. R. White, L. L. Guan, L. Harthan, and M. D. Hanigan. 2021. Metatranscriptomic analyses reveal ruminal pH regulates fiber degradation and

fermentation by shifting the microbial community and gene expression of carbohydrate-active enzymes. Anim. microbiome 3:1–17. https://doi.org/10.1186/s42523-021-00092-6

Li, Q., R. Liang, Y. Li, Y. Gao, Q. Li, D. Sun, and J. Li. 2020. Identification of candidate genes for milk production traits by RNA sequencing on bovine liver at different lactation stages. BMC Genet. 21:1–12. https://doi.org/10.1186/s12863-020-00882-y

Li, S., G. N. Gozho, N. Gakhar, E. Khafipour, D. O. Krause, and J. C. Plaizier. 2012. Evaluation of diagnostic measures for subacute ruminal acidosis in dairy cows. Can. J. Anim. Sci. 92:353–364. https://doi.org/10.4141/cjas2012-004

Li, W., S. Gelsinger, A. Edwards, C. Riehle, and D. Koch. 2019. Transcriptome analysis of rumen epithelium and meta-transcriptome analysis of rumen epimural microbial community in young calves with feed induced acidosis. Sci. Rep. 9:1–13. https://doi.org/10.1038/s41598-019-39286-z

Lima, R. F., J. C. Resende Júnior, S. F. Costa, J. L. P. Daniel, T. S. Teófilo, and M. G. Cardoso. 2015. Morphological response of the ruminal and omasal mucosae to the variation in diet energy. Cienc. e Agrotecnologia. 39:574–582. https://doi.org/10.1590/S1413-70542015000600004

Lindmark-Månsson, H., C. Bränning, G. Alden, and M. Paulsson. 2006. Relationship between somatic cell count, individual leukocyte populations and milk components in bovine udder quarter milk. Int. Dairy J. 16:717–727. https://doi.org/10.1016/j.idairyj.2005.07.003

Liu, J., M. Zhang, R. Zhang, W. Zhu, and S. Mao. 2016. Comparative studies of the composition of bacterial microbiota associated with the ruminal content, ruminal epithelium and in the faeces of lactating dairy cows. Microb. Biotechnol. 9:257–268. https://doi.org/10.1111/1751-7915.12345

Liu, J., T. Xu, Y. Liu, W. Zhu, and S. Mao. 2013. A high-grain diet causes massive disruption of ruminal epithelial tight junctions in goats. Am. J. Physiol. Integr. Comp. Physiol. 305:R232–R241. https://doi.org/10.1152/ajpregu.00068.2013

Liu, J., T. Xu, Y. Liu, W. Zhu, and S. Mao. 2013. A high-grain diet causes massive disruption of ruminal epithelial tight junctions in goats. Am. J. Physiol. Integr. Comp. Physiol. 305:R232–R241. https://doi.org/10.1152/ajpregu.00068.2013

Logan, C. M., and A. S. Menko. 2019. Microtubules: Evolving roles and critical cellular interactions. Exp. Biol. Med. 244:1240–1254. https://doi.org/10.1177/1535370219867296

Lopes, J. C., R. D. Shaver, P. C. Hoffman, M. S. Akins, S. J. Bertics, H. Gencoglu, and J. G. Coors. 2009. Type of corn endosperm influences nutrient digestibility in lactating dairy cows. J. Dairy Sci. 92:4541–4548. https://doi.org/10.3168/jds.2009-2090

Love, M. I., W. Huber, and S. Anders. 2014. Moderated estimation of fold change and dispersion for RNA-seq data with DESeq2. Genome Biol. 15:1–21.

Ma, N., J. A. Abaker, G. Wei, H. Chen, X. Shen, and G. Chang. 2022. A high-concentrate diet induces an inflammatory response and oxidative stress and depresses milk fat synthesis in the mammary gland of dairy cows. J. Dairy Sci. 105:5493–5505. https://doi.org/10.3168/jds.2021-21066

Macy, J. M. and I. Probst. 1979. The biology of gastrointestinal bacteroides. Annu. Rev. Microbiol. 33:561-594. https://doi.org/10.1146/annurev.mi.33.100179.003021.

Madureira, A. R., C. I. Pereira, A. M. P. Gomes, M. E. Pintado, and F. X. Malcata. 2007. Bovine whey proteins–Overview on their main biological properties. Food Res. Int. 40:1197–1211. https://doi.org/10.1016/j.foodres.2007.07.005

Maes, P., D. Damart, C. Rommens, J. Montreuil, G. Spik, and A. J. Tartar. 1988. The complete amino acid sequence of bovine milk angiogenin. FEBS Lett. 241:41-45. https://doi.org/10.1016/0014-5793(88)81027-5

Malekkhahi, M., A. M. Tahmasbi, A. A. Naserian, M. Danesh-Mesgaran, J. L. Kleen, O. AlZahal, and M. H. Ghaffari. 2016. Effects of supplementation of active dried yeast and malate during sub-acute ruminal acidosis on rumen fermentation, microbial population, selected blood metabolites, and milk production in dairy cows. Anim. Feed Sci. Technol. 213:29–43. https://doi.org/10.1016/j.anifeedsci.2015.12.018

Martin, C., and A. M. Smith. 1995. Starch biosynthesis. Plant Cell. 7:971. https://doi.org/10.1105%2Ftpc.7.7.971

Matsui, H., K. Ogata, K. Tajima, M. Nakamura, T. Nagamine, R. I. Aminov, and Y. Benno. 2000. Phenotypic characterization of polysaccharidases produced by four Prevotella type strains. Curr. Microbiol. 41:45-49. https://doi.org/10.1007/s002840010089.

McCann, J. C., T. A. Wickersham, and J. J. Loor. 2014. High-throughput methods redefine the rumen microbiome and its relationship with nutrition and metabolism. Bioinform. Biol. Insights. 8:BBI-S15389. https://doi.org/10.4137/BBI.S15389

McDonald, P. 2002. Animal nutrition. Pearson Education Publisher, Harlow, UK.

McSweeney, C., and R. Mackie. 2012. Commission on genetic resources for food and agriculture. Micro-organisms and ruminant digestion: State of knowledge, trends and future prospects. Background Study Paper (FAO). 61:1–62.

Meissner, S., F. Hagen, C. Deiner, D. Günzel, G. Greco, Z. Shen, and J. R. Aschenbach. 2017. Key role of short-chain fatty acids in epithelial barrier failure during ruminal acidosis. J. Dairy Sci. 100:6662–6675. https://doi.org/10.3168/jds.2016-12262

Memon, M. A., Y. Wang, T. Xu, N. Ma, H. Zhang, A.-C. Roy, Z. ul Aabdin, and X. Shen. 2019. Lipopolysaccharide induces oxidative stress by triggering MAPK and Nrf2 signalling pathways in mammary glands of dairy cows fed a high-concentrate diet. Microb. Pathog. 128:268-275. https://doi.org/10.1002/vms3.615

Mentschel, J., R. Leiser, C. Mülling, C. Pfarrer, and R. Claus. 2001. Butyric acid stimulates rumen mucosa development in the calf mainly by a reduction of apoptosis. Arch. Anim. Nutr. 55:85–102. https://doi.org/10.1080/17450390109386185

Mi, H., S. Poudel, A. Muruganujan, J. T. Casagrande, and P. D. Thomas. 2016. PANTHER version 10: expanded protein families and functions, and analysis tools. Nucleic Acids Res. 44:D336–D342.

Miglio, A., L. Moscati, G. Fruganti, M. Pela, E. Scoccia, A. Valiani, and C. J. Maresca. 2013. Use of milk amyloid A in the diagnosis of subclinical mastitis in dairy ewes. J. Dairy Res. 80:496-502. https://doi.org/10.1017/S0022029913000484

Miyazaki, K., J. C. Martin, R. Marinsek-Logar, and H. J. Flint. 1997. Degradation and utilization of xylans by the rumen anaerobe Prevotella bryantii (formerly P. ruminicola subsp. brevis) $B_1$4. Anaerobe. 3:373-381. https://doi.org/10.1006/anae.1997.0125.

Mizrahi, I. 2013. Rumen symbioses. Springer-Verlag Berlin Heidelberg. https://doi.org/10.1007/978-3-642-30194-0_1

Monte, M., R. Benetti, G. Buscemi, P. Sandy, G. Del Sal, and C. Schneider. 2003. The cell cycle-regulated protein human GTSE-1 controls DNA damage-induced apoptosis by affecting p53 function. J. Biol. Chem. 278:30356–30364. https://doi.org/10.1074/jbc.M302902200

Morar, D., C. Văduva, A. Morar, M. Imre, C. Tulcan, and K. Imre. 2022. Paraclinical Changes Occurring in Dairy Cows with Spontaneous Subacute Ruminal Acidosis under Field Conditions. Animals. 12:2466.

Morgavi, D. P., E. Forano, C. Martin, and C. J. Newbold. 2010. Microbial ecosystem and methanogenesis in ruminants. Animals. 4:1024–1036. https://doi.org/10.1017/S1751731110000546

Morgavi, D. P., E. Rathahao-Paris, M. Popova, J. Boccard, K. F. Nielsen, and H. Boudra. 2015. Rumen microbial communities influence metabolic phenotypes in lambs. Front Microbiol. 6:1060. https://doi.org/10.3389/fmicb.2015.01060

Moyes, K. M., J. K. Drackley, D. E. Morin, S. L. Rodriguez-Zas, R. E. Everts, H. A. Lewin, and J. J. Loor. 2010. Mammary gene expression profiles during an intramammary challenge reveal potential mechanisms linking negative energy balance with impaired immune response. Physiol. Genomics. 41:161-170. https://doi.org/10.1152/physiolgenomics.00197.2009

Mulakala, B. K. 2022. Impact of dietary carbohydrate profile on the dairy cow rumen meta-proteome. Mendeley Data, V1. https://data.mendeley.com/datasets/bv3y4ffnc6/1.

Mulakala, B., K. Smith, M. Snider, A. Ayers, M. Honan, and S. Greenwood. 2022. Influence of dietary carbohydrate profile on the dairy cow rumen meta-proteome. J. Dairy Sci. 105:8485-8496. https://doi.org/10.3168/jds.2022-21812

Mulakala, Bharath kumar (2022), "Mulakala et al. 2022. JDS, Supplementary Tables", Mendeley Data, v1.

Murata, M., H. Wakabayashi, K. Yamauchi, and F. J. Abe. 2013. Identification of milk proteins enhancing the antimicrobial activity of lactoferrin and lactoferricin. J. Dairy Sci. 96:4891-4898. https://doi.org/10.3168/jds.2013-6612

National Academies of Sciences, Enginnering, and Medicine. 2021. Nutrient Requirements of Dairy Cattle. 8th rev. ed. Natl. Acad. Sci., Washington, DC. https://doi.org/10.17226/25806

Newman, L. A., Z. Useckaite, J. Johnson, M. J. Sorich, A.M. Hopkins, and A. Rowland. 2022. Selective isolation of liver-derived extracellular vesicles redefines performance of miRNA biomarkers for non-alcoholic fatty liver disease. Biomedicines 10:195.

Nielsen, T. S., K. Sejrsen, H. R. Andersen, P. Lund, and E. M. Straarup. 2004. Effect of silage type and energy concentration on conjugated linoleic acid (CLA) in milk fat from dairy cows. J. Anim. Feed Sci. 13:697–700.

Nissen, A., E. Bendixen, K. L. Ingvartsen, and C. M. Røntved. 2013. Expanding the bovine milk proteome through extensive fractionation. J. Dairy Sci. 96:7854–7866. https://doi.org/10.3168/jds.2013-7106

Nocek, J. E. 1997. Bovine acidosis: Implications on laminitis. J. Dairy Sci. 80:1005–1028.

Nocek, J. E., and J. Russell. 1988. Protein and energy as an integrated system. Relationship of ruminal protein and carbohydrate availability to microbial synthesis and milk production. J. Dairy Sci. 71:2070–2107. https://doi.org/10.3168/jds.S0022-0302(97)76026-0

Oba, M., and M. S. Allen. 2003. Intraruminal infusion of propionate alters feeding behavior and decreases energy intake of lactating dairy cows. J. Nutr. 133:1099. https://doi.org/10.1093/jn/133.4.1094

Oba, M., and M. S. Allen. 2003a. Dose-response effects of intrauminal infusion of propionate on feeding behavior of lactating cows in early or midlactation. J. Dairy Sci. 86:2922–2931. https://doi.org/10.3168/jds.S0022-0302(03)73889-2

Oetzel, G. R. 2004. Monitoring and testing dairy herds for metabolic disease. Vet. Clin. North Am. Food Anim. 20:651–674. https://doi.org/10.1016/j.cvfa.2004.06.006

Ogata, T., H. Makino, N. Ishizuka, E. Iwamoto, T. Masaki, K. Kizaki, Y. H. Kim, and S. Sato. 2020. Long-term high-grain diet alters ruminal pH, fermentation, and epithelial transcriptomes, leading to restored mitochondrial oxidative phosphorylation in Japanese Black cattle. Sci. Rep. 10:1–11. https://doi.org/10.1038/s41598-020-63471-0

Ogunade, I., A. Pech-Cervantes, and H. J. Schweickart. 2019. Metatranscriptomic analysis of sub-acute ruminal acidosis in beef cattle. Animals. 9:232. https://doi.org/10.3390/ani9050232

Ong, J. M., B. Saffari, R. B. Simsolo, and P. A. Kern. 1992. Epinephrine inhibits lipoprotein lipase gene expression in rat adipocytes through multiple steps in post-transcriptional processing. Mol. Endocrinol. 6:61-69. https://doi.org/10.1210/mend.6.1.1738372

Orpin, C. G., and K. N. Joblin. 1997. The rumen anaerobic fungi. Springer.

Overton, T., J. McArt, and D. J. Nydam. 2017. A 100-Year Review: Metabolic health indicators and management of dairy cattle. J. Dairy Sci. 100:10398-10417. https://doi.org/10.3168/jds.2017-13054

Parker, R., and S. G. Ring. 2001. Aspects of the physical chemistry of starch. J. Cereal Sci. 34:1–17. https://doi.org/10.1006/jcrs.2000.0402

Pengpeng, W. and Z. Tan. 2013. Ammonia assimilation in rumen bacteria: a review. Anim. Biotechnol. 24:107-128. https://doi.org/10.1080/10495398.2012.756402.

Penner, G. B. 2014. Mechanisms of volatile fatty acid absorption and metabolism and maintenance of a stable rumen environment. Pages 92–104 in 25th Florida Ruminant Nutrition Symposium.

Pertea, M., D. Kim, G.M. Pertea, J. T. Leek, and S. L. Salzberg. 2016. Transcript-level expression analysis of RNA-seq experiments with HISAT, StringTie and Ballgown. Nat. Protoc. 11:1650–1667.

Petri, R. M., T. Schwaiger, G. B. Penner, K. A. Beauchemin, R. J. Forster, J. J. McKinnon, and T. A. McAllister. 2013. Characterization of the core rumen microbiome in cattle during transition from forage to concentrate as well as during and after an acidotic challenge. PLoS One. 8:e83424. https://doi.org/10.1371/journal.pone.0083424

Philippeau, C., J. Landry, and B. Michalet-Doreau. 2000. Influence of the protein distribution of maize endosperm on ruminal starch degradability. J. Sci. Food Agric. 80:404–408. https://doi.org/10.1002/1097-0010(200002)80:3%3C404::AID-JSFA541%3E3.0.CO;2-Z

Pilachai, R., J. T. Schonewille, C. Thamrongyoswittayakul, S. Aiumlamai, C. Wachirapakorn, H. Everts, and W.H. Hendriks. 2012. Starch source in high concentrate rations does not affect rumen pH, histamine and lipopolysaccharide concentrations in dairy cows. Livest. Sci. 150:135–142. https://doi.org/10.1016/j.livsci.2012.08.009

Piñeiro, M., M. A. A. Alava, N. González-Ramón, J. Osada, P. Lasierra, L. Larrad, A. Piñeiro, and F. Lampreave. 1999. ITIH4 serum concentration increases during acute-phase processes in human patients and is up-regulated by interleukin-6 in hepatocarcinoma HepG2 cells. Biochem. Biophys. Res. Commun. 263:224-229. https://doi.org/10.1006/bbrc.1999.1349

Pirondini, M., S. Colombini, M. Mele, L. Malagutti, L. Rapetti, G. Galassi, and G. M. Crovetto. 2015. Effect of dietary starch concentration and fish oil supplementation on milk

yield and composition, diet digestibility, and methane emissions in lactating dairy cows. J. Dairy Sci. 98:357-372. https://doi.org/10.3168/jds.2014-8092.

Pitta, D. W., N. Indugu, B. Vecchiarelli, D. E. Rico, and K. J. Harvatine. 2018. Alterations in ruminal bacterial populations at induction and recovery from diet-induced milk fat depression in dairy cows. J. Dairy Sci. 101:295–309. https://doi.org/10.3390/metabo9070154

Plaizier, J. C., D. O. Krause, G. N. Gozho, and B. W. McBride. 2008a. Subacute ruminal acidosis in dairy cows: the physiological causes, incidence and consequences. Vet. J. 176:21–31. https://doi.org/10.1016/j.tvjl.2007.12.016

Pollock, J., L. Glendinning, T. Wisedchanwet, and M. Watson. 2018. The madness of microbiome: attempting to find consensus "best practice" for 16S microbiome studies. Appl. Environ. Microbiol. 84:e02627-17. https://doi.org/10.1128/AEM.02627-17

Poppi, D. P., R. E. Hendricksen, and D. J. Minson. 1985. The relative resistance to escape of leaf and stem particles from the rumen of cattle and sheep. J. Agric. Sci. 105:9–14. https://doi.org/10.1017/S0021859600055623

Puppel, K., M. Gołębiewski, J. Slósarz, G. Grodkowski, P. Solarczyk, P. Kostusiak, K. Grodkowska, M. Balcerak, and T. Sakowski. 2021. Interaction between the level of immunoglobulins and number of somatic cells as a factor shaping the immunomodulating properties of colostrum. Sci. Rep. 11:1–9. https://doi.org/10.1038/s41598-021-95283-1

Puppel, K., P. Staniszewska, M. Gołębiewski, J. Slósarz, G. Grodkowski, P. Solarczyk, M. Kunowska-Slósarz, P. Kostusiak, B. Kuczyńska, and T. J. Przysucha. 2021. Using the Relationship between Concentrations of Selected Whey Proteins and BHBA to Characterize the Metabolism of Dairy Cows in Early Lactation. Animals. 11:2298. https://doi.org/10.3390/ani11082298

Purushe, J., D. E. Fouts, M. Morrison, B. A. White, R. I. Mackie, P. M. Coutinho, B. Henrissat, and K. E. Nelson. 2010. Comparative genome analysis of Prevotella ruminicola and Prevotella bryantii: insights into their environmental niche. Microb. Ecol. 60:721-729. https://doi.org/10.1007/s00248-010-9692-8.

Raffrenato, E., D. Ross, and M. J. Van Amburgh. 2018. Development of an in vitro method to determine rumen undigested aNDFom for use in feed evaluation. J. Dairy Sci. 101:9888-9900. https://doi.org/10.3168/jds.2018-15101

Rajendhran, J., and P. Gunasekaran. 2011. Microbial phylogeny and diversity: small subunit ribosomal RNA sequence analysis and beyond. Microbiol. Res. 166:99–110. https://doi.org/10.1016/j.micres.2010.02.003

Ramos, S. C., C. D. Jeong, L. L. Mamuad, S. H. Kim, S. H. Kang, E. T. Kim, Y. I. Cho, S. S. Lee, and S. S. Lee. 2021. Diet transition from high-forage to high-concentrate alters rumen bacterial community composition, epithelial transcriptomes and ruminal fermentation parameters in dairy cows. Animals. 11:838. https://doi.org/10.3390/ani11030838

Reeve, J. N., J. Nölling, R. M. Morgan, and D. R. Smith. 1997. Methanogenesis: genes, genomes, and who's on first?. J. Bacteriol. 179:5975-5986. https://doi.org/10.1128/jb.179.19.5975-5986.1997.

Reinhardt, T. A., and J. D. Lippolis. 2006. Bovine milk fat globule membrane proteome. J. Dairy Res. 73:406–416. https://doi.org/10.1017/S0022029906001889

Rooke, J. A., R. J. Wallace, C. A. Duthie, N. McKain, S. M. de Souza, J. J. Hyslop, D. W. Ross, T. Waterhouse, and R. Roehe. 2014. Hydrogen and methane emissions from beef cattle and their rumen microbial community vary with diet, time after feeding and genotype. Br. J. Nutr. 112:398-407. https://doi.org/10.1017/S0007114514000932.

Rosenberg, H. F. and J. B. Domachowske. 2001. Eosinophils, eosinophil ribonucleases, and their role in host defense against respiratory virus pathogens. J. Leukoc. Biol. 70:691-698.

Russell, J. B. 2002. Rumen microbiology and its role in ruminant nutrition. Department of Microbiology, Cornell University. https://www.ars.usda.gov/research/software/download/?softwareid=409 , Ithaca, NY.

Sadet-Bourgeteau, S., C. Martin, and D. P. Morgavi. 2010. Bacterial diversity dynamics in rumen epithelium of wethers fed forage and mixed concentrate forage diets. Vet Microbiol. 146:98–104. https://doi.org/10.1016/j.vetmic.2010.04.029

Santana, Á. L., and M. A. A. Meireles. 2014. New starches are the trend for industry applications: a review. Food Public Health. 4:229–241.

Schiebenhoefer, H., T. van den Bossche, S. Fuchs, B. Y. Renard, T. Muth, and L. Martens. 2019. Challenges and promise at the interface of metaproteomics and genomics: an overview of recent progress in metaproteogenomic data analysis. Expert Rev. Proteomics. 16:375–390. https://doi.org/10.1080/14789450.2019.1609944

Schloss, P. D., M. L. Jenior, C. C. Koumpouras, S. L. Westcott, and S. K. Highlander. 2016. Sequencing 16S rRNA gene fragments using the PacBio SMRT DNA sequencing system. Peer J. 4:e1869. https://doi.org/10.7717/peerj.1869

Schulz, H. 2013. Fatty acid oxidation. Pages 281-284 in Encyclopedia of biological chemistry (second edition). W. J. Lennarz, and M. D. Lane. Academic Press, Waltham. https://doi.org/10.1016/B978-0-12-378630-2.00071-2.

Schwartzkopf-Genswein, K. S., K. A. Beauchemin, D. J. Gibb, D. H. Crews Jr, D. D. Hickman, M. Streeter, and T.A. McAllister. 2003. Effect of bunk management on feeding behavior, ruminal acidosis and performance of feedlot cattle: A review. J. Anim. Sci. 81:E149–E158. https://doi.org/10.2527/2003.8114_suppl_2E149x

Shirley, J., R. Emery, E. Convey, and W. J. Oxender. 1973. Enzymic changes in bovine adipose and mammary tissue, serum and mammary tissue hormonal changes with initiation of lactation. J. Dairy Sci. 56:569-574.

Skillman, L. C., P. N. Evans, C. Strömpl, and K. N. Joblin. 2006. 16S rDNA directed PCR primers and detection of methanogens in the bovine rumen. Lett. Appl. Microbiol. 42:222–228. https://doi.org/10.1111/j.1472-765X.2005.01833.x

Skillman, L. C., P. N. Evans, C. Strömpl, and K. N. Joblin. 2006. 16S rDNA directed PCR primers and detection of methanogens in the bovine rumen. Lett. Appl. Microbiol. 42:222–228. https://doi.org/10.1111/j.1472-765X.2005.01833.x

Smith, K. M. 2021. The effect of physically effective undegradable neutral detergent fiber and rumen fermentable starch on lactating Holstein cows. MS Thesis. The University of Vermont, Burlington, VT.

Smith, W. A. 2019. Relationships between undigested and physically effective fiber in lactating dairy cow diets. MS Thesis. The University of Vermont, Burlington, VT.

Smolenski, G., S. Haines, F. Y.-S. Kwan, J. Bond, V. Farr, S. R. Davis, K. Stelwagen, and T. T. Wheeler. 2007. Characterisation of host defence proteins in milk using a proteomic approach. J. Proteome Res. 6:207–215. https://doi.org/10.1021/pr0603405

Snelling, T. J. and R. J. Wallace. 2017. The rumen microbial metaproteome as revealed by SDS-PAGE. J. Dairy Sci. 95:318-327. https://doi.org/10.1186/s12866-016-0917-y.

Snelling, T. J., and R. J. Wallace. 2017. The rumen microbial metaproteome as revealed by SDS-PAGE. BMC Microbiol. 17:1–10. https://doi.org/10.1186/s12866-016-0917-y

Sniffen, C. J., J. D. O'connor, P. J. van Soest, D. G. Fox, and J. B. Russell. 1992. A net carbohydrate and protein system for evaluating cattle diets: II. Carbohydrate and protein availability. J. Anim. Sci. 70:3562–3577. https://doi.org/10.2527/1992.70113578x

Soergel, D. A. W., N. Dey, R. Knight, and S. E. Brenner. 2012. Selection of primers for optimal taxonomic classification of environmental 16S rRNA gene sequences. ISME J. 6:1440–1444. https://doi.org/10.1038/ismej.2011.208

Solano, J., F. Galindo, A. Orihuela, and C. S. Galina. 2004. The effect of social rank on the physiological response during repeated stressful handling in Zebu cattle (*Bos indicus*). Physiol. Behav. 82:679–683. https://doi.org/10.1016/j.physbeh.2004.06.005

Soler, L., R. Dąbrowski, N. García, M. A. Alava, F. Lampreave, M. Piñeiro, W. Wawron, M. Szczubiał, and M. J. Bochniarz. 2019. Acute-phase inter-alpha-trypsin inhibitor heavy chain 4 (ITIH4) levels in serum and milk of cows with subclinical mastitis caused by *Streptococcus* species and coagulase-negative *Staphylococcus* species. J. Dairy Sci. 102:539-546. https://doi.org/10.1016/j.physbeh.2004.06.005

Steele, M. A., J. Croom, M. Kahler, O. AlZahal, S. E. Hook, K. Plaizier, and B. W. McBride. 2011. Bovine rumen epithelium undergoes rapid structural adaptations during grain-induced subacute ruminal acidosis. Am. J. Physiol. Regul. 300:R1515–R1523. https://doi.org/10.1152/ajpregu.00120.2010

Steele, M., L. Dionissopoulos, O. AlZahal, J. Doelman, and B. W. McBride. 2012. Rumen epithelial adaptation to ruminal acidosis in lactating cattle involves the coordinated

expression of insulin-like growth factor-binding proteins and a cholesterolgenic enzyme. J. Dairy Sci. 95:318-327. https://doi.org/10.3168/jds.2011-4465.

Stefańska, B., J. Komisarek, and W. Nowak. 2020. Noninvasive indicators associated with subacute ruminal acidosis in dairy cows. Ann. Anim. Sci. 20:1325–1338.

Stefanska, B., W. Człapa, E. Pruszynska-Oszmałek, D. Szczepankiewicz, V. Fievez, J. Komisarek, K. Stajek, and W. Nowak. 2018. Subacute ruminal acidosis affects fermentation and endotoxin concentration in the rumen and relative expression of the CD14/TLR4/MD2 genes involved in lipopolysaccharide systemic immune response in dairy cows. J. Dairy Sci. 101:1297–1310.

Steijns, J. M., and A. C. M. van Hooijdonk. 2000. Occurrence, structure, biochemical properties and technological characteristics of lactoferrin. Br. J. Nutr. 84:11–17. https://doi.org/10.1017/S0007114500002191

Sterk, A., B. E. O. Johansson, H. Z. H. Taweel, M. Murphy, A. M. van Vuuren, W. H. Hendriks, and J. Dijkstra. 2011. Effects of forage type, forage to concentrate ratio, and crushed linseed supplementation on milk fatty acid profile in lactating dairy cows. J. Dairy Sci. 94:6078–6091. https://doi.org/10.3168/jds.2011-4617

Stevenson, D. M., and P. J. Weimer. 2007. Dominance of Prevotella and low abundance of classical ruminal bacterial species in the bovine rumen revealed by relative quantification real-time PCR. Appl. Microbiol. Biotechnol. 75:165–174. https://doi.org/10.1007/s00253-006-0802-y

Stevnebø, A., S. Sahlström, and B. Svihus. 2006. Starch structure and degree of starch hydrolysis of small and large starch granules from barley varieties with varying amylose content. Anim. Feed Sci. Technol. 130:23–38. https://doi.org/10.1016/j.anifeedsci.2006.01.015

Stins, M. F., F. R. Maxfield, and I. J. Goldberg. 1992. Polarized binding of lipoprotein lipase to endothelial cells. Implications for its physiological actions. Arterioscler. Thromb. Vasc. Bio. 12:1437-1446.

Stone, W. C. 1999. The effect of subclinical rumen acidosis on milk components. Page. Proceedings Cornell Nutrition Conference For Feed Manufacturers.

Sun, Y. Z., S. Y. Mao, and W. Y. Zhu. 2010. Rumen chemical and bacterial changes during stepwise adaptation to a high-concentrate diet in goats. Animals. 4:210–217. https://doi.org/10.1017/S175173110999111X

Tacoma, R., J. Fields, D. B. Ebenstein, Y. W. Lam, and S. L. Greenwood. 2016. Characterization of the bovine milk proteome in early-lactation Holstein and Jersey breeds of dairy cows. J. Proteomics. 130:200–210. https://doi.org/10.1016/j.jprot.2015.09.024

Tajima, K., R. I. Aminov, T. Nagamine, H. Matsui, M. Nakamura, and Y. Benno. 2001. Diet-dependent shifts in the bacterial population of the rumen revealed with real-time PCR.

Appl. Environ. Microbiol. 67:2766–2774. https://doi.org/10.1128/AEM.67.6.2766-2774.2001

Tajima, K., S. Arai, K. Ogata, T. Nagamine, H. Matsui, M. Nakamura, R. I. Aminov, and Y. Benno. 2000. Rumen bacterial community transition during adaptation to high-grain diet. Anaerobe. 6:273–284. https://doi.org/10.1006/anae.2000.0353

Terry, S. A., G. de O. Ribeiro, R. J. Gruninger, M. Hunerberg, S. Ping, A. Chaves, J. Burlet, K.A. Beauchemin, and T. A. McAllister. 2018. Effect of humic substances on rumen fermentation, nutrient digestibility, methane emissions, and rumen microbiota in beef heifers. J. Anim. Sci. 96:3863–3877.

Théry, C., L. Zitvogel, and S. Amigorena. 2002. Exosomes: composition, biogenesis and function. Nat. Rev. Immunol. 2:569–579.

Thoetkiattikul, H., W. Mhuantong, T. Laothanachareon, S. Tangphatsornruang, V. Pattarajinda, L. Eurwilaichitr, and V. Champreda. 2013. Comparative analysis of microbial profiles in cow rumen fed with different dietary fiber by tagged 16S rRNA gene pyrosequencing. Curr. Microbiol. 67:130-137. https://doi.org/10.1007/s00284-013-0336-3.

Toyoda, A., W. Iio, M. Mitsumori, and H. Minato. 2009. Isolation and identification of cellulose-binding proteins from sheep rumen contents. Appl. Environ. Microbiol. 75:1667–1673. https://doi.org/10.1128/AEM.01838-08

Uppal, S. K., K. Wolf, and H. Martens. (2003). The effect of short chain fatty acids on calcium flux rates across isolated rumen epithelium of hay-fed and concentrate-fed sheep. J. Anim. Physiol. Anim. Nutr. 87:12-20. https://doi.org/10.1046/j.1439-0396.2003.00401.x

van Altena, S. E. C., B. de Klerk, K. A. Hettinga, R. J. J. van Neerven, S. Boeren, H. F. J. Savelkoul, and E. J. Tijhaar. 2016. A proteomics-based identification of putative biomarkers for disease in bovine milk. Vet. Immunol. Immunopathol. 174:11–18. https://doi.org/10.1016/j.vetimm.2016.04.005

van Soest, P. J. 1994. Nutritional Ecology of the Ruminant. Cornell university press.

Verlhac, M.-H., H. De Pennart, B. Maro, M. H. Cobb, and H. J. Clarke. 1993. MAP kinase becomes stably activated at metaphase and is associated with microtubule-organizing centers during meiotic maturation of mouse oocytes. Dev. Biol. 158:330–340.

Villalba, J. J., F. D. Provenza, and K. C. Olson. 2006. Terpenes and carbohydrate source influence rumen fermentation, digestibility, intake, and preference in sheep. J. Anim. Sci. 84:2463-2473. https://doi.org/10.2527/jas.2005-716.

Vlaeminck, B., V. Fievez, D. Demeyer, and R. J. Dewhurst. 2006. Effect of forage: concentrate ratio on fatty acid composition of rumen bacteria isolated from ruminal and duodenal digesta. J. Dairy Sci. 89:2668–2678. https://doi.org/10.3168/jds.S0022-0302(06)72343-8

Wada, Y., and B. Lönnerdal. 2014. Bioactive peptides derived from human milk proteins—mechanisms of action. J. Nutr. Biochem. 25:503–514. https://doi.org/10.1016/j.jnutbio.2013.10.012

Wallace, R. J., J. A. Rooke, N. McKain, C. A. Duthie, J. J. Hyslop, D. W. Ross, A. Waterhouse, M. Watson, and R. Roehe. 2015. The rumen microbial metagenome associated with high methane production in cattle. BMC Genomics. 16:1–14. https://doi.org/10.1186/s12864-015-2032-0

Wang, X., H. Zhou, J. G. Hickford, S. Li, J. Wang, X. Liu, J. Hu and Y. Luo. (2020). Variation in the yak lipin-1 gene and its association with milk traits. J. Dairy Res. 87:166-169. https://doi.org/10.1017/S002202991900089X

Weijland, A., K. Harmark, R. H. Cool, P. H. Anborgh, and A. Parmeggiani. 1992. Elongation factor Tu: a molecular switch in protein biosynthesis. Mol. Microbiol. 6:683-688. https://doi.org/10.1111/j.1365-2958.1992.tb01516.x.

Weimer, P. J. 2015. Redundancy, resilience, and host specificity of the ruminal microbiota: implications for engineering improved ruminal fermentations. Front. Microbiol. 6:296. https://doi.org/10.3389/fmicb.2015.00296

White, B. A., I. K. O. Cann, S. A. Kocherginskaya, R. I. Aminov, L. A. Thill, R. I. Mackie, and R. Onodera. 1999. Molecular analysis of Archaea, Bacteria and Eucarya communities in the rumen-review. Asian-Australas J. Anim. Sci. 12:129–138. https://doi.org/10.5713/ajas.1999.129

Whitford, M. F., R. J. Forster, C. E. Beard, J. Gong, and R. M. Teather. 1998. Phylogenetic analysis of rumen bacteria by comparative sequence analysis of cloned 16S rRNA genesß. Anaerobe 4:153–163. https://doi.org/10.1006/anae.1998.0155

Williams, A. G., and G. S. Coleman. 1997. The rumen protozoa. Springer. https://doi.org/10.1007/978-94-009-1453-7_3

Winter, K. A., and D. P. Collins. 1987. Fibrosity index as an estimate of forage digestibility. Can. J. Plant Sci. 67:445–449. https://doi.org/10.4141/cjps87-063

Wirth, R., G. Kádár, B. Kakuk, G. Maróti, Z. Bagi, Á. Szilágyi, G. Rákhely, J. Horváth, and K. L. Kovács. 2018. The planktonic core microbiome and core functions in the cattle rumen by next generation sequencing. Front. Microbiol. 9:2285. https://doi.org/10.3389/fmicb.2018.02285

Woolpert, M. E., H. M. Dann, K. W. Cotanch, C. Melilli, L. E. Chase, R. J. Grant, and D. M. Barbano. 2017. Management practices, physically effective fiber, and ether extract are related to bulk tank milk de novo fatty acid concentration on Holstein dairy farms. J. Dairy Sci. 100:5097–5106.

Wright, S. D., R. A. Ramos, A. Hermanowski-Vosatka, P. Rockwell, and P. A. Detmers. 1991. Activation of the adhesive capacity of CR3 on neutrophils by endotoxin: dependence

on lipopolysaccharide binding protein and CD14. J. Exp. Med. 173:1281-1286. https://doi.org/10.1084/jem.173.5.1281

Xu, C., T. Shen, W. Yang, H. Yu, S. Gao, and B. Huang. 2016. The effect of subacute ruminal acidosis of dairy cows on productivity, digestibility and greenhouse gas emission. J. Agric. Sci. 8:92. http://dx.doi.org/10.5539/jas.v8n4p9

Xu, C., T. Shen, W. Yang, H. Yu, S. Gao, and B. Huang. 2016. The effect of subacute ruminal acidosis of dairy cows on productivity, digestibility and greenhouse gas emission. J. Agric. Sci. 8:92. http://dx.doi.org/10.5539/jas.v8n4p9

Yakubovich, E. I., A. G. Polischouk, and V. I. Evtushenko. 2022. Principles and Problems of Exosome Isolation from Biological Fluids. Biochem. (Moscow), Suppl. Ser. A Membr. Cell Biol. 16:115–126.

Yamamoto, T., N. Kosaka, and T. Ochiya. 2019. Latest advances in extracellular vesicles: from bench to bedside. Sci. Technol. Adv. Mater. 20:746–757.

Yáñez-Ruiz, D. R., B. Macías, E. Pinloche, and C. J. Newbold. 2010. The persistence of bacterial and methanogenic archaeal communities residing in the rumen of young lambs. FEMS Microbiol. Ecol. 72:272–278. https://doi.org/10.1111/j.1574-6941.2010.00852.x

Yang, W. and K. A. Beauchemin. 2006. Increasing the physically effective fiber content of dairy cow diets may lower efficiency of feed use. J. Dairy Sci. 89:2694-2704. https://doi.org/10.3168/jds.2008-1379.

Yang, W. Z., K. A. Beauchemin, and L. M. Rode. 2000. Effects of barley grain processing on extent of digestion and milk production of lactating cows. J. Dairy Sci. 83:554–568. https://doi.org/10.3168/jds.S0022-0302(00)74915-0

Zebeli, Q., J. Dijkstra, M. Tafaj, H. Steingass, B. Ametaj, and W. J. Drochner. 2008. Modeling the adequacy of dietary fiber in dairy cows based on the responses of ruminal pH and milk fat production to composition of the diet. J. Dairy Sci. 91:2046-2066. https://doi.org/10.3168/jds.2007-0572

Zebeli, Q., J. Dijkstra, M. Tafaj, H. Steingass, B. N. Ametaj, and W. Drochner. 2008. Modeling the adequacy of dietary fiber in dairy cows based on the responses of ruminal pH and milk fat production to composition of the diet. J. Dairy Sci. 91:2046–2066. https://doi.org/10.3168/jds.2007-0572

Zebeli, Q., M. Tafaj, H. Steingass, B. Metzler, and W. Drochner. 2006. Effects of physically effective fiber on digestive processes and milk fat content in early lactating dairy cows fed total mixed rations. J. Dairy Sci. 89:651–668. https://doi.org/10.3168/jds.S0022-0302(06)72129-4

Zeng, H., C. Guo, D. Sun, H. E. Seddik, and S. Mao. 2019. The ruminal microbiome and metabolome alterations associated with diet-induced milk fat depression in dairy cows. Metabolites. 9:154. https://doi.org/10.3390/metabo9070154.

Zhan, K., T. Y. Yang, Y. Chen, M. C. Jiang, and G. Q. Zhao. 2020. Propionate enhances the expression of key genes involved in the gluconeogenic pathway in bovine intestinal epithelial cells. J. Dairy Sci. 103:5514–5524. https://doi.org/10.3168/jds.2019-17309

Zhang, L., S. Boeren, A. Van Hooijdonk, J. Vervoort, and K. J. Hettinga. 2015. A proteomic perspective on the changes in milk proteins due to high somatic cell count. J. Dairy Sci. 98:5339-5351. https://doi.org/10.3168/jds.2014-9279

Zhang, R., W. Zhu, W. Zhu, J. Liu, S. Mao. 2014. Effect of dietary forage sources on rumen microbiota, rumen fermentation and biogenic amines in dairy cows. J. Sci. Food Agric. 94:1886-1895. https://doi.org/10.1002/jsfa.6508.

Zhang, W., and H. T. Liu. 2002. MAPK signal pathways in the regulation of cell proliferation in mammalian cells. Cell Res. 12:9–1.

Zhang, X., H. Zhang, Z. Wang, X. Zhang, H. Zou, C. Tan, and Q. Peng. 2015. Effects of dietary carbohydrate composition on rumen fermentation characteristics and microbial population in vitro. Ital. J. Anim. Sci. 14:3366. https://doi.org/10.4081/ijas.2015.3366

Zhao, M., D. Bu, J. Wang, X. Zhou, D. Zhu, T. Zhang, J. Niu, and L. Ma. 2016. Milk production and composition responds to dietary neutral detergent fiber and starch ratio in dairy cows. Anim. Sci. J. 87:756–766. https://doi.org/10.1111/asj.12482

Zhao, W. S., S. L. Hu, K. Yu, H. Wang, W. Wang, J. Loor, and J. Luo. 2014. Lipoprotein lipase, tissue expression and effects on genes related to fatty acid synthesis in goat mammary epithelial cells. Int. J. Mol. Sci. 15:22757-22771.

CHAPTER 7: APPENDICES

Supplementary Table S1. Ingredient and chemical composition of TMR (% of DM) (adapted from Smith, 2021).

	Low peuNDF240[1]		High peuNDF240[2]	
	Low RFS[3]	High RFS[4]	Low RFS	High RFS
Ingredients				
Conventional corn silage	-	-	47.6	47.6
Brown midrib corn silage	47.6	47.6	-	-
Timothy hay	7.94	7.94	7.94	7.94
Wheat strew chopped	1.59	1.59	1.59	1.59
Corn meal	2.78	7.94	3.57	8.73
Beet pulp pellets	7.14	5.16	6.35	4.37
Concentrate mix	32.95	29.77	32.95	29.77
Composition				
DM	53.3	55.3	54.4	54.2
CP	16.1	15.3	16.0	15.2
Ether extract	3.83	3.76	3.81	3.75
Starch	20.7	24.6	20.8	24.7
aNDFom[5]	33.1	32.4	33.3	32.6
RFS[6]	16.7	19.2	16.7	19.2
peuNDF240[7]	6.35	6.07	8.60	8.00

[1]High peuNDF240 = High physically effective undigested NDF after 240-h of in vitro fermentation

[2]Low peuNDF240 = Low physically effective undigested NDF after 240-h of in vitro fermentation

[3]LRFS = High rumen fermentable starch

[4]HRFS = Low rumen fermentable starch

[5]Amylase- and sodium sulfite-treated neutral detergent fiber, ash corrected

[6]Rumen fermentable starch

[7]Physically effective undigested neutral detergent fiber after 240 hours of in vitro fermentation.

Supplementary Table S2. Particle size distribution of diets containing different concentrations of peuNDF240 and RFS (adapted from Smith, 2021).

	Low peuNDF240[1]		High peuNDF240[2]	
	Low RFS[3]	High RFS[4]	Low RFS	High RFS
Particle size, % as-fed				
>19.0 mm	4.7±0.2	4.9±0.3	5.6±0.3	6.1±0.5
8.0 to 19.0 mm	45.4±0.6	43.5±1.1	40.8±0.6	41.1±1
4.0 to 8.0 mm	10.3±0.2	10.2±0.4	10.4±0.1	9.8±0.4
<4.0 mm	39.6±0.5	41.4±1.2	43.3±0.6	43.1±0.7

[1]High peuNDF240 = High physically effective undigested NDF after 240-h of in vitro fermentation

[2]Low peuNDF240 = Low physically effective undigested NDF after 240-h of in vitro fermentation

[3]LRFS = High rumen fermentable starch

[4]HRFS = Low rumen fermentable starch

Supplementary Table S3. Proteins characterized across 26 microbial species in rumen fluid samples collected from Holstein dairy cows fed with varying peuNDF240 and RFS content in the diet.

Accession no	Description	Species
A0A011V1T4	Pyruvate, phosphate dikinase	*Ruminococcus albus*
A0A011V4S8	Glyceraldehyde-3-phosphate dehydrogenase	*Ruminococcus albus*
A0A0E3SMD8	Cell division protein FtsH	*Methanosarcina barkeri*
A0A0L6JLZ7	Chaperone protein DnaK	*Pseudobacteroides cellulosolvens*
A0A1D9P506	Electron transfer flavoprotein beta subunit EtfB	*Butyrivibrio hungatei*
A0A1G5B831	Pyruvate, phosphate dikinase	*Butyrivibrio hungatei*
A0A1G5BZL0	GGGtGRT protein	*Butyrivibrio hungatei*
A0A1G5C0N4	10 kDa chaperonin	*Butyrivibrio hungatei*
A0A1G5CJY8	Pyruvate-ferredoxin/flavodoxin oxidoreductase	*Butyrivibrio hungatei*
A0A1G5DIH3	Glyceraldehyde-3-phosphate dehydrogenase	*Butyrivibrio hungatei*
A0A1G5F3F3	Rubrerythrin	*Ruminococcus bromii*
A0A1G5FJB3	60 kDa chaperonin	*Ruminococcus bromii*
A0A1G5G911	Glyceraldehyde-3-phosphate dehydrogenase	*Ruminococcus bromii*
A0A1G5GUI7	Glutamate dehydrogenase	*Ruminococcus bromii*
A0A1G5H9J7	Elongation factor Tu	*Ruminococcus bromii*
A0A1G5IDN6	30S ribosomal protein S3	*Ruminococcus bromii*
A0A1G5IE59	50S ribosomal protein L15	*Ruminococcus bromii*
A0A1G5IH81	Pyruvate-ferredoxin/flavodoxin oxidoreductase	*Ruminococcus bromii*
A0A1G7QQ04	Methylmalonyl-CoA mutase, N-terminal domain	*Selenomonas ruminantium*
A0A1H4CEQ1	Heterodimeric methylmalonyl-CoA mutase large subunit	*Prevotella ruminicola*
A0A1H4EA56	DNA-directed RNA polymerase subunit beta	*Prevotella ruminicola*
A0A1H4EUY7	Chaperone protein DnaK	*Prevotella ruminicola*
A0A1H5RLC4	Pseudouridine synthase	*Prevotella ruminicola*
A0A1H5SU14	Phosphoenolpyruvate carboxykinase (ATP)	*Prevotella ruminicola*
A0A1H5TKQ7	TonB-linked outer membrane protein, SusC/RagA family	*Prevotella ruminicola*
A0A1H5TZH1	Rubrerythrin	*Prevotella ruminicola*
A0A1H5U9A3	Pyruvate, phosphate dikinase	*Prevotella ruminicola*

A0A1H5UBN2	30S ribosomal protein S16	*Prevotella ruminicola*
A0A1H5ULG9	Glyceraldehyde-3-phosphate dehydrogenase	*Prevotella ruminicola*
A0A1H5VSL2	Pyruvate-ferredoxin/flavodoxin oxidoreductase	*Prevotella ruminicola*
A0A1H5VT00	Acetyl-CoA carboxylase, carboxyltransferase component	*Prevotella ruminicola*
A0A1H5WM35	Elongation factor G	*Prevotella ruminicola*
A0A1H5WV20	Elongation factor Tu	*Prevotella ruminicola*
A0A1H5WVE5	50S ribosomal protein L7/L12	*Prevotella ruminicola*
A0A1H5WWH7	30S ribosomal protein S3	*Prevotella ruminicola*
A0A1H5X530	NifU homolog involved in Fe-S cluster formation	*Prevotella ruminicola*
A0A1H6GDE8	Phosphoenolpyruvate carboxykinase (ATP)	*Selenomonas ruminantium*
A0A1H6JAY3	Elongation factor G	*Prevotella ruminicola*
A0A1H7FGA7	Glycine--tRNA ligase	*Pseudobutyrivibrio ruminis*
A0A1H7G5V3	NifU homolog involved in Fe-S cluster formation	*Pseudobutyrivibrio ruminis*
A0A1H7ITM8	Glutamate dehydrogenase	*Pseudobutyrivibrio ruminis*
A0A1H7JCC9	Elongation factor Tu	*Pseudobutyrivibrio ruminis*
A0A1H9I1I4	GGGtGRT protein	*Treponema bryantii*
A0A1H9IAR9	Flagellin	*Treponema bryantii*
A0A1I0C755	Iron(III) transport system substrate-binding protein	*[Clostridium] aminophilum*
A0A1I0H7X7	Rubrerythrin	*[Clostridium] aminophilum*
A0A1I0LYZ3	Transketolase	*Prevotella aff. ruminicola*
A0A1I0M5Y7	D-3-phosphoglycerate dehydrogenase	*Prevotella aff. ruminicola*
A0A1I0MM67	Phosphoglycerate kinase	*Prevotella aff. ruminicola*
A0A1I0N1Z9	Phosphoenolpyruvate carboxykinase (ATP)	*Prevotella ruminicola*
A0A1I0N3G3	Gluconate 5-dehydrogenase	*Prevotella aff. ruminicola*
A0A1I0P5C6	Glutamate dehydrogenase	*Prevotella aff. ruminicola*
A0A1I0P5I5	DNA-directed RNA polymerase subunit alpha	*Prevotella aff. ruminicola*

A0A1I0P7S8	50S ribosomal protein L1	*Prevotella aff. ruminicola*
A0A1I3BNY5	Elongation factor Tu	*Selenomonas ruminantium*
A0A1I6IDU6	Glutamate dehydrogenase	*[Clostridium] aminophilum*
A0A1I6IX72	30S ribosomal protein S11	*[Clostridium] aminophilum*
A0A1M6SWH6	Polyribonucleotide nucleotidyltransferase	*Prevotella ruminicola*
A0A1M6U7D2	DNA-directed RNA polymerase subunit beta	*Prevotella ruminicola*
A0A1M6U8F7	50S ribosomal protein L22	*Prevotella ruminicola*
A0A1M6U920	30S ribosomal protein S5	*Prevotella ruminicola*
A0A1M6UMJ4	L-fucose isomerase	*Prevotella ruminicola*
A0A1M6V542	Phosphoserine aminotransferase	*Prevotella ruminicola*
A0A1M6WB45	Starch phosphorylase	*Prevotella ruminicola*
A0A1M6X0M2	O-acetylhomoserine sulfhydrylase	*Prevotella ruminicola*
A0A1M6X0T8	Electron transfer flavoprotein alpha subunit apoprotein	*Prevotella ruminicola*
A0A1M6XEW9	Pyruvate-ferredoxin/flavodoxin oxidoreductase	*Prevotella ruminicola*
A0A1M6XNC6	Succinate dehydrogenase / fumarate reductase iron-sulfur subunit	*Prevotella ruminicola*
A0A1M6Y5V8	Acetate kinase	*Prevotella ruminicola*
A0A1M6YIT4	Outer membrane protein OmpA	*Prevotella ruminicola*
A0A1M6YNZ0	Phosphoglucomutase	*Prevotella ruminicola*
A0A1M6YX51	Glutamate dehydrogenase	*Prevotella ruminicola*
A0A1M6Z1D6	HSP20 family protein	*Prevotella ruminicola*
A0A1M7GKC7	ElaA protein	*Prevotella ruminicola*
A0A1M7JI43	30S ribosomal protein S12	*Ruminococcus flavefaciens*
A0A1M7JIG3	Elongation factor Tu	*Ruminococcus flavefaciens*
A0A1M7LEX6	Pyruvate-ferredoxin/flavodoxin oxidoreductase	*Ruminococcus flavefaciens*
A0A1T4JZ88	Acyl-CoA dehydrogenase	*Eubacterium ruminantium*
A0A1T4L550	Carbohydrate ABC transporter ATP-binding protein, CUT1 family	*Eubacterium ruminantium*
A0A1T4NKM7	30S ribosomal protein S3	*Eubacterium ruminantium*
A0A1T4PPS8	Phosphoenolpyruvate carboxykinase (ATP)	*Eubacterium ruminantium*

A0A2G3E7F2	Glyceraldehyde-3-phosphate dehydrogenase	*Pseudobutyrivibrio ruminis*
A0A2G3E9W1	50S ribosomal protein L5	*Pseudobutyrivibrio ruminis*
A0A2G3EDW8	GGGtGRT protein	*Pseudobutyrivibrio ruminis*
A0A2N0UM52	50S ribosomal protein L1	*Ruminococcus bromii*
A0A2N0UMJ2	60 kDa chaperonin	*Ruminococcus bromii*
A0A2N0V0H7	50S ribosomal protein L2	*Ruminococcus albus*
A0A317G314	Glutamate dehydrogenase	*Butyrivibrio fibrisolvens*
A0A317G571	Acyl-CoA dehydrogenase	*Butyrivibrio fibrisolvens*
A0A317G727	Acetyl-CoA C-acetyltransferase	*Butyrivibrio fibrisolvens*
A0A412LBR6	Elongation factor Tu	*Ruminococcus bromii*
A0A412UNB6	Pyruvate, phosphate dikinase	*Ruminococcus bromii*
A0A414DYV0	sn-glycerol-3-phosphate ABC transporter ATP-binding protein UgpC	*Ruminococcus albus*
C3X5Z1	ATP synthase subunit alpha	*Oxalobacter formigenes*
C3X764	Elongation factor Tu	*Oxalobacter formigenes*
C9RNS6	Glutamate dehydrogenase	*Fibrobacter succinogenes (strain ATCC 19169)*
D3DYP9	CoB--CoM heterodisulfide reductase iron-sulfur subunit A	*Methanobrevibacter ruminantium (strain ATCC 35063)*
D3E050	Methyl-coenzyme M reductase subunit alpha	*Methanobrevibacter ruminantium (strain ATCC 35063)*
D3E118	F420-dependent methylenetetrahydromethanopterin dehydrogenase	*Methanobrevibacter ruminantium (strain ATCC 35063)*
D3E1K9	5,10-methylenetetrahydromethanopterin reductase	*Methanobrevibacter ruminantium (strain ATCC 35063)*
D5EUK5	Electron transfer flavoprotein, beta subunit	*Prevotella ruminicola (strain ATCC 19189)*
D5EUX2	50S ribosomal protein L11	*Prevotella ruminicola (strain ATCC 19189)*
D5EUX5	Elongation factor Tu	*Prevotella ruminicola (strain ATCC 19189)*

D5EWF4	Succinate dehydrogenase/fumarate reductase, flavoprotein subunit	*Prevotella ruminicola (strain ATCC 19189*
D5EWS5	60 kDa chaperonin	*Prevotella ruminicola (strain ATCC 19189)*
D5EX27	L-arabinose isomerase	*Prevotella ruminicola (strain ATCC 19189)*
D5EYJ8	Uncharacterized protein	*Prevotella ruminicola (strain ATCC 19189)*
D5EZ55	Pyrophosphate--fructose 6-phosphate 1-phosphotransferase	*Prevotella ruminicola (strain ATCC 19189)*
E0RV83	2-hydroxyglutaryl-CoA dehydratase activator HgdC	*Butyrivibrio proteoclasticus (strain ATCC 51982)*
E0RYA0	Chaperone protein DnaK	*Butyrivibrio proteoclasticus (strain ATCC 51982)*
E6UFE2	ABC transporter related protein	*Ruminococcus albus (strain ATCC 27210*
E9S7A1	Ubiquitin family	*Ruminococcus albus*
E9S9C3	Chaperone protein HtpG	*Ruminococcus albus*
E9SA28	Triosephosphate isomerase	*Ruminococcus albus*
E9SBQ5	Phosphoglycerate kinase	*Ruminococcus albus*
E9SC54	Phosphoenolpyruvate carboxykinase (ATP)	*Ruminococcus albus*
E9SHU2	ABC transporter, ATP-binding protein	*Ruminococcus albus*
G0VNR2	Glyceraldehyde-3-phosphate dehydrogenase	*Megasphaera elsdenii*
H7EN05	Rubrerythrin	*Treponema saccharophilum*
I0GNR2	30S ribosomal protein S19	*Selenomonas ruminantium subsp. lactilytica (strain NBRC 103574)*
I5AS91	Phosphoglycerate kinase	*[Eubacterium] cellulosolvens*
I5ATK3	Chaperone protein ClpB	*[Eubacterium] cellulosolvens*
I5AUV7	ATPase component of ABC-type sugar transporter	*[Eubacterium] cellulosolven*
I5AW29	Polyribonucleotide nucleotidyltransferase	*[Eubacterium] cellulosolvens*
UPI0001D0765C	30S ribosomal protein S12	*Prevotella*
UPI0001D07832	F0F1 ATP synthase subunit alpha	*Prevotella*

UPI0001DB1C19	type I glyceraldehyde-3-phosphate dehydrogenase	*Prevotella bryantii*
UPI0001DB225B	pyruvate:ferredoxin (flavodoxin) oxidoreductase	*Prevotella bryantii*
UPI00031FF12C	30S ribosomal protein S5	*Ruminococcus*
UPI0008DFA946	type I glyceraldehyde-3-phosphate dehydrogenase	*Prevotella ruminicola*
UPI0008E5C2F6	phosphoenolpyruvate carboxykinase (ATP)	*Prevotella ruminicola*
UPI0008EA07DC	TonB-dependent receptor	*Prevotella ruminicola*
UPI0008ED1137	phosphoglycerate kinase	*Prevotella ruminicola*
UPI0008EEAC0D	30S ribosomal protein S1	*Prevotella ruminicola*
UPI0008EED52C	class II fructose-1,6-bisphosphate aldolase	*Prevotella ruminicola*
UPI0009596E56	type I glyceraldehyde-3-phosphate dehydrogenase	*Ruminococcus*
W7ULJ1	Glyceraldehyde-3-phosphate dehydrogenase	*Ruminococcus flavefaciens*
W7ULJ1	Glyceraldehyde-3-phosphate dehydrogenase	*Ruminococcus flavefaciens*

Supplementary Table S4. List of 129 proteins identified across 23 microbial species in rumen fluid samples collected from Holstein dairy cows fed with two different concentrations of peuNDF240 and RFS content in the diet.

Accession no	Description	Species
A0A317G314	Glutamate dehydrogenase	*Butyrivibrio fibrisolvens*
A0A317G571	Acyl-CoA dehydrogenase	*Butyrivibrio fibrisolvens*
A0A317G727	Acetyl-CoA C-acetyltransferase	*Butyrivibrio fibrisolvens*
A0A1G5CJY8	Pyruvate-ferredoxin/flavodoxin oxidoreductase	*Butyrivibrio hungatei*
A0A1G5DIH3	Glyceraldehyde-3-phosphate dehydrogenase	*Butyrivibrio hungatei*
E0RUF2	Phosphoenolpyruvate carboxykinase (ATP)	*Butyrivibrio proteoclasticus (strain ATCC 51982)*
E0RV83	2-hydroxyglutaryl-CoA dehydratase activator HgdC	*Butyrivibrio proteoclasticus (strain ATCC 51982)*
E0RWM0	Ketol-acid reductoisomerase (NADP(+))	*Butyrivibrio proteoclasticus (strain ATCC 51982)*
A0A1I0CPA8	BMC domain-containing protein	*Clostridium aminophilum*
A0A1I6JNS0	Pyruvate, phosphate dikinase	*Clostridium aminophilum*
A0A1I0H7X7	Rubrerythrin	*Clostridium aminophilum*
I5AS89	Pyruvate, phosphate dikinase	*Eubacterium cellulosolvens 6*
I5AS91	Phosphoglycerate kinase	*Eubacterium cellulosolvens 6*
I5AS92	Glyceraldehyde-3-phosphate dehydrogenase	*Eubacterium cellulosolvens 6*
A0A1T4MUX0	Enolase	*Eubacterium ruminantium*
A0A1T4JZ88	Acyl-CoA dehydrogenase	*Eubacterium ruminantium*
A0A1T4L550	Carbohydrate ABC transporter ATP-binding protein, CUT1 family	*Eubacterium ruminantium*
D3DYP9	CoB--CoM heterodisulfide reductase iron-sulfur subunit A	*Methanobrevibacter ruminantium (strain ATCC 35063)*
D3E050	Methyl-coenzyme M reductase subunit alpha	*Methanobrevibacter ruminantium (strain ATCC 35063)*
D3E051	Methyl-coenzyme M reductase subunit gamma	*Methanobrevibacter ruminantium (strain ATCC 35063)*

D3E1K9	5,10-methylenetetrahydromethanopterin reductase	*Methanobrevibacter ruminantium (strain ATCC 35063)*
D3E118	F420-dependent methylenetetrahydromethanopterin dehydrogenase	*Methanobrevibacter ruminantium (strain ATCC 35063)*
A0A0E3SMD8	Cell division protein FtsH	*Methanosarcina barkeri 3*
C3X5Q1	Adenosylhomocysteinase	*Oxalobacter formigenes HOxBLS*
R5IY35	Phosphoglycerate kinase	*Peptostreptococcus anaerobius CAG:621*
A0A1I0LYZ3	Transketolase	*Prevotella aff. ruminicola Tc2-24*
A0A1I0MAA6	30S ribosomal protein S1	*Prevotella aff. ruminicola Tc2-24*
A0A1I0NI44	30S ribosomal protein S2	*Prevotella aff. ruminicola Tc2-24*
A0A1I0P5C6	Glutamate dehydrogenase	*Prevotella aff. ruminicola Tc2-24*
A0A1I0P7F2	DNA-directed RNA polymerase subunit beta	*Prevotella aff. ruminicola Tc2-24*
A0A1I0P7S8	50S ribosomal protein L1	*Prevotella aff. ruminicola Tc2-24*
A0A1I0PW57	Elongation factor G	*Prevotella aff. ruminicola Tc2-24*
A0A1I0QFN0	Iron complex outermembrane recepter protein	*Prevotella aff. ruminicola Tc2-24*
A0A1I0N1Z9	Phosphoenolpyruvate carboxykinase (ATP)	*Prevotella aff. ruminicola Tc2-24*
A0A1I0P5I5	DNA-directed RNA polymerase subunit alpha	*Prevotella aff. ruminicola Tc2-24*
A0A1I0P6V2	50S ribosomal protein L2	*Prevotella aff. ruminicola Tc2-24*
A0A1I0QJC9	Elongation factor P	*Prevotella aff. ruminicola Tc2-24*
UPI0001DB1C19	glyceraldehyde-3-phosphate dehydrogenase	*Prevotella bryantii*
UPI0001DB225B	pyruvate:ferredoxin (flavodoxin) oxidoreductase	*Prevotella bryantii*
A0A1H3YTU1	Acetate kinase	*Prevotella ruminicola*
A0A1H4EA56	DNA-directed RNA polymerase subunit beta'	*Prevotella ruminicola*
A0A1H5VSL2	Pyruvate-ferredoxin/flavodoxin oxidoreductase	*Prevotella ruminicola*

A0A1H5WV20	Elongation factor Tu	*Prevotella ruminicola*
A0A1H5WVE5	50S ribosomal protein L7/L12	*Prevotella ruminicola*
A0A1H5X530	NifU homolog involved in Fe-S cluster formation	*Prevotella ruminicola*
A0A1M6TI31	Phosphoenolpyruvate carboxykinase (ATP)	*Prevotella ruminicola*
A0A1M6U920	30S ribosomal protein S5	*Prevotella ruminicola*
A0A1M6UMJ4	L-fucose isomerase	*Prevotella ruminicola*
A0A1M6UYF5	UDP-glucose 4-epimerase	*Prevotella ruminicola*
A0A1M6WVF5	Triosephosphate isomerase	*Prevotella ruminicola*
A0A1M6X0T8	Electron transfer flavoprotein alpha subunit apoprotein	*Prevotella ruminicola*
A0A1M6XEW9	Pyruvate-ferredoxin/flavodoxin oxidoreductase	*Prevotella ruminicola*
A0A1M6XNC7	Succinate dehydrogenase subunit A	*Prevotella ruminicola*
A0A1M6Y5V8	Acetate kinase	*Prevotella ruminicola*
A0A1M6YIT4	Outer membrane protein OmpA	*Prevotella ruminicola*
A0A1M6YNZ0	Phosphoglucomutase	*Prevotella ruminicola*
A0A1M6YX51	Glutamate dehydrogenase	*Prevotella ruminicola*
A0A1M6Z1D6	HSP20 family protein	*Prevotella ruminicola*
UPI0001D07747	molecular chaperone DnaK	*Prevotella ruminicola*
UPI0008DFA946	glyceraldehyde-3-phosphate dehydrogenase	*Prevotella ruminicola*
UPI0008E5C2F6	phosphoenolpyruvate carboxykinase (ATP)	*Prevotella ruminicola*
UPI0008E71882	pyruvate, phosphate dikinase	*Prevotella ruminicola*
UPI0008ED1137	phosphoglycerate kinase	*Prevotella ruminicola*
UPI0008EED52C	class II fructose-1,6-bisphosphate aldolase	*Prevotella ruminicola*
A0A1H3XC50	O-acetylhomoserine sulfhydrylase	*Prevotella ruminicola*
A0A1H5TZH1	Rubrerythrin	*Prevotella ruminicola*
A0A1H5U2M6	ATP synthase subunit beta	*Prevotella ruminicola*
A0A1H5U383	Na(+)-translocating NADH-quinone reductase subunit C	*Prevotella ruminicola*
A0A1H5ULG9	Glyceraldehyde-3-phosphate dehydrogenase	*Prevotella ruminicola*
A0A1H6JAY3	Elongation factor G	*Prevotella ruminicola*
A0A1M6SWH6	Polyribonucleotide nucleotidyltransferase	*Prevotella ruminicola*
A0A1M6V542	Phosphoserine aminotransferase	*Prevotella ruminicola*
A0A1M6VCT7	Fructose-bisphosphate aldolase	*Prevotella ruminicola*
A0A1M6WB45	Starch phosphorylase	*Prevotella ruminicola*

A0A1M6XE37	Acetyl-CoA carboxylase, carboxyltransferase component	*Prevotella ruminicola*
A0A1M6XNC6	Succinate dehydrogenase / fumarate reductase iron-sulfur subunit	*Prevotella ruminicola*
D5EUK5	Electron transfer flavoprotein, beta subunit	*Prevotella ruminicola (strain ATCC 19189)*
D5EUA2	50S ribosomal protein L19	*Prevotella ruminicola (strain ATCC 19189)*
D5EUX5	Elongation factor Tu	*Prevotella ruminicola (strain ATCC 19189)*
D5EWS5	60 kDa chaperonin	*Prevotella ruminicola (strain ATCC 19189)*
D5EX27	L-arabinose isomerase	*Prevotella ruminicola (strain ATCC 19189)*
D5EX68	Acyl carrier protein	*Prevotella ruminicola (strain ATCC 19189)*
D5EY19	Plug domain-containing protein	*Prevotella ruminicola (strain ATCC 19189)*
D5EYJ8	Uncharacterized protein	*Prevotella ruminicola (strain ATCC 19189)*
UPI00048FAA24	acyl-CoA carboxylase subunit beta	*Prevotella sp.*
A0A0L6JXI6	NifU_N domain-containing protein	*Pseudobacteroides cellulosolvens ATCC 35603*
A0A0L6JLZ7	Chaperone protein DnaK	*Pseudobacteroides cellulosolvens ATCC 35603*
A0A1H7FBX7	Pyruvate, phosphate dikinase	*Pseudobutyrivibrio ruminis*
A0A1H7JCC9	Elongation factor Tu	*Pseudobutyrivibrio ruminis*
A0A2G3DUJ4	Phosphoglycerate kinase	*Pseudobutyrivibrio ruminis*
A0A2G3DY38	ABC transporter substrate-binding protein	*Pseudobutyrivibrio ruminis*
A0A1H7ITM8	Glutamate dehydrogenase	*Pseudobutyrivibrio ruminis*
A0A2G3E7F2	Glyceraldehyde-3-phosphate dehydrogenase	*Pseudobutyrivibrio ruminis*
A0A2G3EDW8	GGGtGRT protein	*Pseudobutyrivibrio ruminis*
UPI0009596E56	type I glyceraldehyde-3-phosphate dehydrogenase	*Ruminococcus*

E6UJ21	Phosphoenolpyruvate carboxykinase (ATP)	*Ruminococcus albus (strain ATCC 27210)*
E6UH00	Uncharacterized protein	*Ruminococcus albus (strain ATCC 27210)*
E6UK84	Ubiquitin	*Ruminococcus albus (strain ATCC 27210)*
E9S7A1	Ubiquitin family	*Ruminococcus albus 8*
E9S9C3	Chaperone protein HtpG	*Ruminococcus albus 8*
E9SA66	Pyruvate synthase	*Ruminococcus albus 8*
E9SBQ5	Phosphoglycerate kinase	*Ruminococcus albus 8*
A0A011V1T4	Pyruvate, phosphate dikinase	*Ruminococcus albus SY3*
A0A011V4S8	Glyceraldehyde-3-phosphate dehydrogenase	*Ruminococcus albus SY3*
A0A011VUA2	Heat-shock protein Hsp20	*Ruminococcus albus SY3*
A0A011VWT5	60 kDa chaperonin	*Ruminococcus albus SY3*
A0A1G5IG65	Fructose-bisphosphate aldolase, class II	*Ruminococcus bromii*
A0A2N0UM52	50S ribosomal protein L1	*Ruminococcus bromii*
A0A2N0UMJ2	60 kDa chaperonin	*Ruminococcus bromii*
A0A2N0V0H7	50S ribosomal protein L2	*Ruminococcus bromii*
A0A412LBR6	Elongation factor Tu	*Ruminococcus bromii*
A0A412UP21	Pyruvate:ferredoxin (Flavodoxin) oxidoreductase	*Ruminococcus bromii*
A0A414DYV0	sn-glycerol-3-phosphate ABC transporter ATP-binding protein UgpC	*Ruminococcus bromii*
A0A1G5BWW0	30S ribosomal protein S9	*Ruminococcus bromii*
A0A1G5F3F3	Rubrerythrin	*Ruminococcus bromii*
A0A1G5G911	Glyceraldehyde-3-phosphate dehydrogenase	*Ruminococcus bromii*
A0A1G5GUI7	Glutamate dehydrogenase	*Ruminococcus bromii*
A0A1G5H9J7	Elongation factor	*Ruminococcus bromii*
A0A2N0UTQ0	Polyribonucleotide nucleotidyltransferase	*Ruminococcus bromii*
A0A412UNB6	Pyruvate, phosphate dikinase	*Ruminococcus bromii*
A0A1M7HAP1	Rubrerythrin	*Ruminococcus flavefaciens*
A0A1M7JIG3	Elongation factor Tu	*Ruminococcus flavefaciens*
A0A1M7L8N4	Pyruvate, phosphate dikinase	*Ruminococcus flavefaciens*
W7ULJ1	Glyceraldehyde-3-phosphate dehydrogenase	*Ruminococcus flavefaciens 007c*
A0A1I3BNY5	Elongation factor Tu	*Selenomonas ruminantium*

A0A1I6Z320	Flagellin	*Selenomonas ruminantium*
H7EPU6	Enolase	*Treponema saccharophilum DSM 2985*
H7EKI7	Monosaccharide ABC transporter substrate-binding protein, CUT2 family	*Treponema saccharophilum DSM 2985*
H7EN05	Rubrerythrin	*Treponema saccharophilum DSM 2985*

Supplementary Table S5. List of 159 milk whey protein in milk samples collected from Holstein dairy cows fed with two different concentrations of peuNDF240 and RFS content in the diet.

Accession no	Description	Biological function
Q3ZBZ1	45 kda calcium-binding protein	Cell differentiation
Q0VCX2	78 kda glucose-regulated protein	Immunity
P60712	Actin, cytoplasmic 1	Protein synthesis
Q5GN72	Alpha-1-acid glycoprotein	Immunity
P34955	Alpha-1-antiproteinase	Immunity
P28800	Alpha-2-antiplasmin	Immunity
P12763	Alpha-2-HS-glycoprotein	Cell differentiation
Q7SIH1	Alpha-2-macroglobulin	Immunity
Q9XSJ4	Alpha-enolase	Immunity
P00711	Alpha-lactalbumin	Immunity
P02662	Alpha-S1-casein	Immunity
P02663	Alpha-S2-casein	Immunity
A6H6X2	ANG2 protein (angiogenin2 isoformx1)	angiogenesis
P10152	Angiogenin-1	Angiogenesis
Q3SZH5	Angiotensinogen precursor	Vasoconstrictor
F6QVC9	Annexin A5	Cell proliferation
F1MSZ6	Antithrombin-III	Protease inhibitor
P15497	Apolipoprotein A-I	Transport
B2D1N9	ATP-binding cassette sub-family G member 2 isoform X2	Transport
P08037	Beta-1,4-galactosyltransferase 1	Lipid metabolism
P17690	Beta-2-glycoprotein 1	Transport
P01888	Beta-2-microglobulin	Immunity
P02666	Beta-casein	Immunity
P02754	Beta-lactoglobulin	Immunity
P18892	Butyrophilin subfamily 1 member	Transport
P52193	Calreticulin precursor	Calcium metabolism
P25975	Cathepsin L1	Immunity
P30932	CD9 antigen	Immunity
Q2KJ93	Cell division control protein 42 homolog	Cell migration
G3X7D2	Chitinase-3-like protein 1	Immunity
P17697	Clusterin	Immunity
Q2UVX4	Complement C3	Immunity
F1N045	Complement component C7	Immunity
Q3MHN2	Complement component C9	Immunity
P81187	Complement factor B	Immunity
Q28085	Complement factor H	Immunity
A4IFS7	CTSL1 protein	Protein catabolism
F1MD23	C-X-C motif chemokine	Immunity

G3N3P6	Cystatin	Immunity
F6QEL0	Cystatin	Immunity
P15396	Ectonucleotide pyrophosphatase/phosphodiesterase family member 3	Immunity
P79345	Epididymal secretory protein E1	Transport
P31976	Ezrin	Cell shape
P10790	Fatty acid-binding protein, heart	Cell growth
Q3SZZ9	FGG protein	Angiogenesis
P02672	Fibrinogen alpha chain	Inflammation
F1MAV0	Fibrinogen beta chain	Angiogenesis
Q9MZ06	Fibroblast growth factor-binding protein 1	Angiogenesis
P02702	Folate receptor alpha	Transport
E1BJL8	Folate receptor alpha	Transport
P50291	Follistatin	Bone maturation
F1MJH1	Gelsolin	Transport
P80195	Glycosylation-dependent cell adhesion molecule 1	Immunity
P19120	Heat shock cognate 71 kda	Immunity
Q3SZV7	Hemopexin	Transport
Q3SYR8	Immunoglobulin J chain	Immunity
F1MMD7	Inter-alpha-trypsin inhibitor heavy chain	Immunity
Q0VCM5	Inter-alpha-trypsin inhibitor heavy chain H1	Immunity
F1MNW4	Inter-alpha-trypsin inhibitor heavy chain H2	Immunity
F1MNW4	Isocitrate dehydrogenase [NADP]	Transport
A0A140T8A9	Kappa-casein	Lactation
A6QNZ7	Keratin 10 (Epidermolytic hyperkeratosis; keratosis palmaris et plantaris)	Transport
F1MNV5	Kininogen-1	Immunity
Q95114	Lactadherin	Immunity
P80025	Lactoperoxidase	Immunity
P24627	Lactotransferrin	Immunity
Q95M12	Legumain	Transport
Q2KIF2	Leucine-rich alpha-2-glycoprotein 1	Inflammation
P11151	Lipoprotein lipase	Transport
Q95122	Monocyte differentiation antigen CD14	Immunity
Q8WML4	Mucin-1	Immunity
Q8MI01	Mucin-15	Immunity
P12624	Myristoylated alanine-rich C-kinase substrate	Transport

Q58CS8	N-acetylglucosamine-1-phosphotransferase subunit gamma	Transport
Q0IIH5	Nucleobindin 2	Immunity
Q0P569	Nucleobindin-1	Immunity
Q32KV6	Nucleotide exchange factor SIL1	Transport
Q0IIA2	Odorant-binding protein-like	Transport
P31096	Osteopontin	Immunity
M5FKI8	zymogen granule protein 16 homolog B-like	Transport
P00974	Pancreatic trypsin inhibitor	Protein degradation
P58073	Parathyroid hormone-related protein	cell differentiation
P62935	Peptidyl-prolyl cis-trans isomerase A	Immunity
P80311	Peptidyl-prolyl cis-trans isomerase B	Immunity
F1N1N6	Perilipin	Transport
Q3SX32	Perilipin	Transport
P13696	Phosphatidylethanolamine-binding protein 1	Transport
Q95121	Pigment epithelium-derived factor	Cell growth
P06868	Plasminogen	Immunity
P26201	Platelet glycoprotein 4	Immunity
P81265	Polymeric IgM receptor	Immunity
P0CH28	Polyubiquitin-C	Protein degradation
Q29437	Primary amine oxidase, liver isozyme	Amine metabolic process
P26779	Prosaposin	Transpoprt
O02853	Prostaglandin-H2 D-isomerase	Inflammation
F1MX65	Protein OS-9 precursor	Nervous system maturation
F1MMK9	Protein AMBP	Immunity
Q2KIT0	Protein HP-20 homolog	Immunity
Q2KIU3	Protein HP-25 homolog 2	Immunity
A6QR11	Protein kinase C-binding protein NELL2	Cell differentiation
P00735	Prothrombin	Angiogenesis
P50397	Rab GDP dissociation inhibitor beta	Transport
A1L528	RAB1A, member RAS oncogene family	Transport
Q9TU25	Ras-related C3 botulinum toxin substrate 2	Cell differentiation
Q0IIG8	Ras-related protein Rab-18	Cell growth
P19803	Rho GDP-dissociation inhibitor 1	Signal transduction
Q58DP6	Ribonuclease 4	Immunity
A0JNP2	Secretoglobin family 1D member	Transport
Q29443	Serotransferrin	Immunity
Q9TTE1	Serpin A3-1	Transport
A0A0A0MP92	Serpin A3-7	Protein degradation

A0A140T897	Serum albumin	Angiogenesis
Q8SQ28	Serum amyloid A protein	Immunity
F1N6D4	Sodium-dependent phosphate transport protein 2B	Transport
G8JKX0	Spermadhesin-1	Transport
F1MM32	Sulfhydryl oxidase	Transport
P00442	Superoxide dismutase [Cu-Zn]	Cell homeostasis
Q3T000	Synaptobrevin homolog YKT6	Transport
Q2KIS7	Tetranectin	Cell growth
A6QQ20	Trans-Golgi network integral membrane protein 2 (Fragment)	Golgi-associated
O46375	Transthyretin	Cell growth
E1BI01	Dual specificity mitogen-activated protein kinase 5	Transport
G5E5H7	beta-lactoglobulin precursor	Immunity
G5E513	Igm heavy chain secretory form	Immunity
E1BH06	Complement C4 precursor	Immunity
G5E5T5	Igm heavy chain secretory form	Immunity
F1N726	Pancreatic secretory granule membrane major glycoprotein GP2 precursor	Immunity
F1N076	Ceruloplasmin isoform X1	Cell growth
G3N0V0	Immunoglobulin gamma2 heavy chain	Immunity
F1MNT4	Laminin subunit beta-1	Nervous system maturation
F1MZ96	IGK protein	Immunity
F1N4M7	Complement factor I isoform X1	Immunity
E1BHY6	Granulin isoform X2	Cell growth
G8JKW7	TPA: serpin A3-6	Protein degradation
F6R3I5	Cysteine-rich secretory protein 3 precursor	Immunity
E1BF27	Putative sodium-coupled neutral amino acid transporter 10 isoform X6	Transport
F1N514	CD5 antigen-like precursor	Immunity
F1MPE1	CD109 antigen	Cell differentiation
E1BGX8	HHIP-like protein 2 isoform X2	Transport
F1MLW8	Immunoglobulin lambda-1 light chain-like isoform X5	Immunity
G3N2D8	Gamma-glutamyl Transpeptidase 1	Cell growth
E1BMJ0	Factor xiia inhibitor isoform X1	Blood coagulation pathway
F1MX50	CREG1 isoform X1	Transport
F1MFI4	Cartilage acidic protein 1 isoform 1 precursor	Cell differentiation
F1MCF8	IGL protein	Immunity

G3MXB5	IgM precursor	Immunity
G3N2K4	Golgi apparatus protein 1 precursor	Golgi-associated
E1B6Z6	Neutrophil gelatinase-associated lipocalin	Immunity
G3N0V2	Keratin, type II cytoskeletal 1	Cell growth
G5E604	TPA: IgM iota chain-like	Immunity
G3N2D7	Immunoglobulin light chain variable region	Immunity
M0QVY0	Keratin, type II cytoskeletal 6A	Cell growth
G5E5V1	TPA: IgM iota chain-like	Immunity
F1MT39	Trophoblast Kunitz domain protein 3	trophoblast differentiation
F1N5M2	Vitamin D-binding protein	Transport
Q3T0Z0	WAP four-disulfide core domain 2	Cell growth
F1MUT3	Xanthine dehydrogenase/oxidase	Immunity
P80457	Xanthine dehydrogenase/oxidase	Immunity
Q3ZCH5	Zinc-alpha-2-glycoprotein	Cell growth

Supplementary Table S6. Ingredient and chemical composition of TMR (% of DM)

	Value
Ingredients	
Corn silage	37.3
CREAM low cow mash	88
3rd cut haylage	31.3
Composition	
DM	46.93
CP	17.95
Neutral detergent fiber	31.53
Starch	24.15
Acid detergent fiber	21.02
physically effective neutral detergent fiber	24.38
Ether extract	4.63
Calcium	0.86
Phosphorus	0.38
Magnesium	0.42
Potassium	1.07
Sodium	0.40
Monensin	365.17
Selenium (PPM)	0.49
DCAD (meq/kg)	122.03
Lysine (g)	228.58

Supplementary Table S7. List of identified differentially expressed genes in rumen epithelium collected from cows dosed with intra-ruminal sodium propionate (propionate) or sodium chloride (control). n = 4 cows/treatment (propionate or control).

Gene symbol	Entrez gene ID	Description	Log2Fold change	P_{FDR} - value
Down-regulated				
RBSN	511484	rabenosyn, RAB effector	-11.05	1.8E-06
CLN6	617615	CLN6 transmembrane ER protein	-10.477	1.8E-06
GDAP2	508774	ganglioside induced differentiation associated protein 2	-10.268	1.8E-06
POLE4	613730	DNA polymerase epsilon 4, accessory subunit	-10.188	1.3E-05
SRSF11	513451	serine and arginine rich splicing factor 11	-10.158	1.6E-05
EMD	399681	emerin	-10.149	2.1E-06
FLII	514446	FLII actin remodeling protein	-9.8279	4.1E-06
MLYCD	512341	malonyl-CoA decarboxylase	-9.5768	0.00012
C15H11ORF96	100270684	chromosome 15 C11orf96 homolog	-9.4805	0.00019
RAB11FIP4	100848380	RAB11 family interacting protein 4	-9.3187	0.00017
C7H19orf24	ND	Unchratcerized	-9.2994	4.1E-05
MUC1	281333	mucin 1, cell surface associated	-9.1849	0.0001
LOC104974155	104974155	myb/SANT-like DNA-binding domain-containing protein 4 pseudogene	-9.0552	0.00025
PINX1	525027	PIN2	-9.0378	3.8E-05
CDCA3	614434	cell division cycle associated 3	-8.9415	0.00032
HAT1	509329	histone acetyltransferase 1	-8.9414	0.00065
CDK2	519217	cyclin dependent kinase 2	-8.8858	0.00052
VWA2	530237	von Willebrand factor A domain containing 2	-8.8025	1.4E-05
GTF2H1	513510	general transcription factor IIH subunit 1	-8.7978	5.9E-06
ARHGEF11	511220	Rho guanine nucleotide exchange factor 11	-8.785	0.00011

ACTR1A	514371	actin related protein 1A	-8.5818	0.00025
STAMBPL1	538785	STAM binding protein like 1	-8.556	0.0008
LOC112449304	112449304	uncharacterized	-8.4805	0.00144
LOC112447732	112447732	uncharacterized	-8.4048	0.00106
NKAPD1	513716	NKAP domain containing 1	-8.3489	1.4E-05
ANO6	521784	anoctamin 6	-8.3235	0.00114
LOC112447087	112447087	bisphosphoglycerate mutase	-8.2526	0.00043
SMS	615950	spermine synthase	-8.2438	0.00198
SERTAD4	614583	SERTA domain containing 4	-8.1298	0.00052
PMVK	513533	phosphomevalonate kinase	-8.1127	7.6E-06
GABARAPL2	282531	major facilitator superfamily domain containing 4A	-8.1098	0.00024
TG	280706	thyroglobulin	-8.0391	0.00304
PIK3CB	517948	phosphatidylinositol-4,5-bisphosphate 3-kinase catalytic subunit beta	-8.0307	0.00086
FAM118B	540626	family with sequence similarity 118 member B	-8.0243	0.00053
GPIHBP1	512826	glycosylphosphatidylinositol anchored high density lipoprotein binding protein 1	-8.0142	0.00117
FOXRED1	510097	FAD dependent oxidoreductase domain containing 1	-8.0112	0.00476
EVPL	510502	envoplakin	-7.9667	0.00182
ZNF768	100847165	zinc finger protein 768	-7.9369	0.00015
WNK3	100337119	WNK lysine deficient protein kinase 3	-7.8879	0.00764
DENND4C	536760	DENN domain containing 4C	-7.8815	0.00741
LOC112447304	112447304	uncharacterized	-7.8649	0.00707
LOC107132327	107132327	cytochrome P450 2J2-like	-7.8638	0.00169
LOC788036	788036	protein FAM92A pseudogene	-7.7938	0.00781
LOC107131803	107131803	serpin B3-like	-7.7882	0.00107

TMEM110	538654	transmembrane protein 110	-7.7178	0.00276
HM13	512534	histocompatibility minor 13	-7.6388	0.00276
LOC101907697	101907697	homeobox protein CDX-1-like	-7.6012	0.00997
CCT5	533784	chaperonin containing TCP1 subunit 5	-7.4925	0.00492
YTHDC1	613858	YTH domain containing 1	-7.4834	0.00227
APRT	519017	adenine phosphoribosyltransferase	-7.4804	0.00441
STARD8	535900	StAR related lipid transfer domain containing 8	-7.4572	0.00564
LOC112447903	112447903	U6 spliceosomal RNA	-7.4565	0.00521
UBE2K	281225	ubiquitin conjugating enzyme E2 K	-7.4523	0.00046
STAG3	515399	stromal antigen 3	-7.3971	0.00454
LOC112446151	112446151	small nucleolar RNA U3	-7.32	0.01114
HSPA8	281831	heat shock protein family A	-7.2986	0.00276
LOC101904768	101904768	chromobox protein homolog 3 pseudogene	-7.2893	0.00164
TRIP4	533430	thyroid hormone receptor interactor 4	-7.2186	0.00988
SLC25A1	282476	solute carrier family 25 member 1	-7.2124	0.01585
ACY1	768058	aminoacylase 1	-7.2017	0.00106
CTHRC1	538634	collagen triple helix repeat containing 1	-7.1852	0.01642
PAQR3	534876	progestin and adipoQ receptor family member 3	-7.1538	0.00048
IRF2BPL	613845	interferon regulatory factor 2 binding protein like	-7.0644	0.00281
RPE	533764	ribulose-5-phosphate-3-epimerase	-7.0589	0.00601
MAOB	338445	monoamine oxidase B	-7.0458	0.00582
OTUB1	540984	OTU deubiquitinase, ubiquitin aldehyde binding 1	-7.0392	0.00812
SNCAIP	540156	synuclein alpha interacting protein	-7.0361	0.0203
PARM1	518368	prostate androgen-regulated mucin-like protein 1	-7.0123	0.00521
CALM2	100297344	calmodulin 2	-6.9983	0.01129

SLC6A6	282366	solute carrier family 6 member 6	-6.9855	0.01237
LOC101903064	101903064	COMM domain-containing protein 6	-6.9725	0.00987
LRRC8E	507824	leucine rich repeat containing 8 VRAC subunit E	-6.9307	0.00142
PRR7	538641	proline rich 7, synaptic	-6.9278	0.00582
RREB1	789017	ras responsive element binding protein 1	-6.9235	0.01383
LOC112443564	112443564	small nucleolar RNA SNORD69	-6.8851	0.02212
LOC101905876	101905876	Uncharacterized	-6.8616	0.0136
ATP23	514014	ATP23 metallopeptidase and ATP synthase assembly factor homolog	-6.8391	0.02212
LOC112446416	112446416	uncharacterized	-6.8125	0.0138
PSMB4	506203	proteasome 20S subunit beta 4	-6.79	0.01578
RPL39	767908	ribosomal protein L39	-6.7836	0.04759
ZCCHC11	ND	Unchratcerized	-6.7834	0.0138
TAF5L	510413	TATA-box binding protein associated factor 5 like	-6.7819	0.00902
HBEGF	522921	heparin binding EGF like growth factor	-6.7813	0.00482
PLA2G5	614911	phospholipase A2 group V	-6.757	0.0351
LRP1	533894	LDL receptor related protein 1	-6.7124	0.02363
MRPL15	510347	mitochondrial ribosomal protein L15	-6.7097	0.00283
SPOUT1	100138783	SPOUT domain containing methyltransferase 1	-6.7078	0.0081
ZNF397	506448	zinc finger protein 397	-6.6888	0.00253
PTBP1	282018	polypyrimidine tract binding protein 1	-6.6809	0.00744
PSME3	100336105	proteasome activator subunit 3	-6.6788	0.01509
KIT	280832	KIT proto-oncogene, receptor tyrosine kinase	-6.6449	0.00641
RAB6B	526526	RAB6B, member RAS oncogene family	-6.5918	0.03759
LOC112447371	112447371	uncharacterized	-6.5899	0.02556
PDE6D	281976	phosphodiesterase 6D	-6.5767	0.00831

PUM3	514957	pumilio RNA binding family member 3	-6.5656	0.00789
LOC615559	615559	uncharacterized	-6.5639	0.01987
LOC112446664	112446664	uncharacterized	-6.5493	0.04946
EFNB2	100139818	ephrin B2	-6.5457	0.00842
PSMC3IP	508530	PSMC3 interacting protein	-6.5429	0.0081
MAP2K2	510434	mitogen-activated protein kinase kinase 2	-6.5385	0.02381
UQCC1	618503	ubiquinol-cytochrome c reductase complex assembly factor 1	-6.5384	0.00489
S100A12	282467	S100 calcium binding protein A12	-6.5341	0.01464
SESN1	538226	sestrin 1	-6.5287	0.00914
SYN2	782758	synapsin II	-6.521	0.01334
LOC112442039	112442039	40S ribosomal protein S29 pseudogene	-6.4664	0.03933
DERL2	508465	derlin 2	-6.4625	0.00741
LOC100337328	100337328	Uncharacterized	-6.462	0.04432
PCLO	517284	piccolo presynaptic cytomatrix protein	-6.4542	0.04592
PDZD7	511930	PDZ domain containing 7	-6.445	0.02691
WFDC18	100336022	extracellular proteinase inhibitor	-6.439	0.01289
HKDC1	614824	hexokinase domain containing 1	-6.4316	0.0115
HERC6	527520	HECT and RLD domain containing E3 ubiquitin protein ligase family member 6	-6.4226	0.01642
SRRT	527938	serrate, RNA effector molecule	-6.3676	0.0136
CFL2	539332	cofilin 2	-6.3603	0.00375
ZNF516	519449	zinc finger protein 516	-6.3593	0.00847
LOC100138864	100138864	eukaryotic initiation factor 4A-II pseudogene	-6.346	0.04973
CAMKK2	509084	calcium/calmodulin dependent protein kinase kinase 2	-6.3415	0.00937
RALGPS1	616166	Ral GEF with PH domain and SH3 binding motif 1	-6.3024	0.01129

CCNT1	407194	cyclin T1	-6.2897	0.00902
TMEM200C	786855	transmembrane protein 200C	-6.2755	0.02911
LOC112447466	112447466	uncharacterized	-6.2735	0.04167
RHOQ	100139988	ras homolog family member Q	-6.2604	0.0351
LOC788634	788634	BOLA class I histocompatibility antigen, alpha chain BL3-7-like	-6.2475	0.02928
SBNO2	512682	strawberry notch homolog 2	-6.2424	0.01174
BTBD10	505888	BTB domain containing 10	-6.2364	0.04061
LTBR	504653	lymphotoxin beta receptor	-6.219	0.00375
NAA40	517933	N-alpha-acetyltransferase 40, NatD catalytic subunit	-6.2082	0.01383
STK17A	513665	serine/threonine kinase 17a	-6.2016	0.00552
HEATR4	101902938	HEAT repeat containing 4	-6.1894	0.01638
LOC100138660	100138660	uncharacterized	-6.1874	0.03982
ZBTB7B	509019	zinc finger and BTB domain containing 7B	-6.1801	0.03219
EHBP1	100300164	EH domain binding protein 1	-6.1758	0.03121
COQ10B	514221	coenzyme Q10B	-6.1586	0.02832
LARS	ND	Uncharacterized	-6.1415	0.04981
ATG101	513049	autophagy related 101	-6.1303	0.01486
TRNAG-GCC	112445489	transfer RNA glycine	-6.1146	0.04032
MXRA5	786844	matrix remodeling associated 5	-6.0855	0.02977
ZC3H18	523958	zinc finger CCCH-type containing 18	-6.0842	0.01486
RPS28	282877	ribosomal protein S28	-6.0564	0.04432
BUB1	514777	BUB1 mitotic checkpoint serine/threonine kinase	-6.0522	0.03424
TSPAN31	510619	tetraspanin 31	-6.0511	0.04434
TLR2	281534	toll like receptor 2	-6.0477	0.04548
PTPRJ	508150	protein tyrosine phosphatase receptor type J	-6.0252	0.04013

HNRNPD	527471	heterogeneous nuclear ribonucleoprotein D	-6.0128	0.02321
CXADR	281733	CXADR Ig-like cell adhesion molecule	-6.0084	0.02736
KIAA0391	ND	Uncharacterized	-5.9909	0.00252
ATM	526824	ATM serine/threonine kinase	-5.9536	0.02691
USP38	534262	ubiquitin specific peptidase 38	-5.9328	0.04973
ATP5MD	ND	Uncharacterized	-5.9087	0.04692
PPP2R2C	782110	protein phosphatase 2 regulatory subunit Bgamma	-5.8953	0.03403
NXPH3	541093	neurexophilin 3	-5.8875	0.04494
LOC112444869	112444869	uncharacterized	-5.8494	0.0496
RPL36AL	613592	ribosomal protein L36a like	-5.8373	0.0376
PSPN	518266	persephin	-5.79443	0.046247
LOC782884	782884	dihydrodiol dehydrogenase 3	-5.7728	0.04434
SERPINB10	510205	serpin family B member 10	-5.7701	0.04173
TGM2	281528	transglutaminase 2	-5.761	0.00896
RAB38	533332	RAB38, member RAS oncogene family	-5.7605	0.02407
MTCH2	337927	mitochondrial carrier 2	-5.7512	0.04494
SPTAN1	540108	spectrin alpha, non-erythrocytic 1	-5.7465	0.02881
DLST	506888	dihydrolipoamide S-succinyltransferase	-5.7388	0.01585
ZNF774	100125278	zinc finger protein 774	-5.7375	0.01492
CCL20	281666	C-C motif chemokine ligand 20	-5.7343	0.0365
SH3BGRL3	614672	SH3 domain binding glutamate rich protein like 3	-5.672	0.02411
PAPD7	ND	Uncharacterized	-5.6716	0.03701
NUP188	504307	nucleoporin 188	-5.6576	0.03136
DYNC1LI2	519789	dynein cytoplasmic 1 light intermediate chain 2	-5.6524	0.02588
EIPR1	613935	EARP complex and GARP complex interacting protein 1	-5.5816	0.04015

CD46	280851	CD46 molecule	-5.5695	0.03601
NF2	540479	NF2, moesin-ezrin-radixin like	-5.5663	0.04432
KIAA0232	514704	KIAA0232	-5.5612	0.01454
SLC39A2	508989	solute carrier family 39 member 2	-5.5555	0.04974
AMBRA1	517263	autophagy and beclin 1 regulator 1	-5.5313	0.03138
GLMN	504211	glomulin, FKBP associated protein	-5.497	0.04973
ATP7A	541275	ATPase copper transporting alpha	-5.4572	0.03123
CD63	404156	CD63 molecule	-5.3665	0.00885
SIX5	513676	SIX homeobox 5	-5.2864	0.0253
TMEM115	532459	transmembrane protein 115	-5.2713	0.04941
TTC37	ND	Uncharacterized	-5.1819	0.03257
TSEN54	511091	tRNA splicing endonuclease subunit 54	-5.1646	0.0233
AREG	538751	amphiregulin	-5.0791	0.04329
ARFRP1	525394	ADP ribosylation factor related protein 1	-5.0375	0.04472
ANKRD9	532402	ankyrin repeat domain 9	-4.9858	0.03884
RAN	540457	RAN, member RAS oncogene family	-4.9806	0.04632
SYT4	539867	synaptotagmin 4	-4.9479	0.04015
GNAI3	539521	G protein subunit alpha i3	-4.6436	0.04015
FABP4	281759	fatty acid binding protein 4, adipocyte	-3.5548	0.03168
Up-regulated				
LOC104973427	104973427	uncharacterized	5.10204	0.03424
LOC101905648	101905648	39S ribosomal protein L53, mitochondrial pseudogene	5.15517	0.02699
LDHAL6B	509519	lactate dehydrogenase A like 6B	5.21155	0.022
LOC112443447	112443447	uncharacterized	5.24672	0.04032
LOC112446710	112446710	uncharacterized	5.25078	0.02158
FAM129C	ND	Uncharacterized	5.29914	0.04494

LOC101905156	101905156	non-histone chromosomal protein HMG-14 pseudogene	5.31729	0.04692
GIF	ND	Uncharacterized	5.34179	0.03829
LOC112442794	112442794	small nucleolar RNA SNORA70	5.36271	0.04484
LOC112446114	112446114	small nucleolar RNA SNORA55	5.44644	0.02058
TERB1	100295202	telomere repeat binding bouquet formation protein 1	5.52499	0.02053
LOC112443499	112443499	uncharacterized	5.56311	0.04434
LOC101905398	101905398	Uncharacterized	5.62777	0.03065
LOC112441663	112441663	uncharacterized	5.64161	0.0302
MIR2285K-2	102466168	microRNA mir-2285k-2	5.6785	0.04469
LOC781565	781565	40S ribosomal protein S6 pseudogene	5.68232	0.02788
MEFV	529195	MEFV innate immunity regulator, pyrin	5.73612	0.00653
LOC101906271	101906271	zinc finger protein 705A-like	5.73832	0.03374
LOC112446123	112446123	small nucleolar RNA SNORA79	5.84205	0.03999
LOC112443931	112443931	U6 spliceosomal RNA	5.86146	0.04592
NEFH	528842	neurofilament heavy chain	5.86561	0.03701
MYO1H	525975	myosin IH	5.90333	0.0172
LOC112448024	112448024	uncharacterized	5.9296	0.01859
LOC112445951	112445951	uncharacterized	6.00249	0.01484
MIR2338	100313356	microRNA mir-2338	6.01603	0.03224
NLRP10	104974255	NLR family pyrin domain containing 10	6.02072	0.04548
LOC101904822	101904822	Uncharacterized	6.0537	0.01896
LOC101906692	101906692	Uncharacterized	6.06505	0.00757
PHOX2A	507670	paired like homeobox 2A	6.08427	0.0122
PDE11A	524446	phosphodiesterase 11A	6.0931	0.00532
SLBP2	100848789	oocyte-specific histone RNA stem-loop-binding protein 2-like	6.09998	0.03827

GPD1	525042	glycerol-3-phosphate dehydrogenase 1	6.10821	0.00886
LOC101902022	101902022	small EDRK-rich factor 1 pseudogene	6.12663	0.04288
CNPPD1	507473	cyclin Pas1/PHO80 domain containing 1	6.14949	0.03966
LOC112449624	112449624	small nucleolar RNA SNORD87	6.15496	0.01807
LOC112444650	112444650	uncharacterized	6.16196	0.04432
LOC112443906	112443906	small nucleolar RNA SNORA38	6.17371	0.00489
LOC112442435	112442435	small nucleolar RNA SNORD71	6.18818	0.02186
LOC112444250	112444250	small nucleolar RNA SNORD36	6.20426	0.0081
SLC23A1	505492	solute carrier family 23 member 1	6.22646	0.03916
TRNAG-UCC	ND	uncharacterized	6.2302	0.00678
TRNAD-AUC	ND	uncharacterized	6.23812	0.02691
CTSV	281108	cathepsin V	6.24508	0.01642
S100G	281658	S100 calcium binding protein G	6.26518	0.00997
IL37	786493	interleukin 37	6.29109	0.03561
LOC101904962	101904962	U11/U12 small nuclear ribonucleoprotein 35 kDa protein-like	6.31283	0.01642
LOC112441677	112441677	small nucleolar RNA SNORD97	6.32148	0.04494
TRNAG-UCC	ND	uncharacterized	6.32193	0.02778
TTLL4	511853	tubulin tyrosine ligase like 4	6.32249	0.00117
LOC617130	617130	60S ribosomal protein L12 pseudogene	6.33663	0.03156
LOC101905399	101905399	dual specificity mitogen-activated protein kinase kinase 1 pseudogene	6.34136	0.04332
LOC112441460	112441460	immunoglobulin lambda-1 light chain-like	6.38904	0.00939
LOC107133112	107133112	40S ribosomal protein S26-like	6.42141	0.02315
LOC112442110	112442110	U4 spliceosomal RNA	6.4434	0.04494
LOC104975198	104975198	uncharacterized	6.44963	0.03963
MIR2300B	100313278	microRNA mir-2300b	6.46586	0.00643
LOC101909777	101909777	T cell receptor alpha variable 25-like	6.47332	0.02616

LOC112443346	112443346	U2 spliceosomal RNA	6.48008	0.01972
LOC104973096	104973096	T cell receptor alpha variable 22-like	6.49114	0.02928
LOC112442857	112442857	U2 spliceosomal RNA	6.50044	0.01833
LOC112447103	112447103	uncharacterized	6.57554	0.02428
LOC112444555	112444555	small nucleolar RNA SNORA70	6.64207	0.00997
LOC112446016	112446016	uncharacterized	6.70031	0.00182
LOC112444472	112444472	uncharacterized	6.70662	0.02881
LOC107132308	107132308	uncharacterized	6.70788	0.0299
LOC112449049	112449049	translation initiation factor IF-2-like	6.72922	0.00956
STC2	540573	stanniocalcin 2	6.74801	0.00793
LOC112445941	112445941	uncharacterized	6.7508	0.04692
LOC112441775	112441775	uncharacterized	6.7722	0.02952
LOC784525	784525	interferon beta-2	6.83681	0.04432
RBP5	539418	retinol binding protein 5	6.86771	0.01649
LOC112443325	112443325	small Cajal body-specific RNA 13	6.8806	0.001
PDX1	538927	pancreatic and duodenal homeobox 1	6.91838	0.0134
LOC112442557	112442557	uncharacterized	6.92602	0.00659
LOC112447392	112447392	membrane magnesium transporter 1 pseudogene	6.95182	0.02401
HIST1H2BM	ND	uncharacterized	6.97939	0.00956
LOC104973767	104973767	uncharacterized	7.00622	0.01534
LOC112448196	112448196	U6 spliceosomal RNA	7.02147	0.00352
TRNAG-UCC	ND	uncharacterized	7.05835	0.00339
TRNAE-UUC	ND	uncharacterized	7.05992	0.01078
LOC112448492	112448492	uncharacterized	7.07126	0.00793
LOC112445399	112445399	liprin-alpha-1-like	7.07873	0.01346
TRNAD-AUC	112446192	transfer RNA aspartic acid	7.08171	0.0029
STXBP5L	536735	syntaxin binding protein 5L	7.13319	0.00896

LOC107132302	107132302	60S ribosomal protein L23a pseudogene	7.15694	0.01128
TMEM174	618642	transmembrane protein 174	7.16484	0.00476
LOC783508	783508	UL16-binding protein 27-like	7.19563	0.00184
LOC112442015	112442015	uncharacterized	7.19982	0.01237
LOC112443671	112443671	U4atac minor spliceosomal RNA	7.22043	0.01569
LOC112446537	112446537	U6 spliceosomal RNA	7.23916	0.00941
LOC112441823	112441823	uncharacterized	7.2488	0.00117
LOC100335792	100335792	selenoprotein W pseudogene	7.26062	0.00998
LOC112448033	112448033	uncharacterized	7.27908	0.01115
MOBP	508625	myelin associated oligodendrocyte basic protein	7.27988	0.00622
LOC112446419	112446419	uncharacterized	7.38274	0.00812
LOC101903101	101903101	40S ribosomal protein S3a pseudogene	7.44184	0.00314
LOC112446089	112446089	U6 spliceosomal RNA	7.44996	0.0011
LOC112446862	112446862	small nucleolar RNA SNORA23	7.45054	0.0065
TRNAE-UUC	ND	uncharacterized	7.46636	0.00489
LOC112449363	112449363	thymidylate synthase pseudogene	7.48183	0.00047
TRNAE-UUC	ND	Uncharacterized	7.52814	0.00168
SPAG4	618468	sperm associated antigen 4	7.56148	0.00279
TAAR3	785678	trace amine-associated receptor 3	7.56896	0.00939
LOC100296102	100296102	Uncharacterized	7.57529	0.01096
LOC112448630	112448630	U2 spliceosomal RNA	7.58954	0.00586
LOC112442704	112442704	60S ribosomal protein L10-like	7.60617	0.00052
LOC112448739	112448739	uncharacterized	7.64607	0.00542
GPR17	782442	G protein-coupled receptor 17	7.66436	0.00376
LOC107132831	107132831	T cell receptor alpha variable 22-like	7.73246	0.00801
MIR2421	100313206	microRNA mir-2421	7.77077	0.00884
LOC107132785	107132785	60S ribosomal protein L30 pseudogene	7.77655	0.00143

TRNAG-GCC	ND	Uncharacterized	7.78819	0.00263
LOC112447875	112447875	interferon beta-3-like	7.79393	0.00816
UCP3	281563	uncoupling protein 3	7.82793	0.00121
LOC112442588	112442588	translation initiation factor IF-2-like	7.83838	0.00509
LOC112446028	112446028	uncharacterized	7.8388	0.00252
LOC112449157	112449157	U6 spliceosomal RNA	7.84508	0.00161
LOC100139065	100139065	uncharacterized	7.95664	0.00256
TRNASTOP-UCA	112448671	transfer RNA opal suppressor	7.96319	0.00097
ANKAR	100140244	ankyrin and armadillo repeat containing	7.97409	0.00521
LOC112443378	112443378	small nucleolar RNA SNORA62/SNORA6 family	8.18328	0.00227
LOC112448408	112448408	T cell receptor alpha variable 14/delta variable 4-like	8.23759	0.00117
LOC112448078	112448078	uncharacterized	8.336	0.00252
LOC100298434	100298434	T cell receptor alpha variable 38-1-like	8.43952	0.00252
LOC112446441	112446441	T-cell receptor beta chain V region 3H.25-like	8.53783	0.0023
MIR9-1	100313091	microRNA mir-9-1	8.56909	0.00197
LOC107132241	107132241	uncharacterized	8.70849	0.00086
LOC112442607	112442607	uncharacterized	8.71894	0.00095
LOC112443310	112443310	small nucleolar RNA SNORD113/SNORD114 family	8.74618	0.00117
ABCA12	523479	ATP binding cassette subfamily A member 12	8.81541	0.00015
LOC112449399	112449399	small nucleolar RNA U2-30	8.83881	0.00069
LOC104975179	104975179	uncharacterized	8.86532	0.00021
LOC112448377	112448377	U6 spliceosomal RNA	8.89035	0.00061
KCNS1	521338	potassium voltage-gated channel modifier subfamily S member 1	8.89049	0.00022
LOC786158	786158	proteasome assembly chaperone 3 pseudogene	8.9385	0.00039

TRNAS-GGA	ND	Uncharacterized	8.99333	0.00015
MIR760	100313318	microRNA mir-760	9.03191	0.00021
MIR2387	100313426	microRNA mir-2387	9.04507	0.00052
TRNAC-ACA	112445361	transfer RNA cysteine	9.14148	0.00032
LOC107131651	107131651	uncharacterized	9.26865	8.2E-06
LOC104971329	104971329	Uncharacterized	9.40392	3.8E-05
HEATR1	617204	HEAT repeat containing 1	9.60453	4.1E-06
DGAT2L6	505958	diacylglycerol O-acyltransferase 2 like 6	10.1214	1.7E-05
MIR2285O-4	102465276	microRNA mir-2285o-4	10.47	1.3E-05

ND = not identified by Entrez Gene ID

Supplementary Table S8. Milk fat content, milk protein content, and the average concentration of other solids and MUN in the milk samples from cows dosed with intra-ruminal sodium propionate (propionate) or sodium chloride (control) at two different sampling points. n = 4 cows/treatment (propionate or control).

	0430 h		1630 h		*P* - value
	Control	Propionate	Control	Propionate	
Milk fat (%)	4.2[a]	4.5[a]	4.3[a]	5.0[b]	>0.05
Milk protein (%)	3.5[a]	3.5[a]	3.2[a]	3.1[a]	>0.05
Other solids (%)	5.6[a]	5.9[a]	6.0[a]	5.7[a]	>0.05
Milk urea nitrogen (mg/dL)	11.9[a]	11.6[a]	11.7[a]	11.8[a]	>0.05

[a-b]Mean values in the sampling point with different superscripts differ ($P < 0.05$)